MASTERARBEIT / MASTER'S THESIS

Titel der Masterarbeit / Title of the Master's Thesis

„Porosity and Permeability of the main Lithologies of the Kuhschneeberg"

verfasst von / submitted by

Mario Theyer BSc

angestrebter akademischer Grad / in partial fulfilment of the requirements for the degree of

Master of Science (MSc)

Wien, 2022 / Vienna 2022

1 Inhalt

2 Danksagung / Preface

Vor dem fachlichen Teil meiner Arbeit möchte Ich noch allen Personen danken, die mich bei dem Schreiben dieser Arbeit unterstützt haben.

Zuerst möchte ich dem Betreuer meiner Arbeit, Kurt Decker, danken, welcher sich stets bemüht hat alle meine Fragen und Probleme schnellstmöglich zu lösen. Egal ob fachliche Fragen, Empfehlungen für die Visualisierung der Daten, Unklarheiten bei den Laborgeräten oder Literaturempfehlungen, man konnte sich sicher sein, dass Kurt sich bei jedem Problem mit fachlicher Kenntnis und Hilfsbereitschaft Zeit nimmt dieses zu lösen.

Ebenfalls zu erwähnen ist meine Mitbetreuerin Mariella Penz-Wolfmayr, welche mit eigenen Erfahrungen zum Coreval 700 und dem Immersionsmessungen hilfreiche Erfahrungen und Rat hatte. Ein weiterer besonderer Dank gilt Julian Huemer, welcher sehr engagiert dafür gesorgt hat, dass ich schnellstmöglich wieder meine Arbeit am UV-Mikroskop aufnehmen konnte, als dessen Lichtleiter defekt war.

Natürlich gilt mein Dank auch allen anderen Professoren, Mitarbeitern und Studenten der Uni Wien, die mich bei sonstigen Fragen und Problemen unterstützt haben.

Nicht vergessen will ich auch meine Mitstudenten, mit welchen so einige Tage an der Uni durch ausgedehnte gemeinsame Kaffeepausen aufgelockert wurden. Besonders durch die ungewöhnlich Covid-bedingte Stille und Ruhe im Uni-Gebäude, waren diese Treffen eine willkommene Zerstreuung bei der man sich gemeinsam ausschweifend unterhalten konnte.

Der größte Dank gilt allerdings meiner Familie und meiner langjährigen Freundin, welche mich stets bedingungslos unterstützt haben und deren Beisein mir jeden Tag die Kraft gibt neue Herausforderungen und Lebensabschnitte zu meistern.

3 Kurzfassung

Diese Arbeit gibt Einsicht in die Porosität und Permeabilität der Lithologien des Kuhschneebergs und ist die erste Arbeit, welche Fluorol-gefüllte Dünnschliffe, vergleichend zu den Messungen eines Porosi- und Permeameter, untersucht.

Die Ergebnisse der Immersionsmethode zeigen einen systematischen Unterschied in den Porositäten von Dolomiten (≈2-4 %), Kalksteinen (≈0,5-3%) und verkarsteten Kalksteinen (≈5-9%). Stylobrekzien weisen ähnliche Porositäten wie ihre Protolithen auf, während die Kataklasite höhere Porositäten als die Muttergesteine aufweisen (≈3-6 %). Unterschiede in den Lithologien sind erkennbar, der Einfluss von "fracture density classes" auf die Porosität ist hingegen nicht erkennbar. Handstücke weisen eine höhere Porosität auf als die Bohrkerne, da die Bohrkerne stabiler sind (weniger Brüche und Poren) als die Handstücke und die Bohrkerne mehr Wasser in ihren Oberflächenporen verlieren (prozentual), da ihr Volumen/Oberflächen-Verhältnis geringer ist.

Ähnliche Unterschiede in den Porositäten der Lithologien wurden auch bei den Coreval 700-Messungen festgestellt, die Permeabilität hingegen ist weniger von der Lithologie abhängig. Hohe Durchlässigkeiten (>1 mD) wurden nur in Proben mit ausgeprägter Bruchbildung oder Verkarstung beobachtet. Der grundsätzliche Porositätswert einer Probe ist im Vergleich zu der Bruchbildung/Verkarstung für die Permeabilität von untergeordneter Bedeutung. Nicht frakturierte und nicht verkarstete Proben weisen Permeabilitäten von nur 0.00x - 0,4 mD auf.

Die Porositäten der Immersionsmethode sind konsistent niedriger als die Ergebnisse der Bohrkerne im Coreval 700 (im Mittel um 4% absolute Porosität). Mögliche Erklärungen hierfür sind die Viskosität und das Verhalten des verwendeten Mediums, der Verlust von Porenwasser an der Oberfläche bei der Immersionsmethode und Abweichungen von der perfekten zylindrischen Form bei den Coreval 700-Messungen.

Die Betrachtung von, mit Fluorol imprägnierten, Proben unter UV-Licht ist eine nützliche ergänzende Untersuchungsmethode, da sie eine qualitative Untersuchung des mechanischen Hintergrunds (Poren-/Bruchverteilung und -struktur) der Coreval 700-Ergebnisse ermöglicht. Die Betrachtung von Fluorol-gefüllten Dünnschliffen zeigt auch, dass der prozentuale Verlust von Permeabilität und Porosität der Proben mit der Verteilung des Porenraums (Poren und Brüche) zusammenhängt. Der Verlust ist deutlicher bei Proben mit

einer starken räumlichen Konzentration des Porenraums und weniger diffuser UV-Emission.

Messungen mit der Immersionsmethode sind der schnellste Weg, um Erkenntnisse über die Porosität größerer Probenmengen zu gewinnen, da mehrere Proben gleichzeitig gemessen werden können. Auch die Unterschiede zwischen den Lithologien sind bei der Immersionsmethode im Vergleich zu den Coreval 700-Messungen ausgeprägter, weshalb sie eine nützliche ergänzende Methode darstellt. Die Untersuchung von mit Fluorol gefüllten Proben ist zeitaufwändig, kann aber durchgeführt werden, wenn Mechanismen des Fließvorganges von Interesse sind (durch Porenform, Zementierung, Bruchverbindungen usw.). Es ist auch von Interesse, ob künftige Studien den Einfluss der Porenraumverteilung auf den prozentualen Verlust von Permeabilität und Porosität bestätigen.

Die beobachteten Lithologien, welche Merkmale von Wasserstauern aufweisen, sind der Hornsteinkalk und die Stylobrekzien. Die zahlreichen Quellen am Kontakt zwischen Wetterstein und Hornsteinkalk bestätigen diese Beobachtung. Kataklasite und Dolomite weisen eine höhere Porosität bei ähnlicher Durchlässigkeit wie andere Karbonatproben auf, sie haben daher ein höheres Wasserrückhaltevermögen und benötigen mehr Zeit zum Austrocknen. Der Hauptfaktor für die Permeabilität ist jedoch die Bruchbildung und Verkarstung der Gesteine am Kuhschneeberg.

4 Abstract

This thesis gives insight into the porosity and permeability of the lithologies of the Kuhschneeberg and is the first thesis that uses thin sections stained with Fluorol to accompany the measurements of a gas porosi- and permeameter.

The results of porosity measurements using the immersion method show a systematic difference between the porosity of dolomites (≈2-4 %), limestones (≈0.5-3%) and karstified limestones (≈5-9%). Stylobreccias show similar porosities as their protoliths, whereas the cataclasites reveal higher values than the parent rocks (≈3-6 %). While differences of the porosity between different lithologies are clearly recognized, results indicate no influence of fracture density on porosity. Porosity measurements from handpieces show higher porosities than values derived from smaller sized core plugs from the same specimen, because the core plugs tend to be sampled from parts of the samples containing less fractures than the full-sized samples, and core plugs lose more water from pores intersected by the sample surface due to their lower volume to surface ratio.

Similar differences in porosities between the lithologies were also observed in measurements performed with a Coreval 700 gas porosi- and permeameter. Permeability, on the other hand, is less dependent on lithology. High permeabilities (>1 mD) were only observed in samples with pronounced fracturing or karstification. Fracturing and karstification outweigh the effects of matrix porosity on permeability. Unfractured and nonkarstified samples show permeabilities of between about less than 0.01 mD and 0.4 mD.

Porosity values derived from the immersion method are consistently lower than the results from plugs analysed by the gas porosimeter Coreval 700 (in the mean around 4% absolute porosity). Possible explanations for this are the viscosity and behaviour of the used medium, loss of surface pore water in the immersion method and deviations from the perfect cylindric form of plugs used in the Coreval 700 measurements.

The analysis of thin sections stained with Fluorol under UV light in the microscope proved a useful supplementary method, as it enables a qualitative examination of the matrix pore and fracture distribution. Comparing the observations from Fluorol-stained thin sections with the Coreval 700 results showed, that the loss of permeability and porosity of samples measured under high confining stresses is governed by the relative amount of pore space provided by "spherical" matrix pores and fractures. The loss of permeability and porosity

is significantly higher for samples with a prevalence of fracture porosity as documented by UV light microscopy.

Measurements with the immersion method are the fastest way to obtain porosity data from larger sized samples, since multiple samples can be measured at the same time. The differences between lithologies are also more pronounced in the immersion method in comparison to the Coreval 700 measurements, therefore it is a useful complementary method. Studying Fluorol-stained samples is time-intensive but should be done if the relative contribution of matrix and fractures, pore size, pore geometry, fracture architecture, fracture connectivity, cementation, etc. is of interest to assess mechanisms of fluid flow.

Among the analysed lithologies, Jurassic Hornstein limestone and stylobreccia are classified as aquicludes. The abundant occurrence of springs at the contact between Wetterstein in the hangingwall and Hornstein limestone in the footwall of thrusts support this observation. Cataclasites and dolomites show higher porosities with similar permeabilities to samples from unfractured and non-karstified limestone, they therefore have higher water retention capabilities and are classified as aquifers. However, the primary factor of fluid in the aquifers of the Kuhschneeberg is fracturing/faulting and the karstification of carbonate rocks.

5 Introduction

This thesis concentrates on analysing porosities and permeabilities of rocks from the Kuhschneeberg, as well as the evaluation, and the comparison of methods, used to determine these parameters from hydrogeological reservoir rocks. The Kuhschneeberg lies in the middle of the catchment area of the I. Wiener Hochquellenleitung and is of essential importance for the water supply of the Austrian capital. It is rightly an area worth protecting, and knowledge about the geologic and hydrologic aspects of the area is of great interest.

Porosity and permeability measurements utilize different methods and can differentiate in scale. This thesis studies samples in a range from several decimeters to thin sections, supported by large-scale observations in the field. Porosity measurements were achieved through different filling methods of sample material with fluids and gases, the further measurement of permeability with the use of the Coreval 700 porosi- and permeameter device. Especially the comparison and correlation of the results of porosity/permeability measurements, performed with different confining pressures, with Fluorol-stained thin sections to determine, at least qualitatively, the contribution of (micro-) fractures and pores to the hydrogeological rock properties is a new approach. The methodology and suitability of this correlation is evaluated for future scientific work.

Figure 1: Map showing the two Vienna water mains connecting the city to springs and their catchment areas. The Kuhschneeberg (black dot) is located at a protective area (green zone) forming the catchment of some major tapped springs (like the Kaiserbrunn spring). Modified from Wiener Wasser, 2021.

The Kuhschneeberg is part of the Rax-Schneeberg massif, which is not only known as a popular destination for hikers of Austria and neighbouring countries, but also as a hydrological protective area. It is the catchment area of the First Vienna Water Main (I. Wiener Hochquellwasserleitung), an indispensable part of the Austrian capital´s water supply. Together with the Hochschwab massif´s springs (the source of the Second Vienna Water Main), 95 percent of the water supply of the Austrian capital is provided (Schmid & Pröll, 2020:224f). Two hundred twenty million litres of water flow every day through the First Vienna Water Main over a 150-kilometer distance of canals. The catchment of the tapped springs mostly consists of karstified Triassic carbonates. The danger of contamination is relatively high in such karst waters because of the typically short transit time and soil-cover, which acts as a filter, is generally thin or even absent (Dirnböck & Greimler, 1999:202).

Therefore, it is essential to research and understand the water cycle, from the moment the precipitation water meets the soil and rock until it is discharged from the karst system in one of the many springs and collected in the spring pipelines.

The effort of this thesis concentrates mostly on the two properties porosity and permeability of the aquifer rocks, which are important for the water retention, transit time, water flow and storage capacities of water in the rock masses. Different methods were used to gather the data, including the Immersion Method, the measurements with the Coreval 700 device and analysis of thin sections with the fluorescence microscope.

The results of these methods were also compared with each other to determine their differences, advantages, disadvantages, and suitability. This holistic approach should lead to a better understanding of the reservoir characteristics of the rocks in terms of porosity and permeability and the interplay between fractures and pores. Additionally, field work was done to collect samples on-site and to get a direct overview of the lithologies and the structural geology of the Kuhschneeberg.

Besides providing quantitative data on the reservoir properties, this thesis also evaluates the suitability of different methods to gain meaningful porosity/permeability data. Porosity/permeability data is determined by lab measurements at different confining pressures to simulate the effect of rock overburden on the natural reservoirs as deep groundwater flow below the Kuhschneeberg occurs at levels which are up to 1 km below the mountain´s plateau. The stepwise increase of confining pressure during the measurement also allows for an at least qualitative assessment of the contribution of fractures and pores to porosity/permeability. The validation of such assessments with porosity measurements from Fluorol stained thin sections is a new method.

The following chapter "Theoretical Background" gives information about the actual state of science, about the geologic history of the Rax-Schneeberg Group, the morphology, lithology, tectonics, the hydrogeology of the Kuhschneeberg and information about porosity and permeability in rocks.

In the chapter "Overview of the Geological Mapping" there is a descriptive and graphical overview of the area of interest, the analysed outcrops and the samples taken. There is also information about the use of existing sample material from the Wetterstein Fm. collected by Wimmer (2020).

The chapter "Methods" provides technical information on the procedures of measurement, equipment and theory behind the different methods used. The chapter is divided in "Porosity" and "Permeability", each describing the corresponding analytical methods. This divides information about the Coreval 700 measurements since the device measures porosities as well as permeabilities with different principles and operations. General information of the Coreval 700 is found in the porosity sub-chapter, as well as the method of porosity measurement. The different approach of permeability measuring is still found in the permeability sub-chapter.

In "Results", the obtained data is shown in figures and the presentation of the data is explained. This includes the results of the different methods applied, as well as the comparison between the results of different methods.
Summaries of the obtained data, possible and definitive interpretations of the data, answers to the aims of the thesis and new questions are found in the "Discussion" chapter. A concise summary of the whole information given in the thesis is found in the "Conclusion".

The descriptions of the analysed samples are found in "Samples", a summary of figures and tables is found in "Lists" and the "References" conclude this thesis.
Further, detailed data tables from the measurements are found as an "Appendix".

6 Theoretical Background

6.1 Geologic History of the Rax-Schneeberg Group
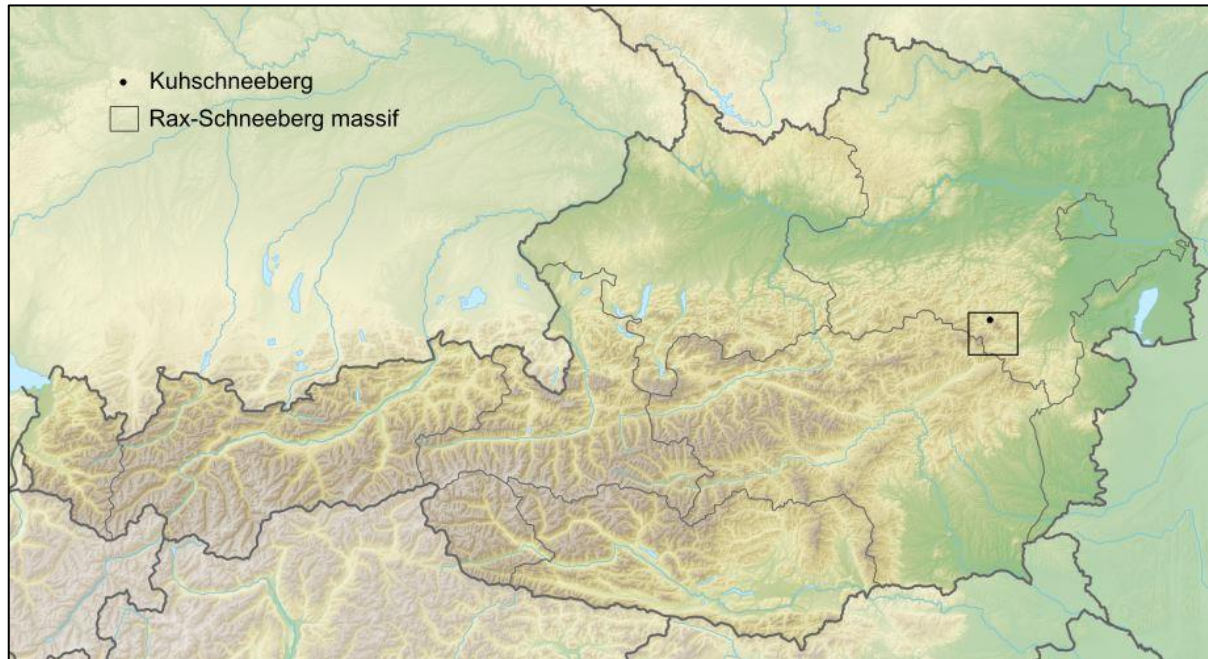
Figure 2: The location of the Rax-Schneeberg massif (box) and of the Kuhschneeberg (black dot) shown on a modified relief map of Austria. Modified from https://www2.jpl.nasa.gov/srtm/ (NASA Shuttle Radar Topography Mission), download on 05.05.2022.

The Rax- and the Schneeberg massif, located at the south-western border of Lower Austria (Figure 2), is dominated by Mesozoic carbonate rocks of mainly Triassic age. Not as common, but especially important under hydrogeologic aspects, are the different siliciclastic and clayey sediments accompanying them because of their potential to work as aquitards or aquicludes (Mandl, 2006:3).

The base of the Mesozoic sedimentary succession of the Schneeberg massif is the Greywacke zone, which consists of Palaeozoic rocks, deformed in the Variscic deformation. It was the last orogeny in Europe before the Alpine orogeny (Matte 1986:329f). The pre-Permian rocks of the Greywacke zone are discordantly overlayed by the Präbichl Formation, terrestrial red beds of Permian age (Krainer & Stingl, 1986:231-234). Hypersaline evaporitic and volcanic intercalations were also formed during the Permian. The reason for this was an N-S-directed spreading of continental crust, which occurred together with volcanic activity and marine ingression. Through the onset of the marine inundation into the rift arm, evaporitic facies developed on the continent (Mandl, 2006:3, Spötl, 1989:122f, Raumer & Neubauer 1993:547). This saline facies is known as "Haselgebirge", one of its deposits is located at "Pfennigbach/Puchberg am Schneeberg". It is the only actively mined gypsum deposit in Lower Austria (Grösel, 2018:34). Because of its

strong dissolution, this lithology is also important for hydrogeologic models, as it not only dissolves fast but also changes the water chemistry in the process (Mandl, 2006:3).

In the Mesozoic period, several hundred meters of the Werfen Formation deposited (Figure 3), an accumulation of sandy to shaly sediments. These lithologies represent a fluvial to marginal marine facies of the Lower Triassic epoch. Towards the hanging wall, this lithology gets more calcareous (Krainer 1987:77). The Werfen Fm. acts as an aquitard (Mandl, 2006:3).
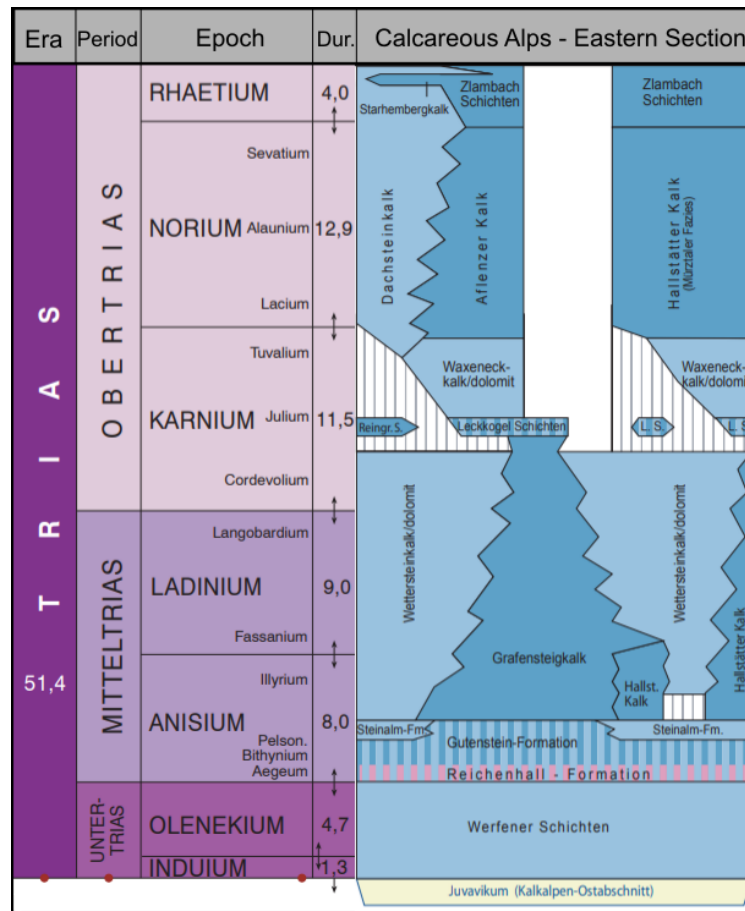
Figure 3: Overview of the lithologies in the Eastern Calcareous Alps during the Trias. The unit of duration is million years. The Era of Trias began 251 million years ago and ended 199,6 million years ago. Modified from Piller et al., 2004.

At the beginning of the Middle Triassic epoch (Anisian age), sedimentation of the Gutenstein and Steinalm Formation took place. The sedimentation marked the beginning of intensive carbonate sedimentation in the Rax-Schneeberg Group. Both formations contain limestone and dolomite. The Steinalm Fm. was following the Gutenstein Formation after some differentiation took place in the anoxic Gutenstein Formation. The Steinalm Fm. developed in a shallow-marine environment as documented by the accumulation of green algae (Mandl, 2006:3, Nittel 2006:93f).

In the middle of the Anisian, faulting led to the formation of a deepened and strongly differentiated relief. The relief provided the base for the strong facies differentiation of

carbonate sedimentation in the remaining Triassic epoch (Gawlick et al., 2021:419). Sedimentation happened in deep seas basins, shallow marine, and intermediate zones (Mandl, 2006:3). The most prominent lithology, which followed, is the Wetterstein Fm. with limestone or dolomite. It forms a large part of the Schneeberg-Rax massif. It represents a carbonate platform up to 1000 meters thick in this area. Carbonates are bedded or massive. The bedded facies developed in a lagoonal setting, the massive facies contains former reef structures, including calcispongae, corals, and encrusting organisms (Mandl, 2006:3, Piros et al., 1994:349-352).

Deeper basins and ridges between the shallow platforms were the sedimentation areas of the Grafensteig, Reiflinger, and Hallstätter limestone. (Mandl, 2006:3,8f, Moser, 2014:200, Pistotnik, 1973/1974:143). During the Middle Triassic, the Wetterstein Formation prograded over the deep basin facies. The fact that the Wetterstein Formation is fractured and partly transformed to dolomite is interesting in hydrogeological aspects for the region. The fractures represent the rock´s secondary porosity and work as a water pathway through the rock. Dolomized parts of the formation have a higher water retention ability, leading to a more stable spring discharge (Mandl, 2006:3).

In the early Carnian, the carbonate platform was lying dry, and the Raibl Formation sedimented on top. It is an intercalation of sandstone, marl and shales, another aquiclude in this research area. (Mandl, 2006:3,10). The beginning of terrigenous sedimentation is known as "Reingrabener Wende" (Schlager & Schöllnberger, 1973/1974:171ff).

In the later Carnian, carbonate platforms developed again. The rising sea level led to the deposition of the Hauptdolomit and Dachstein Fm. The former is the intertidal to subtidal facies, the later the reef and lagoon facies (Mandl, 2006:3,14,23, Czurda, 1973:397, Schwarzacher, 2005:93f). In Upper Triassic, the platform development got restricted by terrigenous sedimentation again. Kössen Formation and Zlambach Formation are the products of this time frame. Both formations are characterized by calcareous marls (Gawlick et al., 2013:178, Krystyn L., 1987:22-25). At the Triassic/Jurassic-split, the platform development came to an end, and rifting processes happened in the crust. (Mandl, 2006:4, Bernoulli & Jenkyns, 1974:148f).

The Jurassic epoch is characterized by marl- and silica-rich limestones on top of the sunken platforms. In deeper basins, the Ruhpolding radiolarite formed (Schlager & Schöllnberger, 1973/1974:175). In the Upper Jurassic, global tectonics led to the transpressive uplift of parts of the Calcareous Alps, which glided into the radiolarite basins. These tectonic movements are known under the term "Kimmerische Orogenese" ("kimmeric orogeny", Frisch & Gawlick, 2003:715).

In the Lower Cretaceous, the whole of the NCA (Northern Calcareous Alps) was dominated by nappe stacking and folding of rock. (Kilian et al, 2021:3ff) The nappes witnessed deep terrestrial erosion, followed by the marine transgression of the Upper Cretaceous to Eocene Gosau Group. The Gosau Group often discordantly overlies the folded underlying formations (Weigl, 1937:30,36 Mandl, 2006:4). Folding and thrusting went on after the Gosau sedimentation ended and moved the nappes towards the north, bringing the NCA over the accretionary wedge of the Rhenodanubic Flysch units. With this thrusting, the sedimentation of marine sediment ended in the remnants of the South Pennic Ocean (Egger 1990:147, Mandl, 2006:4).

Today´s plateau character of the Rax-Schneeberg Group evolved in the Oligocene through erosion processes. Sediments of rivers ("Augenstein formation"), flowing from the Central Alps to the Molassic Zone, were deposited on top of the NCA (Mandl, 2006:4,16, Frisch et al. 2001:500).

Fold-thrusting continued through the Oligocene to Early Miocene because of the ongoing shortening between the Adriatic Plate and the Eurasian Plate, overlapping in time with the lateral extrusion of the central Eastern Alps (Ratschbacher et al., 1991; Beidinger & Decker, 2014:229).

Strike-slip faults form a large part of the brittle deformation structures in the NCA. The locally most important fault are the so-called SEMP Fault ("Salzach-Ennstal-Mariazell-Puchberg Fault", Decker et al., 2002:211ff) and other SW-NE striking strike-slip fault systems that parallel the Mur-Mürz-Vienna Basin fault system (Linzer et al., 2002). The formed faults have a considerable potential for the permeabilities of the deformed lithologies through their influence on karst formation (Mandl, 2006:4, Plan & Decker, 2006:29f). Data from GNSS (Globate Navigating Satellite Systems) shows the extrusion from the Eastern Alps towards the Pannonian Basin has a velocity of around 1-2 mm per year (Möller et al., 2011:144). The tectonic processes in the Eastern Alps are still active but are diminishing.
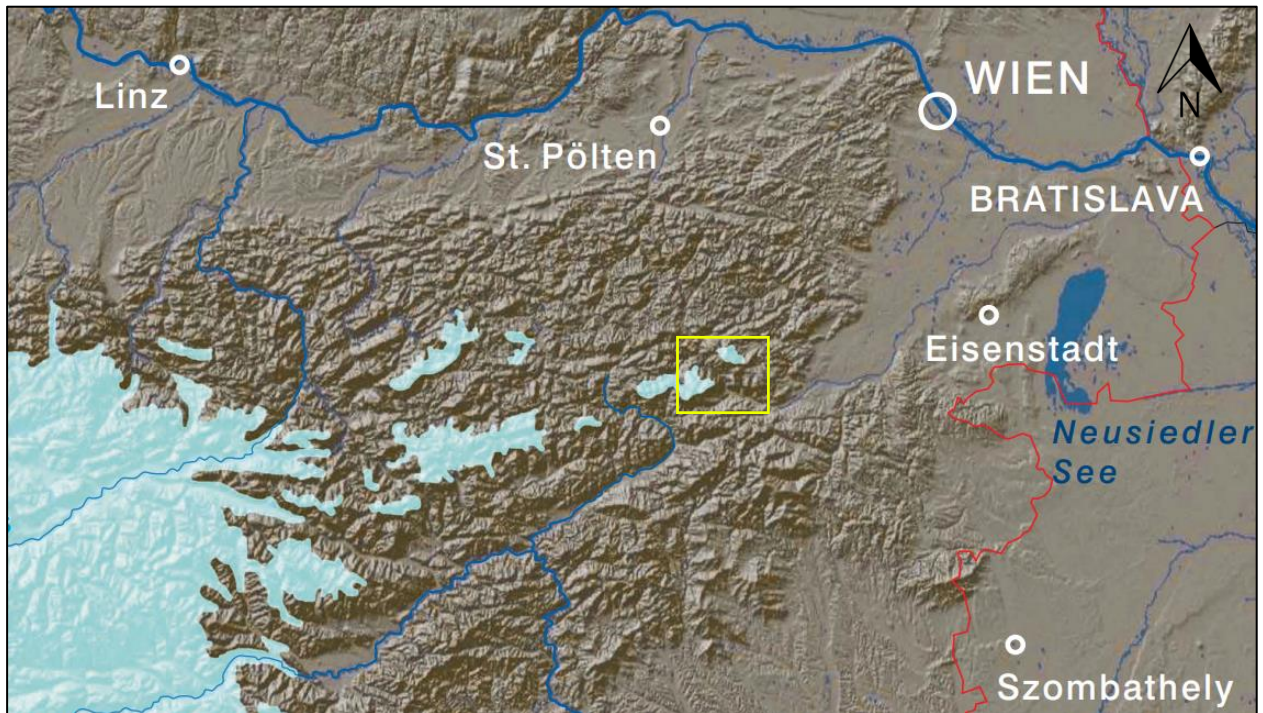
Figure 4: Cut-out showing the extent of the last glaciation in the Würm glacial. The yellow box indicates the Rax-Schneeberg massif and is the easternmost glaciation, separated from the main glaciation at the western part of the map. Modified from Schuster et al., 2015:67.

The youngest sedimentation happened through the Pleistocene and recent Holocene. Pleistocene (Würmian) glacial deposits are recognized in the Rax-Schneeberg massif. In the "Würm" ice age (Fig. 4), however, the Rax-Schneeberg Group was isolated from the extensive ice flow network in the west of Austria and the Western Alps (Ivy-Ochs et al., 2008:559f).

6.2 The Morphology, Lithology, Tectonics, and Hydrogeology on and around the Kuhschneeberg

6.2.1 Morphology

The Kuhschneeberg, as his higher neighbour, the Hochschneeberg, has steep slopes and a plateaued character at the top. The plateau of the Kuhschneeberg is located at around 1400-1550 meters altitude. The highest point is the Saukogel at 1545 meters, around 500 meters lower than the highest point of the Hochschneeberg in the east: the Klosterwappen at 2076 meters. The plateaued character of the Kuhschneeberg is as apparent as the plateau of the Hochschneeberg. Northwards of the Kuhschneeberg, the Gutensteiner Alps are located, which are also part of the Northern Eastern Alps (after AVE - Alpine Club classification of the Eastern Alps in Graßler, 1984:215-224). The Kuhschneeberg faces towards the Klostertal in the North. Springs from the Kuhschneeberg flow into the Voisbach, a stream, which flows from the Klostertal into the "Schwarza"-river.

In the West and South-West, the mentioned Schwarza river flows in a roughly N-S trend through the Höllental. The latter separates the Rax- from the Schneeberg-massif. The south-facing side of the Kuhschneeberg is marked through the Frohnbachgraben. It is a deepening in the morphology, which brings water into the Schwarza.

6.2.2 Lithology
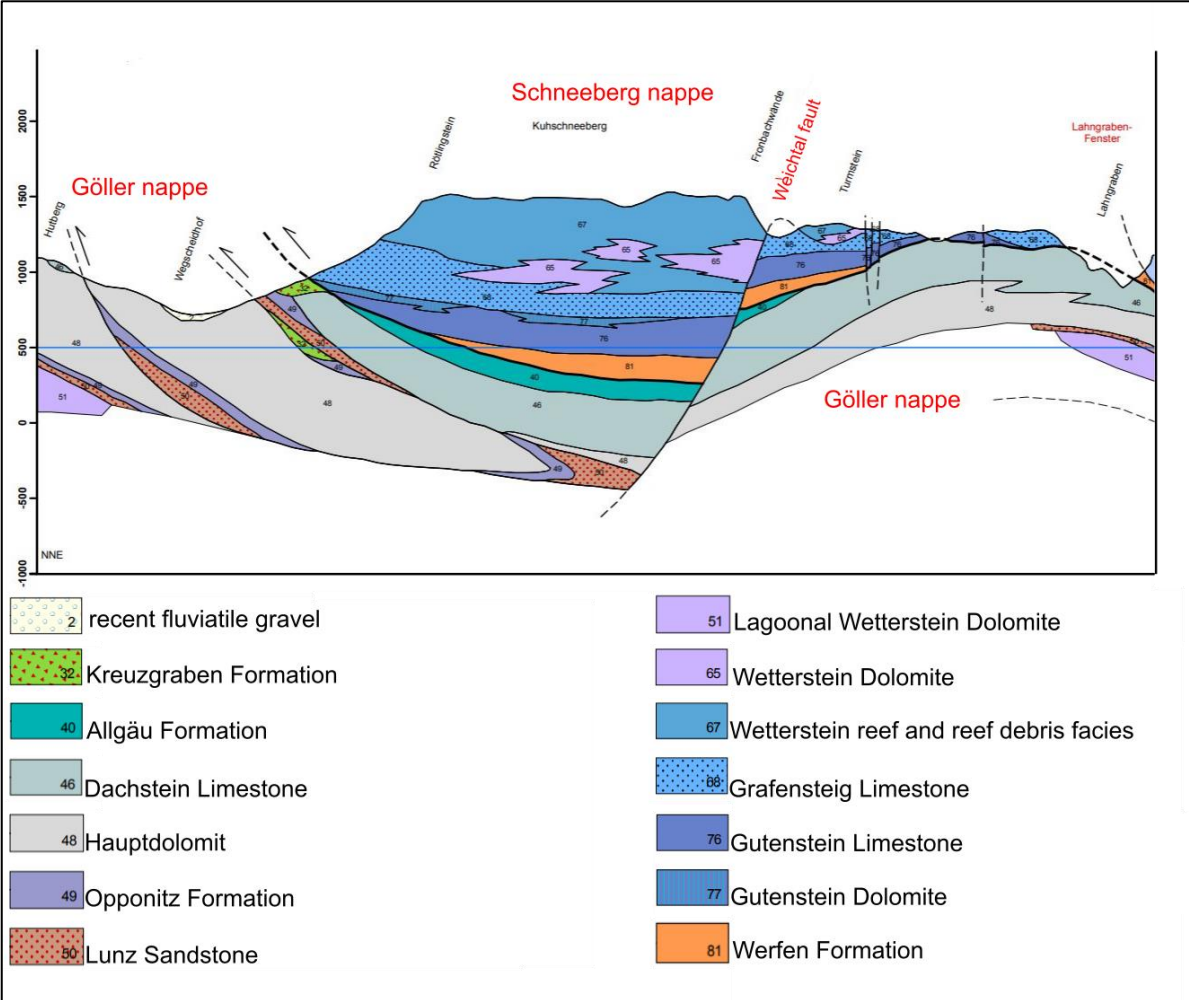
Figure 5: NNE-SSW profile through the eastern part of the Kuhschneeberg. Lithologies from the Schneeberg nappe form the major parts of the elevation relative to the Kuhschneeberg´s surroundings. Modified cut-out from Mandls (2006) profile 1.

On the surface, the lithology of the central Kuhschneeberg is almost exclusively Wetterstein Formation. Further away from the center, the lithology variates much more. Profile 1 of Gerhard W. Mandl´s "Explanatory notes to the digital geological map of the Rax-Schneeberg-Region" (Mandl, 2006) shows an NNE-SSW profile (Figure 5), which crosses the plateau of the Kuhschneeberg. The uppermost part of the Kuhschneeberg consists of Wetterstein limestone and Wetterstein dolomite. The Wetterstein limestone can principally be found as lagoonal, reef, or reef-debris facies. No lagoonal outcrops are found at the Kuhschneeberg, they are restricted to the area opposite of the Höllental (Rax). On the Kuhschneeberg, only the reef and reef debris facies of the Wetterstein limestone is present, as well as Wetterstein dolomite. These lithologies are massive and build up a

large part of the Kuhschneeberg, as does the underlying Grafensteig limestone. Other lithologies of the Schneeberg nappe underlying here are, from top to bottom: Gutenstein dolomite, Gutenstein limestone, and schists/sandstones of the Werfen Formation. Below and around 1000 meters height, lithologies of the Göller nappe can be expected on the surface. Prominent examples are the Hauptdolomit Formation and the Dachstein limestone.

6.2.3 Tectonics
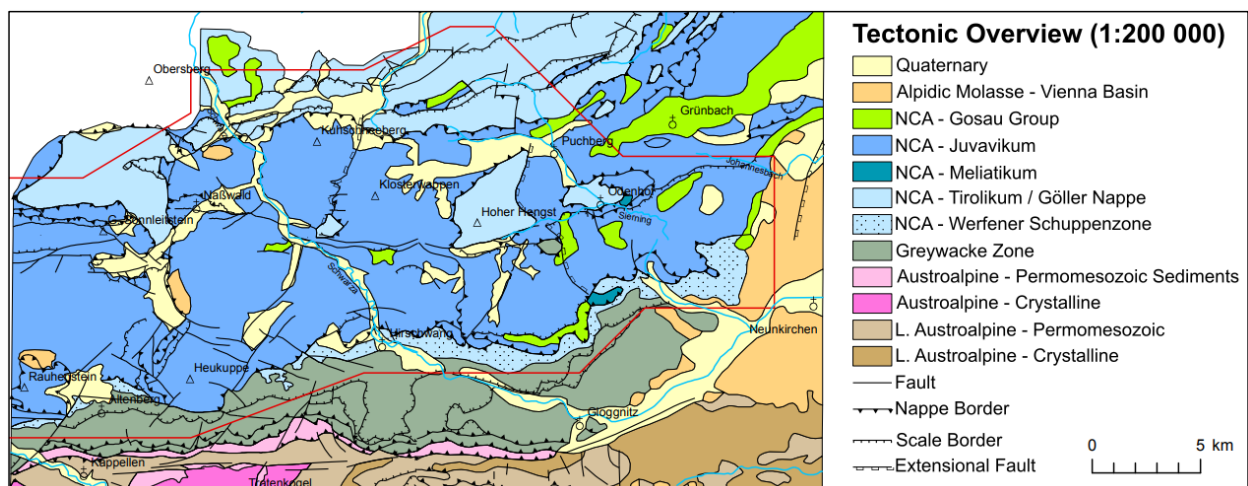
Figure 6: Tectonic overview over the Kuhschneeberg and his surroundings. The Juvavic Schneeberg-nappe thrusts over the Tirolic Göller nappe. Modified from Mandl (2006).

As explained in the previous chapter Lithology, rocks of the Schneeberg nappe are overlying rocks of the Göller nappe. The Schneeberg nappe had been thrust northwards along a shallow dipping thrust fault over the Jurassic rocks of the Göller nappe (Figure 6). The place of detachment of this thrust movement was an evaporitic and siliciclastic-shaly lithology. In the area of the Kuhschneeberg, this happens to be the Werfen Formation.

Peripheral to the southern part of the Kuhschneeberg, in the Höllental, the Krummbach Fault System is trending roughly EW (Mandl, 2006:21fff). The nearest of these faults are found around and south of the Weichtal house and in the Stadlwandgraben. They represent a flower structure of a strike-slip fault, which also implies a vertical displacement component, where the inner parts of the structure are uplifted, as well as the northern edge relative to the southern edge. The Krummbach fault system led to a fractured Wetterstein Formation and elevation of some part of the Werfen Formation up to the surface, which is also relevant to the hydrogeologic situation.

More near the central area of the Kuhschneeberg is the Weichtal normal fault. The estimated offset of the fault is 600 meters. Without this offset, Kuhschneeberg and Hochschneeberg would have approximately the same elevation. The Weichtal normal

fault is also responsible for splitting of the Göller nappe´s synclinal form into a western and eastern part. The faults of the Großes Höllental have the same strike direction, but they have elevated the western side relatively to the eastern side.

Internal thrusts in the Schneeberg nappe do not seem to play a big role in the geology of the Kuhschneeberg, even if they are found in the Rax-Schneeberg massif. An example of this is the Markgraben thrust; a westward directed thrusting in the Gahns plateau.

6.2.4 <u>Hydrogeology of the Kuhschneeberg</u>

In the NCA, the Mesozoic carbonates are the dominant lithologies and form the main aquifer and the karst morphology, we see nowadays in this region (Mandl, 2006:3). Limestones and dolomites might be initially characterized by low permeability, but carbonate dissolution nucleating at fractures change this attribute over time by widening natural fractures and forming connected volumes of karst conduits (Thurner, 1967:36). The main aquicludes are the siliciclastic layers below or between some of these carbonates. A prominent aquiclude is the Werfen Formation in the Rax-Schneeberg massif (Dirnböck & Greimler, 1999:203).

Around the Kuhschneeberg, the Wetterstein limestone is the most significant aquifer like it is over the whole Schneeberg-Rax massif. Despite losing its primary porosity during cementation, the Wetterstein limestone can form many different karst forms like sinkholes and provides fast transportation of precipitation water to the springs.

Locally, the dolomitic Wetterstein Fm. might have an influence on the water cycle because of a lower percolation rate and a more constant spring discharge (Mandl, 2006:3). Other Triassic limestones and dolomites, which are important aquifers, are the Gutenstein, Steinalm Formation and the limestones of the Grafensteig Formation (Mandl, 2006:21). Evaporitic lithologies, like the Präbichl Formation, have the potential to alter the water chemistry but are not mapped on the Kuhschneeberg and were not found during the field investigations during this thesis.

Jurassic sediments of the Göller Nappe exposed below the Schneeberg Nappe at the N slope of the Kuhschneeberg mostly act as aquicludes. This is indicated by numerous springs emerging at the contact between overlying Triassic carbonates and the Jurassic formations (Mandl, 2006:24).

Especially the compressions of Miocene and, therefore, the creation of strike-slip fault systems are driving forces of the development of the karst system in the Rax-Schneeberg massif. The later sedimentation of Pleistocene and Holocene sediments is not known to

be a significant influence, and major springs are not bound to those layers (Mandl 2006:4).

Another question is the independence of the drainage from the Kuhschneeberg to its neighbouring mountain, the Hochschneeberg. An experiment from A. Thurner (1967:129ff) showed that tracers used at the plateau of the Hochschneeberg are measurable at the springs around the Kuhschneeberg, even at its north-west flanks. It means the Kuhschneeberg is not independent of the drainage of the Hochschneeberg, at least in one direction and the fracture systems of the Hochschneeberg allow outflow in all directions. Such a direct link also means that any contamination on the grounds of the Hochschneeberg will also affect the springs around the Kuhschneeberg. This risk should be considered for the future planning Vienna´s water supply network.

7 Overview of the Geological Mapping

7.1 Surveyed Area and Sample Collection

Most of the mapped areas of the Kuhschneeberg (Figure 7) are easily accessible as various forest roads climb the Kuhschneeberg from north, west, and south. Additionally, the plateau of the Kuhschneeberg is relatively easily accessible. Most of the outcrops were mapped at the lower parts of the mountain as the plateau itself is less interesting in variety and outcrop density. Classical karst forms are abundant on the plateau, whereas the lithology there consists mostly of limestone of the Wetterstein Formation. Recorded outcrops are very dense from the Frohnbachgraben and the Weichtalklamm in the south, as well as in the north-western edge towards the conjunction of the Höllental with the Klostertal.

Field work in the southern and western parts of the region provided only samples of the Wetterstein Formation, as well as the plateau. Towards the north and north-east of the Kuhschneeberg, the sampled lithologies became more diverse: the dolomites of the Hauptdolomit Formation, limestones of the Hornsteinkalk Formation and Opponitzer Formation were collected.

Samples were taken from different locations on and around the Kuhschneeberg to get an overall view on the lithologies. There are also some lithologies only found locally at very restricted areas, like the Hornsteinkalk Formation.

Although samples were not taken from every outcrop, it is crucial to know the entirety of the geology of the Kuhschneeberg to interpret data from the laboratory.
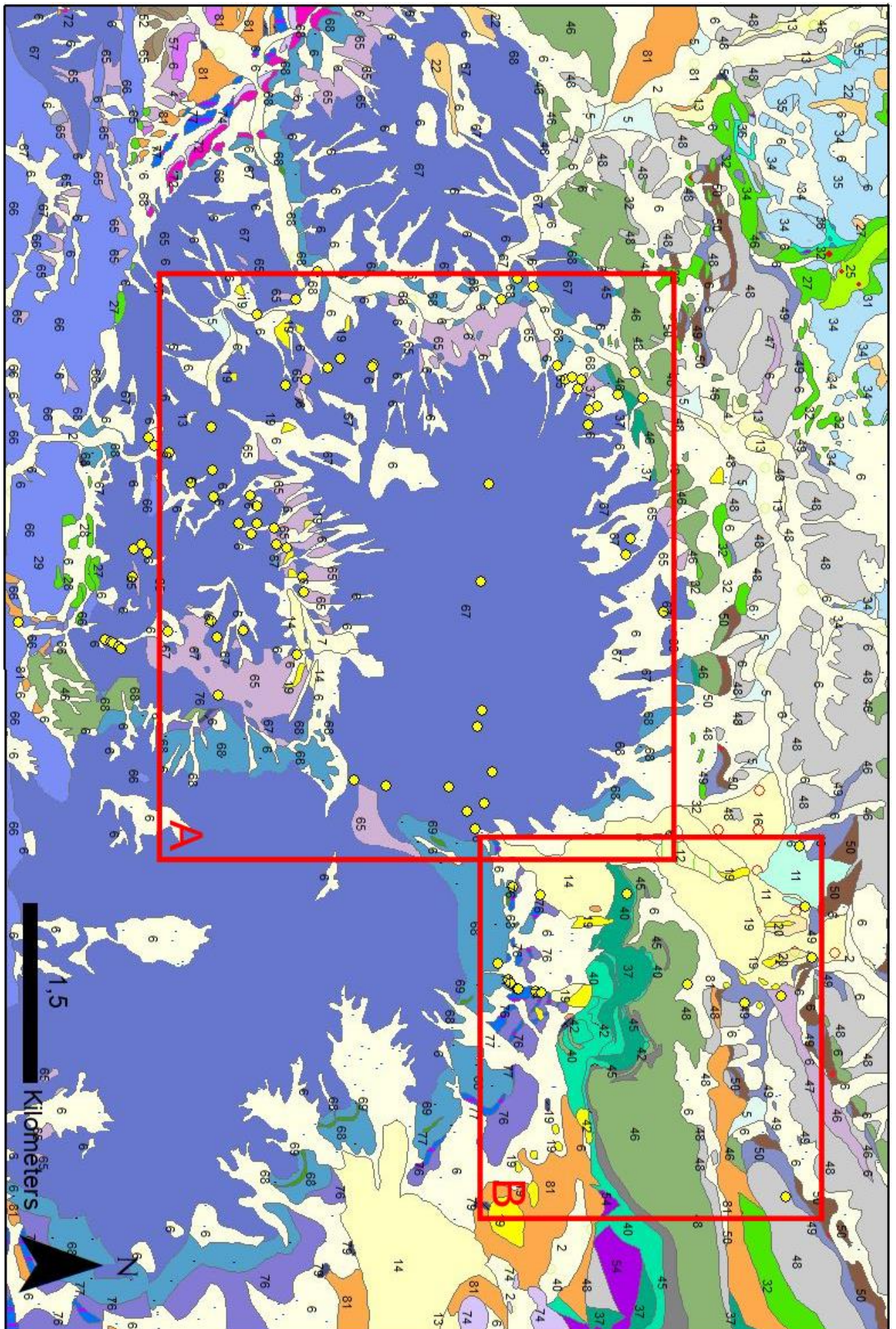
Figure 7: Locations of outcrops (yellow circles) documented and sample during this thesis. Digitalized cut-out modified from Mandl´s (2006) map of the Rax-Schneeberg-group. Red boxes denote the locations of enlarged maps in Figure 9 and 10. The legend for this map is found in Figure 8.

Legend

Lithology

Quaternary

Pleistocene - Holocene

- 2 Young River Sediment
- 4 Swamp/Moor
- 5 Alluvial Fan
- 6 Slope Debris and Debris Fans
- 7 Blocky Debris
- 8 Creeping Soil/Debris
- 11 Late Glacial Alluvial Fan
- 12 Late Glacial Sediment

Pleistocene

Würm

- 13 Lower Terrace
- 14 Moraine
- 16 Advanced Gravel

Riss

- 18 Moraine

Mindel/Riss Interglacial

- 19 Slope Breccia

Pre-Riss

- 20 Conglomerated Gravel

Inner Alpine Molasse

- 22 Red Clay

Gosau Group

- 25 Turbitidic Sandstone
- 27 Piesting Formation
- 28 Orbitoid Sandstone
- 29 Biodetritic Limestone with Rudists
- 31 Red Marls with Conglomerate Layers
- 32 Kreuzgraben Formation

Tirolikum

- 34 Plassen and Tressen Limestone
- 35 Oberalm Limestone
- 36 Ruhpolding Radiolarite
- 37 Red Radiolarite
- 40 Allgäu Formation
- 41 Jurassic Limestones in general
- 42 Adnet Limestone
- 44 Upper Dachstein Limestone
- 45 Kössen Formation
- 46 Dachstein Limestone (Lagoon)
- 47 Platten Limestone
- 48 Haupt Dolomite
- 49 Opponitz Formation
- 50 Lunz Sandstone

Juvavikum (Mürztal Nappe and Schneeberg Nappe)

- 52 Zlambach Formation
- 53 Zlambach Formation (Dark Banked Limestone)
- 54 Hallstatt Limestone of Salzberg Facies
- 57 Hallstatt Limestone at Nasswald
- 60 Waxeneck Limestone
- 65 Wetterstein Dolomite
- 66 Wetterstein Lagoonal Facies
- 67 Wetterstein Reef and Reef Debris Facies
- 68 Grafensteig Limestone
- 69 Volcanic Tuffite
- 72 Hallstatt Limestone
- 74 Steinalm Limestone
- 76 Gutenstein Limestone
- 77 Gutenstein Dolomite
- 79 Rauwacke
- 81 Werfen Formation
- 83 Carbonates of Unknown Stratigraphic Origin

Figure 8: Legend of the geological maps shown in Figure 7, 9 and 10. Modified from Mandl (2006).

As the three maps (Figure 7, 9 and 10) show, the rocks of the Schneeberg nappe are the most prominent lithologies on the Kuhschneeberg. Only towards the northern flanks lithologies of the Göller nappe are found. These include the Hauptdolomit and Opponitz Formation, as well as a succession of Jurassic sediments. At this height the vegetation and Holocene-Pleistocene sediments and debris already cover many parts of the Göller nappe. Therefore, the rocks of the Göller nappe are mostly found as roadside outcrops.
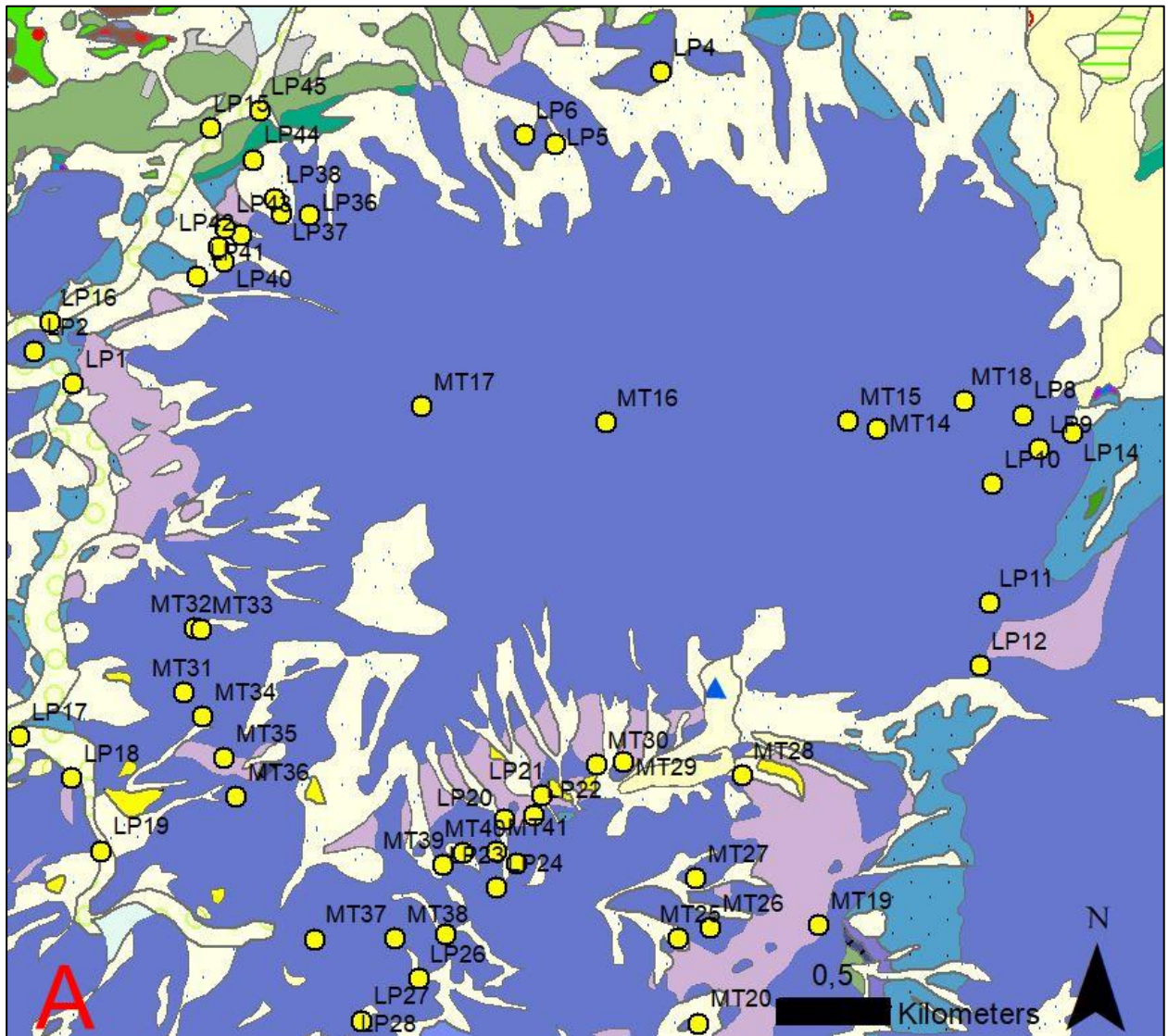
Figure 9: Locations of outcrops on the Kuhschneeberg (yellow circles) documented and sampled during this thesis. See Figure 7 for location of the map and Figure 8 for legend.

Cut-Out A and B (shown separately in Figure 9 and 10) were chosen to visualize different characteristics of the areas.

A (Figure 9) shows the lithologically homogeneous plateau of the Kuhschneeberg. The relatively low density of outcrops also is clearly recognizable in the central plateau, whereas outcrop densities are much more pronounced at the surrounding flanks. It must be mentioned tough, that these maps do not depict every outcrop of the shown areas. Towards the northern flanks, the Göller nappe is visible but mostly covered by slope debris and debris fans.

B (Figure 10) gives a clearer picture of the NE, where many outcrops were studied and some of the handpieces of the Göller nappe were collected. The rocks in this area are strongly differentiated with many different lithologies in a small space.
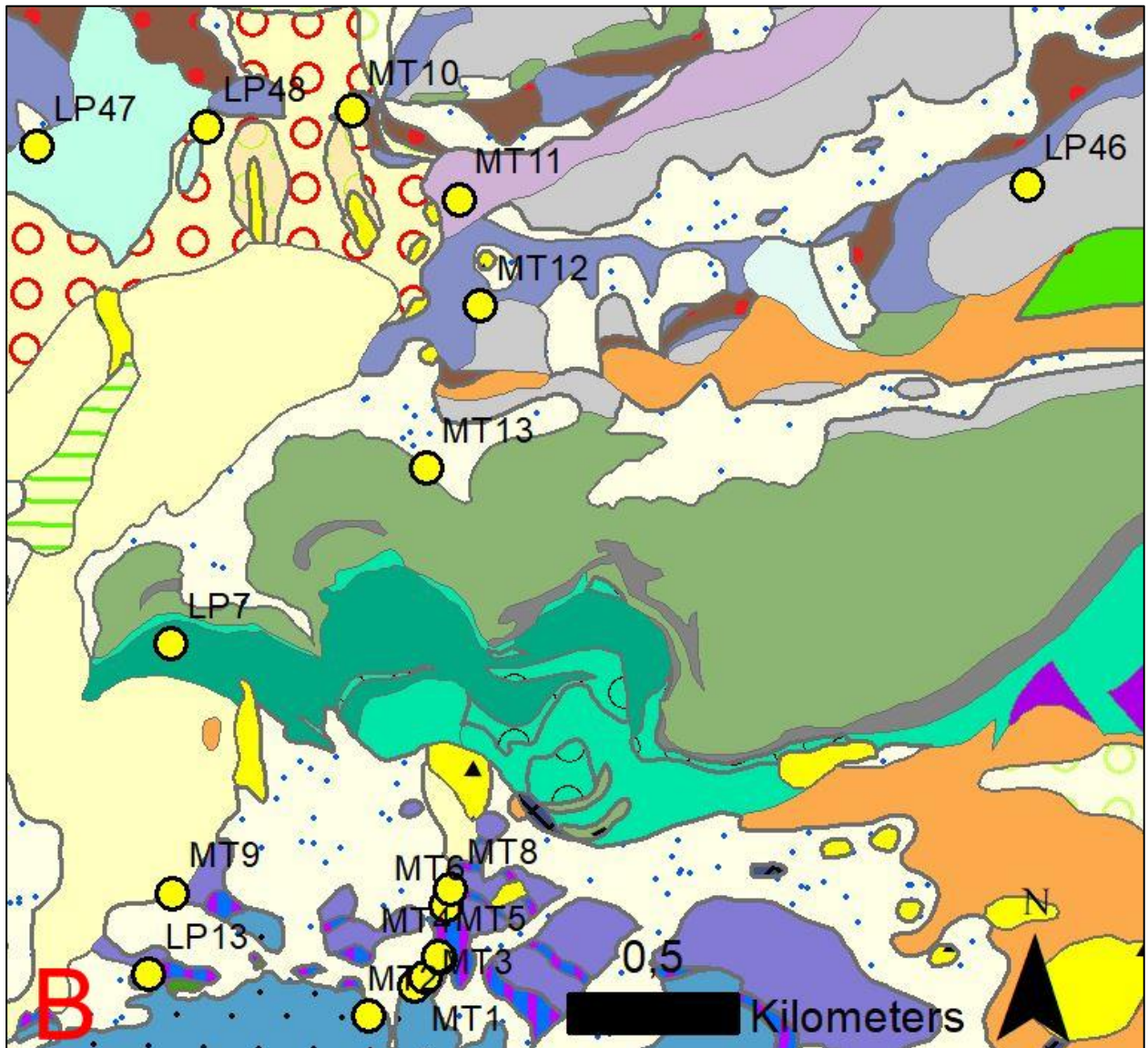
Figure 10: Locations of outcrops on the NE flanks of the Kuhschneeberg and northern flank of the Hochschneeberg (yellow circles). See Figure 7 for location of the map and Figure 8 for legend.

7.2 Samples from other authors

To increase the number of data, further samples were included in this thesis. From Wimmer (2020) multiple samples of Wetterstein limestones and dolomites were used. These samples mainly serve the purpose of increasing the sample size with comparable material. Their closeness to the Kaiserbrunn spring (Figure 1) and to the Kuhschneeberg itself makes them a useful addition to the data pool.

Most of the sample material was not drilled, so additional core plugs were manufactured for measurements with the Coreval 700. Over 30 core plugs were made from the material. Included Lithologies are Wetterstein dolomites, Wetterstein reef Limestones and Wetterstein lagoonal limestones. The lagoonal Wetterstein limestones do not occur on the mapped area on the Kuhschneeberg but are an interesting point of reference.

7.3 Outcrop Locations

Table 1: Location of the outcrops and Cataclasite Types and FDC of collected samples. This list also includes Wimmers (2020) samples. Outcrop numbers LP, PW and MT refer to Prandstätter (2022), Wimmer (2020) and this thesis, respectively.

Outcrop Coordinates MGI GK M34				
Outcrop	**E**	**N**	**Lithology**	**Sample FDC or Cataclasite Type**
LP1	705191	294440	Wetterstein reef debris limestone	-
LP2	705020	294585	Wetterstein reef debris limestone	1
LP3	704749	294579	Wetterstein reef limestone	-
LP4	707824	295775	Wetterstein reef limestone	-
LP5	707347	295467	Wetterstein dolomite	-
LP6	707212	295507	Wetterstein dolomite	-
LP7	710180	295422	Hornstein limestone	1
LP8	709399	294227	Wetterstein reef limestone	-
LP9	709468	294072	Wetterstein reef limestone	-
LP10	709260	293922	Wetterstein reef limestone	-
LP11	709236	293395	Karstified Wetterstein limestone*	1
LP12	709190	293117	Wetterstein dolomite	-
LP13	710100	294450	-	-
LP14	709618	294141	Wetterstein reef limestone	-
LP15	705818	295564	Dachstein limestone	-

LP16	705092	294714	Wetterstein reef limestone	-
LP17	704926	292882	Wetterstein reef limestone	-
LP18	705154	292691	Wetterstein reef limestone	-
LP19	705278	292366	Wetterstein reef limestone / Kar-stified Wetter-stein limestone	1, 2
LP20	707068	292475	Wetterstein reef limestone	-
LP21	707235	292578	Wetterstein reef limestone	-
LP22	707203	292492	Wetterstein reef limestone	-
LP23	707118	292280	Wetterstein reef limestone	-
LP24	707028	292174	Wetterstein reef limestone	-
LP25	706799	291970	Wetterstein reef limestone	-
LP26	706675	291774	Wetterstein reef limestone	-
LP27	706420	291593	Wetterstein reef limestone	-
LP28	706363	291471	Wetterstein reef limestone	-
LP29	706294	291422	Wetterstein reef limestone	-
LP30	707821	290292	Wetterstein reef limestone	-
LP31	707978	291019	Wetterstein reef limestone	-
LP32	707992	291068	Wetterstein reef limestone	-
LP33	708002	291093	Wetterstein reef limestone	-
LP34	708034	291143	Wetterstein reef limestone	-

LP35	708057	291156	Wetterstein reef limestone	-
LP36	706254	295167	Wetterstein reef limestone	1
LP37	706125	295179	Wetterstein reef limestone	-
LP38	706097	295242	Wetterstein reef limestone / Sty-lobreccia from a protolith of Wet-terstein reef limestone	-
LP39	705947	295085	Wetterstein reef limestone	-
LP40	705871	294971	Wetterstein reef limestone	-
LP41	705751	294907	Wetterstein reef limestone	1
LP42	705847	295032	Wetterstein reef limestone	-
LP43	705875	295115	Wetterstein reef limestone	2
LP44	706006	295419	Wetterstein do-lomite	-
LP45	706038	295637	Hornstein limes-tone	1
LP46	712735	296727	Haupt dolomite	1
LP47	709811	296894	Haupt dolomite	-
LP48	710316	296941	Opponitz limes-tone	1
MT1	710885	294397	Grafensteig li-mestone	-
MT2	710747	294315	Grafensteig li-mestone	-
MT3	710915	294423	Gutenstein li-mestone	-
MT4	710958	294479	Gutenstein li-mestone	-
MT5	710956	294487	Gutenstein li-mestone	-

MT6	710980	294634	Gutenstein limestone	-
MT7	710990	294658	Gutenstein limestone	-
MT8	710996	294682	Gutenstein limestone	-
MT9	710173	294686	Gutenstein limestone	-
MT10	710743	296985	Opponitz limestone	1
MT11	711055	296717	Wetterstein dolomite	-
MT12	711114	296404	Haupt dolomite	-
MT13	710945	295928	Haupt dolomite	-
MT14	708756	294177	Wetterstein reef limestone	-
MT15	708627	294216	Wetterstein reef limestone	-
MT16	707550	294229	Wetterstein reef limestone	-
MT17	706735	294311	Wetterstein reef debris limestone / Stylobreccia from a protolith of Wetterstein reef debris limestone	-
MT18	709144	294293	Wetterstein reef limestone	-
MT19	708455	291979	Wetterstein reef limestone	-
MT20	707913	291555	Wetterstein reef limestone	-
MT21	707452	291270	Wetterstein reef limestone	-
MT22	707224	291276	Wetterstein reef limestone	-
MT23	707181	291349	Wetterstein reef limestone	-
MT24	707253	291391	Wetterstein reef limestone	-

MT8 row: right margin note "28"

MT25	707831	291931	Wetterstein reef limestone	-
MT26	707976	291976	Wetterstein reef limestone	-
MT27	707914	292198	Wetterstein reef limestone	-
MT28	708127	292652	Wetterstein reef limestone	-
MT29	707604	292720	Wetterstein reef limestone	-
MT30	707481	292712	Wetterstein reef limestone	-
MT31	705659	293061	Wetterstein reef limestone	Cataclasite T-1
MT32	705712	293346	Wetterstein reef limestone	-
MT33	705738	293340	Wetterstein reef limestone	-
MT34	705739	292956	Wetterstein reef limestone	-
MT35	705831	292769	Wetterstein reef limestone	-
MT36	705880	292597	Wetterstein reef limestone	-
MT37	706216	291958	Wetterstein reef limestone	-
MT38	706574	291957	Wetterstein reef limestone	-
MT39	706796	292278	Wetterstein reef limestone	-
MT40	706885	292330	Wetterstein reef limestone	-
MT41	707029	292331	Wetterstein reef limestone	-
PW1	709564	288785	Wetterstein do-lomite	4
PW3	710117	288741	Wetterstein reef limestone	2, 3
PW4	710294	288712	Wetterstein reef limestone	2

PW5	701477	288687	Wetterstein reef limestone / Wetterstein cataclasite	1, 2, 3
PW6	710953	288820	Lagoonal Wetterstein limestone / Stylobreccia from a protolith of lagoonal Wetterstein limestone	1, 2, 3
PW7	709176	288751	Wetterstein dolomite / Wetterstein cataclasite	1, 2, Cataclasite Type 1 + 2
*LP11 is just a hand sample, not an outcrop				

8 Methods

8.1 Porosity

8.1.1 Porosity

Porosity is defined as "*the ratio of the volume of the pores to the total bulk volume of the media*" (Heinemann, 2005:6). The porosity can then be displayed as a fraction or percent.

Mathematically, the porosity can be expressed through V_T, V_p and V_s:

Equation 1:

$$V_T = V_p + V_s$$

V_T	Total volume of the medium
V_p	Volume of the pore space in V_T
V_s	Volume of the solid material in V_T

Table 2: Explanation of variables in Equation 1

The sum of V_p and V_s results in V_T.

Equation 2:

The definition of porosity can further be described in this Equation:

$$p = \frac{V_p}{V_T} = \frac{V_T - V_s}{V_T}$$

p	Porosity

Table 3: Explanation of variables in Equation 2

There are different terms for the classification of porosity. Important for fluid circulation is to distinguish between Total and Effective Porosity (Heinemann, 2005:7). Whereas the Total Porosity is equal to the porosity V_p in Equation 1, the Effective Porosity (also often

just called "Open Porosity") is only a part of the pore space´s volume: the pores, which are effective in the sense of fluid transport. A clear example of "ineffective pore spaces" are isolated pores, these are not connected to a pore system, which means they are not part of the circulation of fluids.

Porosity can also be subdivided into Primary and Secondary Porosity (Heinemann, 2005:12). The Primary Porosity includes the intragranular and intergranular porosities during the sediment´s deposition. After this, Secondary Porosity evolves through processes of diagenesis, dissolution, dolomitization, and fracturing. Intragranular (or also: intraparticular) as well as intergranular porosity can be abundant in carbonate rocks and is often mostly during the processes of secondary porosity (Heinemann, 2005:12).

There are further possibilities to address the process of pore development: fracture porosity, vuggy porosity, dissolution porosity, etc. (Heinemann, 2005:12-13, Grotzinger et al. 2008:468).

Important to note is the possibility of a strong influence of fracture porosity around the Kuhschneeberg. Although the intensity varies locally, the carbonates are often strongly fractured. The importance for hydrogeology is only given if these fractures are not filled with cement blocking the water flow and upholding the porosity (Heinemann, 2014:5), even possibly decreasing it. The carbonates´ Secondary Porosity is another crucial factor, as the carbonates make out large parts of the Kuhschneeberg. Secondary porosity forms, e.g., during diagenesis and dolomitization of limestone, and by carbonate dissolution during karstification. Porosity can be very diverse in carbonates, making it very difficult to name a range for porosities. Das & Mukherjee (2020:14) for example name 5-15 % as a range for older lithified carbonates.

However, unfractured porous material itself is permeable too, since most rocks have interconnected pores, providing permeability for fluid flow (Walsh & Brace, 1984:9425). Changes in the porosity also lead to a change in the transport properties of a rock (Hassanzadegan et al., 2013:421).

8.1.2 <u>Immersion Method</u>

With the Immersion method, it is possible to calculate the open porosity and the raw density (grain density) of rock samples. The basic concept of this method is the ÖNORM EN 1936 (2006) despite a minor difference: The water saturation in this experiment is not done under vacuum because this condition does not represent the natural environment

from which the samples are derived. As there are no strict upper limits for the volumes of the samples in this method, the collected samples are often multiple sizes of what they need to have for further methods. The reason for this is to try to minimize the effects of statistical anomalies in local pore space, the smaller the sample the more it is possible to get an unrepresentative result, not replicating the outcrop conditions, where the sample is taken from.

First, the samples are cleaned from any outer impurities, dirt, or plants. Subsequently, the samples are put into an oven and dried for 24 hours at 105 °C. The samples are weighted after drying. The process of drying for 24 hours is repeated afterward. If there is any sample with a weight derivative of more than 0,1% from the first weight measurement, then the drying process is repeated until mass consistency is reached.

The following step is the saturation of the samples in demineralized water for 24 hours and weighting of the saturated samples afterward in air and under buoyancy in water. For the air measurement of the wet rocks, any surface water is removed from the sample. The samples are again put underwater for 24 hours until mass consistency is reached (derivation of max. 0.1%).

The last step includes the weighting of the wet samples under submersion, where the measurements are again repeated every 24 hours until mass consistency is reached.

8.1.2.1 Calculation of porosity from the immersion method

Through the different weights of the samples (dry, wet, in water), it is possible to calculate the raw (grain) density and the sample´s open porosity.

Equation 3:

Raw (grain) Density:
$$\rho = \frac{(m_d * \rho_{H2O})}{(m_s - m_h)}$$

ρ	Raw (grain) density [g/cm³]
m_d	Mass of the dry sample [g]
m_h	Mass of the submerged sample [g]

m_s	Mass of the water-saturated sample [g]
ρ_{H2O}	Density of H$_2$O [g/cm^3]

Table 4: Explanation of variables in Equation 3

Equation 4:

Open Porosity:
$$p_0 = \left(\frac{m_s - m_d}{m_s - m_h}\right) * 100$$

p_0	Open porosity [%]

Table 5: Explanation of variables in Equation 4

8.1.2.2 Limits of the Immersion Method

The most significant advantage of this method is the simplicity and the relatively low cost. The only limit for the sample size is space and the scale´s weight limit. This paper, therefore, includes samples up to more than 7 kg. The bigger size of the samples helps to get a general understanding of the whole rock´s porosity and density, which might be more varied and deviant in smaller masses or thin sections. The size of the samples allows analysing volumes which are large enough to be representative for fractured rocks with fracture spacings of several centimetres. Negatives are the limits of sampling, as unstable rocks will not reach mass consistency due to the break-off of grains in this method and the relatively slow progress through the 24-hour time-windows. This makes some measurements impossible or difficult. During the weighing of the water-saturated samples, there is also a small fraction of water, which will instantly be lost from large pores, when the rock is removed from the water column and therefore not measured in the weighting process (see Figure 11).

Figure 11: Left: Simplified two-dimensional view of rock sample with round (dark grey) pores on the surface. Due to the inability to hold water after extraction of the sample out of the water column, larger pores volumes directly on the surface do not get measured. Right: Example of LP19/2.5 with a possible high influence of this effect on the measured porosity.

There is also no way to say anything about the rock´s total porosity using this method. Many small pores might not be filled with water, depending on their size, the connectivity of pores and the water surface tension.

8.1.3 Porosity Measurements with the Coreval 700 gas porosimeter

The Coreval 700 is an instrument developed by Vinci Technologies and enables the measurement of porosities and permeabilities of cylindrical rock samples (plugs). Information on the function, specifications, and theoretical background was given by Vinci Technologies and the Coreval 700 porosi- and permeameter manual.

The specifications of the Coreval 700 are following:

Permeability range:	1µD to 10D
Porosity range:	0.1 to 60%
Max pore pressure:	250 psi
Length:	0.5 to 3 inches

Diameter:	1.5 inch or 30 mm
Confining pressure:	400 psi to 10,000 psi
Temperature:	ambient
Temperature accuracy:	+/- 0.1 °C
Pressure transducer accuracy:	0.1% F.S.
Helium:	400 psi
Nitrogen:	500 psi
Air:	100 psi (dry)
Power:	110/220 VAC, 50/60 Hz

Table 6: Specifications of the Coreval 700 gas porosimeter and permeameter

The used model of the Coreval 700 during the paper´s creation is located at the "University Centrum Althanstraße" in Vienna. It is from the inventory of the Department for Geodynamics and Sedimentology.

8.1.3.1 General Description of the Coreval 700

Porosity and permeability measurements must be made with rock plugs, which are further described in the next chapter (8.1.3.2). The gas-phase used for the plugs in this thesis is N_2. It is possible to measure under different confining pressure conditions (400 psi *[pounds per square inch]* to 10,000 psi), which is practical to simulate pressure conditions of reservoir rocks in different depth and overburden.

There are different proceedings for the measurement of porosity and permeability. The porosity is measured with Boyle's and Charles' law technique. Other factors, which are also measured are the rock compressibility factor and the pore volumes under different pressures.

8.1.3.2 Preparation of rock samples:

To use the rock samples for the measurements, they must be drilled into plugs first. As the specifications state, the plugs must have a length between 0.5 and 3 inches and a diameter of 1.5 inches (38.1 mm).

The plugs need to have a flat surface orthogonal to the length of the plug, need to have ambient temperature, and be completely dry before they can be used in the Coreval 700. Therefore, they were dried in the oven for 24 hours and cooled to ambient temperature before they were used for measurements.

8.1.3.3 Theory behind the porosity measurements with the Coreval 700

The method used by the Coreval 700 is the *"Boyle's law Single Cell Method for direct void volume measurement"*, a recommended practice of the API (American-Petroleum-Institute). The Coreval 700 can measure porosities up to 60 %. A properly calibrated system can measure the porosity up to +/- 0.03 cm³ if the used plug is a perfect cylinder. Actual core samples deviate around +/- 0.1 cm³ for samples of 50 cm³ size.

Using a gas-charged reference cell (with initial pressure and reference volume) and a sample core holder, measurement through confining pressure is possible. The sample core holder utilizes additional end plugs to fill the volume and an elastomer sleeve.

The proceeding starts with the venting of gas (N_2 or He) into the sample´s pore volume with an isostatic confining pressure. In this thesis, only N_2 was used. The whole experiment happens under isothermal conditions.

Using the mathematical equation from the ideal gas law, we can describe the experiment´s initial and final conditions (Vinci Technologies, 2013).

Equation 5 (Ideal gas law):

$$PV = nRT$$

P	Pressure [Pa or N/m^2]
V	Volume [m^3]
n	Number of moles

R	Universal gas constant [J / Kmol]
T	Temperature [K]

Table 7: Explanation of variables in Equation 5

Equation 6 (State at initial conditions):

$$n_{total} = n_{N2} + n_{air}$$

Equation 7 (Initial conditions):

$$n_{total} = \frac{P_1 * (V_r + V_v)}{Z_{N_2} * RT} + \frac{P_a * (V_d + V_p)}{Z_{air} * RT}$$

n_{total}	Number of total moles
n_{N2}	Number of moles of helium
n_{air}	Number of moles of air
P_1	Initial pressure in valve and reservoir volume [Psi]
P_a	Initial pressure in dead and pore volume [Psi]
Z_{N2}	Compressibility factor of N2 at initial conditions
Z_{air}	Compressibility factor of air at initial conditions
V_r	Volume of reservoir [cm^3]
V_v	Volume of valve [cm^3]

V_d	Dead volume (rest of volume in the tubes) [cm^3]
V_p	Pore volume [cm^3]

Table 8: Explanation of variables in Equation 6 and 7

Equation 8 (Final conditions):

$$n_{total} = \frac{n_{N2}}{n_{total}} * \frac{P_2 * (V_r + V_v + V_d + V_p)}{Z_{N_2(2)} * RT} + \frac{n_{air}}{n_{total}} * \frac{P_2 * (V_r + V_v + V_d + V_p)}{Z_{air(2)} * RT}$$

P_2	final pressure in the whole volume [Psi]
$Z_{N2(2)}$	compressibility factor of N$_2$ at final conditions
$Z_{air(2)}$	compressibility factor of air at final conditions

Table 9: Explanation of variables in Equation 8

Equation 9:

Two assumptions can simplify the equation: P1 is much larger than Pa, and the number of moles of nitrogen is much larger than the number of moles of air.

$$P_1 \gg P_a, \; n_{N2} \gg n_{air}$$

Equation 10:

In conclusion:

$$\frac{n_{N2}}{n_{total}} \cong 1, \frac{n_{air}}{n_{total}} \cong 0$$

Equation 11:

Adding the simplifications of Equation 10 to Equation 8 the Equation for n_{total} reads:

$$n_{total} = \frac{n_{N2}}{n_{total}} * \frac{P_2 * (V_r + V_v + V_d + V_p)}{Z_{N2(2)} * RT} + \frac{n_{air}}{n_{total}} * \frac{P_z * (V_r + V_v + V_d + V_p)}{Z_{air(2)} * RT}$$

Equation 12:

$$n_{total} = 1 * \frac{P_2 * (V_r + V_v + V_d + V_p)}{Z_{N2(2)} * RT}$$

Equation 13:

$$n_{total} = \frac{P_2 * (V_r + V_v + V_d + V_p)}{Z_{N2(2)} * RT}$$

Equation 14:

Considering that the temperature is not changing in this experiment, deduction leads to:

$$Vp = \frac{V_r \left(\frac{P_1 * Z_{N_2(2)}}{P_2 * Z_{N_2(1)}} - 1 \right) - V_v}{1 - \frac{P_a * Z_{N_2(2)}}{P_2 * Z_{air}}} - V_d$$

Equation 15:

The result of the porosity is then obtained through:

$$\phi \ (\%) = 100 * Vp/BV$$

Equation 16:

$$BV = \left(\pi * \frac{D^2}{4} \right) * L$$

ϕ	porosity [%]	
BV	Apparent volume of the sample [cm^3]	
D	Diameter of the sample [mm]	
L	Length of the sample [mm]	

Table 10: Explanation of variables in Equation 15 and 16

Which Type of Porosity gets Measured?

Since the principles of this measurement are founded on the Boyle´s Law Single Cell, the method yields us the **effective porosity (open porosity)**. Depending on how much the N$_2$ can fills the pores of the sample, the value will differ. N$_2$ is not influenced much by the size of pore connections but it still cannot flow into completely isolated pore volumes.

8.1.3.4 Correction for High Confining Stress

With stresses of over 500 Psi, the reduction of the sample´s apparent volume can be a factor that needs to be considered (Vinci Technologies, 2013). We assume that the decrease in apparent volume is the same as the reduction in pore volume. In conclusion, this means the grain volume (GV) will be viewed as a constant, as changes in grain volume are insignificant relative to the change in pore volume.

The value of the grain volume is deducted from the porosity (ϕ), which first needs to be measured without applied confining pressure. From the measured value of porosity, the GV will be calculated.

Equation 17:

$$GV = BV - \phi$$

Equation 18:

Hence the correction for the reduction in pore volume reads:

$$\phi = V_p/(GV + V_p)$$

GV	Grain Volume [cm^3]
BV	Volume of the sample [cm³]
ϕ	Porosity [%]
V_p	Pore Volume [cm³]

Table 11: Explanation of variables in Equation 17 and 18

8.2 Analysis of thin-sections

12 circular slices from the top or bottom of drilled plugs were chosen to be cut into thin sections with 30 µm thickness. Thin sections are therefore oriented orthogonal to the length of the plugs. The following procedure includes treating of these samples with

"Fluorol Grüngold 084" (abbreviated as "Fluorol" in the following chapters), a fluorophore, to fill the pore space and open fractures of the rocks, which then are easily seen under UV-light during microscopic observation.
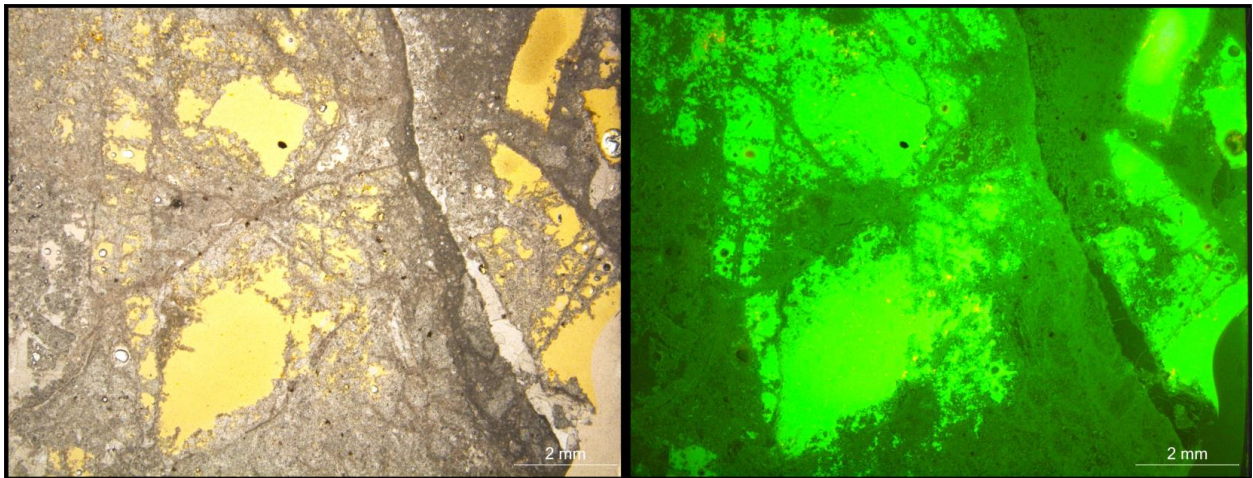
Figure 12: Thin-section of sample LP11 (Karstified Wetterstein Limestone), stained with Fluorol under normal transmit-ted light (left) and under UV-light (right). This example shows areas of strong light emission through the pore spaces.
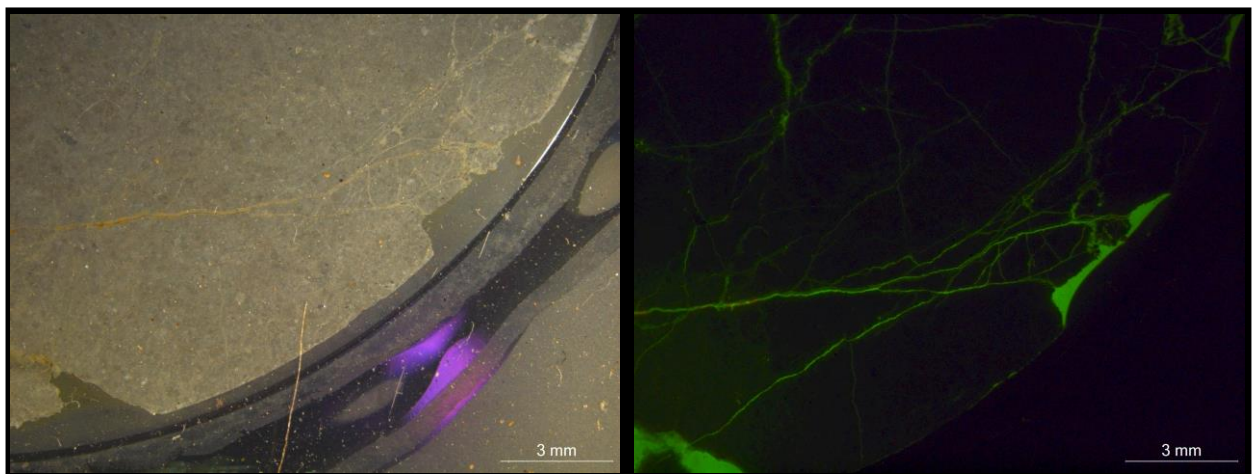
Figure 13: Thin section of sample PW1/6 (Wetterstein Dolomite) stained with Fluorol under normal transmitted light (left) and under UV-light (right). This sample has only minor light emission through small fractures. These fractures are not visible under normal light microscopy and can be clearly separated from filled fractures under UV-light.
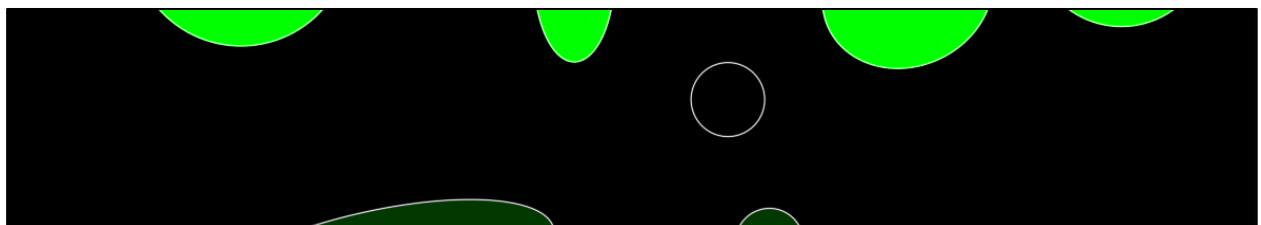
Figure 14: As visible in Fig. 12 and 13, there are different intensities of the fluorescent coloration. A weak fluorescent emission can mean different things. First, the pores could simply be extremely small and numerous in between solid material. The obtained effect is an area with a weaker coloration than areas with a large uninterrupted pore space. The other possibility is shown in this figure: Pores on the backside of the thin section (here on the bottom) are still saturated with Fluorol and can be visible through non-opaque materials. Pores in the middle of the thin section should not be visible, unless they are connected to other pore spaces, then they also emit lower-intensity light.

The percentage of pore spaces and the length of open microfractures are the results obtained from analysing the photos from the UV-microscope. In this thesis, the pores were determined through point-counting with a grid, containing at least 200 intersections over the sample space. Points of strong emission were counted as pore space, weakly emitting or non-emitting points were counted as solid space.

The pore space was determined through point counting (at least 200 points per sample), the length of cleavages was determined through tracing of the cleavages and measuring of their length and the area of the sample. AutoCAD was used for the determination of the pore spaces and the cleavage lengths.

8.3 Permeability

8.3.1 Permeability

The development of the following formula is based on Henry Darcy´s experiments in 1856 (Heinemann, 2005:39). Therefore, today´s formula is known as "Darcy´s law" and describes the laminar and steady-state on-phase flow through a porous medium. One condition being, that the fluid phase must be largely incompressible.
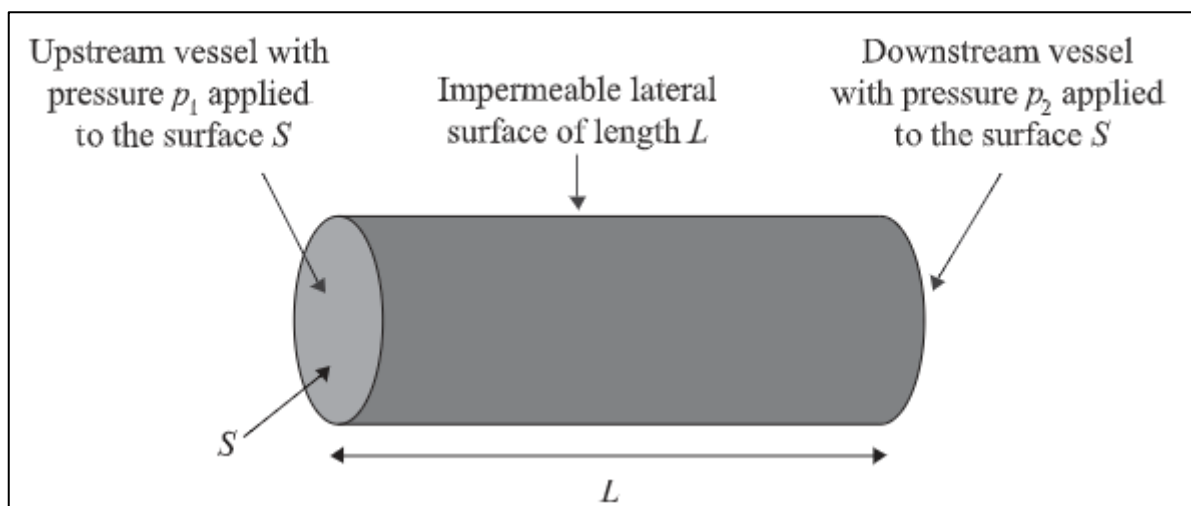
Figure 15: Visualization of the concept of permeability, similarly to Darcy´s experiment (from Adler et al., 2012:4).

Permeability is defined as *"The permeability of a porous media will be 1 [Darcy], if at a 1 [cm2] cross-section a fluid with 1 [cP] viscosity flowing with a rate of 1 [cm3/s] will cause a pressure drop of 1 [atm/cm]"* (Heinemann, 2005:40). This definition can also be written in SI-units, but it is arguable if the use of the SI-unit [m²] or Darcy makes more sense, as

the unit Darcy is commonly used in the scientific world. Common pore volumes of geologic materials are also in the range of a few microns. This thesis will use the Darcy-system for calculations because of its commonness and it´s fit to the common size of pores.

Equation 19:

$$k = \frac{\frac{\mu q}{A}}{\frac{\Delta P}{\Delta L}}$$

k	Permeability as the Material Property of the Porous Medium [Darcy]
ΔL	Length of the Medium in Direction of Flow [cm]
ΔP	Pressure Difference along the Length of the Porous Medium [atm]
μ	Viscosity of the Fluid [cp]
A	Cross-Section of the Porous Medium perpendicular to the Direction of Flow [cm^2]
q	Water Flow Rate [cm^3/s]

Table 12: Explanation of variables in Equation 19

In other words, permeability describes the ability of a porous medium to transmit fluids and gives us a way to describe it in numbers.

Equation 20:

Darcy is related to the SI-unit through this formula:

$$1 \, Darcy = 0.987 * 10^{-12} [m^2]$$

8.3.2 Permeability in Fractured Porous Media

The permeability of many rocks is often described through the characteristics of their "fracture network", a term which describes the rock as impervious, whereas the connected fractures between the solid material allow for permeability (Adler et al.,2012:3). However, rocks are more accurately to be described as "fractured porous media", since the rock itself has a porous matrix with its own permeability. Therefore, a fractured porous medium can be viewed as a composition of a porous medium with non-zero permeability and fractures (Adler et al., 2012:109) as seen in Figure 16.
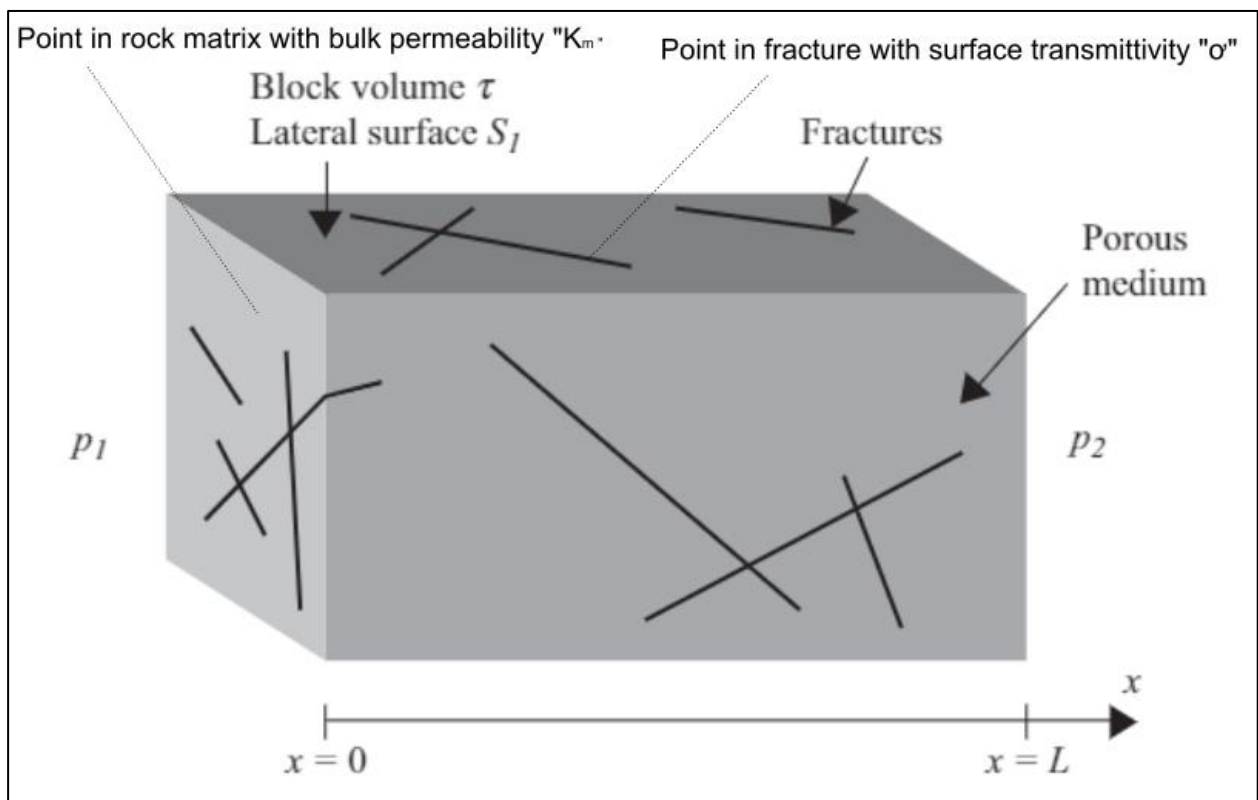
Figure 16: A permeability experiment with a fractured porous rock. Every point in the rock matrix can be assigned a bulk permeability Km and every point in the fractures can be assigned a surface transmittivity σ. Modified figure from Adler et al. (2012:112).

Although fractures are not the only pathway for flow of fluid phases, connected fractures can dominate flow patterns in different media (Berre et al., 2018:215ff). They can act as major conduits or barriers for fluid flow. Subsurface rocks themselves are, always fractured to some degree by tectonic deformation, if they are deformed in the brittle regime (Adler et al. 2012:1).

Fractures can result in an effective permeability, multiple magnitudes higher than the porosity does through connected pores (Berre et al., 2018:215ff). Even fractures with a thickness of 0.1 mm can reach extensions of a few m in the plane space, which enables fractures to build a connected "fracture network" over great distances (Adler et al. 2012:3).

FDC-Values

Some samples in the description of the rock samples are described with their FDC ("Fracture Density Class"). It is a way to describe the fracture densities of a rock in a semi-quantitative manner. This method was proposed by Decker (2007:72) and used in the works of Wimmer (2020), Bauer et al. (2016) and Bauer (2010). In different works, the fracture density classes differ in details of definition, so comparing data must be done carefully.

The samples in this thesis were classified in the FDC classes 1-4, as was done in Decker (2007).

In Detail, this means:

FDC 1 - Rock volumes with a maximum of three differently oriented fracture sets with an average spacing of more than 10 cm. This class correlates to P_{32}-values (fracture m² per m³ of rock volume) of 0-20 m²/m³.

FDC 2 – Rock volumes with 3 or more fracture sets of different orientation with average spacing of 5 to 10 cm. P_{32}-values of 20-60 m²/m³.

FDC 3 – Rock volumes with more than three fracture sets of different orientation with average spacing of 1 to 5 cm. P_{32}-values range from 60-200 m²/m³.

FDC 4 – Rock volumes with numerous fracture sets with spacings of 1 cm or less. P_{32}-values are >300 m²/m³.

If the fractures are filled with an impermeable material, like cements or clay, the permeability can

even decrease. This decreasing and increasing of permeability can also be dependent on direction if the fractures have a pattern (Berre et al., 2018:215ff.).

Although rocks are more accurately described as "Fractured porous media", proportion of fractures and pores can vary greatly, this can also have an influence on the permeability of these rocks over different pressure conditions (Fig. 17).
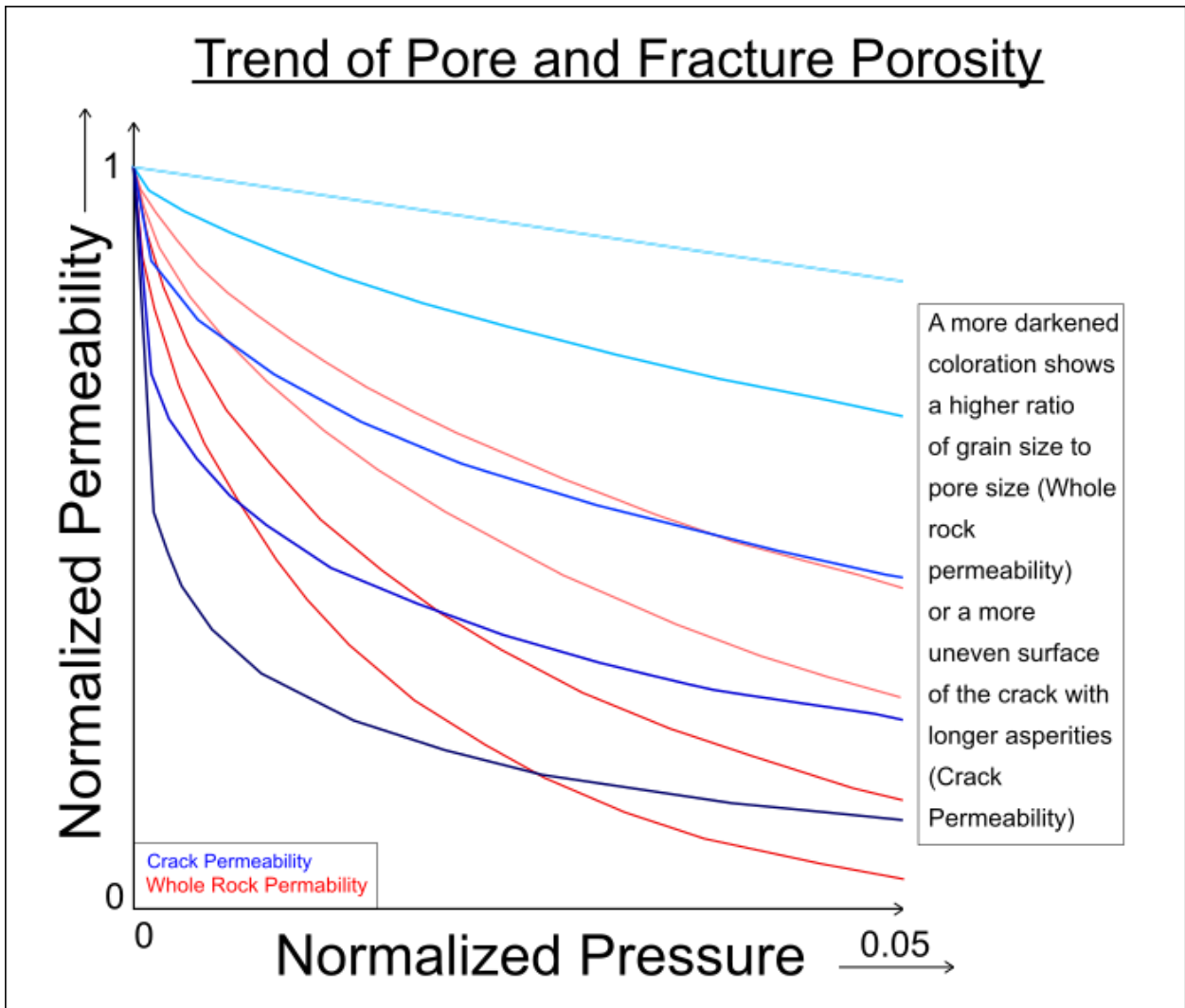
Figure 17: Theoretical change in permeability over different pressure conditions for a porous rock model and a fractured rock-model. This figure is a combined depiction of Figure 4. and 7 of Gangi (1978). The normalisation was made over the bulk modulus (Normalized Pressure) and the permeability at ambient pressure (Normalized Permeability). These models are for pure pore or fracture rocks, a real sample therefore normally would represent something in between these outcomes.

Fig. 17 shows, that rocks, which have more fractured than porous characteristics, potentially lose a lot of permeability in the first few hundred psi of pressure (since the bulk modulus of limestones and similar objects amounts to GPa). This only counts for "effective cracks", which in this case means cracks with relative uneven surface and longer asperities. The change in permeability is more gradual in samples with a more porous character. The more the grain size to pore size ratio is, the higher is the loss of permeability at any given confining pressure.

8.3.3 The Correlation of Permeability and Porosity

Many sediments tend to have higher permeabilities if the porosity is higher. This roughly linear correlation does not always apply for limestones since they are often more complex

(Heubeck, 2007:41f). Limestones often have large pores with small connections between them or big connected areas with almost no pore space (fracture porosity).

Different factors lead to this, from karstic developments and the reactivity of carbonate with fluids, high fracture porosity in many carbonates and complex pore shapes through the original lifeforms.

8.3.4 Permeability measurements with the Coreval 700 gas permeameter

The source for the theory behind the permeability measurements is information provided by Vinci Technologies and the manual of the Coreval 700 (Vinci Technologies, 2013). It is also noteworthy that the principles of the permeability measurements are based on Darcy´s law, therefore they have the same limitations: The upper limit of Darcy´s law is the point, where laminar flow changes into turbulent flow and the lower limit sets in, through adsorption effects of small pores in fine-grained clay sediments (Langguth & Voigt, 1980:40f).

The Coreval 700 device can measure a permeability range from 0.001 mD to 10 D. The prerequisites are the same for the permeability measurements with the Coreval 700: The samples must be drilled into plugs with pre-defined diameters, have a pre-defined range of length, have flat surfaces orthogonal to the length, and be cooled off to room temperature.

The technique behind the permeability is the use of Pressure-Falloff (API, 1998:148ff). This process is also referred to as the *"unsteady state pressure drop method"*. With this method, it is also possible to determine the equivalent liquid permeability, slip, and turbulence factors.

The experiment begins with filling of the upstream gas reservoir with a pressure to be chosen, whereas the downstream end of the sample is vented to atmospheric pressure. After a few seconds, where thermal equilibrium is reached, an outlet valve is opened, which lets gas flow out of the sample holder and ensures a transient pressure. At the exact moment, the gas pressure drops off to 85% of its initial value, the data collection starts. The change in pressure over time enables the determination of the permeability.

Even with an accounting of inertial effects, the permeability measurements are still dependent upon the "mean free path of the flowing gas", which describes the average dis-

tance of a moving particle between successive impacts/collisions, in this case, the particles of N_2. This phenomenon is known as "slip" and was described by Klinkenberg. It is an effect observable only in permeability measurements with gases. A correction is necessary to interpret permeability-data of gas or to compare it with fluid permeabilities.

The slip-phenomenon leads to a decrease in permeability with higher pore-pressures during measurement. The problem of this pressure dependency is addressed through the Klinkenberg permeability (Equation 21). It is an extrapolated method for permeability-measurements and equals the permeability obtained using a non-reactive liquid.

Equation 21:

Thus, the equation follows as described in Vinci Technologies (2013:18):

$$K_{g(x,t)} = K_1 * \left(\frac{1 + b}{P_{x,t} + P_a} \right)$$

K_1	Klinkenberg permeability [mD] = Liquid permeability K_L
Kg	Gas permeability [mD]
b	Slip factor (b>0) [Psi]<<
$P_{x,t}$	Pressure at position "x" at time "t" [Psi]
P_a	Air pressure [Psi]

Table 13: Explanation of variables in Equation 21

The slip-effect, described by Klinkenberg, is more easily recognizable at low Pressures. The K_g and K_1 values differ there more than at higher pressures.

The b-value itself is obtained through incremental and decremental trial-and-error calculations of the software.

After obtaining the uncorrected Gas permeability, the software calculates the Klinkenberg permeability as in Equation 22 (Vinci Technologies, 2013:21).

Equation 22:

$$Kg = K_1 * (\frac{1 + \frac{b_m * \mu_c}{\mu_m} * \sqrt{\frac{T_c * M_m}{T_m * M_c}}}{\frac{1}{2} * P_g * P_a})$$

Kg	Gas permeability [mD]
K_1	Klinkenberg permeability [mD]
b_m	Measured slip-factor [psi]
μ_c	Theoretical viscosity of gas [cP (centipoise)]
μ_m	Measured viscosity of gas [cP]
T_c	Theoretical temperature [°F]
T_m	Measured temperature [°F]
M_m	Measured molecular weight of gas [g/mol]
M_c	Theoretical molecular weight of gas [g/mol]
P_g	Geometrical mean pressure [psia (pounds per square inch absolute)]
P_a	Atmospheric pressure [psi]

Table 14: Explanation of variables in Equation 22

8.3.5 About the Importance of the Klinkenberg Correction at Low Pressures (400 Psi)

As mentioned in the previous sub-chapter of the permeability measurements with the Coreval 700, the Klinkenberg correction gives us another permeability-value, the Klinkenberg permeability. This permeability, often also known as "liquid permeability" differs strongly in its value to the gas permeability, especially at low pressures.

Primary interest in this paper is the Klinkenberg permeability, since water is the medium of focus around the Kuhschneeberg and the Klinkenberg correction gives us more fitting results (Tanikawa & Shimamoto, 2006:1315-1326).

8.3.6 About the limits of the maximum pressure at 6500 psi

As the volume of interest includes the whole of the Kuhschneeberg, from the top to the base, where the springs flow into the adjacent Voisbach and Schwarza. Assuming a lithology of mainly Wetterstein Reef Limestone, overburden pressures up to 20.000 psi could be expected for the lowest of lithologies in the area. However, much of the Kuhschneebergs volume is represented through the range of 0-6.500 psi, the Coreval 700 can measure. Additionally, most of the change in permeability and porosity already happens in the first 6500 psi, so there are no further findings to be expected with additional higher pressures.

8.3.7 <u>The Repeatability of Coreval Measurements</u>

Repeated measurements with the same core in the Coreval 700 lead to a loss of information, as seen in Fig. 18 and Fig. 19. Repeated measurements of four samples at confining pressure of 400, 1500 and 6500 psi show, that porosities and permeabilities are lower during the second measurement.

Permeabilities tend to change quite drastically during the second measurement cycle. The higher the permeability-value is during the first measurement, the more pronounced is the difference in the second cycle. The permeability values of "PW3/2" differ greatly on the second measurement cycle for all three psi-values (only 40.8 % percent of the initial value at 1500 psi), whereas the values of the low-permeability rock "PW7/2.2" almost don't change.

This trend also shows for the porosity measurements in Fig. 19. However, the percentual changes are smaller than those observed for permeability. Most of the second measurements still show more than 90% of the initial porosities of the first measurements.
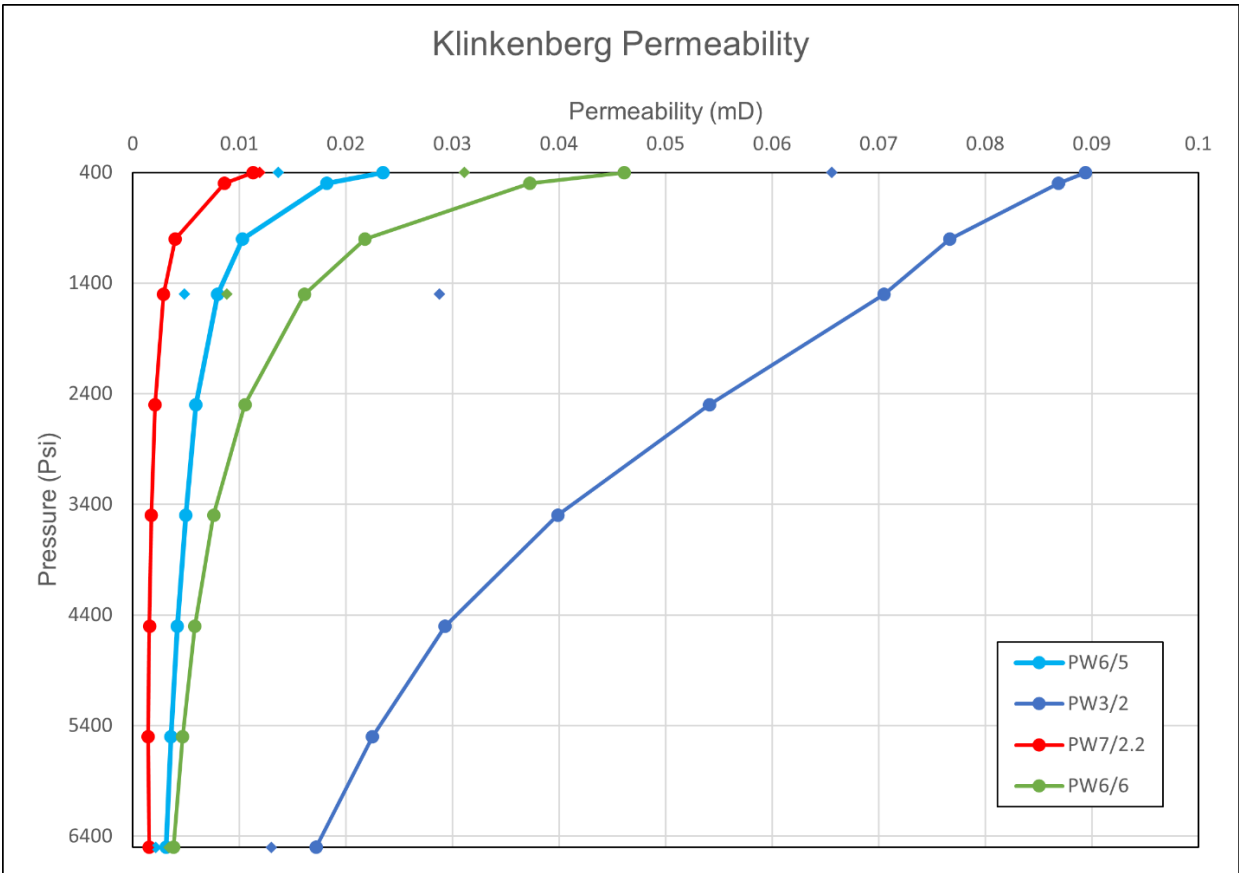
Figure 18: Repeatability of permeability measurements using the Coreval 700 permeameter. The dots connected by continuous lines indicate the initial measurements of 4 samples. The squares in corresponding colours show the change in permeability of each sample in the second measurement. The measurements for the second run were done at 400, 1500 and 6500 psi.
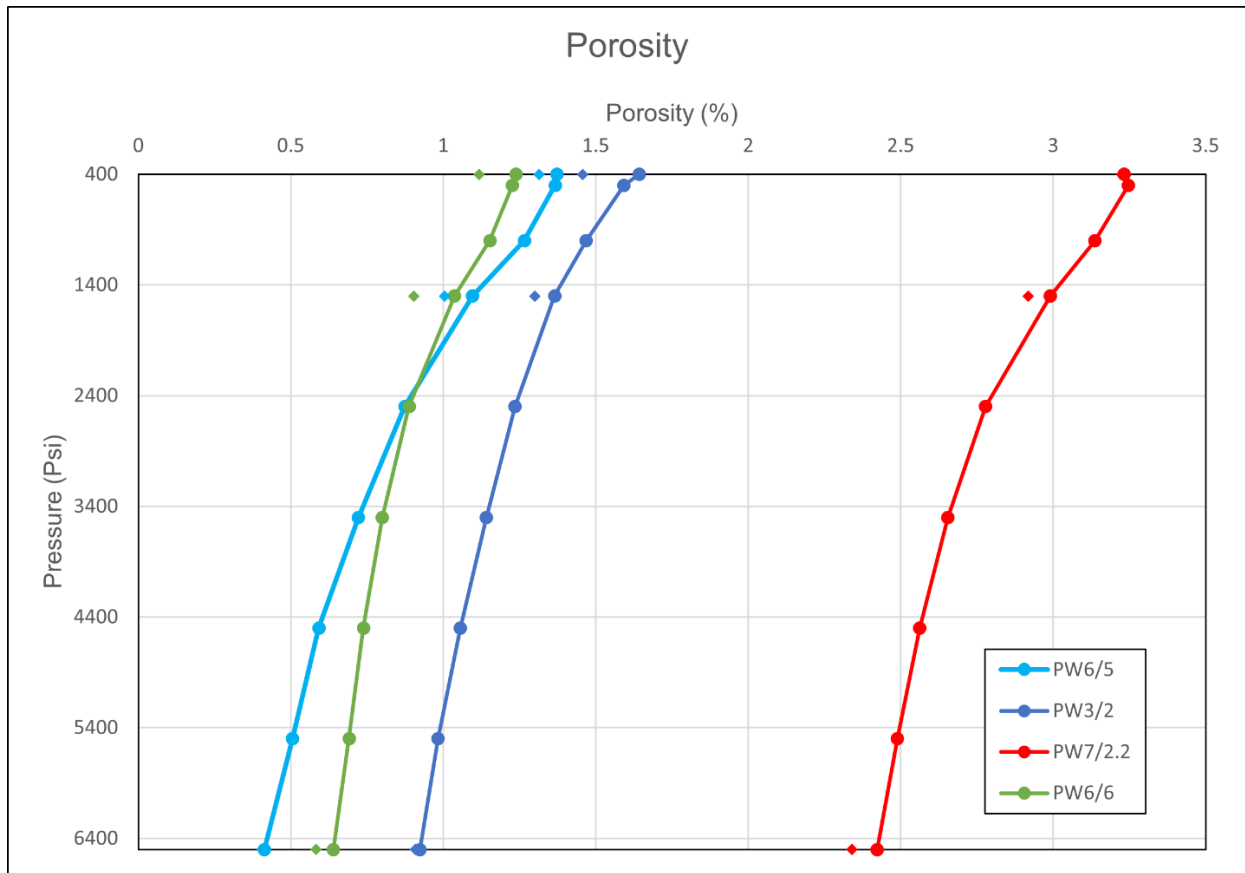
Figure 19: Repeatability of porosity measurements using the Coreval 700 porosimeter. The dots connected by continuous lines are the initial measurements of 4 samples. The squares in corresponding colours show the change in porosity of each sample in the second measurement. The measurements for the second run were done at 400, 1500 and 6500 psi.

9 Results

9.1 Results determined by the immersion method

The raw density and the open porosity of 109 samples were measured. 57 of these samples are handpieces from the Kuhschneeberg and surroundings, the other 52 samples are core plugs, made from the handpieces. The 22 of the handpieces collected during this thesis are described in the chapter "Data and Samples".

The rest of the 35 handpiece samples are Wetterstein carbonates, collected by Wimmer (2020). These results were added, because limestones and dolomites of the Wetterstein Formation build up most of the Kuhschneeberg and therefore supplement the data set from the two most important lithologies. The samples by Wimmer (2020) were collected in vicinity of the Kaiserbrunn spring. This spring is found in the Höllental, between Rax and Kuhschneeberg.

> **Separate Measurements of Handpieces and Core Plugs**
>
> Measuring the porosity and raw density values of both, the handpieces, and the core plugs, has two advantages:
>
> - First, it is possible to judge the amount of information lost, due to the inhomogeneities in rocks, when only analysing a small portion (the plug) out of the sample.
> - Second, it is possible to make a meaningful and direct comparison between the porosity derived from the Coreval 700 gas porosimeter and the immerged core plugs, since the samples (core plugs) are the same in both measurements.

Data results of this method are raw density and open porosity (effective porosity). The Open Porosity is already explained in the chapter "Porosity", whereas the raw density needs further explanation. This type of density does consider the grain volume and all pore volumes in the sample. Therefore, it says nothing about the grain density without knowledge about the porosities.

Fig. 20 shows the open porosities and raw densities of most handpieces, the karstified samples are found in Fig 27. Data ranges from 0.28 to 12.87% porosity and from 2.22 to 2.78 g/cm³ density. The arithmetic mean for the entirety of the handpiece samples is

2.36% (porosity) and 2.65 g/cm³ (density). Some lithologies form clusters, like the lagoonal Wetterstein limestone or Opponitz limestone samples, whereas others like the Wetterstein reef limestone are more dispersed.
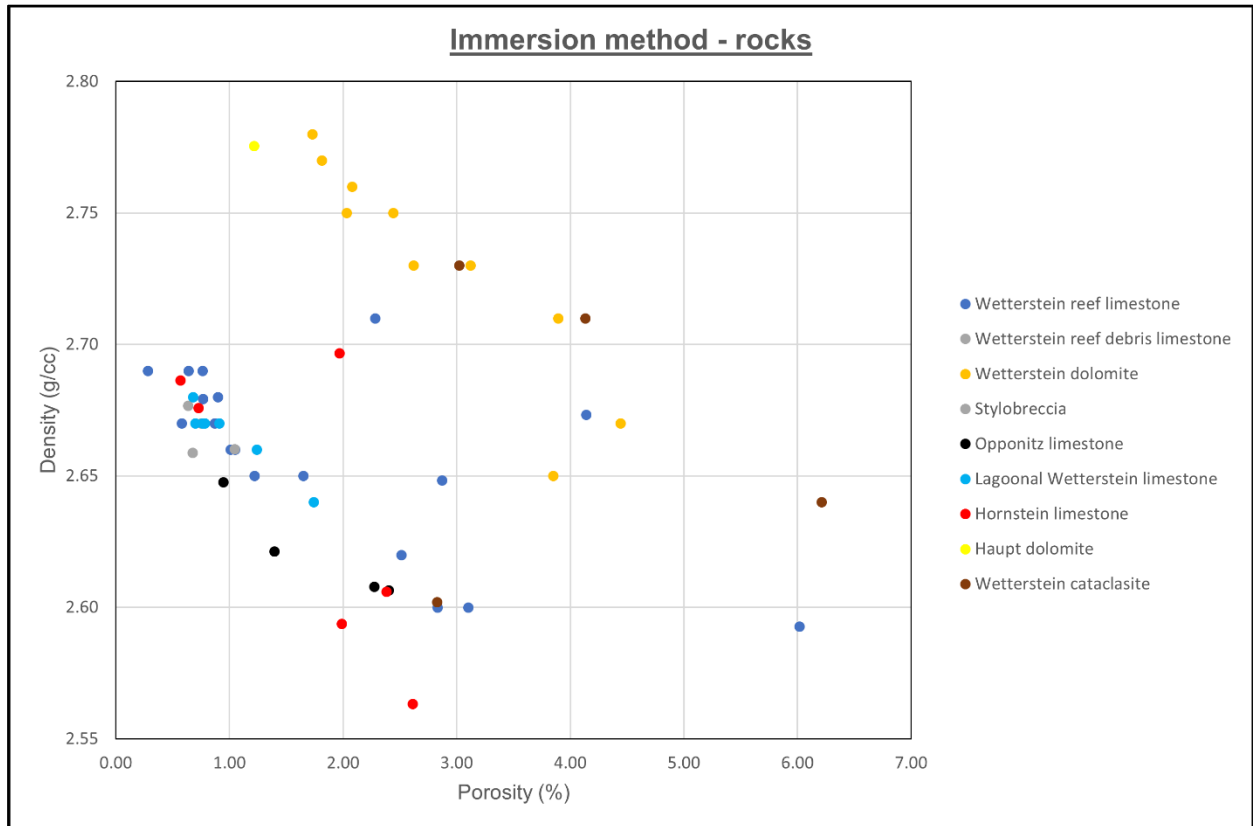
Figure 20: Cross plot of raw density (g/cm³) vs. porosity (%) obtained from handpieces by the immersion method. This figure does not include the data of the karstified Wetterstein samples, which are shown in Figure 27. Most of the lithologies tend to have low to medium densities (2.60-2.70 g/cm³) with porosities less than 3%.

The dataset in Fig. 20 shows two clusters, there is a division between the high-density samples of Wetterstein dolomite and Haupt dolomite relative to the limestone samples. The stylobreccia samples show similar densities as the unaltered limestone samples. The cataclasites are the most diverse group in terms of porosity and density and are found in both clusters. Another lithology, which does occur in both clusters is the Wetterstein reef limestone.

Since data about the FDC-values was also recorded, data was also categorized into the 4 FDC classes in Fig. 21. The idea behind this is, that if fractures have a high influence on the porosity/density, this must be seen in the data. The data of Fig. 21 does not indicate any correlation of FDC´s and porosity/density at this scale. Even when observing lithologies separated for each other, no correlation can be proven with this data. The Wetterstein limestones, for example, show decreasing porosity with higher FDC (FDC 1: 1.84%, FDC 2: 1.60%, FDC 3: 1.42 %).
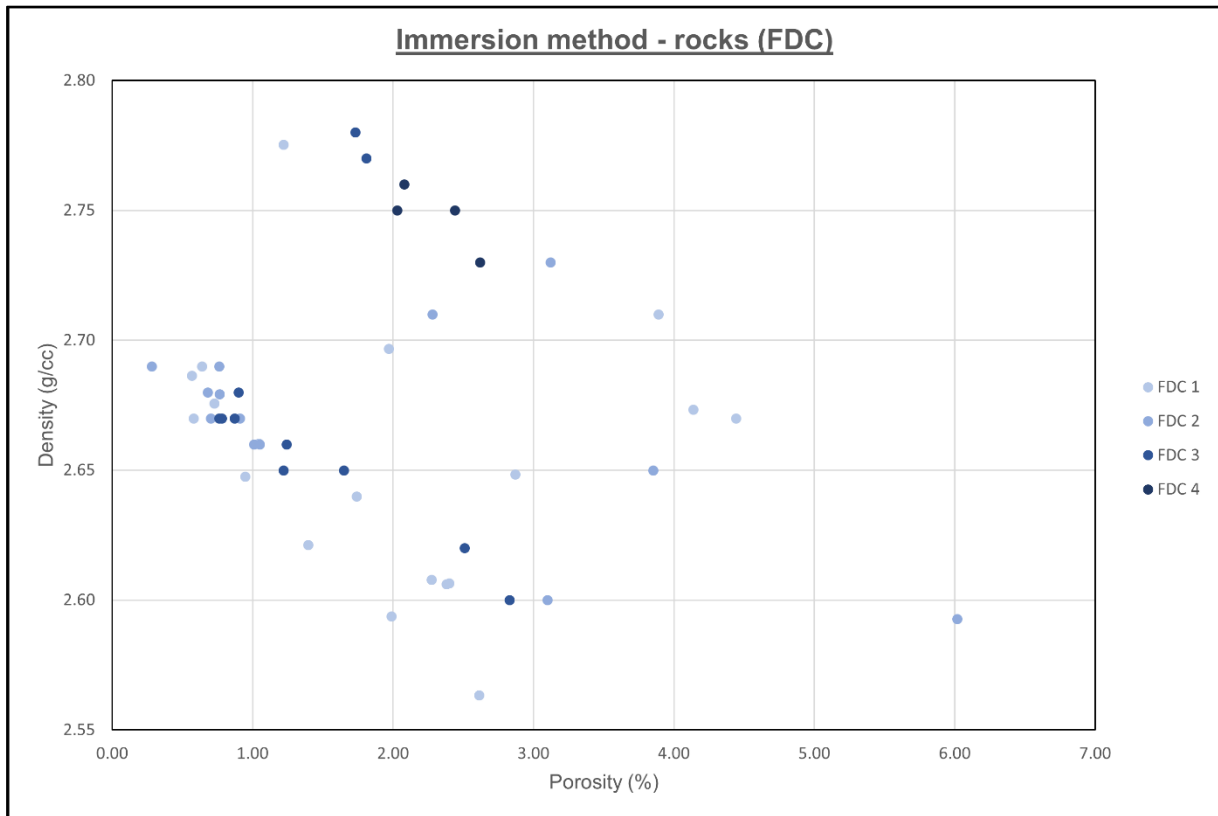
Figure 21: Results of the immersion data (FDCs of handpieces). No stylobreccia, karstified limestones, and cataclasites included.

The results of the porosities of the handpieces are also shown in Fig. 22, where the data of karstified Wetterstein limestones is included. The higher porosity of the karstified Wetterstein limestone is clearly visible, as well as the low porosity of stylobreccias, lagoonal Wetterstein limestones, Wetterstein reef debris limestone and Haupt dolomite.
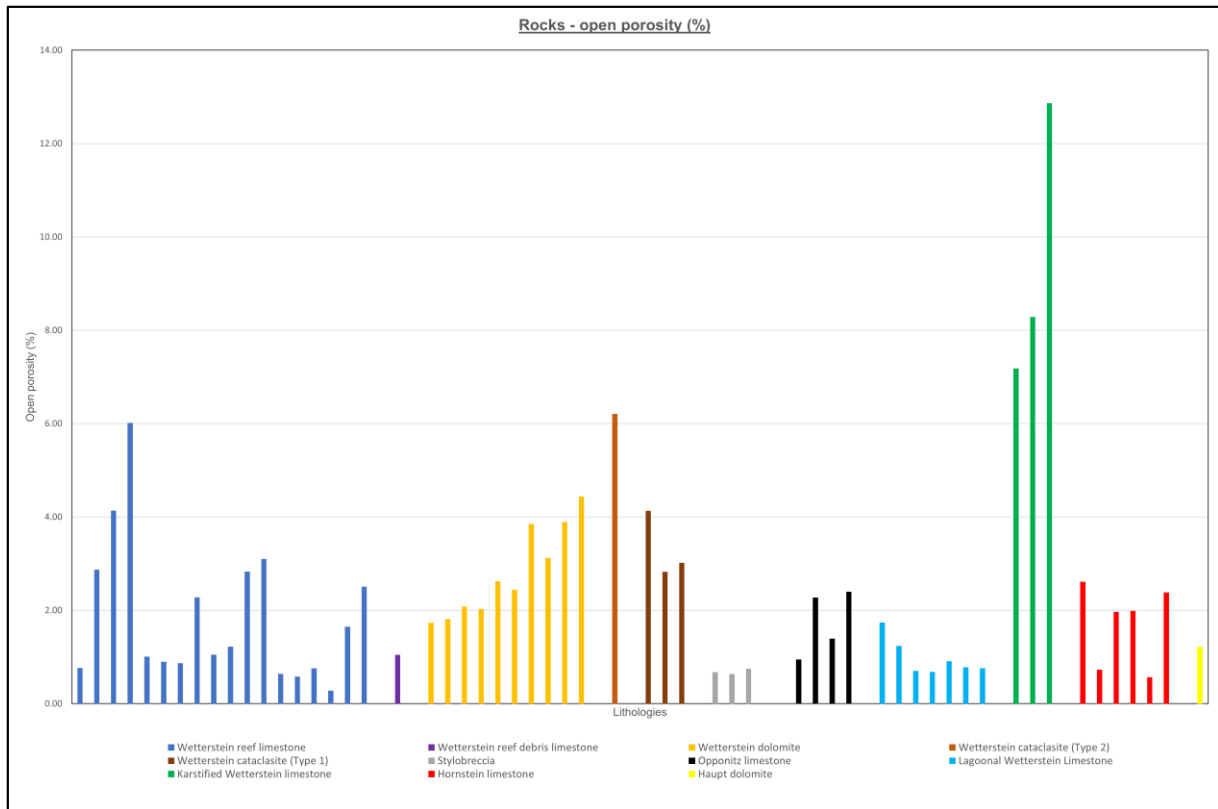
Figure 22: Results of the immersion data (handpieces). The samples are grouped into their different lithologies. The stylobreccias and cataclasites form their own entities.

The results of porosity measurements with the immersion method for core plugs are depicted in Fig. 23 and Fig. 24. Like before, samples from the karstified Wetterstein carbonates are shown in a separate figure (Figure 27).

Minimal and maximal values of the porosities lie between 0.36-9.06%, whereas the raw densities lie between 2.14-2.73 g/cc. The arithmetic mean of the porosity is 1.96 %, the density has a mean of 2.62 g/cc. Clustering is even more pronounced for the core plug samples (Fig. 23 and Fig. 24), both clusters are sharply separated from each other.

As the handpieces, the core plugs of Wetterstein reef limestone are found in both clusters. Another lithology, which happens to occur in both clusters in Fig. 23 is the Hornstein limestone.
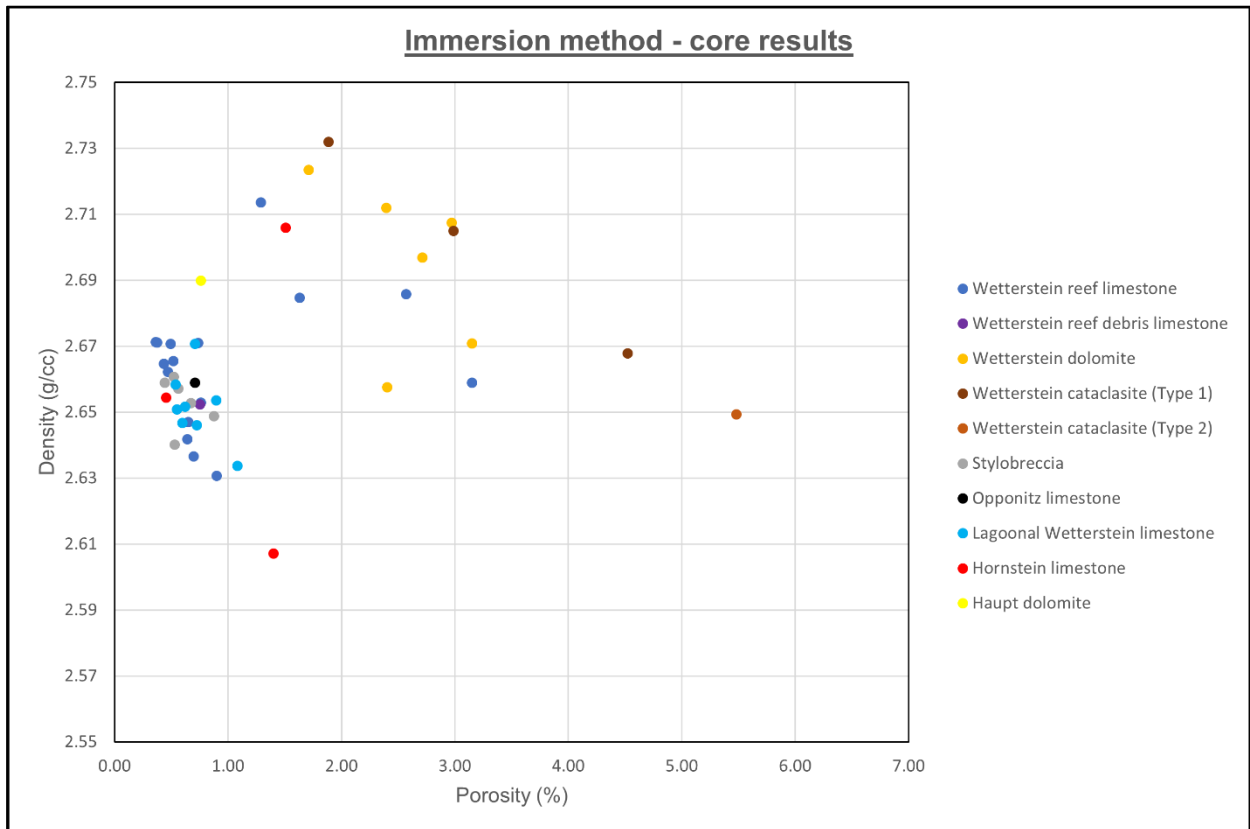
Figure 23: Cross plot of raw density (g/cm³) vs. porosity (%) obtained from core plugs by the immersion method. This figure does not include the data of the karstified samples from the Wetterstein Formation, they are shown separately in figure 27.

Again, the results were grouped into their fracture density classes and are shown in Figure 24. As with the handpieces, a clear correlation between porosity and FDC´s is not visible.
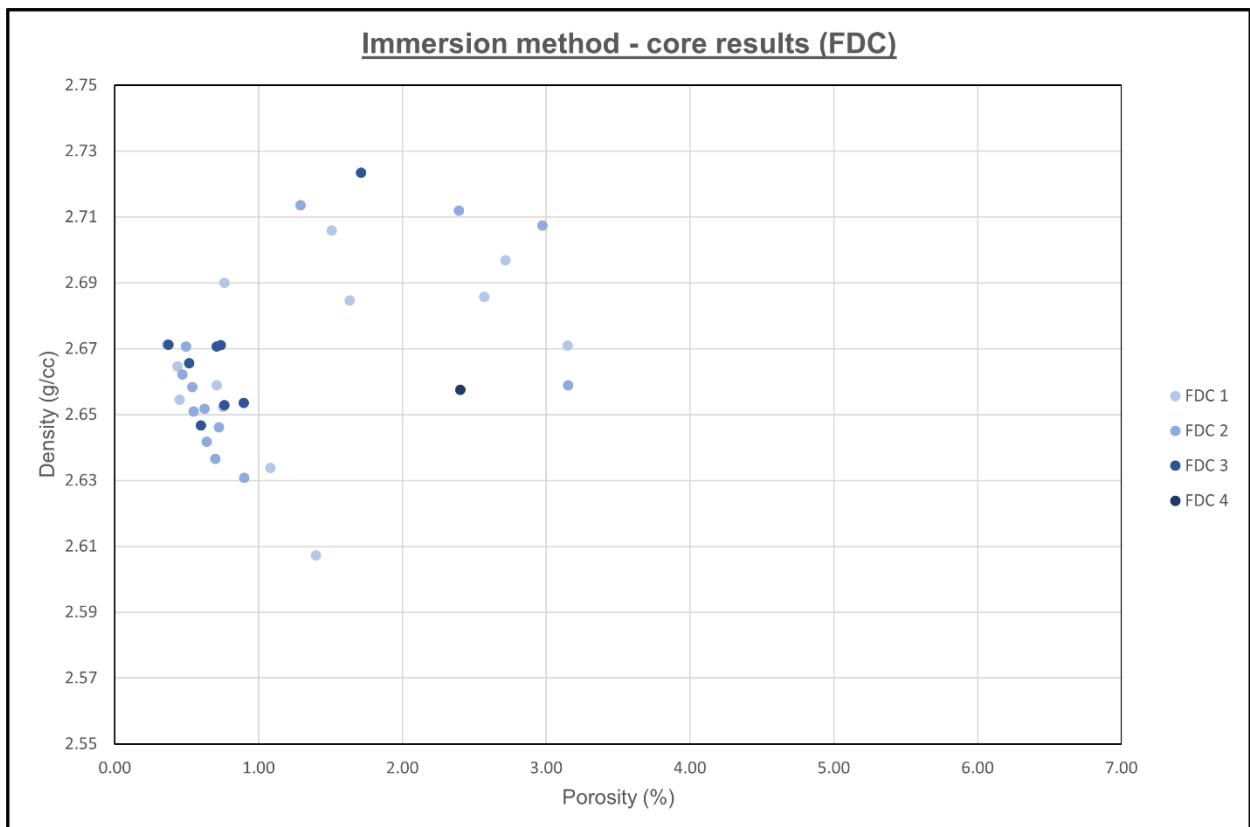
Figure 24: Results of the Immersion Data (FDCs of core plugs). No stylobreccia, karstified limestones, and cataclasites included.

The bar chart (Figure 25) shows the results of the porosity, including the karstified Wetterstein limestones. Values and homogeneity of these results greatly differs over the range of lithologies. The lithologies show the same similarities in their relative porosity to each other, as they do in Fig. 22.
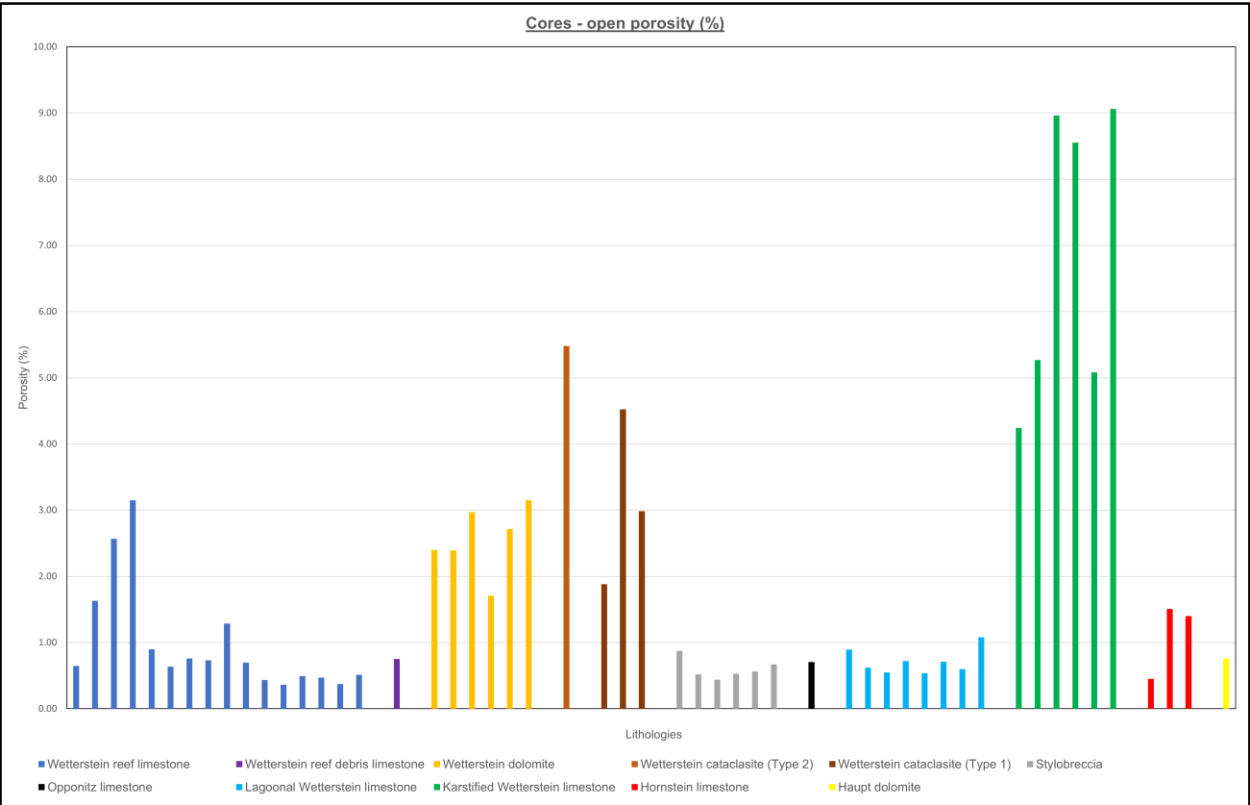
Figure 25: Results of the immersion data (core plugs). The samples are grouped into their different lithologies. The stylobreccias and cataclasites form their own entities.

Fig. 26 shows the FDC-values of all samples (except Stylobreccia and karstified limestones) and their porosities. The trendline shows, that the fracture density class does correlate to the sample porosity with this data set.
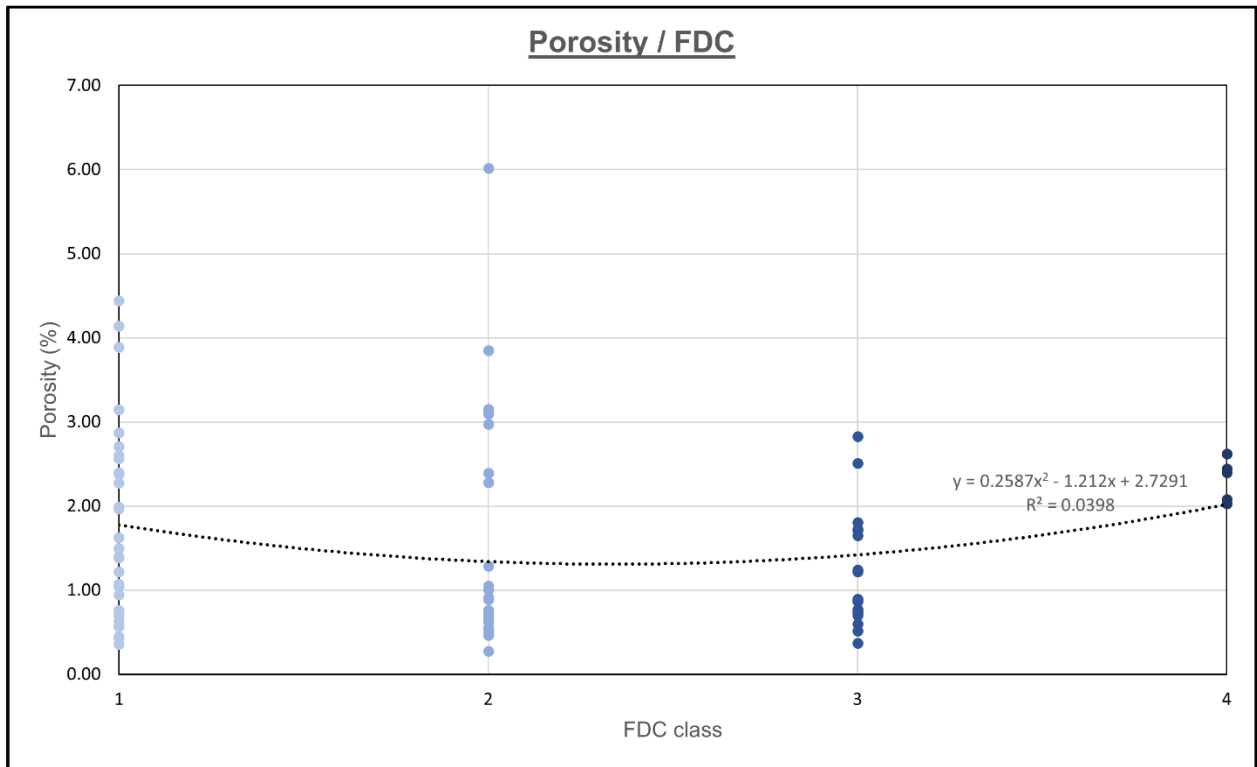
Figure 26: Porosity values of all samples (handpieces and plugs) with an assigned FDC.

Figure 27 depicts the immersion data results of the handpieces and the core plugs from the karstified Wetterstein limestones. 6 core plugs were drilled from 3 handpieces.
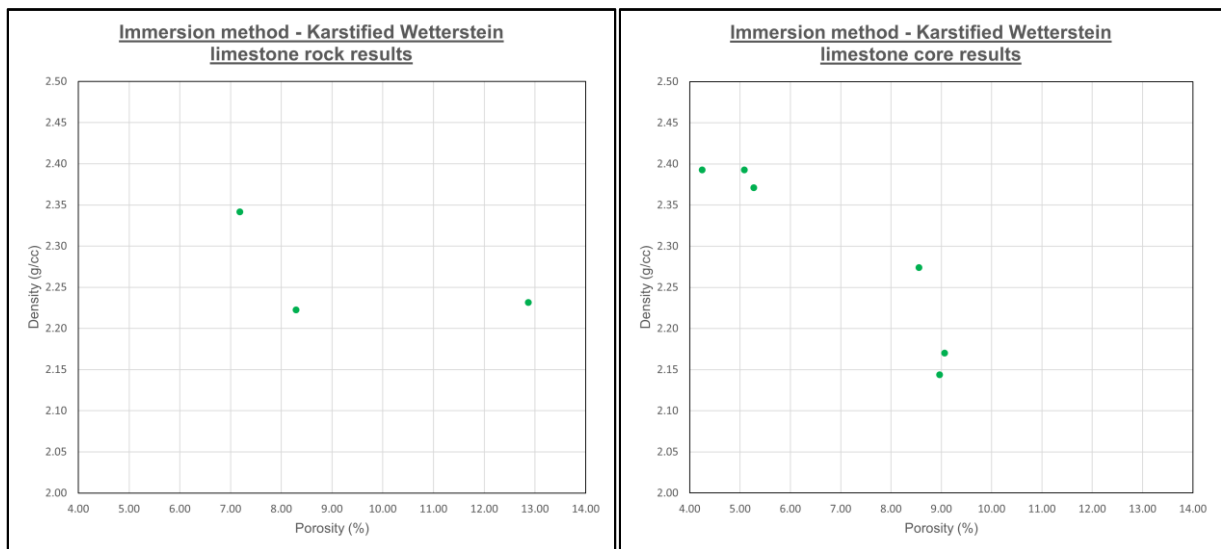
Figure 27: Results of the determination of raw density (g/cm³) and porosity (%) for karstified samples from the Wetterstein Formation (immersion method). Left: data from the handpieces; Right: data from core plugs.
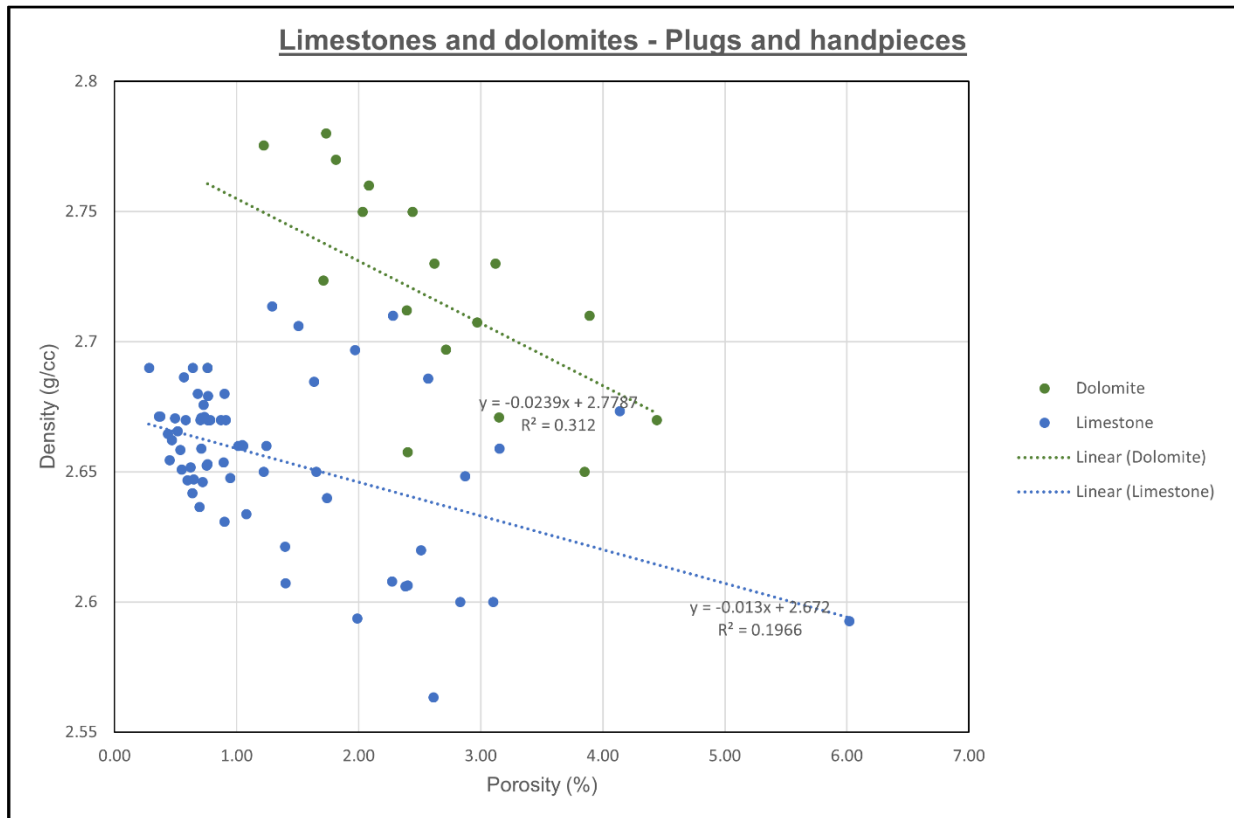
Figure 28: Results of the determination of raw density (g/cm³) and porosity (%) for the samples. Included are all cores and handpieces, except the Karstified Wetterstein samples – The samples are separated into dolomites and limestones. As the function of density to porosity is linear, trend lines are shown for the dolomites and limestones.

Fig. 28 shows all the samples, except the karstified Wetterstein limestones, separated into dolomites and limestones. The figure shows a relatively clear-cut separation, there is an observable difference in the density values between dolomites and limestones.

Table 15: Data of the immersion Method (hand pieces).

Sample	Lithology	Open po-rosity (%)	Raw density (g/cc)	FDC
LP11	Karstified Wetterstein limestone	7.18	2.34	1
LP19.1	Wetterstein reef limestone	0.76	2.68	2
LP19.2	Karstified Wetterstein limestone	8.29	2.22	1
LP19.3	Karstified Wetterstein limestone	12.87	2.23	1
LP2	Wetterstein reef debris limestone	1.04	2.66	1
LP36	Wetterstein reef limestone	2.87	2.65	1
LP38	Stylobreccia from a protolith of Wetterstein reef limestone	0.68	2.66	-
LP41	Wetterstein reef limestone	4.14	2.67	1
LP43	Wetterstein reef limestone	6.02	2.59	2
LP45	Hornstein limestone	2.61	2.56	1
LP46	Haupt dolomite	1.22	2.78	1
LP48.1	Opponitz limestone	0.94	2.65	1
LP48.2	Opponitz limestone	2.27	2.61	1
LP7.1	Hornstein limestone	0.73	2.68	1
LP7.2	Hornstein limestone	1.97	2.70	1
LP7.3	Hornstein limestone	1.99	2.59	1
LP7.4	Hornstein limestone	0.57	2.69	1
LP7.5	Hornstein limestone	2.38	2.61	1
MT10	Opponitz limestone	1.39	2.62	1
MT10.2	Opponitz limestone	2.40	2.61	1
MT17	Stylobreccia from a protolith of Wetterstein reef debris limestone	0.64	2.68	-
MT31	Cataclasite (Type 1) from a protolith of Wetterstein reef limestone	2.83	2.60	-
PW1/1	Wetterstein dolomite	1.73	2.78	3
PW1/2	Wetterstein dolomite	1.81	2.77	3
PW1/3	Wetterstein dolomite	2.08	2.76	4
PW1/4	Wetterstein dolomite	2.03	2.75	4
PW1/5	Wetterstein dolomite	2.62	2.73	4
PW1/6	Wetterstein dolomite	2.44	2.75	4
PW3/1	Wetterstein reef limestone	1.01	2.66	2
PW3/2	Wetterstein reef limestone	0.90	2.68	3
PW3/3	Wetterstein reef limestone	0.87	2.67	3
PW3/4	Wetterstein reef limestone	2.28	2.71	2
PW4/1	Wetterstein reef limestone	1.05	2.66	2
PW4/2	Wetterstein reef limestone	1.22	2.65	3
PW4/3	Wetterstein reef limestone	2.83	2.60	3
PW4/4	Wetterstein reef limestone	3.10	2.60	2
PW5/1	Wetterstein reef limestone	0.64	2.69	1
PW5/2	Wetterstein reef limestone	0.58	2.67	1
PW5/3	Wetterstein reef limestone	0.76	2.69	2
PW5/4	Wetterstein reef limestone	0.28	2.69	2
PW5/5	Wetterstein reef limestone	1.65	2.65	3
PW5/6	Wetterstein reef limestone	2.51	2.62	3
PW5/7	Cataclasite (Type 1) from a protolith of Wetterstein reef limestone	3.02	2.73	-
PW6/1	Lagoonal Wetterstein limestone	1.24	2.66	3
PW6/2	Lagoonal Wetterstein limestone	0.70	2.67	2

Sample	Lithology			
PW6/3	Lagoonal Wetterstein limestone	0.68	2.68	2
PW6/4	Lagoonal Wetterstein limestone	0.91	2.67	2
PW6/5	Lagoonal Wetterstein limestone	0.78	2.67	3
PW6/6	Lagoonal Wetterstein limestone	0.76	2.67	3
PW6/7	Stylobreccia from a protolith of lagoonal Wetterstein limestone	0.75	2.67	-
PW6/8	Lagoonal Wetterstein limestone	1.74	2.64	-
PW7/1	Wetterstein dolomite	3.85	2.65	2
PW7/2	Wetterstein dolomite	3.12	2.73	2
PW7/3	Cataclasite (Type 2) from a protolith of Wetterstein dolomite	6.21	2.64	-
PW7/4	Cataclasite (Type 1) from a protolith of Wetterstein dolomite	4.13	2.71	-
PW7/5	Wetterstein dolomite	3.89	2.71	1
PW7/6	Wetterstein dolomite	4.44	2.67	1

Table 16: Data of the immersion method (core plugs).

Sample	Lithology	Open porosity (%)	Raw density (g/cc)	FDC
LP11	Karstified Wetterstein limestone	4.24	2.39	1
LP19.1_2	Wetterstein reef limestone	0.65	2.65	2
LP19.2_1	Karstified Wetterstein limestone	5.27	2.37	1
LP19.2_2	Karstified Wetterstein limestone	8.96	2.14	1
LP19.2_3	Karstified Wetterstein limestone	8.55	2.27	1
LP19.2_4	Karstified Wetterstein limestone	5.08	2.39	1
LP19.2_5	Karstified Wetterstein limestone	9.06	2.17	1
LP2	Wetterstein reef debris limestone	0.75	2.65	1
LP36	Wetterstein reef limestone	1.63	2.68	1
LP38	Stylobreccia from a protolith of Wetterstein reef limestone	0.87	2.65	-
LP41	Wetterstein reef limestone	2.57	2.69	1
LP43	Wetterstein reef limestone	3.15	2.66	2
LP46	Haupt dolomite	0.76	2.69	1
LP48.2	Opponitz limestone	0.71	2.66	1
LP7.1	Hornstein limestone	0.45	2.65	1
LP7.2	Hornstein limestone	1.51	2.71	1
LP7.3	Hornstein limestone	1.40	2.61	1
MT17.1	Stylobreccia from a protolith of Wetterstein reef debris limestone	0.52	2.66	-
MT17.2	Stylobreccia from a protolith of Wetterstein reef debris limestone	0.44	2.66	-
MT17.3	Stylobreccia from a protolith of Wetterstein reef debris limestone	0.53	2.64	-
PW1/6	Wetterstein dolomite	2.40	2.66	4
PW3/1_1	Wetterstein reef limestone	0.90	2.63	2
PW3/1_2	Wetterstein reef limestone	0.64	2.64	2
PW3/2	Wetterstein reef limestone	0.76	2.65	3
PW3/3	Wetterstein reef limestone	0.73	2.67	3
PW3/4	Wetterstein reef limestone	1.29	2.71	2
PW4/4	Wetterstein reef limestone	0.70	2.64	2
PW5/1_1	Wetterstein reef limestone	0.43	2.66	1

PW5/1_2	Wetterstein reef limestone	0.36	2.67	1
PW5/3	Wetterstein reef limestone	0.49	2.67	2
PW5/4	Wetterstein reef limestone	0.47	2.66	2
PW5/5	Wetterstein reef limestone	0.37	2.67	3
PW5/6	Wetterstein reef limestone	0.51	2.67	3
PW5/7	Cataclasite (Type 1) from a protolith of the Wetterstein reef limestone	1.88	2.73	-
PW6/1	Lagoonal Wetterstein limestone	0.89	2.65	3
PW6/2	Lagoonal Wetterstein limestone	0.62	2.65	2
PW6/3_1	Lagoonal Wetterstein limestone	0.55	2.65	2
PW6/3_2	Lagoonal Wetterstein limestone	0.72	2.65	2
PW6/4	Lagoonal Wetterstein limestone	0.54	2.66	2
PW6/5	Lagoonal Wetterstein limestone	0.71	2.67	3
PW6/6	Lagoonal Wetterstein limestone	0.60	2.65	3
PW6/7_1	Stylobreccia from a protolith of lagoonal Wetterstein limestone	0.56	2.66	-
PW6/7_2	Stylobreccia from a protolith of lagoonal Wetterstein limestone	0.67	2.65	-
PW6/8	Lagoonal Wetterstein limestone	1.08	2.63	1
PW7/1	Wetterstein dolomite	2.39	2.71	2
PW7/2	Wetterstein dolomite	2.97	2.71	2
PW7/2.2	Wetterstein dolomite	1.71	2.72	3
PW7/3_1	Cataclasite (Type 1) from a protolith of the Wetterstein dolomite	4.52	2.67	-
PW7/3_2	Cataclasite (Type 2) from a protolith of the Wetterstein dolomite	5.48	2.65	-
PW7/4	Cataclasite (Type 1) from a protolith of the Wetterstein dolomite	2.99	2.71	-
PW7/5	Wetterstein dolomite	2.71	2.70	1
PW7/6	Wetterstein dolomite	3.15	2.67	1

9.2 Results of the Coreval 700 measurements

Data about the gas permeability, the Klinkenberg permeability, the slip factor, the inertial coefficient, the turbulence factor, the confining pressure, the pore volume at confining pressure and ambient pressure, the porosity at confining pressure and ambient pressure, the grain density at confining pressure and the raw density (which incorporates the pore volume) at confining pressure is collected during measurements with the Coreval. Although the term is different, the raw density is ident to the raw density, therefore the two terms are to be understood synonymously in this thesis. The most important data points are shown here, full tables with results are found in the appendix. The values for the confining pressures (400, 500, 1000, 1500, 2500, 3500, 4500, 5500, 6500 psi) are fixed for better comparison between the samples. The range of values provides a more detailed insight into the first two-thousand psi, were porosities and permeabilities change fast and ends at 6500 psi, were there is far less change in porosity and permeability.

9.2.1 **Klinkenberg-Permeabilities:**

The Klinkenberg permeabilities ("corrected gas permeability") derived from 47 samples are shown in figures 29 to 32. Figure 29-31 concentrate on the samples from the Wetterstein Formation (lagoonal, reef, and dolomite facies) and Fig. 32 shows the results obtained from samples of the other lithostratigraphic units. Each of the figures also shows the "fitted means" of other lithology measurements at the minimal and maximal measured confined pressures (400 psi and 6500 psi). These fitted means exclude permeabilities over 1 mD (in other words: especially high permeabilities).

The Wetterstein samples of Fig 29-31 (lagoonal, reef and dolomite facies) all include high- and low-permeability results and different slopes of the declining curves from the initial permeability at 400 psi confining pressure. Looking at the fitted means of the low-permeability samples (<1 mD Klinkenberg permeability) shows us, that the dolomite samples have the lowest permeability and the lagoonal facies the highest permeability.

The samples of Fig. 29-31 with permeabilities higher than 1 mD at 400 psi confining pressure all showed fractures in macroscopic observation. At least one of these fractures in each of these samples runs along the stream current (meaning from top to bottom) of the measurements.
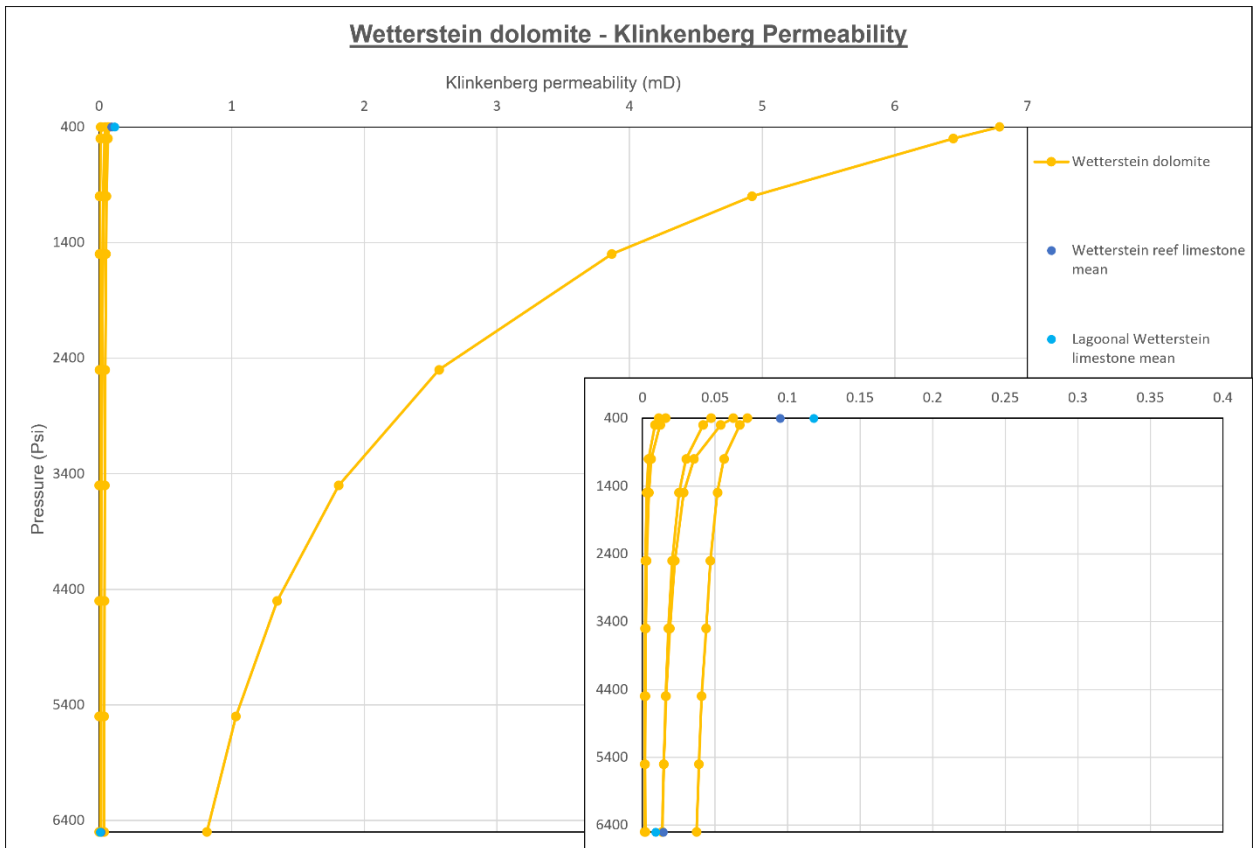
Figure 29: Permeability (Klinkenberg, mD) data from dolomites of the Wetterstein Formation (6 core plugs). The smaller graph is zoomed in on the smaller values on the x-axis.
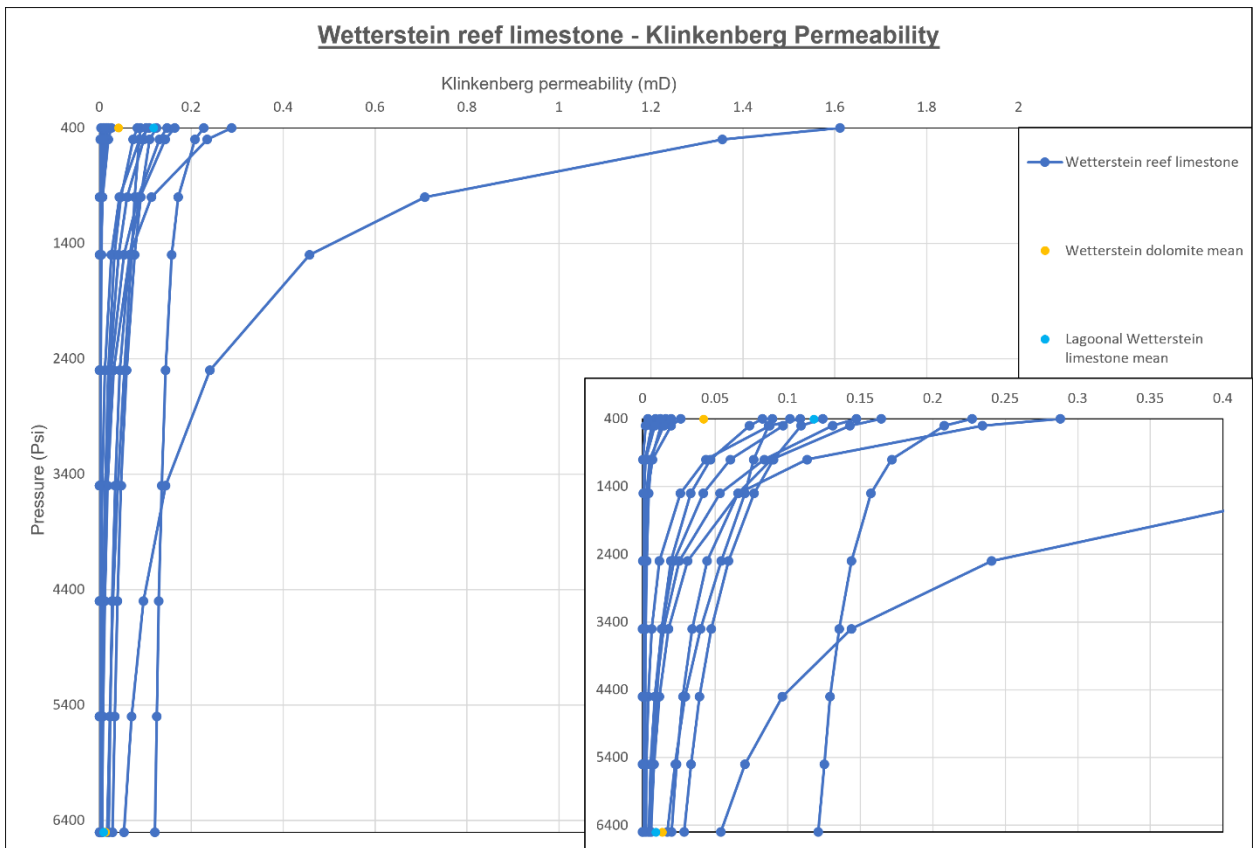
Figure 30: Permeability (Klinkenberg, mD) data from reef limestones of the Wetterstein Formation (16 core plugs). The smaller graph is zoomed in on the smaller values on the x-axis.
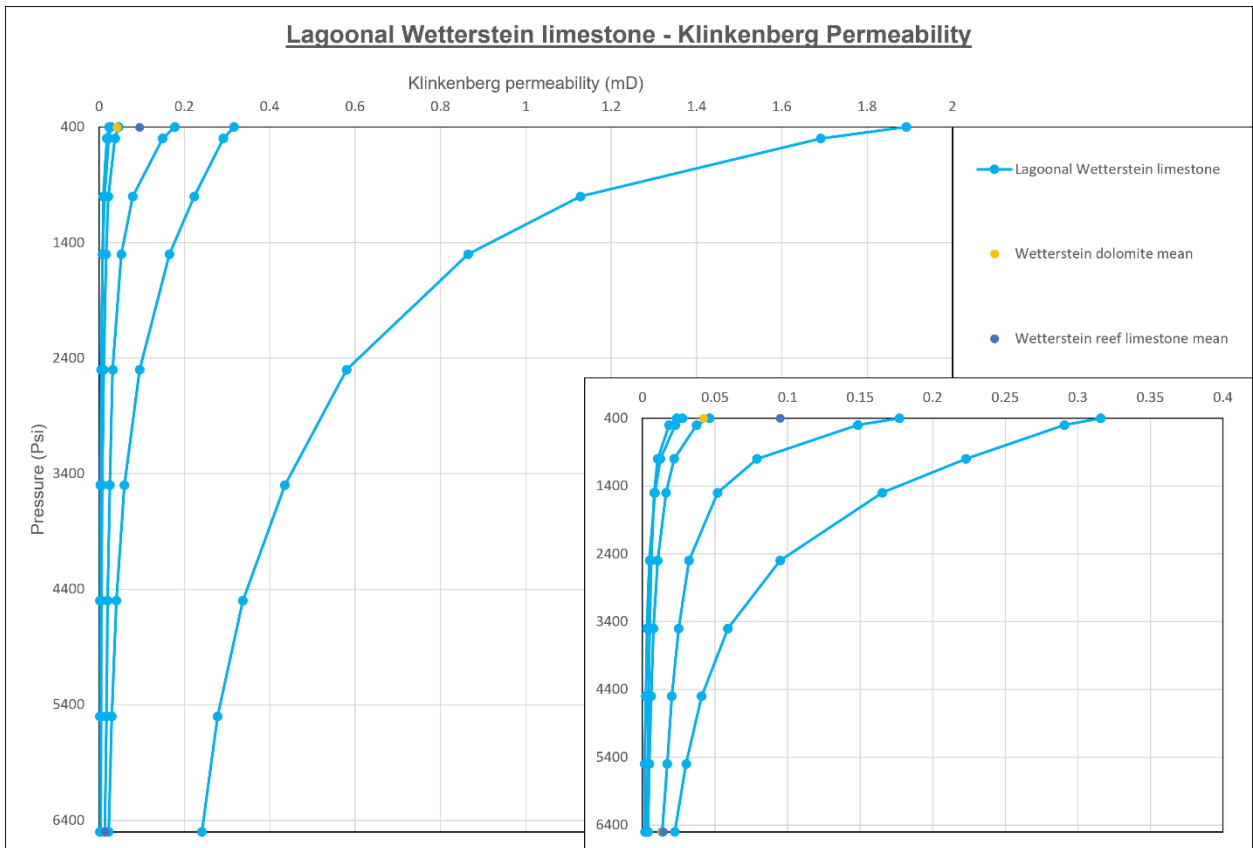
Figure 31: Permeability (Klinkenberg, mD) data from lagoonal limestones of the Wetterstein Formation (6 core plugs). The smaller graph is zoomed in on the smaller values on the x-axis.
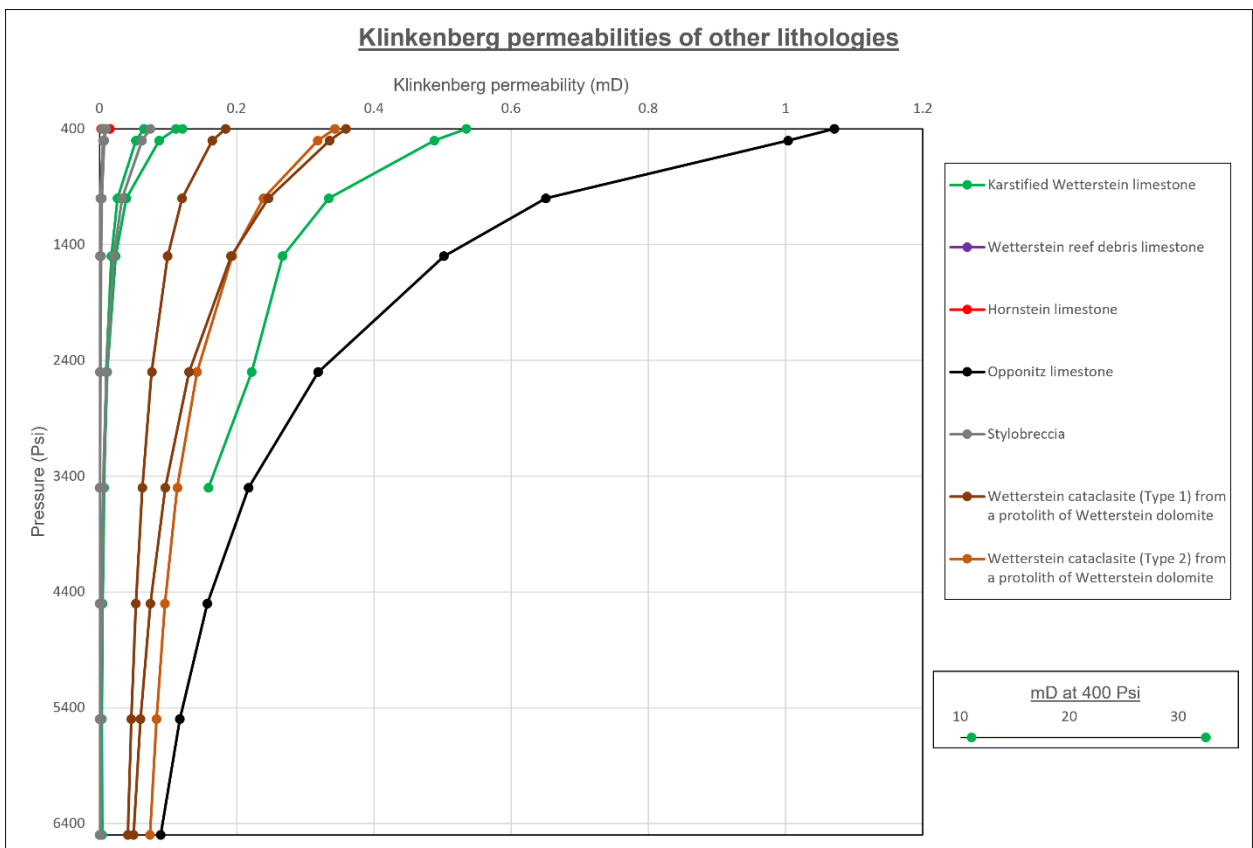
Figure 32: Permeability (Klinkenberg, mD) data from limestones of the Opponitz Fm., Wetterstein Fm. (reef debris), Wetterstein Cataclasite, karstified Wetterstein carbonates and Jurassic Hornstein limestone (19 core plugs). The inset at the bottom of the figure shows the results obtained at 400 psi confining pressure from two especially permeable karstified Wetterstein limestones.

9.2.2 **Porosities:**

The figures (33-36) show the porosities and follow the same arrangement as the figures for the permeabilities. There are no fitted means here, as the porosities are not that different in magnitude, even if the absolute numbers diverge more. The x-scale between the Wetterstein figures is always at the same scale and only was fitted for figure 36.

The Wetterstein reef limestone show a diverse range of porosities, the lagoonal Wetterstein limestone and the Wetterstein dolomites on the other hand are more uniform. Wetterstein dolomite porosities range between 3-5% porosity and lagoonal Wetterstein limestone ranges around 1-2% porosity at 400 psi confining pressure.

Generally, the slopes of the curves do not differ greatly between samples, with few exceptions. Especially the Karstified Wetterstein samples also lose a lot of porosity at higher confining pressure, which normally is only the case for the first few (lower) confining pressure measurements, the samples themselves show strong deformation through shortening after measurement.
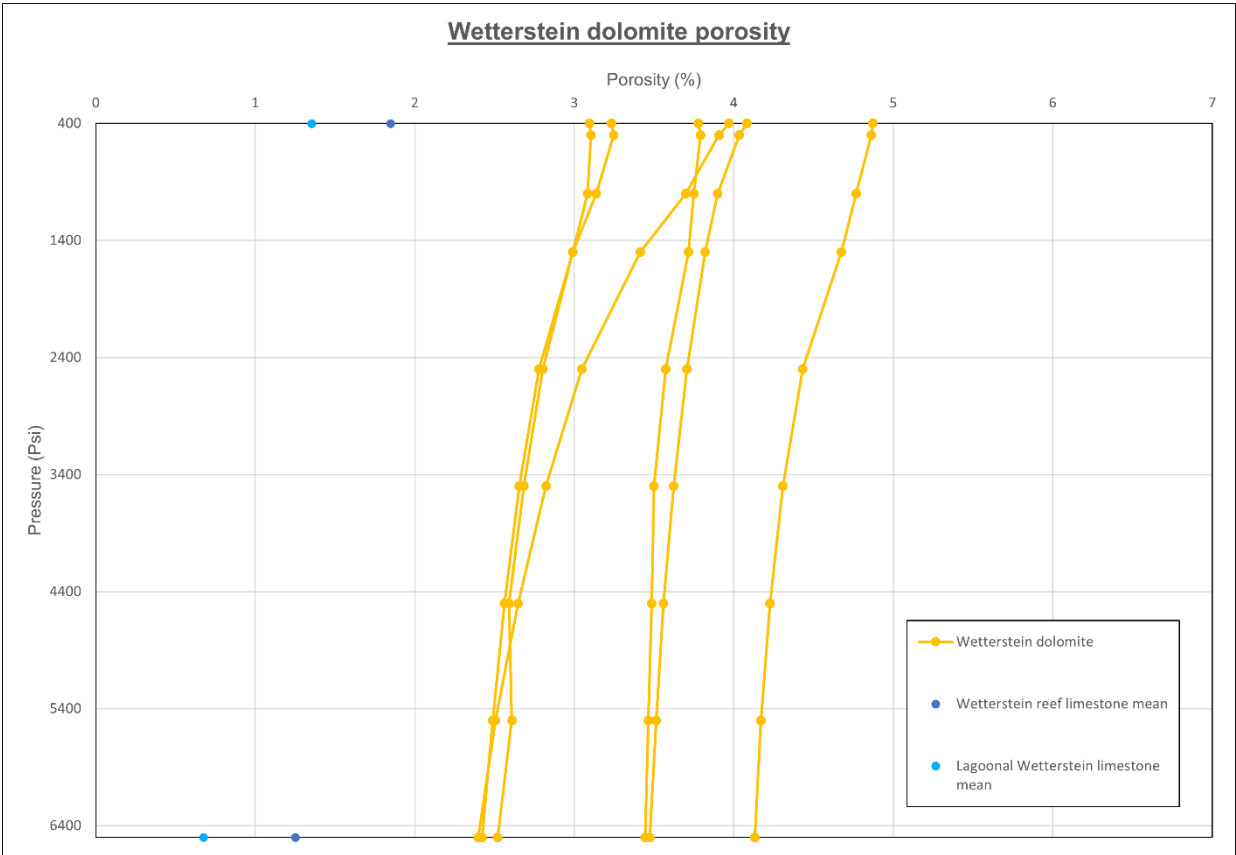
Figure 33: Porosities of dolomites from the Wetterstein Formation (6 core plugs) derived from measurements with the Coreval 700 gas porosimeter at confining pressures between 400 and 6500 psi.
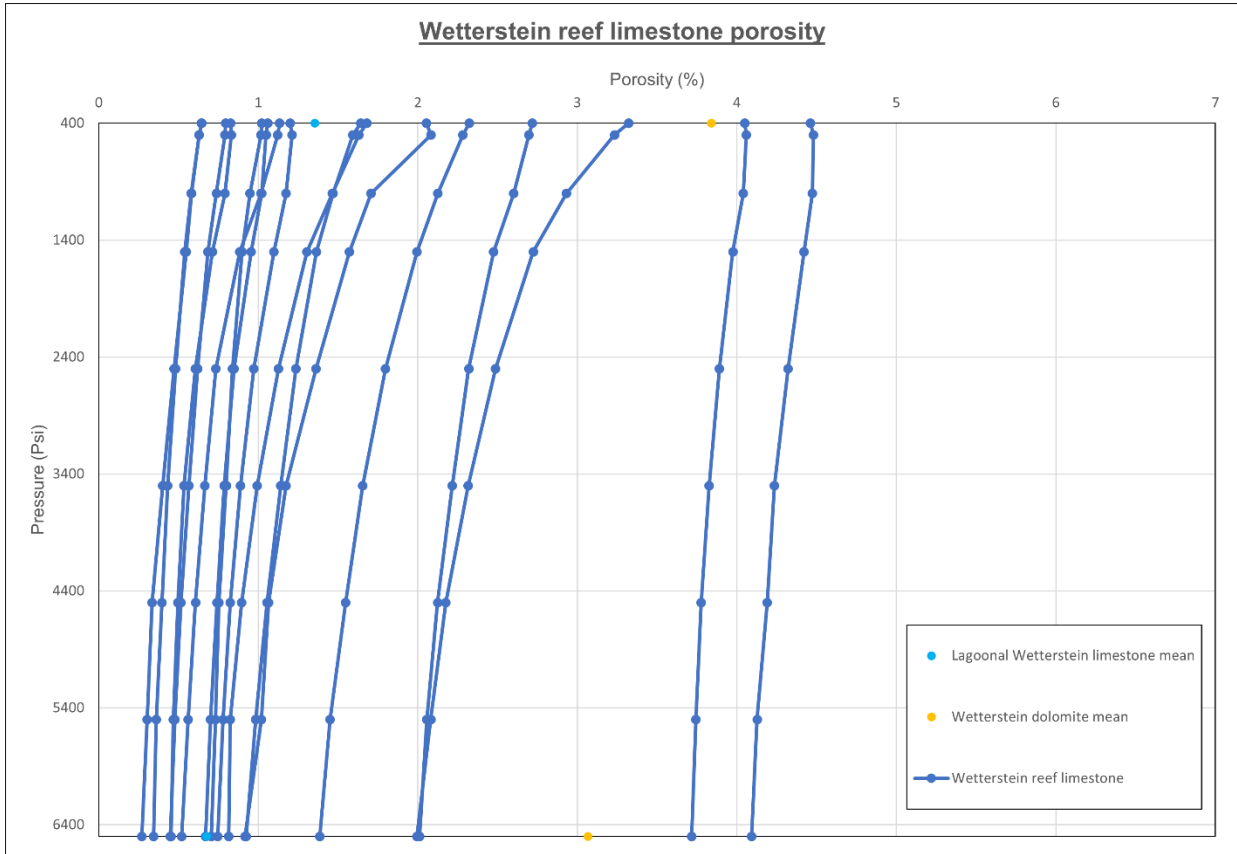
Figure 34: Porosities of reef limestones from the Wetterstein Formation (16 core plugs) derived from measurements with the Coreval 700 gas porosimeter at confining pressures between 400 and 6500 psi.
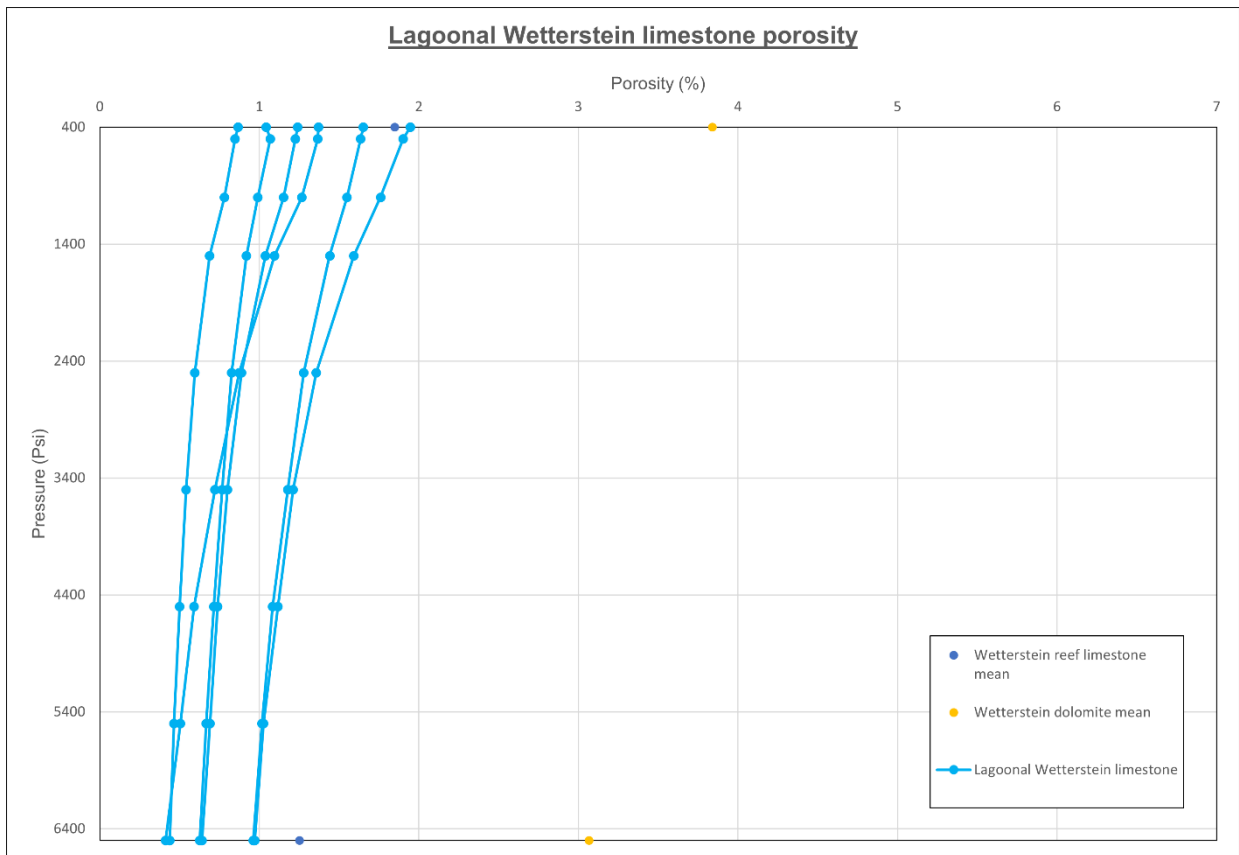
Figure 35: Porosities of lagoonal limestones from the Wetterstein Formation (6 core plugs) derived from measurements with the Coreval 700 gas porosimeter at confining pressures between 400 and 6500 psi.
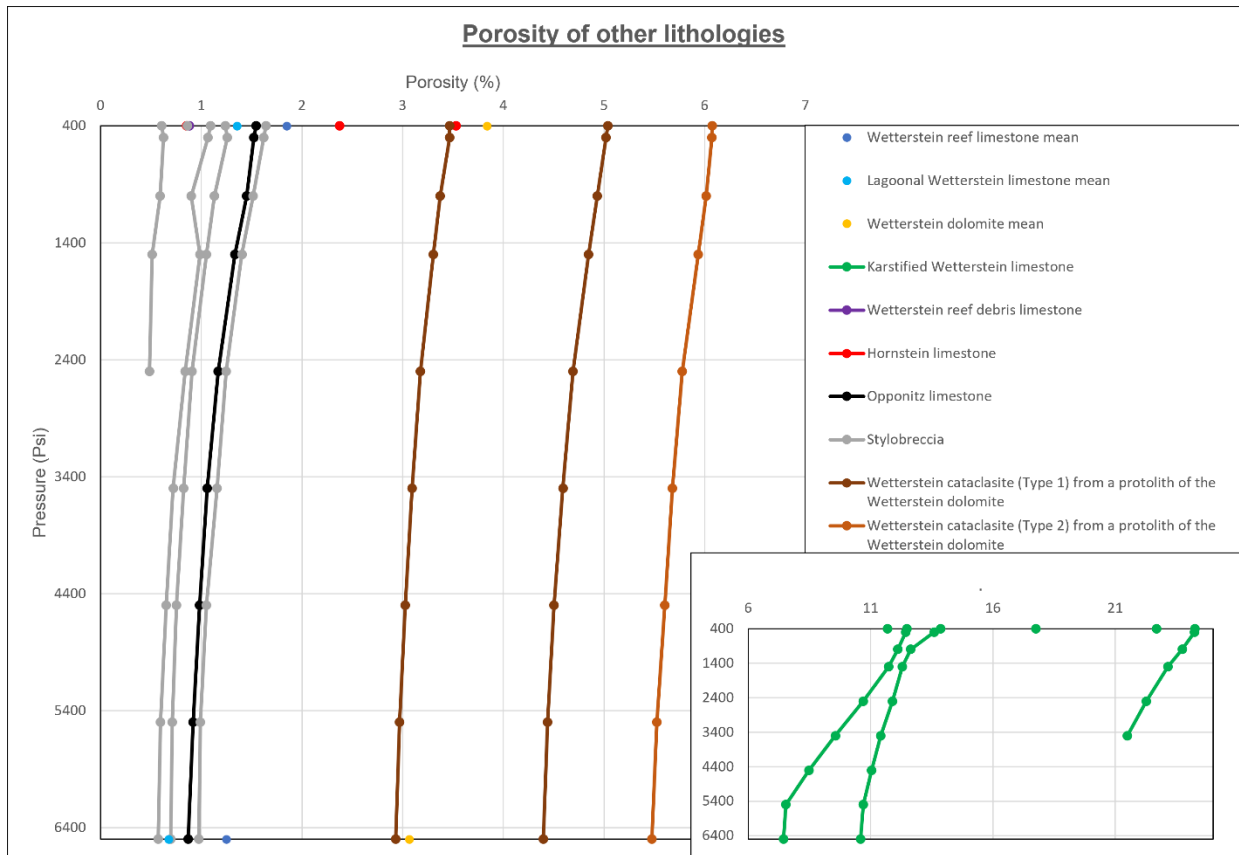
Figure 36: Porosities from limestones of the Opponitz Fm., Wetterstein Fm. (reef debris), Wetterstein Cataclasite, karstified Wetterstein carbonates and Jurassic Hornstein limestone (19 core plugs) derived from measurements with the Coreval 700 gas porosimeter at confining pressures between 400 and 6500 psi. The smaller window shows the Karstified Wetterstein carbonates separately.
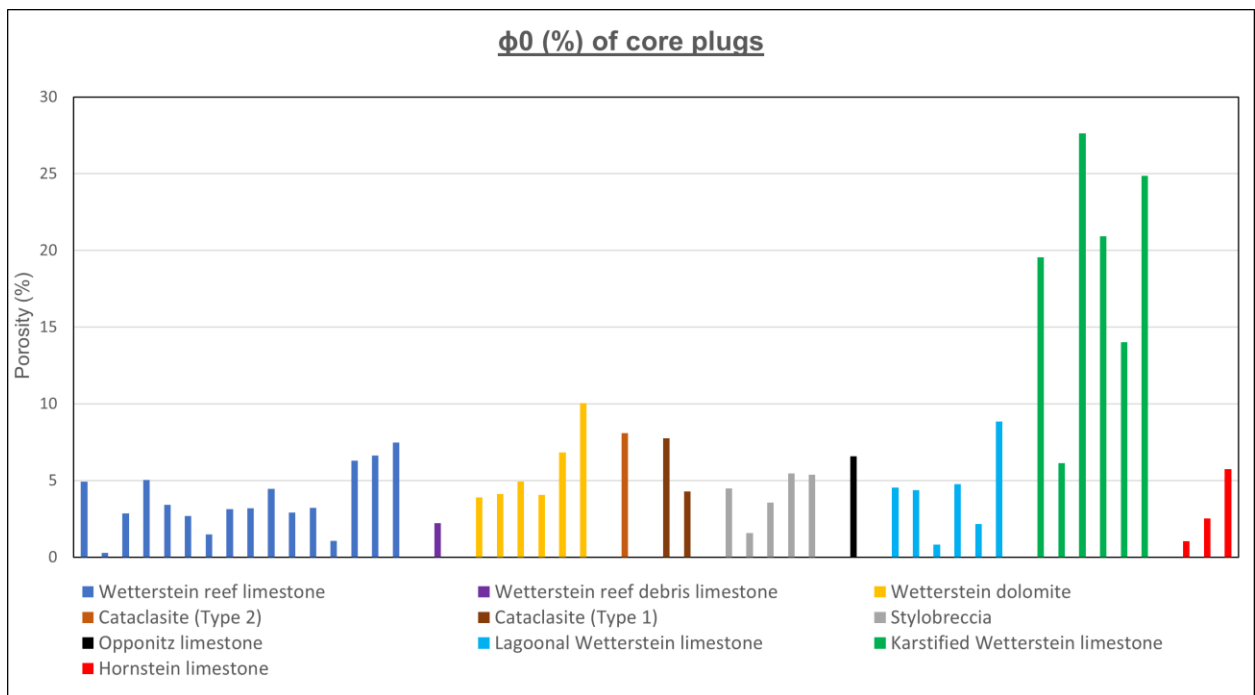
Figure 37: Open porosity at ambient pressure of the core samples measured with the Coreval 700 gas porosimeter.

Figure 37 shows the porosity values at ambient pressure and the data is arranged like Figure 22 and 25. Differences between the porosities of lithologies are not as easy to recognize as it is with the immersion method data.

Figure 38 classifies the result of different samples by their FDC class. The graph does not include karstified Wetterstein limestones, stylobreccia and cataclasites. Although the trend line does show a rising permeability with a higher FDC class, the singular results do not support this.
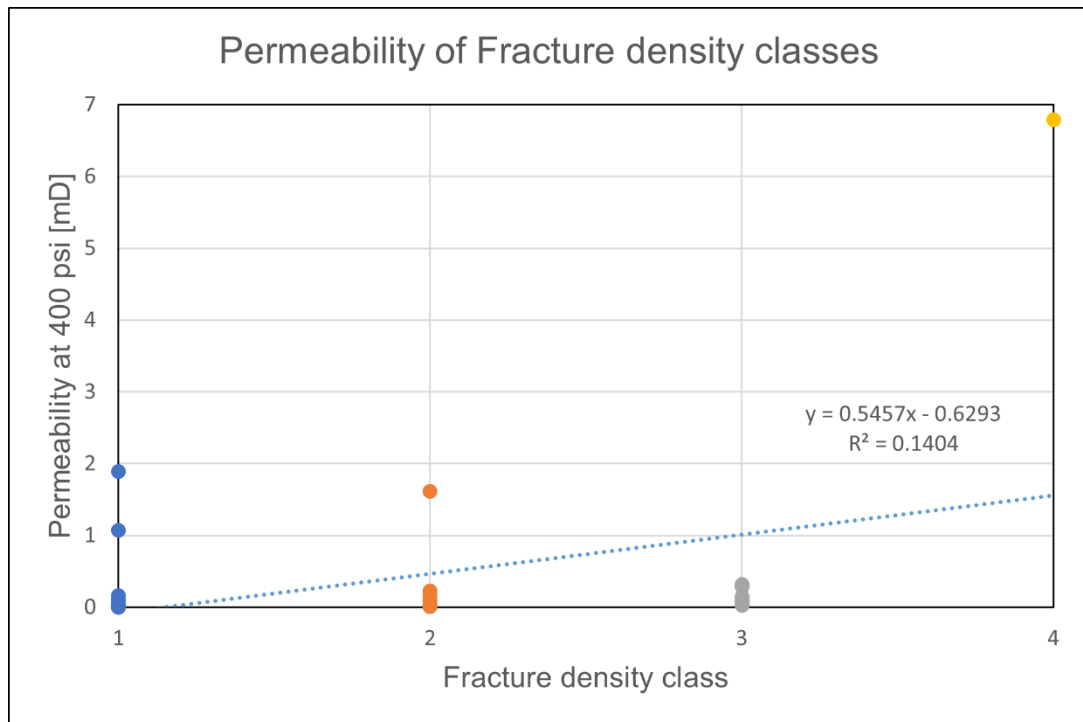
Figure 38: Permeability values of the different samples at 400 psi sorted by their fracture density class (33 data points). No karstified limestones, stylobreccias or cataclasites were included.

A general overview over the porosity and permeability correlations of the whole sample range over different pressure conditions is shown in Figure 39. The data is presented with the $\log_{10}$ values of the permeability and porosity to fit all the data into one figure.
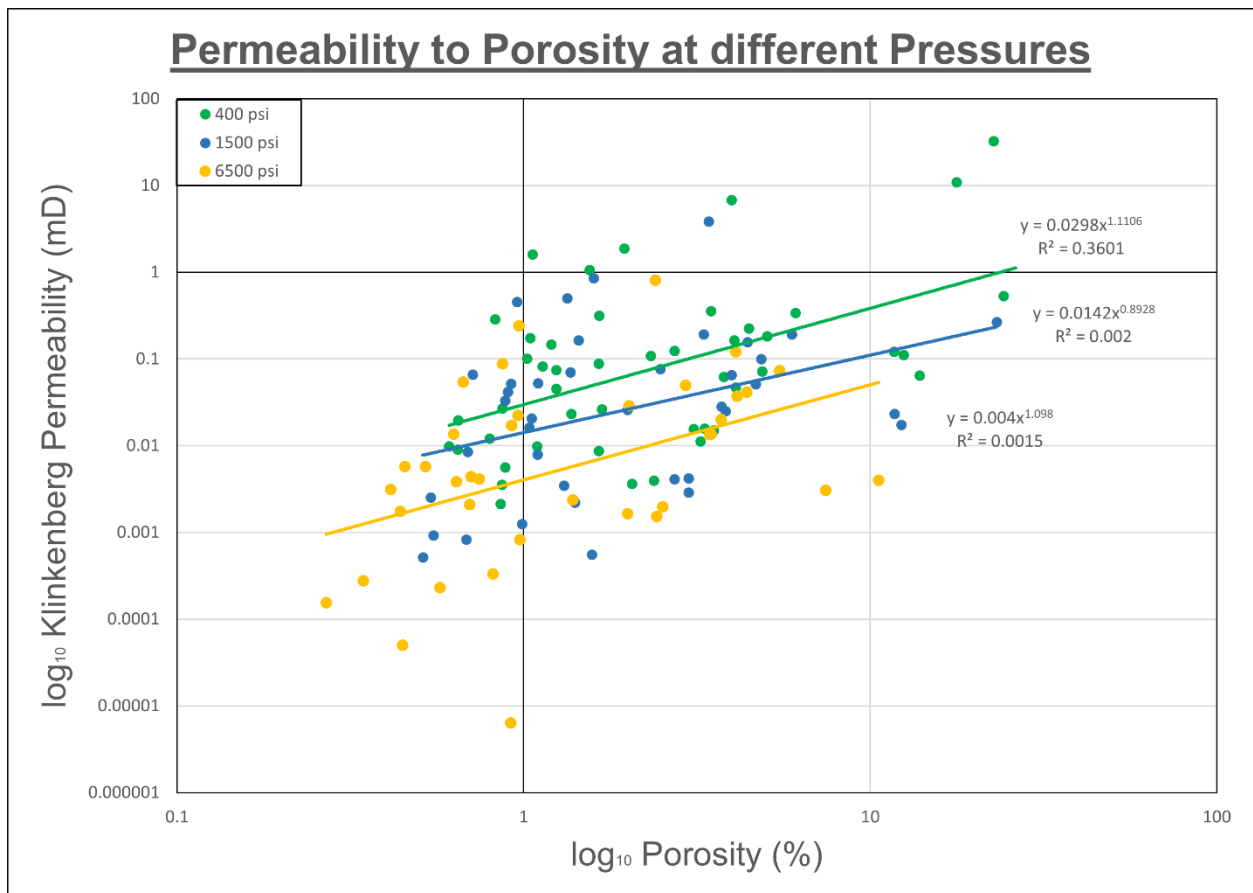
Figure 39: Permeability and porosity cross-plot for all measurements (123 data points). Because of the wide spread of values, a log10 representation of the Klinkenberg permeabilities and the porosities was chosen. Color-codes represent measurements at the confining pressures 400 psi, 1500 psi and 6500 psi. The calculated best fit correlations of the different pressure states show similar slopes.

9.2.3 Loss of permeability and porosity at 1500 psi confining pressure

As seen in Fig. 17, rocks with a strong fractured characteristic can lose much of their initial permeability in the early stages of confined pressure measurements. The different characteristics of the curves is best seen between the measurements at 1000 and 2500 confining pressure. Taking a view on the percentual loss of permeability in this range (Fig. 40) can give an indication of the rocks tendency to act as a fractured rock (with fresh fracture characteristics, meaning bigger asperities and uneven surface).

Figure 40 shows, that percentual loss of permeability is generally to be considered higher than the loss of porosity for an individual sample. Most lithologies do not show any special behaviour different from other lithologies. Only the cataclasite and the stylobreccia samples show relatively homogeneous results. The cataclasite samples retain much of their initial porosity and permeability, whereas the stylobreccia samples retain only minor fractions of their permeability at 1500 psi confining pressure. Other lithology characteristics are less developed, though there are still observations to be made: Wetterstein dolomites and karstified Wetterstein samples retain much of their porosity, the lagoonal Wetterstein limestone on the other hand retains less percentual porosity.
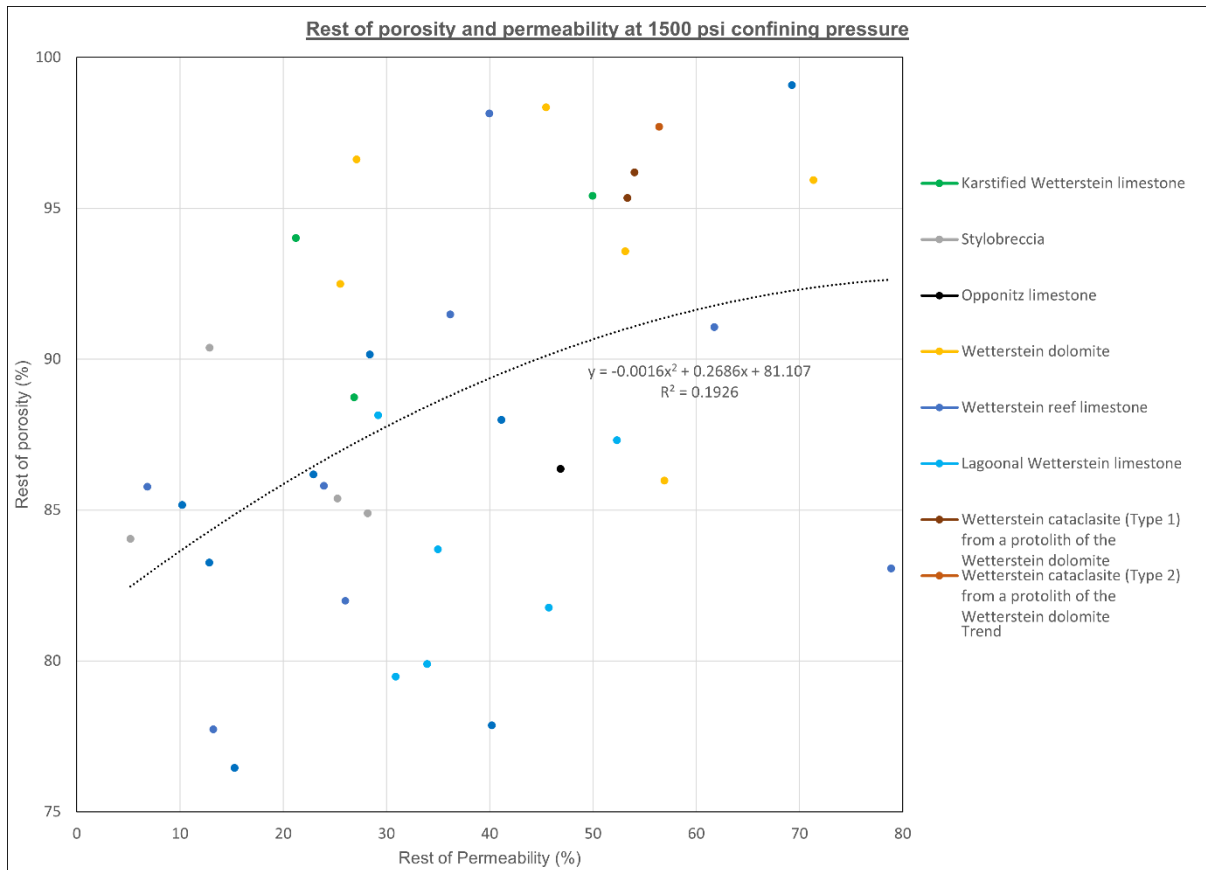
Figure 40: Graph showing the remaining porosity and permeability after increasing the confining pressure from 400 to 1500 psi in % of the value measured at 400 psi. The percentual rest of permeability at 1500 psi can vary strongly. Values from around 80 to 5% can be seen. A very low value of residual permeability shows that, the sample lost already much of its permeability at relatively low confining pressure. The trend line shows the correlation between porosity and permeability loss.

Table 17, 18 and 19 show the collected data of the important parameters Gas permeability, Klinkenberg permeability and porosity at different pressure conditions (400, 1500 and 6500 psi). In the Appendix of this thesis is the full comprehensive table of collected data with the Coreval 700 device.

Why exactly 1500 psi?

Using 1500 psi as a confining pressure value for Figure 39 has two advantages:

-The permeability and porosity-curves of the Coreval 700 measurements show clear differences in their steepness at this confining pressure. At higher pressures the curves tend to have similar slopes and the inherent permeability and porosity at ambient pressure, as well as the pore and fracture characteristics, are barely defining factors anymore.

-1500 psi equals an overburden of roughly 400 m carbonate (2.6 g/cc). This confining pressure therefore resembles the overburden at the base of the Kuhschneeberg more than the other pre-defined psi-values used for the measurements.

Table 17: Permeability- and porosity values of the Coreval 700 device at 400 psi.

Coreval data at 400 psi confining pressure				
Name	**Lithology**	**Gas permeability (mD)**	**Klinkenberg permeability (mD)**	**Φ (%)**
PW1/6	Wetterstein dolomite	8.358299	6.790863	3.97080734
PW3/1.1	Wetterstein reef limestone	0.2196835	0.1085939	2.32365495
PW3/2	Wetterstein reef limestone	0.1874633	0.08938575	1.64291089
PW3/3	Wetterstein reef limestone	0.2826041	0.1474772	1.19951092
PW3/4	Wetterstein reef limestone	0.04852302	0.01596084	3.32171325
PW4/4	Wetterstein reef limestone	2.235301	1.611109	1.05879528
PW5/1.1	Wetterstein reef limestone	0.03165734	0.009034712	0.64410003
PW5/1.2	Wetterstein reef limestone	0.01644247	0.003689446	2.05444969
PW5/3	Wetterstein reef limestone	0.07106849	0.02627252	1.67938519
PW5/4	Wetterstein reef limestone	0.05688974	0.01966925	0.6462659

PW5/5	Wetterstein reef limestone	0.4953323	0.2879667	0.8252535
PW5/6	Wetterstein reef limestone	0.1757325	0.08253473	1.13362199
PW6/1	Lagoonal Wetterstein limestone	0.5356979	0.3157438	1.65070472
PW6/2	Lagoonal Wetterstein limestone	0.07356539	0.02747154	0.86759864
PW6/4	Lagoonal Wetterstein limestone	0.3288542	0.1769923	1.04226719
PW6/5	Lagoonal Wetterstein limestone	0.0652015	0.02349597	1.37203422
PW6/6	Lagoonal Wetterstein limestone	0.1103423	0.04612304	1.23919153
PW6/7.1	Stylobreccia from a protolith of lagoonal Wetterstein limestone	0.03094365	0.008761414	1.64426652
PW6/8	Lagoonal Wetterstein limestone	2.583166	1.891477	1.94676832
PW7/1	Wetterstein dolomite	0.140543	0.06252126	3.77813411
PW7/2.1	Wetterstein dolomite	0.04822081	0.01582988	3.09410961
PW7/2.2	Wetterstein dolomite	0.03735303	0.01127893	3.23291884
PW7/3.1	Wetterstein cataclasite (Type 1) from a protolith of the Wetterstein dolomite	0.3399531	0.1841752	5.03888071
PW7/3.2	Wetterstein cataclasite (Type 2) from a protolith of the Wetterstein dolomite	0.5750399	0.3430808	6.07486696
PW7/4	Wetterstein cataclasite (Type 1) from a protolith of the Wetterstein dolomite	0.5982667	0.3593335	3.46513045
PW7/5	Wetterstein dolomite	0.1124751	0.04725316	4.08286
PW7/6	Wetterstein dolomite	0.1579825	0.07233209	4.8723347
LP2	Wetterstein reef debris limestone	0.02233072	0.005625386	0.88294162
LP7.1	Hornstein limestone	0.01124244	0.00216791	0.85689182
LP7.2	Hornstein limestone	0.01733003	0.003968282	2.37552446
LP7.3	Hornstein limestone	0.04648059	0.0150801	3.53051553
LP11	Karstified Wetterstein limestone	0.1447551	0.06487	13.8624247
LP19.1_1	Wetterstein reef limestone	0.2078062	0.1014506	1.02112564
LP19.1_2	Wetterstein reef limestone	0.0399189	0.01232373	0.79621565

LP19.2	Karstified Wetterstein limestone	0.2248535	0.1117247	12.484619
LP19.2_2	Karstified Wetterstein limestone	0.8430515	0.5348543	24.2627899
LP19.2_3	Karstified Wetterstein limestone	13.17688	11.0379	17.7593087
LP19.2_4	Karstified Wetterstein limestone	0.2400884	0.1210217	11.6976949
LP19.2_5	Karstified Wetterstein limestone	36.8136	32.54081	22.6869276
LP36	Wetterstein reef limestone	0.2453855	0.1242781	2.71767442
LP38	Stylobreccia from a protolith of Wetterstein reef limestone	0.1618366	0.07452969	1.2399138
LP41	Wetterstein reef limestone	0.3092842	0.1644184	4.05001262
LP43	Wetterstein reef limestone	0.4053746	0.2271964	4.46161881
LP48.2	Opponitz limestone	1.551854	1.071163	1.54638224
MT17	Stylobreccia from a protolith of Wetterstein reef debris limestone	0.01595543	0.003538607	0.86401193
MT17.2	Stylobreccia from a protolith of Wetterstein reef debris limestone	0.03388737	0.009900394	0.60840631
MT17.3	Stylobreccia from a protolith of Wetterstein reef debris limestone	0.03367958	0.009819002	1.09333554

Table 18: Permeability- and porosity values of the Coreval 700 device at 1500 psi.

Coreval data at 1500 psi confining pressure				
Name	**Lithology**	**Gas permeability (mD)**	**Klinkenberg permeability (mD)**	**Φ (%)**
PW1/6	Wetterstein dolomite	4.958025	3.865206	3.4139009
PW3/1.1	Wetterstein reef limestone	0.07046033	0.02598201	1.99369673
PW3/2	Wetterstein reef limestone	0.1547447	0.0704938	1.36473999
PW3/3	Wetterstein reef limestone	0.1238396	0.05335013	1.09738538
PW3/4	Wetterstein reef limestone	0.01791405	0.004154442	2.72361378
PW4/4	Wetterstein reef limestone	0.7358526	0.4571249	0.95457969
PW5/1.1	Wetterstein reef limestone	0.006174958	9.23E-04	0.5485999
PW5/1.2	Wetterstein reef limestone	0.004396918	5.64E-04	1.57080747
PW5/3	Wetterstein reef limestone	0.01573905	0.003472097	1.30538548
PW5/4	Wetterstein reef limestone	0.01252374	0.002523308	0.53806734
PW5/5	Wetterstein reef limestone	0.1467466	0.06598522	0.71123499
PW5/6	Wetterstein reef limestone	0.08519536	0.03318077	0.88272423
PW6/1	Lagoonal Wetterstein limestone	0.3105331	0.1652172	1.44132015
PW6/2	Lagoonal Wetterstein limestone	0.03021378	0.00848387	0.68955847
PW6/4	Lagoonal Wetterstein limestone	0.1207457	0.05167812	0.91869837
PW6/5	Lagoonal Wetterstein limestone	0.02884753	0.007969782	1.09621422
PW6/6	Lagoonal Wetterstein limestone	0.04892773	0.01613656	1.03715546
PW6/7.1	Stylobreccia from a protolith of lagoonal Wetterstein limestone	0.01140392	0.002211918	1.4039981
PW6/8	Lagoonal Wetterstein limestone	1.284033	0.8648529	1.59191605
PW7/1	Wetterstein dolomite	0.0755039	0.02840922	3.71584877
PW7/2.1	Wetterstein dolomite	0.01833053	0.004288463	2.98959132
PW7/2.2	Wetterstein dolomite	0.0137587	0.002878593	2.99024587

PW7/3.1	Wetterstein cataclasite (Type 1) from a protolith of the Wetterstein dolomite	0.2045287	0.09949185	4.84674127
PW7/3.2	Wetterstein cataclasite (Type 2) from a protolith of the Wetterstein dolomite	0.3542485	0.1934791	5.93548971
PW7/4	Wetterstein cataclasite (Type 1) from a protolith of the Wetterstein dolomite	0.3513555	0.1915916	3.30366824
PW7/5	Wetterstein dolomite	0.06860409	0.0250991	3.82042657
PW7/6	Wetterstein dolomite	0.1206309	0.05161625	4.67440847
LP11	Karstified Wetterstein limestone	0.05184828	0.01741603	12.3008449
LP19.1_1	Wetterstein reef limestone	0.1019659	0.04173077	0.89847373
LP19.1_2	Wetterstein reef limestone	0.005791601	8.41E-04	0.6829189
LP19.2	Karstified Wetterstein limestone	0.06566008	0.02371085	11.7374615
LP19.2_2	Karstified Wetterstein limestone	0.4648039	0.2671575	23.1496266
LP36	Wetterstein reef limestone	0.165692	0.07673811	2.47472227
LP38	Stylobreccia from a protolith of Wetterstein reef limestone	0.05979077	0.02098978	1.052571
LP41	Wetterstein reef limestone	0.1462103	0.06568457	3.97488869
LP43	Wetterstein reef limestone	0.2982743	0.1573981	4.42050087
LP48.2	Opponitz limestone	0.7975931	0.5017459	1.33552912
MT17.2	Stylobreccia from a protolith of Wetterstein reef debris limestone	0.004137093	5.16E-04	0.51135677
MT17.3	Stylobreccia from a protolith of Wetterstein reef debris limestone	0.007690497	0.001264342	0.98811435

Table 19: Permeability- and porosity values of the Coreval 700 device at 6500 psi.

Coreval data at 6500 psi confining pressure				
Name	**Lithology**	**Gas permeabi- lity (mD)**	**Klinkenberg permeability (mD)**	**Φ (%)**
PW1/6	Wetterstein dolomite	1.215603	0.8127614	2.39827322
PW3/1.1	Wetterstein reef limestone	0.01193626	0.002358617	1.38616773
PW3/2	Wetterstein reef limestone	0.05132376	0.0171848	0.92363212
PW3/3	Wetterstein reef limestone	0.01798393	0.004176859	0.7444325
PW3/4	Wetterstein reef limestone	0.009304145	0.001658671	1.99352678
PW4/4	Wetterstein reef limestone	0.124883	0.05391594	0.66900976
PW5/1.1	Wetterstein reef limestone	0.001830898	1.55E-04	0.26976992
PW5/1.2	Wetterstein reef limestone	2.24E-04	6.40E-06	0.91667405
PW5/3	Wetterstein reef limestone	0.003082551	3.35E-04	0.81454703
PW5/4	Wetterstein reef limestone	0.002705132	2.76E-04	0.34420154
PW5/5	Wetterstein reef limestone	0.02276737	0.005776396	0.45349837
PW5/6	Wetterstein reef limestone	0.02274637	0.005769112	0.51964113
PW6/1	Lagoonal Wetterstein limestone	0.06253193	0.02225263	0.96294047
PW6/2	Lagoonal Wetterstein limestone	0.009691982	0.00175763	0.43982161
PW6/4	Lagoonal Wetterstein limestone	0.04318029	0.01367924	0.62725548
PW6/5	Lagoonal Wetterstein limestone	0.01467219	0.003148875	0.41289935
PW6/6	Lagoonal Wetterstein limestone	0.01689195	0.003830029	0.6401491
PW6/7.1	Stylobreccia from a protolith of la-goonal Wetterstein limestone	0.005726529	8.27E-04	0.97511752
PW6/8	Lagoonal Wetterstein limestone	0.4265095	0.2413196	0.97035848
PW7/1	Wetterstein dolomite	0.04263361	0.01344997	3.4449628
PW7/2.1	Wetterstein dolomite	0.01055713	0.001983764	2.51996282
PW7/2.2	Wetterstein dolomite	0.008758943	0.001522214	2.42185524

PW7/3.1	Wetterstein cataclasite (Type 1) from a protolith of the Wetterstein dolomite	0.1013101	0.04139013	4.39703825
PW7/3.2	Wetterstein cataclasite (Type 2) from a protolith of the Wetterstein dolomite	0.1603122	0.07365924	5.47518533
PW7/4	Wetterstein cataclasite (Type 1) from a protolith of the Wetterstein dolomite	0.1170952	0.04971689	2.9332439
PW7/5	Wetterstein dolomite	0.04315934	0.01367044	3.4721925
PW7/6	Wetterstein dolomite	0.09341766	0.0373295	4.1313394
LP11	Karstified Wetterstein limestone	0.01740056	0.003990651	10.5881795
LP19.1_1	Wetterstein reef limestone	0.01873928	0.004420999	0.70444616
LP19.1_2	Wetterstein reef limestone	8.64E-04	5.01E-05	0.44696328
LP19.2	Karstified Wetterstein limestone	0.01440308	0.003068616	7.43654113
LP36	Wetterstein reef limestone	0.07618272	0.02873895	2.01147947
LP38	Stylobreccia from a protolith of Wetterstein reef limestone	0.01102037	0.002107768	0.6983309
LP41	Wetterstein reef limestone	0.05771928	0.02004513	3.71591456
LP43	Wetterstein reef limestone	0.2403225	0.1211654	4.09277936
LP48.2	Opponitz limestone	0.1874763	0.0893934	0.86880804
MT17.3	Stylobreccia from a protolith of Wetterstein reef debris limestone	0.002397846	2.31E-04	0.57339982

9.3 Comparison of open porosity values derived from handpieces and plugs of Coreval 700 and immersion data

Porosity data using the immersion method was collected both, from the handpieces, as well as the core plugs. Because the core plug is only a fraction of the volume of the initial sample, deviations of porosity are to be expected. The correlation between results of the immersion-derived data with results of the gas-porosimeter is also only meaningful if the cores represent the properties of the handpieces.

Cross-comparing still can help understanding the results and differences between the measurement methods.

Fig. 41 shows the correlation between the porosities determined by measurements using the immersion method from core plugs and handpieces. Although both methods show the same trend over different porosity values (%), differences are recognizable with average deviations of 0.72%. Most of the times the cores show the lower porosity values. The arithmetic mean of the Handpieces is 2.68%, the arithmetic means of the core plugs amounts to only 1.96%.
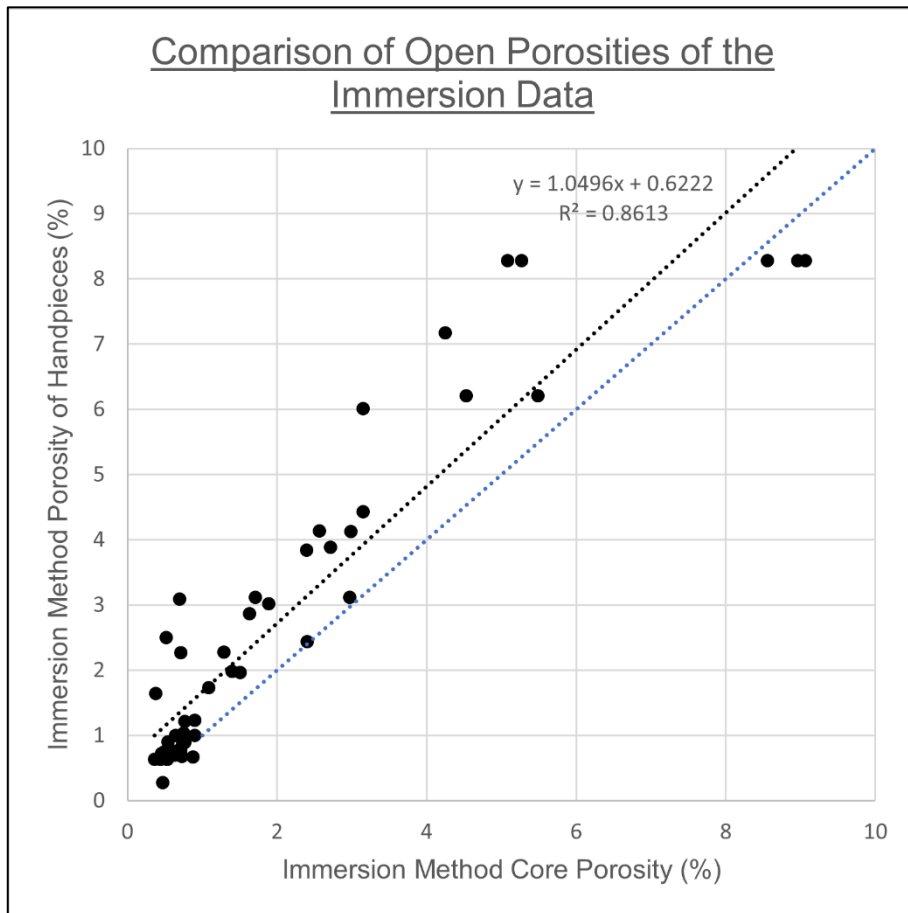
Figure 41: Comparison of the open porosities measured from handpieces and core plugs produced from the same handpiece, measured with the immersion method. The black line shows the linear trend of the measured correlation, whereas the blue line shows an ideal correlation, where every core plug would represent the handpiece 1:1. The lines are almost parallel to each other, so the difference between measurements over the shown porosity range is relatively constant.

The noticeable difference between the porosities determined from core plugs and handpieces suggests, that cross-comparing the immersion data of the handpieces with the Coreval 700-porosities of the plugs is not ideal. Plugs show a lower porosity throughout, which suggests that the plug volume (around a few tens of cm^3) is not large enough to be representative of larger samples (hundreds to thousands cm^3).

A comparison of the porosity values determined from core plugs using the gas permeameter and immersion-measurements, shows clear differences (Fig. 42). Almost all samples show higher porosity when measured with the Coreval 700 device. Despite the clear

difference, there is also an observation to be made in the trend: The higher the porosity-values get, the bigger is the difference between both measurement methods.
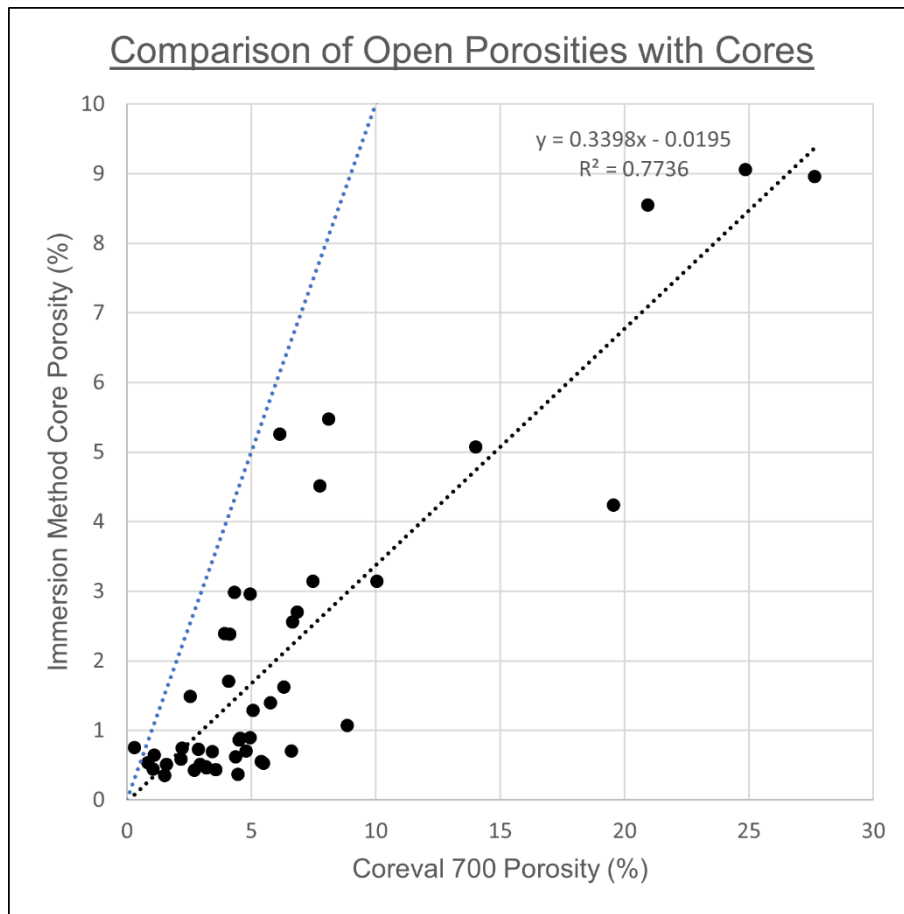
Figure 42: Comparison of the open porosities measured on core plugs with the immersion method and the Coreval 700 gas porosimeter. The black dotted line shows the linear trend of the measured correlation, whereas the blue dotted line shows an ideal correlation, where every core plug would represent the handpiece 1:1. Noticeable is the general deviation of the values, as well as the rising of differences with higher porosity ranges.

9.4 Results of the thin-section measurements

13 different samples were analysed under the microscope with the use of Fluorol staining. The following photographs document the resulting thin sections views and the measured porosity and fracture length per area (P21) determined with the use of Auto-CAD. Fig. 60 and 61 show these thin sections separated into two different categories: The first one (with blue descriptions) are samples with almost no pore space and a clear separation between light emitting and non-emitting areas. These are mostly fracture-dominated samples. The second type (with green descriptions) of samples is characterized by a larger influence of pores and/or a commonness of large areas which are emit-

ting light at least to a degree. This is often the case for pore-dominated samples. Essentially, it is a separation of samples into whether their porosity is mostly concentrated locally in fractures or dispersed in pores.

Every sample has a diameter of 1,5 inches.

LP11

$$2,08 * e^{-3} cm/cm^2 \qquad 20,87 \%$$
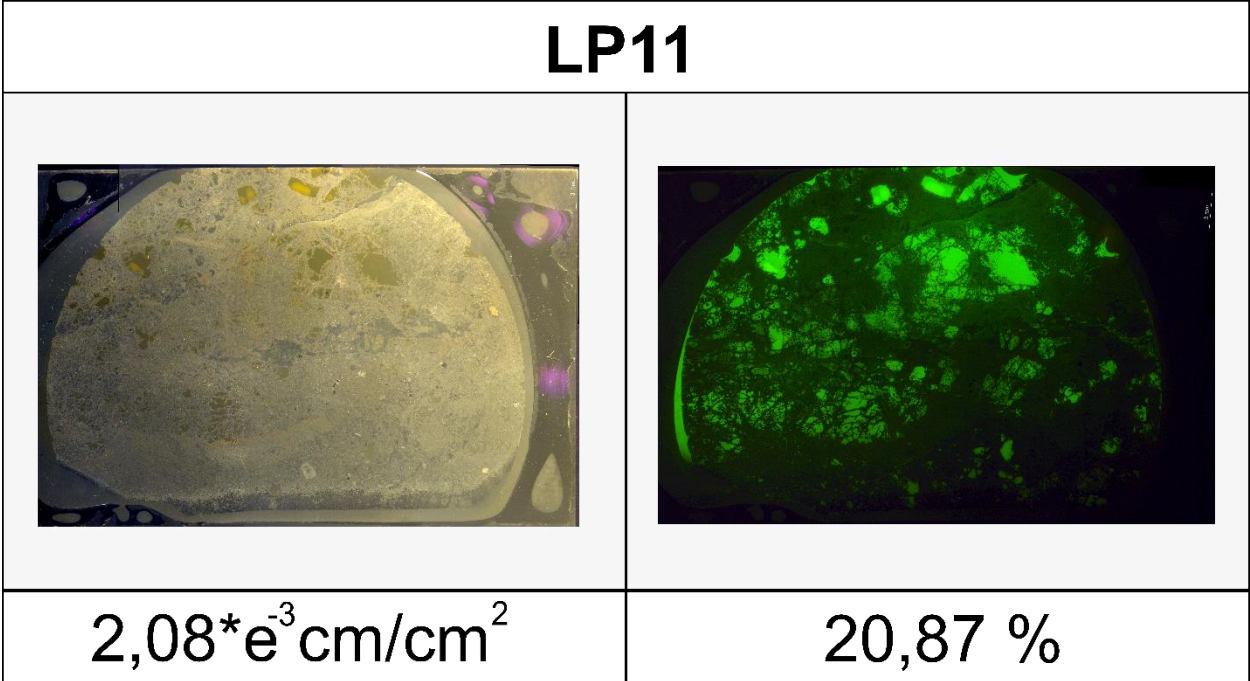
Figure 43: Karstified Wetterstein limestone. Wetterstein Fm. This sample consists of many karst-induced pores. Only minor fractures are to be found, but they do not amount to much porosity. LP11 is the first example belonging to the second group: The whole sample is at least emitting diffuse light through its permeability, even if the large pores are the main emission source The P_{21}-value of the sample (cm/cm²) is shown in the lower left corner, the porosity (%) is shown in the lower right corner.

LP19.1

$$0,4 \ cm/cm^2 \qquad 6,59 \%$$
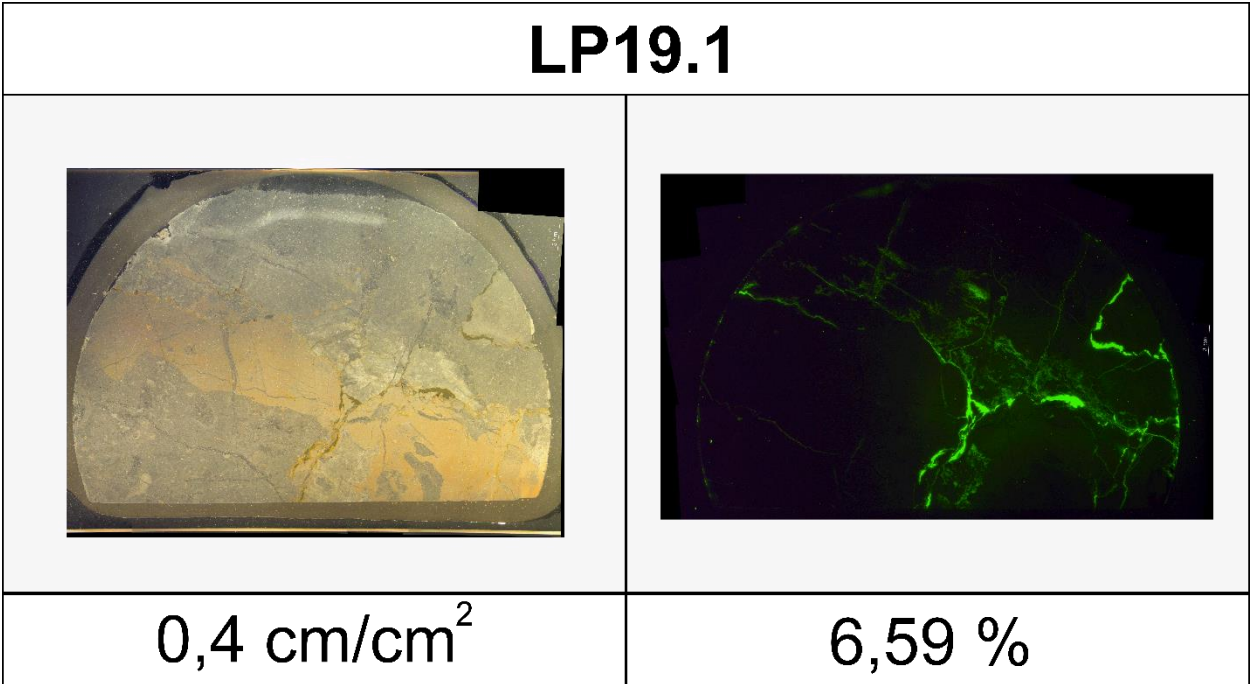
Figure 44: Wetterstein Reef limestone. Wetterstein Fm. This solid sample shows a number of interconnected fractures. Cut-outs through the fractures have widths up to 3mm. The P_{21}-value of the sample (cm/cm²) is shown in the lower left corner, the porosity (%) is shown in the lower right corner.

LP19.2
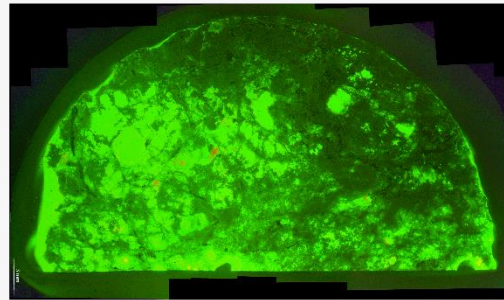
$$1{,}72*e^{-2}\,cm/cm^2$$

$$27{,}16\ \%$$

Figure 45: Karstified Wetterstein limestone. Wetterstein Fm. This sample includes almost exclusively porosity induced through karstification. The P_{21}-value of the sample (cm/cm²) is shown in the lower left corner, the porosity (%) is shown in the lower right corner.

LP36
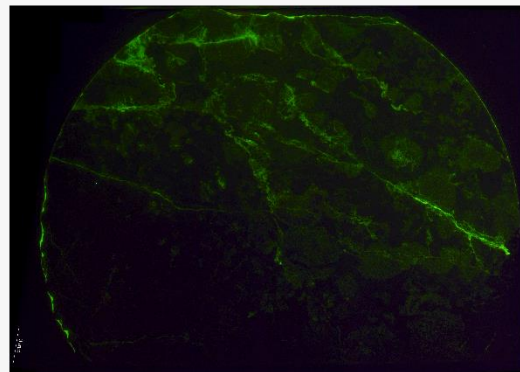
$$0{,}15\ cm/cm^2$$

$$3{,}46\ \%$$

Figure 46: Wetterstein Reef limestone. Wetterstein Fm. This sample shows singular fractures with almost no connection between them. Around the fractures pore spaces are filled partly with Fluorol. The P_{21}-value of the sample (cm/cm²) is shown in the lower left corner, the porosity (%) is shown in the lower right corner.

LP38
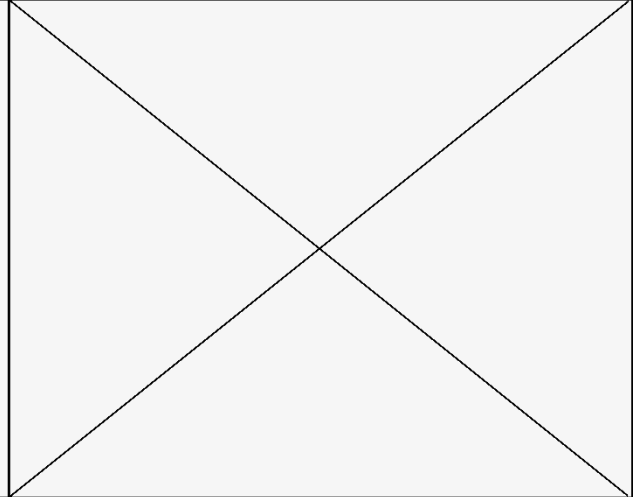
not measureable / stitching not possible

Figure 47: Stylobreccia from a protolith of Wetterstein reef limestone. Wetterstein Fm. LP38 shows almost no pore space, which made it not possible to create a whole picture of the thin section, out of the different frames. The porosity of the sample is therefore very low.

LP41
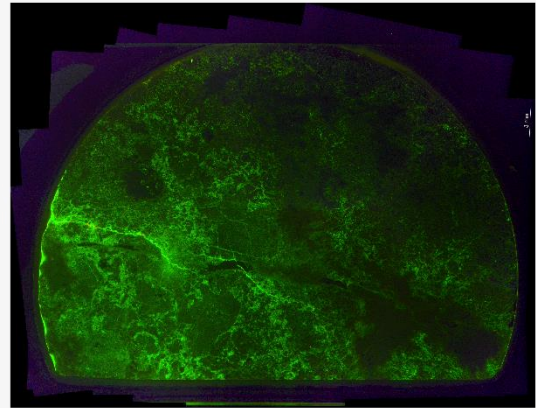
$$4,42 \text{ cm/cm}^2 \qquad 5,33 \text{ \%}$$

Figure 48: Wetterstein reef limestone. Wetterstein Form. The sample shows a lot of fractures, which are connected and spread all over the thin section. From there the Fluorol propagates into the surrounding pores, which leaves only minor parts of the sample without emission of UV-light. The P_{21}-value of the sample (cm/cm²) is shown in the lower left corner, the porosity (%) is shown in the lower right corner.
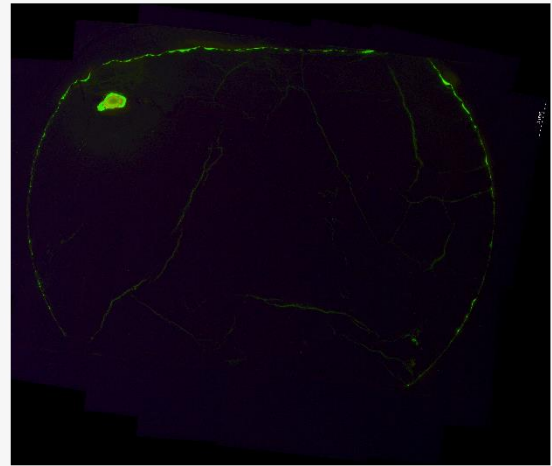
MT17	
0,37 cm/cm^2	1,22 %

Figure 49: Stylobreccia from a protolith of Wetterstein reef debris limestone. Wetterstein Fm. A few thin fractures without many intersections characterize the sample MT17. The rock is almost completely solid without the 2mm wide pore space and the fractures. A large part of the sample is just black, the missing light emission indicates large solid areas without any porosity. The P_{21}-value of the sample (cm/cm²) is shown in the lower left corner, the porosity (%) is shown in the lower right corner.
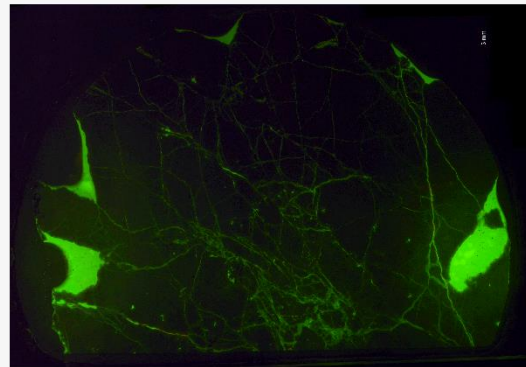
PW1/6	
0,96 cm/cm^2	5,4 %

Figure 50: Wetterstein dolomite. Wetterstein Fm. Many connected and intersected fractures lead to big cut-outs at the sample's edges. These cut-outs are not part of the porosity calculation, the measurement of porosity encompasses all within the solid edges of the sample only. The P_{21}-value of the sample (cm/cm²) is shown in the lower left corner, the porosity (%) is shown in the lower right corner. To save time during the tracing process, only the central part of the sample was measured for the P_{21}-value, possible lowering the P21-value.
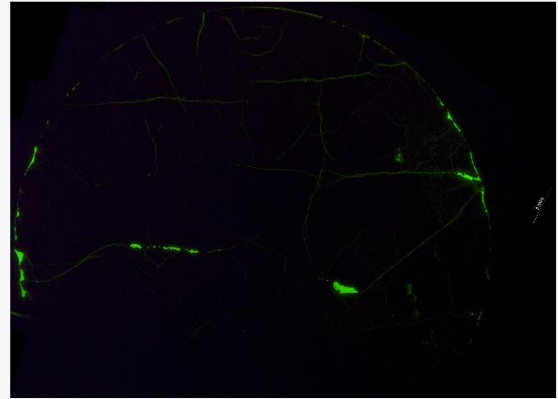
PW4/4	
0,43 cm/cm^2	4,14 %

Figure 51: Wetterstein reef limestone. Wetterstein Fm. Reminiscent of sample MT17, only a few fractures provide pore space in this sample. The P_{21}-value of the sample (cm/cm²) is shown in the lower left corner, the porosity (%) is shown in the lower right corner.
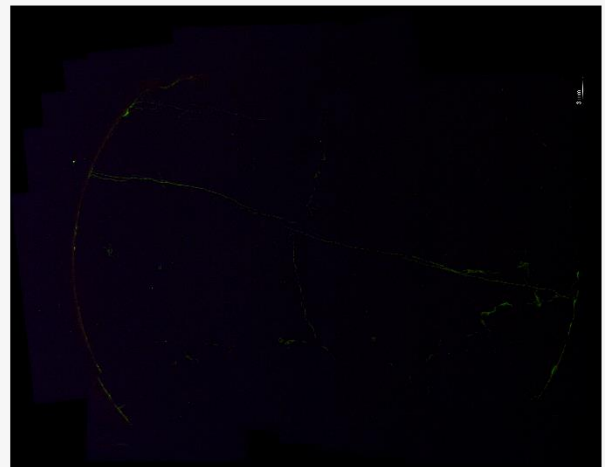
PW5/1.1	
0,11 cm/cm^2	0,83 %

Figure 52: Wetterstein reef limestone. Wetterstein Fm. A few fractures without any intersections and almost no pore space characterize sample PW5/1.1. The P_{21}-value of the sample (cm/cm²) is shown in the lower left corner, the porosity (%) is shown in the lower right corner.

PW5/1.2
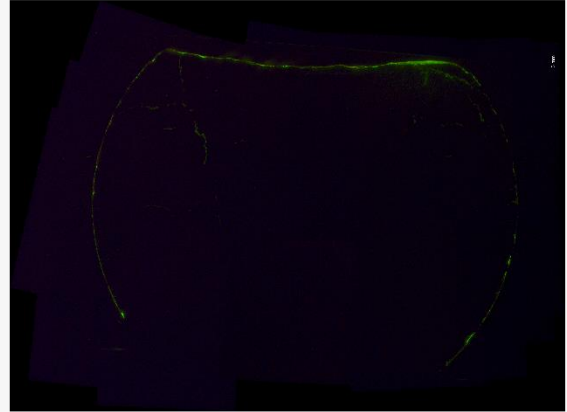
$$3{,}29 * e^{-5} \, cm/cm^2$$

$$0{,}74 \, \%$$

Figure 53: Wetterstein reef limestone. Wetterstein Fm. Like PW5/1.1, this sample is almost without pore space and fractures are almost not to be found. The P21-value of the sample (cm/cm²) is shown in the lower left corner, the porosity (%) is shown in the lower right corner.

PW6/2
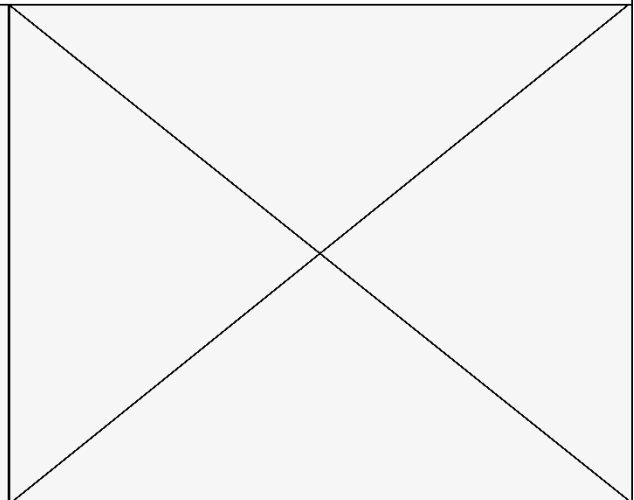
not measureable / stitching not possible

Figure 54: Lagoonal Wetterstein limestone. Wetterstein Fm. PW6/2 is one of the two samples, where the emission of light was too weak to stitch a whole thin section picture, the sample is therefore very low on porosity and cleavages length.
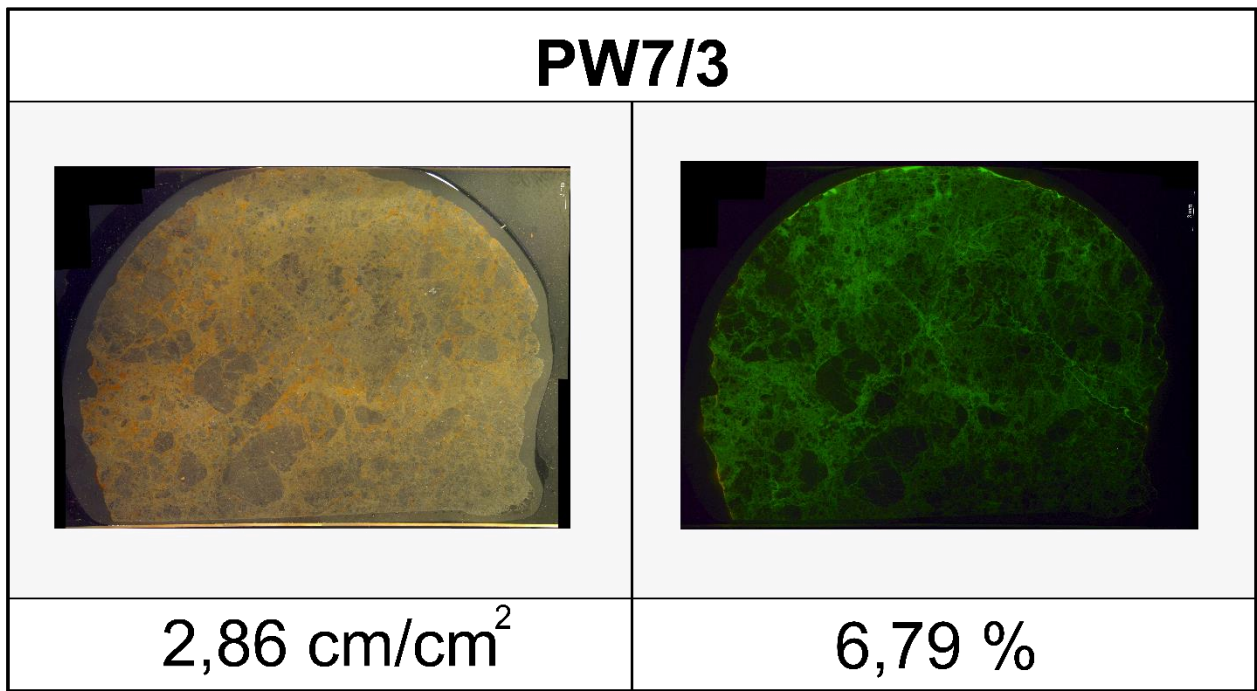
Figure 55: Cataclasite from a protolith of Wetterstein reef limestone. Wetterstein Fm. PW 7/3 is one of the samples with the highest fracture density and porosity from the thin sections. The intersections between the fractures are also numerous. The P_{21}-value of the sample (cm/cm²) is shown in the lower left corner, the porosity (%) is shown in the lower right corner.

Fig. 56 shows the Klinkenberg permeabilities of the listed thin sections measured at confining pressures between 400 and 6500 psi. Although it is tendentially so, that the samples with higher fracture density (higher P_{21} values) determined under the microscope have a higher permeability, this correlation is only vague.

In Figure 57, the relation of P_{21}-value to the permeability is explored further. The permeability data at 400 psi confining pressure is plotted against the exact P_{21}-values of the thin-section samples (logarithmic presentation), a weak correlation between those two parameters is shown.
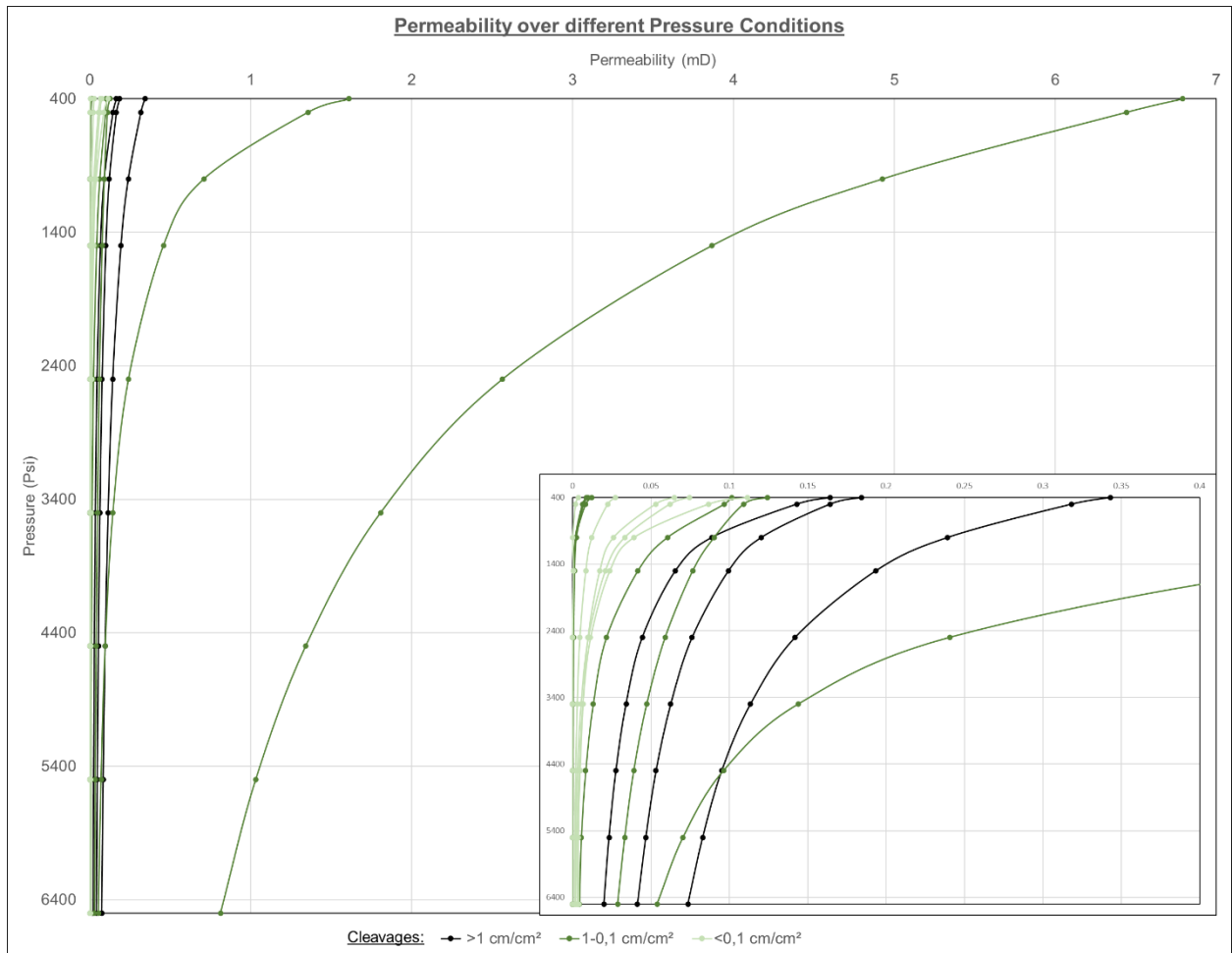
Figure 56: Klinkenberg permeabilities of the thin section samples. Samples with high fracture density determined under the microscope tend to show higher permeabilities.
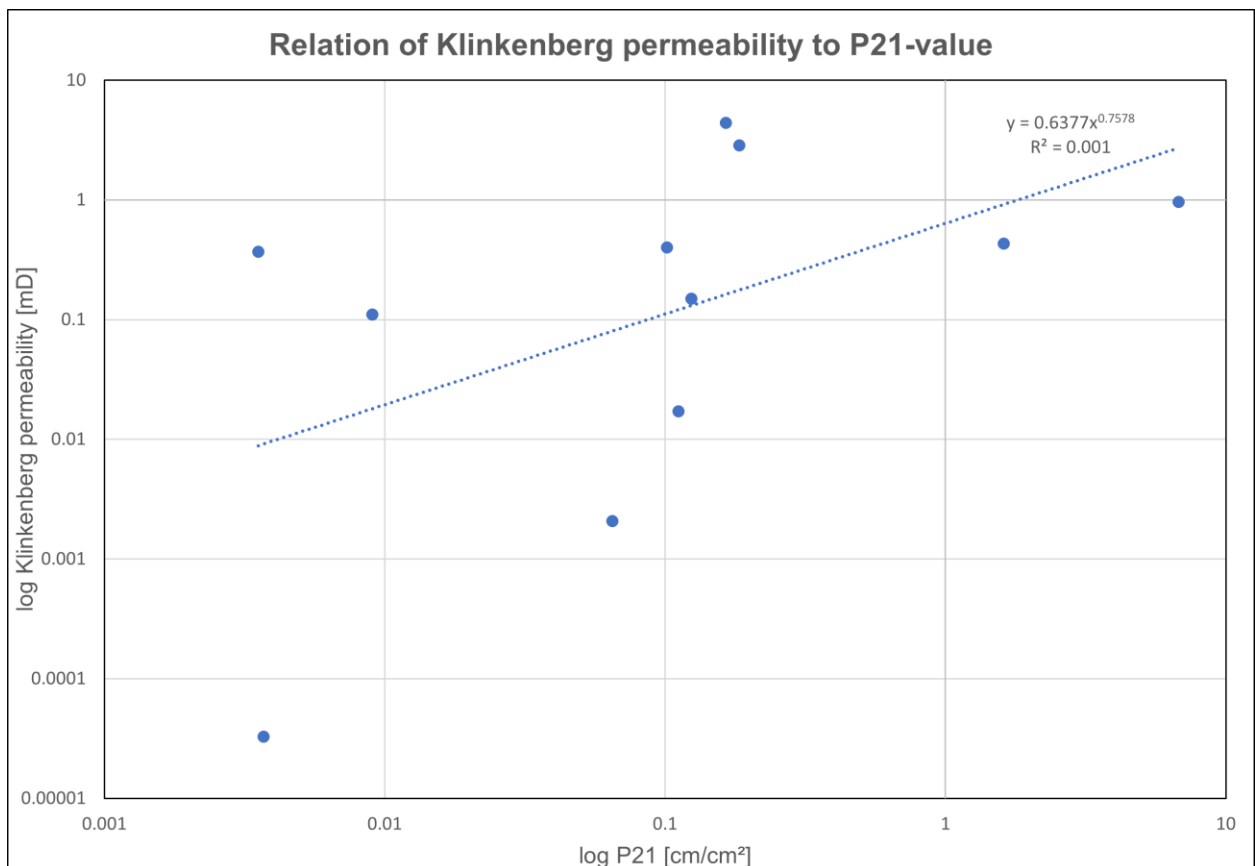
Figure 57: Klinkenberg permeability at 400 psi confining pressure plotted against the P_{21}-values of the corresponding thin-sections (logarithmic presentation).

Fig. 58 shows the core plug porosities of the thin-section samples over rising pressures. Here, the samples with higher porosity in the thin section also tendentially show higher porosity when measured with the Coreval 700 device.
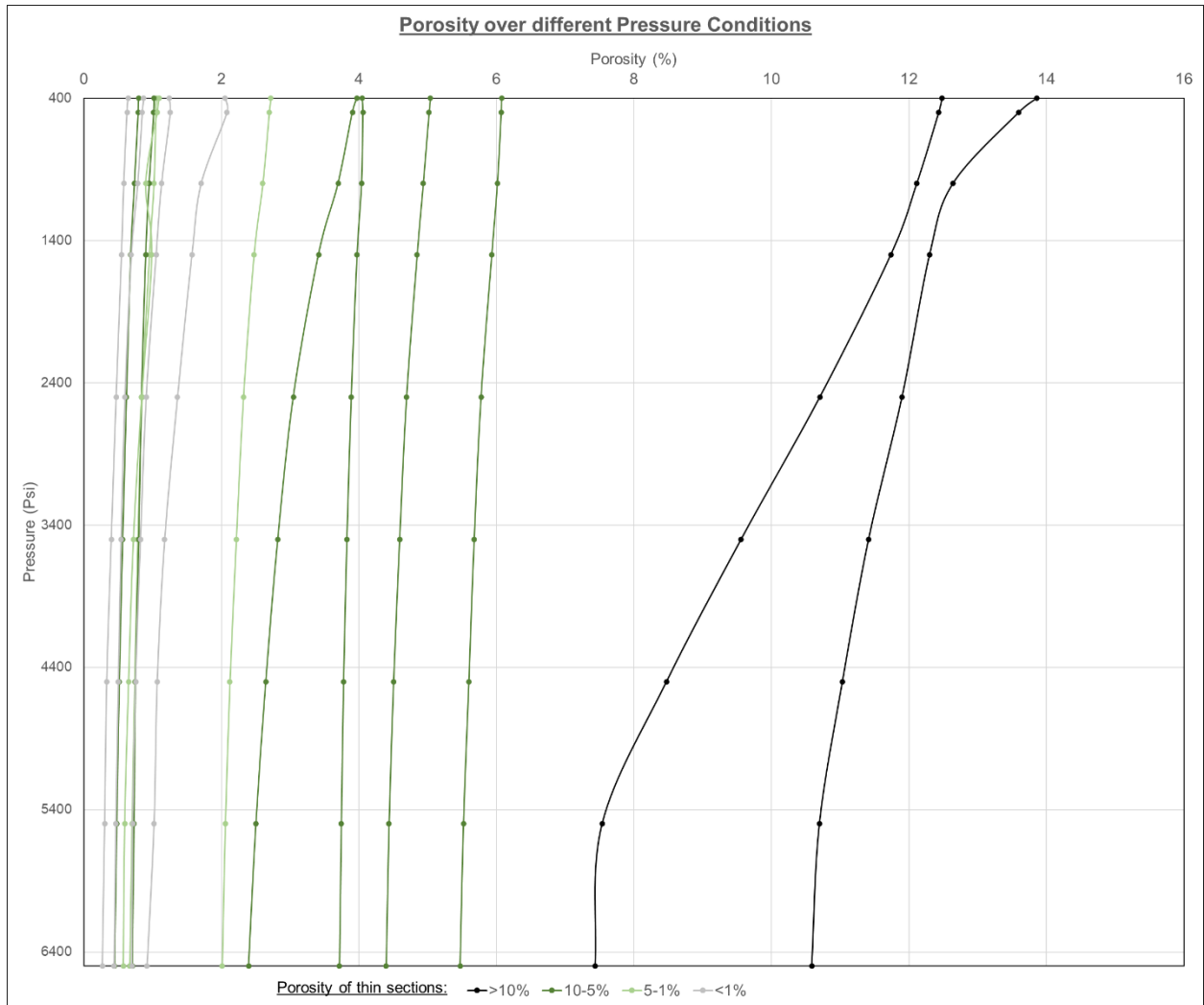
Figure 58: Porosities of the thin-section samples determined with the gas-permeameter Coreval 700. Samples with high porosity under the microscope tendentially also show higher values for the whole core plug in the measurement.

Figure 59 plots the porosity of the thin sections against the porosity of the core plugs at ambient pressure. The correlation is relatively high for this data set, although it is to be considered that the difference in absolute porosities can still be high.
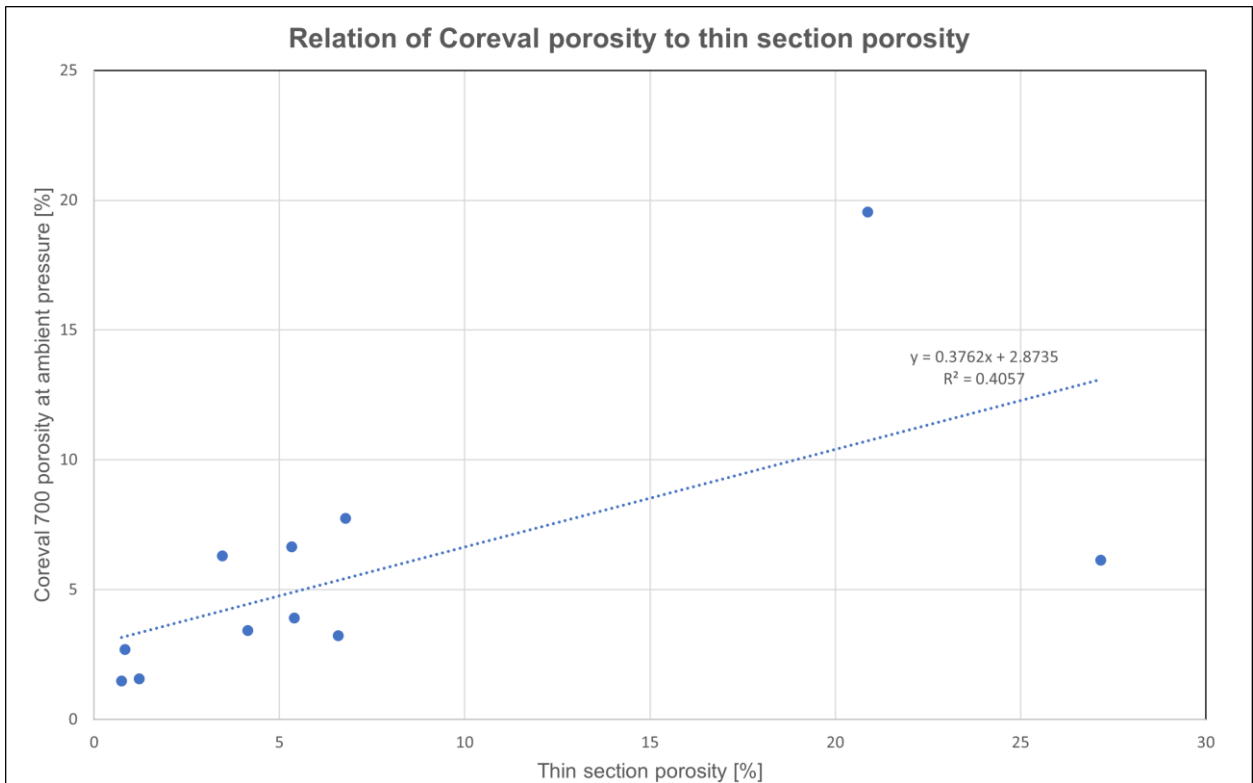
Figure 59: Porosity of core plugs at ambient confining pressure plotted against the porosity-values of the corresponding thin-sections.
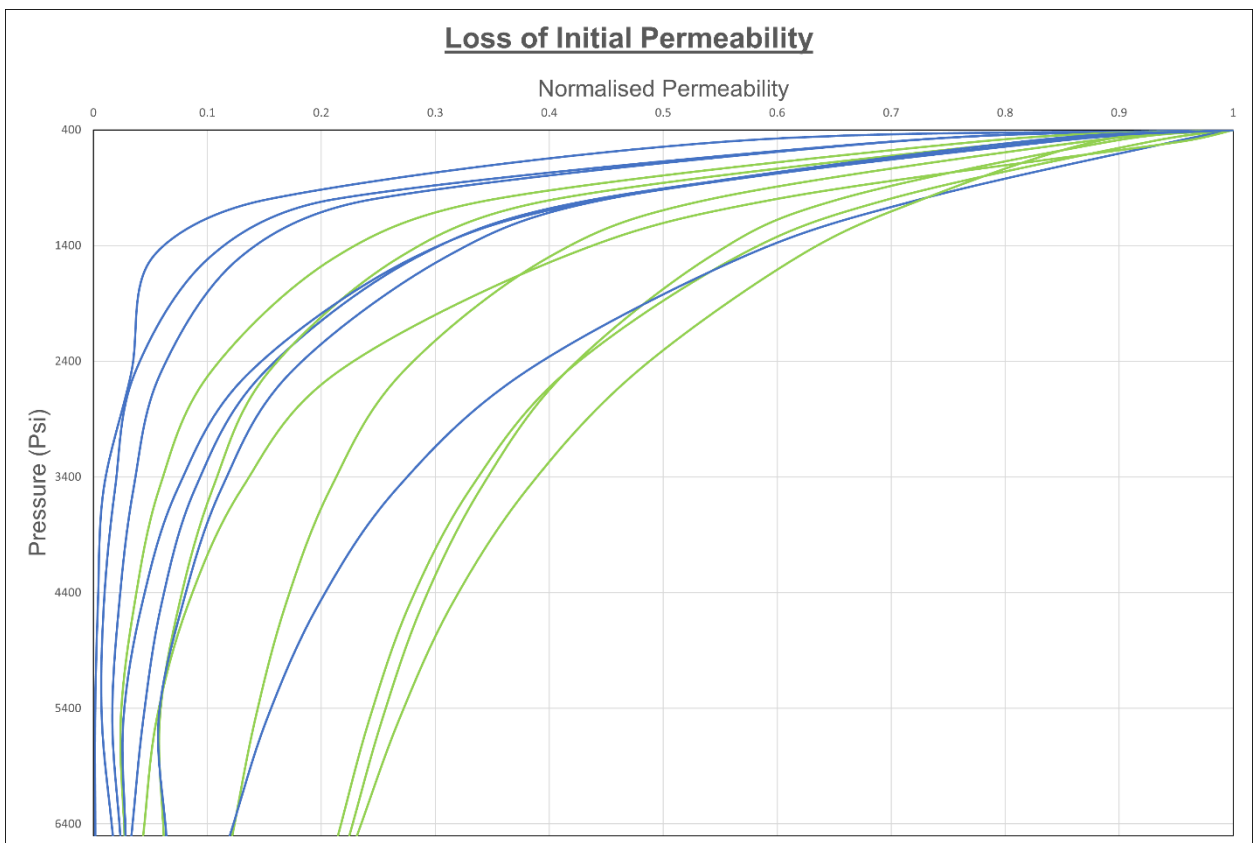
Figure 60: Loss of the initial permeability under increasing confining pressures. Blue marked samples have almost all of their porosity concentrated in the fractures and there is a distinct separation between fluorescent and non-fluorescent areas. Green marked samples also have clearly fluorescent areas, but much of the sample is also fluorescent to a degree and areas completely without any light emission are only found locally.

Fig. 60 and Fig. 61 show the Coreval data of the normalised Klinkenberg permeability and porosity under rising pressure for the samples with thin sections. Although the data itself consists of the Coreval measurement, the samples were divided into the two different groups, according to their thin-section attributes, explained at the chapter beginning (9.4).

Instead of the absolute values, the behaviour of the samples under confining pressures is of interest. The samples with clear separation of light and non-light emitting areas (blue) show a higher loss of permeability and porosity, relative to their initial values, than the diffuse emitting (green) samples do. This applies to the whole range of confining pressures.
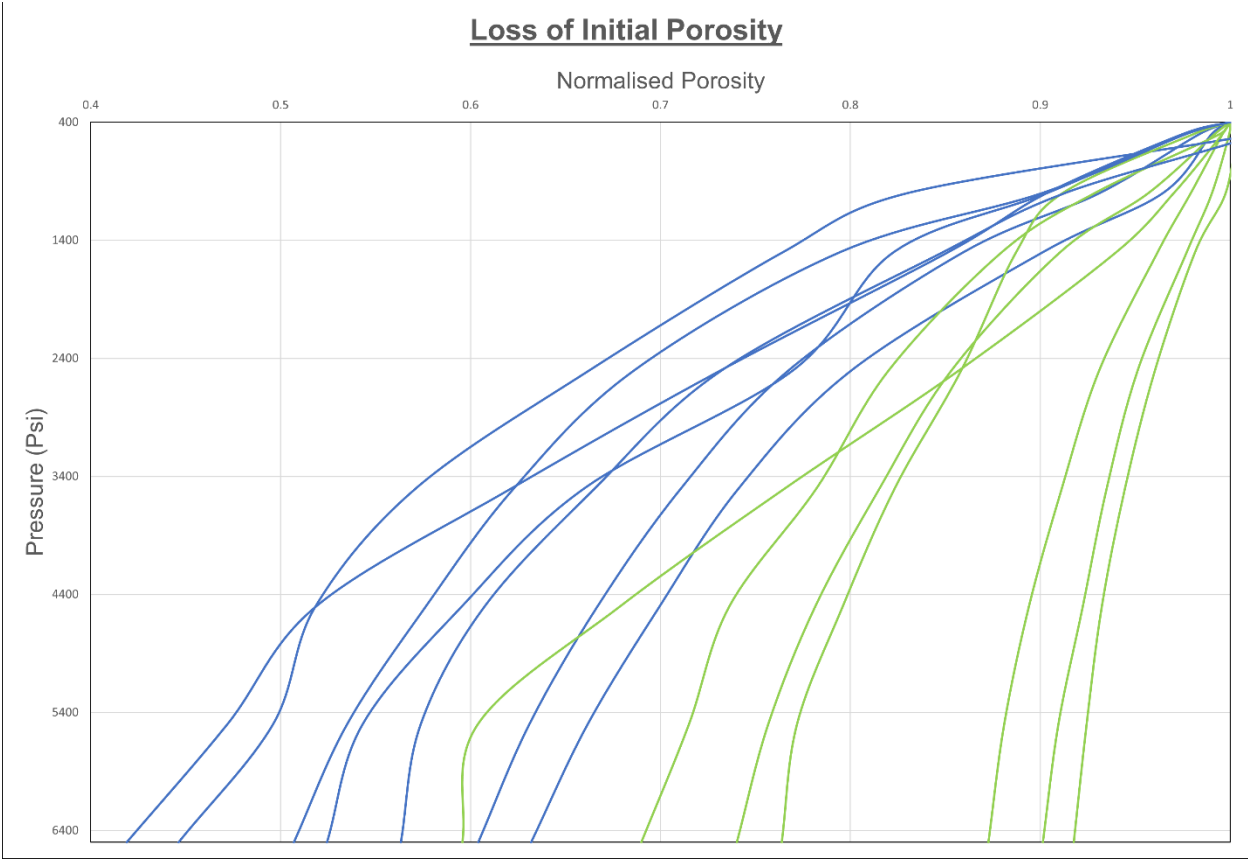
Figure 61: Loss of the initial porosity under rising pressures. The same samples are marked in the same colour as explained in Fig. 60.

10 Discussion

10.1 Immersion data

Most of the samples show typical values for open porosities and raw densities of limestones and dolomites and none of the samples shows a concerning deviation from expected results. The results of the immersion method measurements showed a relatively clear separation between dolomitic, calcitic and karstified samples in terms of porosity and density.

Table 20 orders the results of the different lithologies by their mean porosity. The most porous rocks are the karstified Wetterstein limestone samples, where the high porosity is already visible from a macroscopic view. Matching the high porosity, the raw density of these samples is accordingly low. The interrelationship between high/low porosity and low/high raw density is a unique attribute of the karstified Wetterstein limestone samples. The raw densities of other rock types and lithologies does not reflect the degree of porosity. Naturally, rocks with a high porosity can act as a water storage and have the potential to retain water masses longer in the rock volume before it flows out of springs. This can be doubted in the case of karstified Wetterstein limestone, since the karstification itself is a result of water flow, which suggests a higher permeability.

Samples with relatively high porosity, but still normal values of densities are cataclasites from protoliths of the Wetterstein Fm., Wetterstein dolomites and Wetterstein limestones.

Cataclasite data shows a big spread over both clusters and the density shows no typical values. This is not surprising in any way, if we keep the other dolomite/limestone rock samples in mind. The Wetterstein cataclasites too, consist of samples of dolomitic and calcitic material. Each of these Cataclasites fits into the corresponding cluster/trend, depending on the deformed parent rock material. The porosity of the cataclasites is generally high, it does not matter if the parent material is dolomitic or calcitic origin. As with the karstified examples, a long retention phase of water is not to be expected in cataclasites, since they are generally to be viewed as permeable rocks (Uehara & Shimamoto, 2004). It must be said tough, that fault gouges as accompanying feature of cataclasites in fault zones can act as an impermeable layer. Depending on geologic structures, a build-up of water in cataclasite rocks is imaginable, although it is neither known nor to be expected in the area of the Kuhschneeberg.

Karstified Wetterstein limestone			
Parameter	Mean	Minimum	Maximum
Porosity [%]	9.44	7.18	12.87
Density [g/cc]	2.27	2.22	2.34

Cataclasite			
Parameter	Mean	Minimum	Maximum
Porosity [%]	4.05	2.83	6.21
Density [g/cc]	2.67	2.60	2.73

Wetterstein dolomite			
Parameter	Mean	Minimum	Maximum
Porosity [%]	2.80	1.73	4.44
Density [g/cc]	2.73	2.65	2.78

Wetterstein reef limestone			
Parameter	Mean	Minimum	Maximum
Porosity [%]	1.86	0.28	6.02
Density [g/cc]	2.66	2.59	2.71

Opponitz limestone			
Parameter	Mean	Minimum	Maximum
Porosity [%]	1.75	0.94	2.40
Density [g/cc]	2.62	2.61	2.65

Hornstein limestone			
Parameter	Mean	Minimum	Maximum
Porosity [%]	1.71	0.57	2.61
Density [g/cc]	2.64	2.56	2.70

Haupt dolomite			
Parameter	Mean	Minimum	Maximum
Porosity [%]	1.22	1.22	1.22
Density [g/cc]	2.78	2.78	2.78

Wetterstein reef debris limestone			
Parameter	Mean	Minimum	Maximum
Porosity [%]	1.04	1.04	1.04
Density [g/cc]	2.66	2.66	2.66

Lagoonal Wetterstein limestone			
Parameter	Mean	Minimum	Maximum
Porosity [%]	0.97	0.68	1.74
Density [g/cc]	2.67	2.64	2.68

Stylobreccia			
Parameter	Mean	Minimum	Maximum
Porosity [%]	0.69	0.64	0.75
Density [g/cc]	2.67	2.66	2.68

Table 20: Results of the immersion method measurements of the handpieces. The lithologies are sorted by their mean porosity, from highest to lowest. Density is raw density.

A strong difference is visible, when comparing the dolomite results to the limestone results of the Wetterstein Formation. Dolomitic rocks around the Kuhschneeberg have much higher porosities and raw density than the Wetterstein reef limestones. This trend is relatively clear and only a few limestone samples show comparable results to the dolomites. This is not surprising however, since rocks to not have to be fully dolomitized and Wetterstein dolomite is not as clearly separated from Limestone in the field as geologic maps represent them. The weak overlapping of Wetterstein reef limestones and dolomites is therefore seen because of both lithologies not being purely separated entities. Especially since the dolomitic areas in the region border the Wetterstein limestones directly.

The contrary, Wetterstein dolomite samples, which plot in the cluster of limestones, is not observed. This is interpreted as a subjective bias to only classify dolomites as such, when the HCl test is unambiguously speaking for dolomite.

Wetterstein dolomites have a much higher porosity and only a few samples reach porosity values of under 2%, a clear difference to Wetterstein Limestones with half of the samples of them being under that threshold. The generally higher density as well as the higher porosity of dolomites fits existing literature. It can be arguable that the fine fractures of many of the Wetterstein dolomite samples (Pavuza & Traindl, 1983:17) can give the impression of higher porosity, but the FDC-sorted results show no difference to less fractured samples in this thesis, which indicates the intern structure to be the main factor for the different porosities, not fractures through induced stresses.

The higher porosity of the dolomitic Wetterstein samples would give them a better water retention ability and make them a factor for a more stable spring discharge, if the permeability results do not contradict this.

Unlike the Wetterstein reef limestone, the samples of the lagoonal Wetterstein limestone have low porosities and medium raw densities throughout, although this can just be a result of missing dolomitization in the sample pool of the lagoonal Wetterstein limestones. The same can be applied to the Wetterstein reef debris limestone sample, although the clayey matrix material probably adds to the low porosity too and might be a factor for the permeability of the sample, since the clay could build up an impermeable layer.

The Hauptdolomit Fm., Opponitz limestone and Hornstein limestone samples show medium porosities, and their densities are high (Hauptdolomit Fm.) respectively low (Opponitz and Hornstein limestone), which further emphasizes the difference in density between dolomites and limestones. It must be mentioned that the Haupt dolomite results

consists of only one sample (1 handpiece/ 1 core plug), so conclusions must be made with care.

The spread in the results of the porosity of the Hornstein limestone is noticeable, although not surprising considering the Hornstein limestone is a relatively inhomogeneous lithology in even small scales, as the different samples show.

Continually low in terms of porosity value are the stylobreccia samples, which can be explained through pressure and the pressure induced solution seams. Both factors can be seen as a reason for the loss of porosity or the shutting of pore space, creating isolated pores.

The FDC`s are not found to influence the porosity values. The values of samples with higher FDC show no tendency to be more porous than FDC 2 and FDC 1 samples of the same or other lithologies.

With this, one influential parameter for permeability (the fracture intensity) is not recognizable from results of the immersion method and must be observed in the field before. This also indicates that possible permeability results can differ greatly from expected values from just looking at the immersion data beforehand, even though higher open porosity generally favours fluid transport.

Permeability and porosity are also causally linked as porosity is a result of increased permeability and vice versa, at least for carbonate rocks, as the karstification builds a positive feedback-loop of permeability and porosity.

The porosity itself determines the potential of long-term retention and storage potential of the groundwater reservoir. This does not concern large karst voids, since they are expected to run dry rapidly, therefore karstified rocks have no long-term storage potential.

A note must be made about the comparison of porosity of the handpieces with their matching core plugs. The handpieces have a higher porosity than the core plugs, the difference in porosity gets only slightly higher, the more the sample is porous. Two factors can be considered at fault for the tendency of the handpieces to have larger porosities. First, the drilled samples might simply be less porous, since more porous unstable parts of the handpieces (like a weathered surface) are more likely to be destroyed in the drilling process, whereas the more resistant parts with less porosity rather will be drilled into core plugs.

Another explanation is that the outer pores near the surface easily lose water instantly before the weighting process of the wet sample material. Since core plugs are smaller than the handpieces, more of the pore space volume is to be considered near the surface, where the pores are not filled with water during the measurement. A larger handpiece loses a smaller pore volume through this effect.

10.2 Coreval Data

The two most important results of the Coreval are the Porosities and Klinkenberg-Permeabilities under different confining pressures.

10.2.1 Porosities:

Like the immersion method, the Coreval 700 measurements also give information about the porosity of the plugs at ambient pressure.

What instantly shows is the similarity of porosity values at ambient pressure between the lithologies. Taking out of the equation the karstified Wetterstein samples, the differences between porosity are small between the lithologies. Cataclasites, dolomites and the Opponitz Fm. stand out with tendentially higher porosities, although still much lower than the porosities of the karstified Wetterstein samples.

Clearer is the distinction of porosity ranges between the three Wetterstein lithologies, observed under rising confining pressures. At 400 psi confining pressure lagoonal Wetterstein limestone has values of around 1-2 %, Wetterstein reef limestone of 0.5-4.5% and Wetterstein Dolomite of 3-5 % porosity. The differences between the three lithologies are also still preserved at 6500 psi confining pressure, where the lagoonal limestones generally show around less than 1% porosity, whereas the Wetterstein dolomites still have porosities of around 3%.

The high porosity-values of the Wetterstein dolomite support the observation, that dolomite tends to have a higher water retention ability. Although not solely dictated by the porosity, a higher porosity enables dolomite to keep a steady water supply for longer durations without rain fall/melting ice.

Wetterstein reef samples, again, show more diverse values. This could be explained too by a variation in dolomitization, as explained in the "Immersion Data" (10.1) chapter. The Wetterstein Lagoonal Limestone is characterized by its constant low porosity.

Further lithologies were measured too, although the lower sample numbers make general conclusions more difficult. However, the values fit the overall expectation. Especially the porosities of the karstified Wetterstein limestone reach values of above 10% porosity at 400 psi confining pressure and still have higher porosities at 6500 psi confining pressure than all other samples have at ambient pressure.

Next highest porosities are found for the cataclasites from Wetterstein carbonates, the porosities range from roughly 6 to 3% across the whole pressure range. The higher share of matrix material does not decrease the porosity, instead it is even higher for the cataclasite type 2 sample. An indication for the reason can be seen in the thin-section photo of PW7/3, where the sample parts with more matrix-share also show more UV light emission.

The lowest porosities of the further lithologies are found for the stylobreccia, the Opponitz limestone and the Wetterstein reef debris limestone. Surprisingly high and varied can the porosities of the Hornstein Limestone be, which supports the macroscopic variety of the collected samples. The same reasons for the porosities of these lithologies can be applied as mentioned in the discussion of immersion results (10.1).

Not only the porosity at 400 psi is interesting, also the percentual change in porosity over different pressures. As seen in Fig. 40, the rest of the porosity still preserved after 1500 psi can vary quite a bit for individual samples, although differences in lithologies are more difficult to find. The loss of porosity is not as high as the loss of permeability, every sample still maintains more than 75% of porosity. Even though the numbers are considered under percentual views, there seems to be an overlap with the total porosity data. The lithologies with high porosities under 400 psi also retain more of their percentual porosity at 1500 psi. This makes sense if we consider pore space as a network of individual pores. The more pore space is present in a sample, the more likely every individual pore will maintain a connection to the network, if the overall pore space gets smaller. The open porosity therefore is easier to conserve if the pore space generally is high.

The bulk modulus, describing the resistance of a rock to volume-change, seems unlikely to be a big influence in pore reduction of these samples. Generally, the bulk modulus of

dolomite is lower (Sayers, 2008: Calcite: 76,8 GPa; Dolomite: 76,4 GPa), meaning it should be easier for the dolomite to lose core plug volume and experience a loss of porosity. This is the reverse of what the results show: Dolomites tend to keep their volume (directly linked to porosity in the measurements) more than the limestones.

It is also questionable that the Karstified Wetterstein samples have a high bulk modulus in relation to non karstified material. The structure and pore sizes are more likely to enable Karstified Wetterstein samples and Dolomites to keep their porosity under higher stress, since wider pore apertures and many connections between pores make it more likely to keep pores connected to the open pore system under pressure.

Fractures do not seem to play a noteworthy role in the loss of porosity due to increased confining pressure, as their influence itself on the porosity itself is not seen from the immersion data (Fig. 21, 24, 26). No clear correlation can be seen between the FDC´s and the porosity, which is also shown in the results of Wimmer (2020:35). It is possible that the different lithologies and Wetterstein rock types are a far more deciding factor for the porosity than the FDC-values of the samples.

Other possible influences on the porosity loss are the ratio of grain size to pore sizes and structure of the pore-connections.

10.2.2 <u>Permeabilites:</u>

The permeability measurements of the Coreval 700 show us an influence of open porosity on the permeability (Fig. 39). Samples with higher porosity tend to have higher permeabilities across all confining pressures, as can be seen by the trend lines.

The more deciding factor of permeability is, if present, the degree of fracturing of samples and rock material. Especially interesting are the statistical outliers with high permeability of the three Wetterstein lithologies mentioned (dolomites, reef limestones and lagoonal limestones). Here, every lithology includes one sample with extremely high Klinkenberg permeability (>1 mD at 400 psi confining pressure). Every one of these three samples (PW1/6 [6,8 mD], PW4/4 [1,6 mD], PW6/8 [1,8 mD]), seen in Fig. 29-31, includes at least one clearly visible fracture, which runs along the path of flow, meaning from the top of the

sample to the bottom. This indicates that the inherent characteristics of the rocks at Kuh-schneeberg are of minor importance to the fluid flow in relation to the permeability induced through fractures, which varies much more from sample to sample. Just one fracture can determine the intensity of permeability of the whole sample. The three mentioned samples all show clear signs of permeability loss over increased confining pressure. (3-12 % Klinkenberg permeability left at 6500 psi).
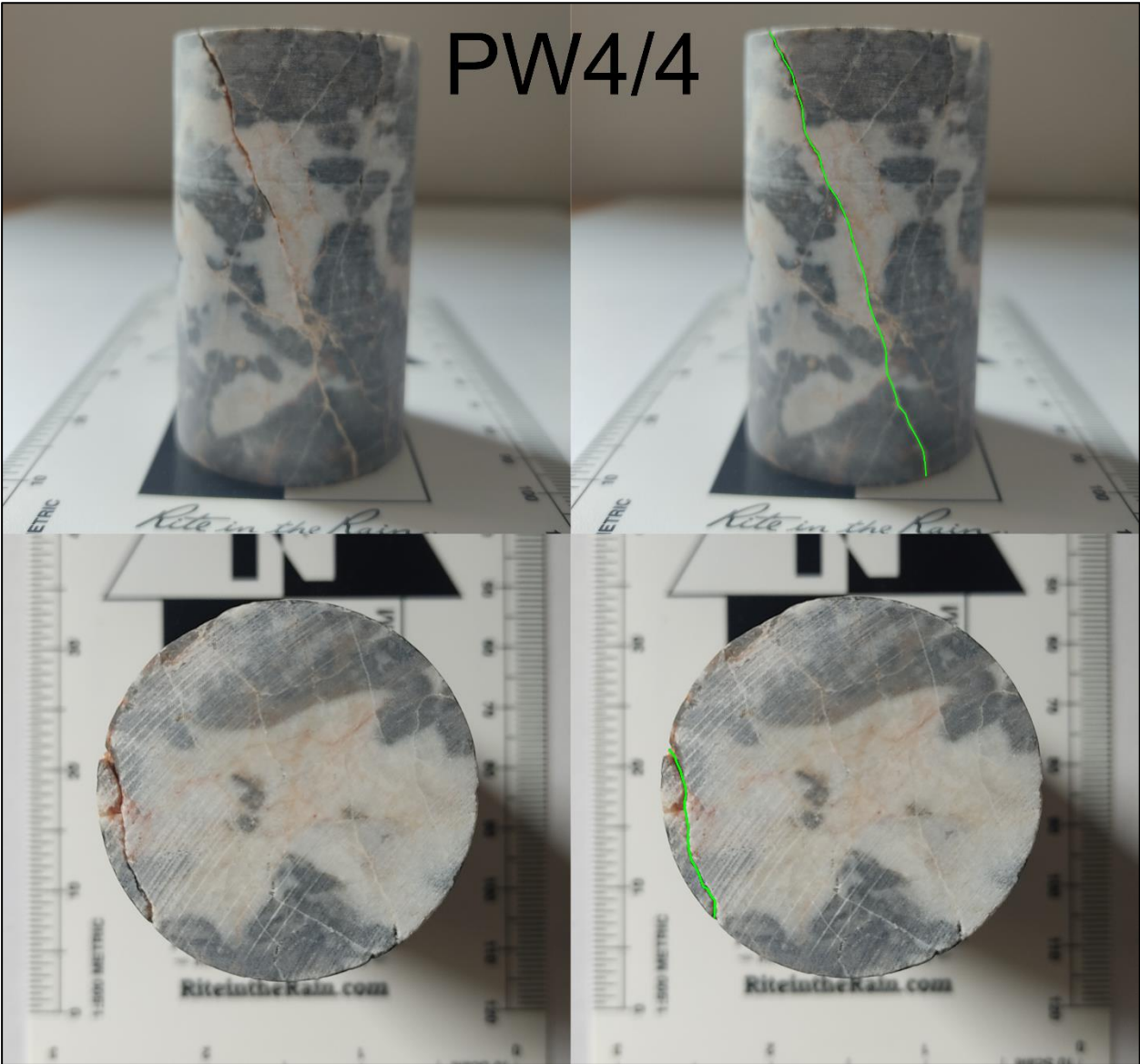
Figure 62: Sample PW4/4 is a good example of a classic high-permeability core plug, as are PW1/6 and PW6/8. At least one pathway for fluid flow is visible from one end to the other of the sample (green marking).

The initial permeability does not give knowledge about the absolute loss of permeability at higher pressures beforehand, although it is true that samples with high permeabilities at 400 psi tend to lose more absolute permeability over the further pressure measurements. Simultaneously, many samples with similar initial permeabilities have different curvatures with rising pressure and the percentual loss of permeability is not necessarily

higher for samples with high initial permeability. Generally, the permeability has the potential to change much more drastically than the porosity with rising pressure and is already at 1500 psi rarely above 50% of its initial value.

The fact that samples with similar permeabilities at 400 psi have different curvature paths along rising confining pressure can have different explanations. It can be dependent on the shaping of the faults/fractures and their asperities or the size of its pores (Fig. 17). For fracture-dominated samples the idea would be that fractures with uneven surfaces and longer asperities cannot be sealed under pressure as easily as fractures with almost planar surfaces. Pore-dominated samples can differ in pore size and therefore also in the size of pore connections, making it more probable to keep fluid flow paths open, if the pore sizes are bigger. Pore form can also make a difference since spherical pores have a high resistance to confining pressure through their pore pressure.

Relatively variable is the permeability of the karstified Wetterstein samples. This samples are missing visible fractures and are therefore a representation of pore-dominated samples with high-porosity. Even though all of them show a high porosity in the handpieces and plugs, the permeability can be very low in certain samples (up to only 0.06 mD at 400 psi confining pressure) and extremely high in others (over 30 mD at 400 psi confining pressure). The samples are exemplary to see the spread of porosity-permeability correlations, as even samples with high porosities can show minor permeability in certain directions.

The collected cataclasite samples have a relatively low permeability for the density of fractures and pore space, yet still higher than most parent rock samples (Wetterstein dolomite). The grain size reduction of the rock material during deformation increases the porosity of the parent's rock. Together with the fracturing, this makes the permeability of the cataclasites even higher than of the non-fractured Wetterstein dolomites.

Surprisingly high is the permeability of the Opponitz Formation. Even if the sample number is not meaningful for detailed analysis, it shows at least that even lithologies, classified as non-permeable, can locally have higher permeabilities. It is therefore not recommendable to automatically assume a low-permeability layer in the regional geology, wherever the Opponitz F. is found. Especially considering the relative thin thickness of the Opponitz Formation.

Samples, which confirm the suspicion of being low-permeability layers are the Wetterstein Reef debris limestone, the Hornstein Fm. and the stylobreccia. Although the cause of their origin is different, these samples most probably have their low-permeability characteristic through their share of finely grained material, cemented seams and/or absence of bigger cracks.

10.3 The correlation between Immersion Porosity and Coreval Porosity

It was already discussed that the handpieces and core plugs show slight differences, when measured with the immersion method. This is expectable and any comparison of the handpieces and the core plugs of the Coreval measurements must consider, that the samples of the Coreval measurement contain less volume (loss of information).

The measurements done with the core plugs, show clear systematic differences in results, as shown in Chapter 9.3.
Three differences stand out: Coreval porosities are almost exclusively higher, the difference in absolute porosity increases, the higher the porosity of the rock is and the Coreval data rarely reveals values less than 1%, a threshold not reached by many immersion method core plugs.

There are three possible explanations for explaining the different porosities recorded by both methods. First, the Coreval 700 works with N_2 instead of water. The viscosity of N_2 is much lower than that of water and no surface tension mechanism is at work. This enables N_2 to fill pore spaces much more easily and leads to higher porosity readings, especially since no mechanism such as water saturation under vacuum conditions was used in the immersion method to overcome the problem of surface tension of water.

Second, the surface pores (pores, which were cut through during drilling) hold no water back in the immersion method, which affects the porosity values negatively as explained in Fig. 11. These pores are not excluded in the Coreval measurements, since the core holder utilizes an elastomer sleeve, which fits around the whole sample, including the partly cut-through pores.
Naturally, the influence will be less high for samples with almost no pore space and no bigger pore spaces after drilling. However, samples like LP19.2 seem to be affected significantly, explaining the increase of differences between immersion and Coreval porosities with increasing porosities.

The third factor is the deviation from the perfect cylinder forms needed for the Coreval 700 device. Not every plane is perfectly orthogonal to the length of the sample and many samples had small cut-outs on their surface, which explains why the samples rarely reach very low porosity values during the Coreval measurements.

Oddly, because the Coreval porosities are often higher than the immersion porosities and the porosity of the handpieces is most of the times higher than the porosity of the core plugs, many handpieces show more similar porosities to the Coreval 700 data, than the core plugs.

10.4 Analysis of thin-sections and their significance

The images of the UV-microscope give a clear overview of the abundance, shape and size of open pores, the open fracture-length per area of the samples as well as the connection and width of the fractures. With this information, it is possible to describe exactly how the permeability and porosity values of the Coreval 700 measurements are to be understood for individual samples and which were the deciding factors.

More important than the detailed view of the individual structures of singular samples in the results are the differences between the two sample groups. A comparison of the Coreval results between the two thin section groups showed different behaviour of the samples under rising confining pressures:

Samples with a very localized UV light emission concentrated in narrow open fractures lose much of their initial permeability and porosity (normalised to their initial values at 400 psi). These samples emit light in only a small part of the samples thin section area and the light emission in a specific part of the sample is either strong (in pores or fractures) or not existent. Naturally, this condition often is showing in fracture dominated samples, where the strong emission of the fractures is present near non-emitting sample material.

In relation, the loss of permeability and porosity for samples with a diffuse distribution of UV light emission is much lower. These are often samples with noticeable pore space, which naturally provides a dispersion of UV light emission.

The degree of localization, respectively dispersion, of UV light emitting porosity therefore may serve as a proxy for the loss of permeability and porosity of a sample due to the increase of confining pressure. The two discussed groups tend to be separable by their

type of porosity in the thin section: fracture- or pore-dominated. This does not reflect all samples tough. A dispersed pattern of UV light can also be reached through a strong fracturing, as shown by sample PW7/3 or LP41. A pervasive dense fracturing network gives much surface, where pore space can connect (open porosity) into the inner parts of the sample. At the same time, samples with a few singular enlarged pores (like MT17) can be strongly localized terms of UV emission.

The main factor for a rock´s resistance to permeability/porosity loss under pressure is therefore the connection of the pore space, recognizable through the dispersion of UV light emission.

Observations from the thin sections for individual samples are found in the chapter 12 "Samples".

Naturally, the thin sections cover only a small part of the plugs and an even smaller part of the whole rock samples, which needs to be considered for every conclusion, as for example LP11 shows. Here the thin section only covers the high porosity characteristics of one side of the plug. The other half of the core plug seems to be much more solid, information the thin section naturally does not include. There is still a rough correlation of the porosity values of the thin sections to the porosity of the Coreval-data, which tells us, that the thin sections can be used to approximately represent the whole core plug in many cases.

11 Conclusion

Most of the Kuhschneebergs lithology consists of fractured carbonatic rocks, with siliciclastic rocks being only a minor fraction of the mountains volume. The most important factors for the porosities and permeabilities are the karstification, fracturing and dolomitization. Whereas porosities are more predictive and more similar in the examined rocks, the permeabilities can change drastically, even within a lithology.

Whereas dolomitic samples have a higher porosity (and density) than limestone samples, the permeability is not noticeable influenced by a dolomitic composition. The fracturing and karstification are the important parameters for the permeability of a sample. Additionally, karstification strongly increases the porosity of a sample.

Lithostratigraphic unit	Tectonic Unit	Por (immersion, handpiece)	Por (gas)	Perm (klink)
Jura Hornstein limestone	Göller N.	1.7	3.1	0.007
Hauptdolomit Fm.	Göller N.	1.2	-	-
Opponitz Fm.	Göller N.	1.75	6.6	1.1
Wetterstein Fm. (reef limestone)	Schneeberg N.	1.9	3.7	0.2
Wetterstein Fm. (lagoonal)	Schneeberg N.	1.0	4.2	0.4
Wetterstein Fm. (dolomite)	Schneeberg N.	2.8	5.6	1.2
Wetterstein Fm. (reef debris)	Schneeberg N.	1.0	2.2	0.006
Wetterstein Fm. (karstified limestone)		9.4	18.8	7.4
Wetterstein Fm. Cataclasite 1 (dolostone)	Schneeberg N.	3.3	6.0	0.3
Wetterstein Fm. Cataclasite 2 (dolostone)	Schneeberg N.	6.2	8.1	0.3
Wetterstein Fm. Stylobreccia (limestone)	Schneeberg N.	0.7	4.1	0.02

Table 21: Overview of mean porosities of the immersion method and the Coreval 700. Permeability values are in mD at 400 psi and porosity in % at ambient pressure.

The fractured carbonatic rocks form the main part of the Kuhschneeberg and therefore are decisive for the fluid flow of the mountain. The characteristics of fractured carbonatic rocks are to be described as having low to medium porosities, ranging from around 0,3 to 5,5 % and permeabilities ranging from almost zero (0,00x mD) to as high as 6,8 mD. However, the permeability is strongly dependent on the intensity of fracturing and the direction of the fractures. The unfractured carbonate matrix itself, is not sufficiently permeable to support "fast" fluid flow. Permeability data obtained from plug-sized samples,

however, is not indicative for the permeability of the rock mass of the Kuhschneeberg at large scales. At the map scale, the aquifers may have a relatively high permeability due to the presence of fault zones containing densely fractured and karstified rock (Prandstätter, 2022). Such fault zones may provide "fast" alternatives for the waterflow, even when the unfractured rock is relatively impermeable.

It is therefore to be expected, that the preferred pathways of deep groundwater flow of the Kuhschneeberg overlaps with the fault system (Prandstätter, 2022). The impermeability of unfractured limestone and dolomite material only add to fractures deciding the fluid flow.

The high influence of the fractures also makes it less relevant which type of carbonate the fluid flows through, although the higher porosity of dolomites gives them a higher water retention ability under similar fracturing conditions.

Karstified rocks show a wide variability in porosity (around 11 to 25 %) and permeability (from around 0.1-30 mD). It is remarkable how low the permeability can be, despite such a high porosity in individual samples. However, since the porosity is a direct result of water flow, it should be considered that the permeability of individual samples could be at least a bit more pronounced in other flow directions. The measurement with the Coreval only considers flow into one specific direction, therefore it is not to be excluded that measurements in other directions yield different results for these rocks. Especially since the inhomogeneity of the material is clearly visible.

Overall, none of the lithologies show increased porosity and have a low enough permeability to be considered a water reservoir, since the permeability is too high through the fracture network. The dolomites continuously showed a higher porosity, which increases the water retention potential, but still is relatively low in relation to classical water reservoirs like sandstone.

Consistently low permeabilities of < 0.1 mD were determined from stylobreccia fault rock and the sampled Jurassic Hornstein limestone. Together with their low porosity values (0.5 to 3 %), these lithologies could be considered as impermeable layers if they reach significant thickness and no breaching by fractures or faults is involved. Although the drilled core plugs do not show signs of fracturing, these lithologies were still involved in faulting.

It is not surprising therefore, that through missing aquicludes in the higher layers of the Kuhschneeberg, springs are mostly found at the base of the Kuhschneeberg (border between Schneeberg and Göller nappe). Often these springs are also associated with a fault-system (Fig. 63). The connected network of cleavages makes the Kuhschneeberg and the surrounding vulnerable for pollutants, as they can advance fast over a wide area and volume.
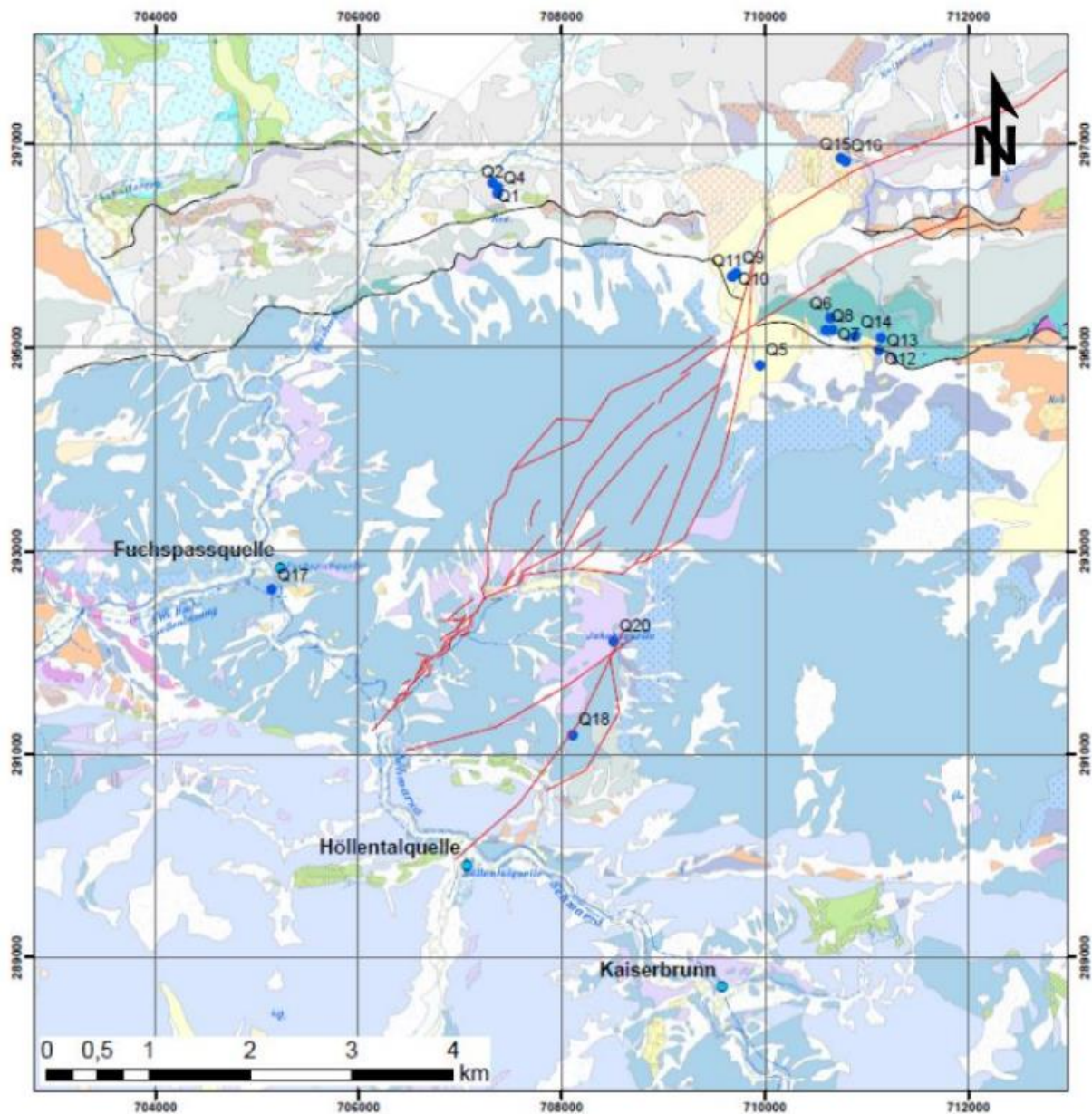
Figure 63: Springs in the area of interest. From Prandstätter (2022:37).

The porosity values of the different methods show clear systematic differences, even within one method (immersion method) the results change drastically (up to 16.5 % absolute difference in a few samples, mostly 0.3-5%).

Measuring the core plugs instead of the whole rock samples continuously delivers lower porosities. The explanation for this effect could be that core plugs tend to consists of less porous (and less fractured) material, since fractured parts of a handpiece do not survive

the process of plug preparation (drilling, cutting). The described effect may result in a significant sample bias. A second explanation, not in contradiction with the first, is that the volume to surface ratio of core plugs is lower, therefore more proportion of water is lost before measurement of the wet core plug material than of the whole rock samples. As a consequence, pore space will be lower for smaller samples, in this case the core plugs. Third, it must be considered that, by their size, core plugs are not representative volumes for fractured rocks with fracture spacings exceeding the plug dimension. Data derived from plug-size samples therefore cannot account for the porosity contribution of such fractures.

A further systematic difference exists between the porosities of the Coreval 700 measurements and the immersion method in the core plugs. The Coreval 700 results are generally higher, which can be attributed to other factors. As determined the three factors changing the porosity values are: the type of fluid, the difference in observed volume through the sleeve and possible deviations from the perfect cylindric form. N_2 is better suited to fill the whole sample through missing hydrogen bonding, the sleeve also includes the outer pores, where water gets lost in the immersion method and deviations from the perfect cylindric form can increase the porosity in the Coreval 700 results.

The coupled effect of the systematic deviations of the immersion method itself and in relation to the Coreval 700 device can lead to the effect, that the porosity of the handpieces is often more similar to the Coreval 700 results than the core plugs themselves.

This does not mean that one method is more fitted to use to find the porosity of a rock than the other. The immersion method will give a tendentially lower porosity value, than it really is because not all the pore space gets filled with water or water is lost before the weight is measured. The Coreval 700 device on the other hand can lead to results, which can potentially be higher than the real results, if the sample material does not represent an ideal cylinder. Most immersion results are lower than 1 % porosity, whereas the Coreval data is mostly concentrated between 1-10 % porosity (Fig. 42).

If the immersion method is chosen for the weighting of rocks it is therefore recommended to utilize larger samples, if possible, to avoid the effect of porosity loss through lower volume to surface ratios. If the Coreval 700 measurement is chosen, further preparation of the sample material is recommended, like filling out the space of broken out pieces with cement or abrasive finishing to eliminate protruding pieces of rock material on the surface; to approach an ideal cylindric form.

The measurements with the immersion method and the Coreval 700 also showed that the fracture density expressed by FDC-values are not significantly informative about the porosity and permeability at this scale. This result is quite different from other studies that have shown clear positive correlations between fracture density and porosity for dolostone of the Hauptdolomit formation (Decker, 2007) and fractured lagoonal Wetterstein limestone (Bauer et al., 2010). A reason could be that the different characteristics of the examined lithologies are far more deciding and outweigh the influence of the FDC-values. A correlation is therefore more expectable if the sample pool consists of only one lithology.

Thin section porosities do not depict the same sample mass as the core plug measurements do and are therefore not to be useful to represent the porosity of a full core plug. The values still are similar in magnitude (Fig. 59) and give more detailed information about specific porosities at distinct parts of the sample. The difference in porosity in the thin sections still can be multiple times the value of the core plug in specific cases (the Coreval 700 porosity of LP19 2.1 is almost 4.5 times as high as the thin section). Caution is important for samples with a clear change in porosity characteristics over the core plug length, since the thin section only shows characteristics of the surrounding part of the sample.

The Fluorol-filled thin section show an important influence of the distribution of porosity on the reduction of porosity and permeability with rising confining pressures. This thesis shows that samples with porosities localized in a few small regions of the sample, often through fractures, show a larger loss of permeability and porosity with rising confining pressure. Samples with very distributed porosity through pores and partly cemented fractures are less susceptible to these changes. This correlation is not seen from Coreval 700 measurements alone and was only possible through the further analysis of thin sections of the core plug samples.

Additionally, the analysis of the thin section samples gives insight over different porosity characteristics of individual samples, which are not detectable through macroscopic observation or the use of immersion and Coreval 700 measurements. The thin sections show the distribution and form of pore space as well as the interconnection between fractures and their form/width. The effectivity of matrix material closing fractures is also only confirmable through the analysis of fluor-filled thin sections.

12 Samples

LP2

Lithology: Wetterstein reef debris limestone

Sample Size: size: 575 cc

Plugs: 1

Location: 705020 E, 294585 N (MGI Austria GK M34)

FDC: 1
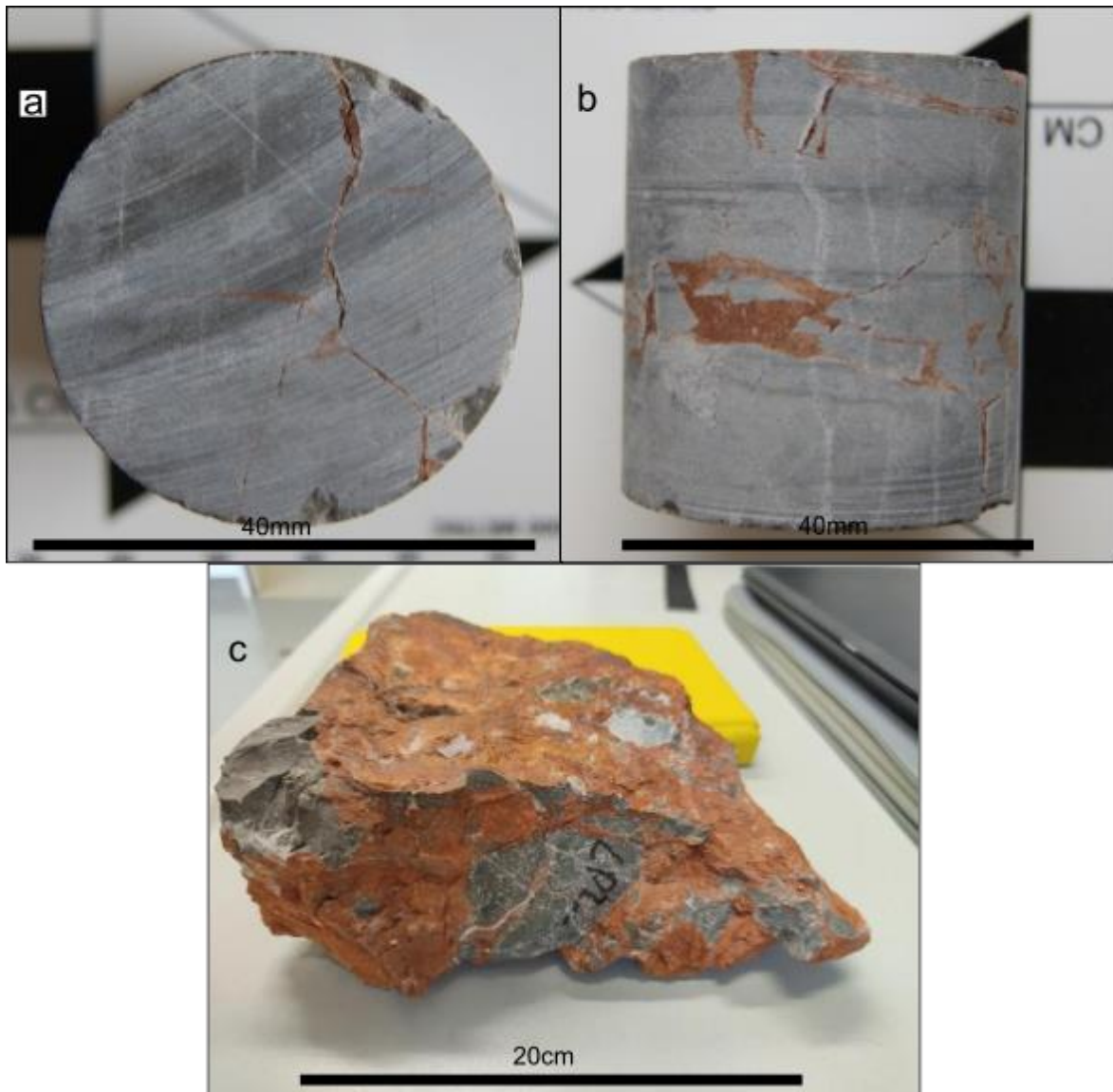
Figure 64: **a)** and **b)** 42,79 mm long core plug of the LP2 Wetterstein limestone (Reef Debris Facies) in top view (a) and lateral view (b), especially the homogeneity of the fragments and the red clay are a visible distinction **c)** Handpiece of the LP2 Wetterstein limestone (Reef Debris Facies), size: 575 cc.

This sample is from a roadcut at the north-western base of the Kuhschneeberg, at the junction between the Höllental and Klostertal. It is an example of the Wetterstein lime-

stone, in this case from the reef-debris facies. It is formed by dark-grey clasts of limestone, with white calcite veins intersecting. The dark- grey limestone is fractured and separated by mm-thick red-brownish clays. All grains are strongly angular. Most of the grains are around 5 cm to a few mm. The main mass seems to be formed from the bigger grains with more than one cm diameter. Veins only cut through the limestone fragments, not through the clay. The rock is massive and is built up of fine crystals, which are not recognizable to the naked eye. Dolomite does not seem to play a significant role, as the rock reacts strongly to hydrochloric acid.

The rock is bedded indistinctly in the handpiece, a feature, which is more distinctive when the whole outcrop is in focus. The clay-layers are often parallel to the bedding but can also cut through it. Surprisingly, the veins are sub-parallel to each other and cut through the bedding planes, despite the rocks being fragmented.

A plug was made from this sample, which is around 1.6 inches long and cuts roughly orthogonal through the banking. The rock reacts robustly during drilling and sawing.

LP7.1

Lithology: Hornstein limestone
Sample Size: 524 cc
Plugs: 1
Location: 710180 E, 295422 N (MGI_Austria_GK_M34)

FDC: 1

Collected near a forest road in the north-western Kuhschneeberg, this is one example of chert-rich limestones from the Hornsteinkalk Formation (Göller nappe). This handpiece looks reddish-brown from the outside but has a considerable amount of white calcite insides. Crystals are recognized with the naked eye, especially the white calcite-crystals from the veins. The calcite grains themselves are mostly around 1 mm diameter and the rock has enough calcite to react strongly to hydrochloric acid. The reddish-brown coloured areas seem to be at least partly consist of chert. The veins are cutting through all features in this sample and seem to be the youngest alteration of rock.

There is no orientation in this 2.7-inch-long rock plug, as there is no inner structure to reference to. There is also no indication of larger porosity/permeability in this rock, as there are no pores and fractures found when viewing the sample and plug.

The form of the calcites often suggests fossil origin, as well as the imprint on the rock sample of a shell.
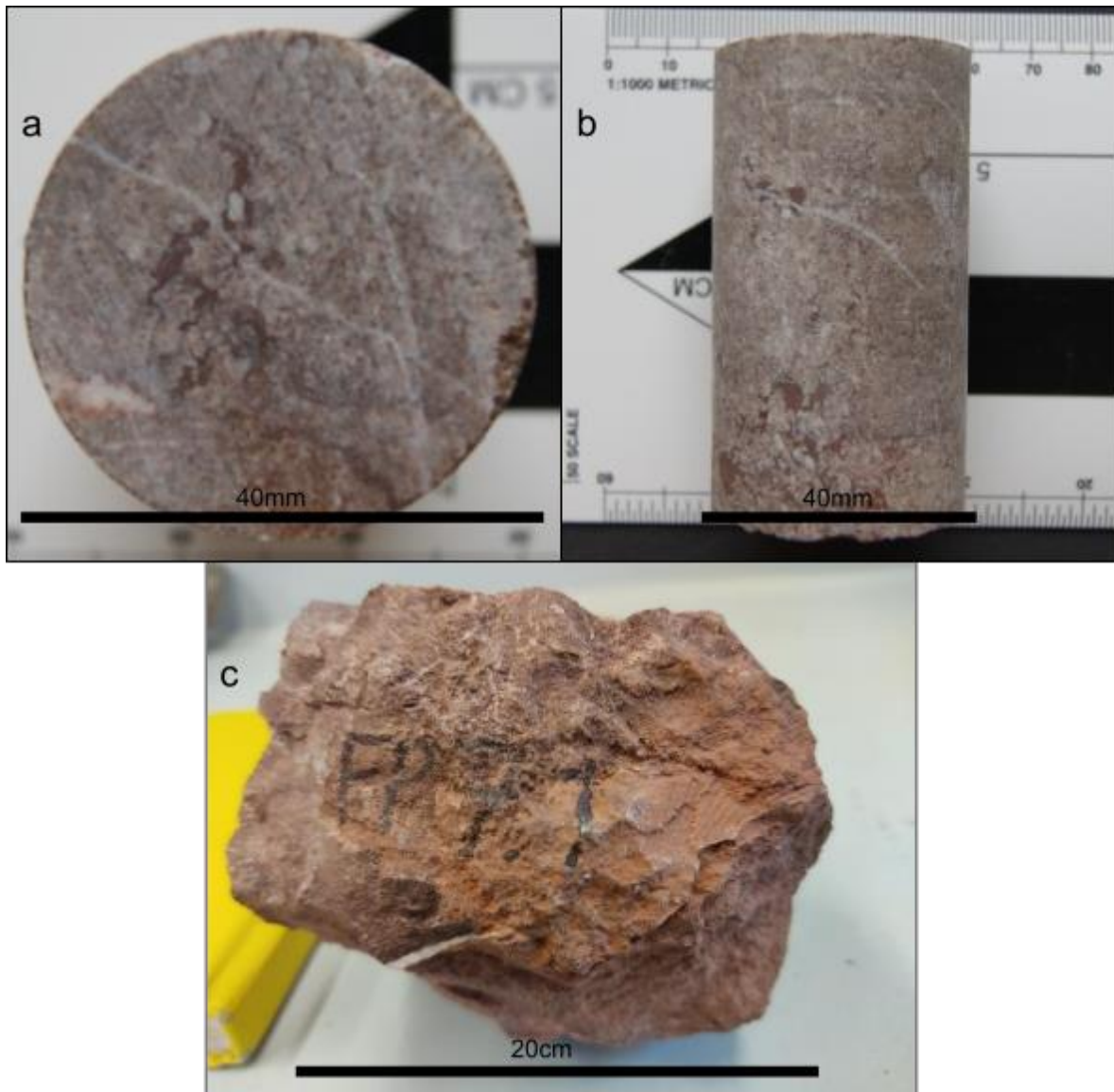
Figure 65: **a) and b)** 69 mm long core plug of the LP7.1 Hornstein Formation in top view (a) and lateral view (b), the numerous white calcite grains are characteristic for LP7.1 and distinct this sample from the other Hornsteinkalk samples, **c)** Handpiece of the LP7.1 Hornstein Formation, a shell-like imprint is visible on the surface, size: 524 cc.

LP7.2

Lithology: Hornstein limestone

Sample Size: 305 cc

Plugs: 1

Location: 710180 E, 295422 N (MGI_Austria_GK_M34)

FDC: 1

From the same outcrop as LP7.1, this sample has a seemingly bigger proportion of chert and clay. There are almost no white calcite grains, and the clay and chert bring in brownish to black tones. The fossil origin of calcites is still recognizable, especially the shell-like structures. Except for those, the grains of this sample are fine and not distinguishable. There is no bedding or lamination of any sort in this handpiece. The sample reacts strongly to HCl.

This sample was in contact with a fault, which is visible in the chert-layer on top of the rock sample, where a few cm offset is visible in the sample. The chert-rich layer has a blistered structure and is found on the sample´s top side. Most of the chert could not be drilled into a plug. However, it was possible to include the offset in the sample.
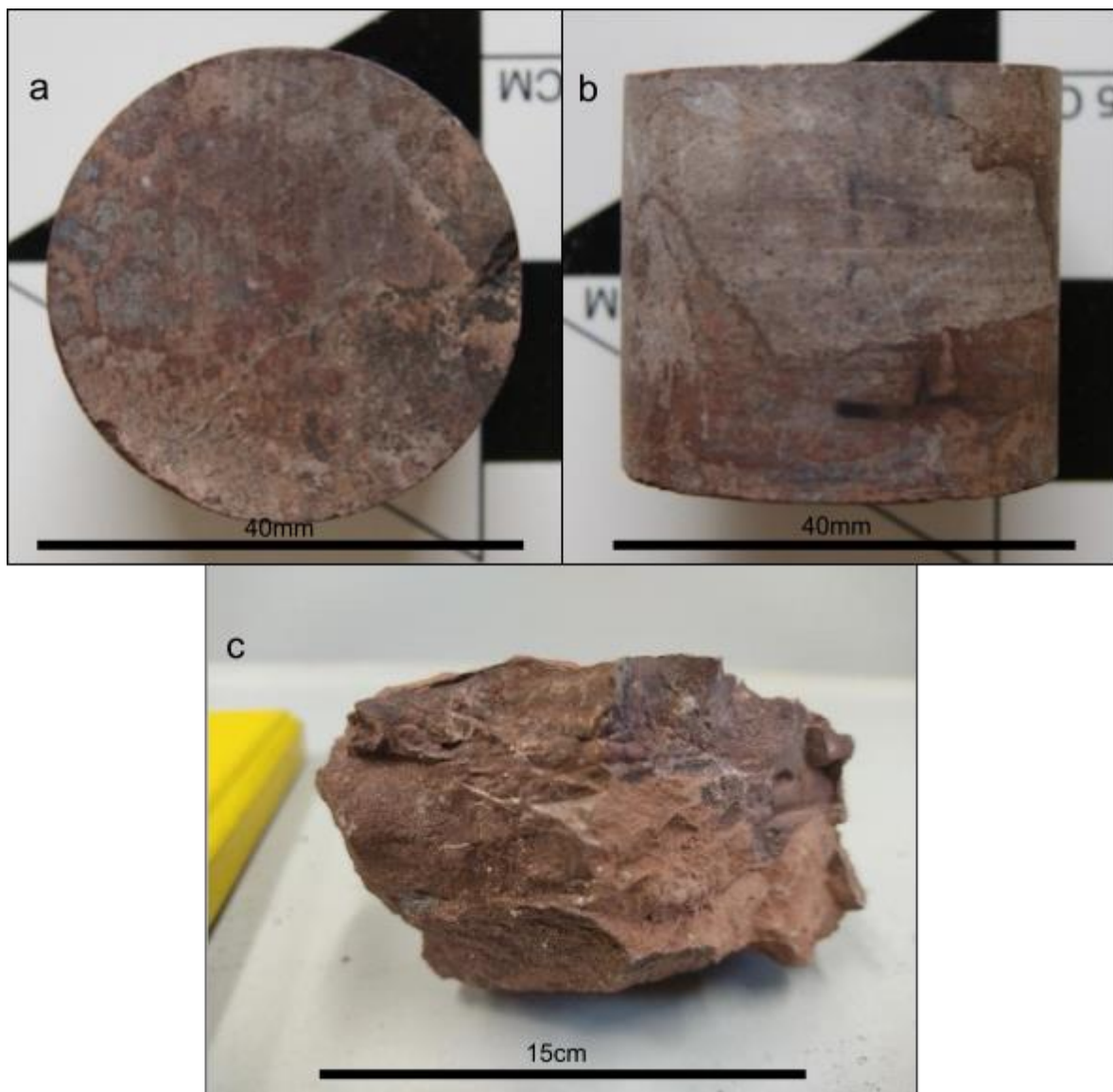
*Figure 66: **a) and b)** 36,2 mm long core plug of the LP7.2 Hornstein Formation in top view (a) and lateral view (b), a disturbance in the layering is visible **c)** Handpiece of the LP7.2 Hornstein Formation, weathered surfaces do not show the differences between LP7.1 and LP7.2, size: 305 cc.*

LP7.3

Lithology: Hornstein limestone

Sample Size: 290 cc.

Plugs: 1

Location: 710180 E, 295422 N (MGI_Austria_GK_M34)

FDC: 1
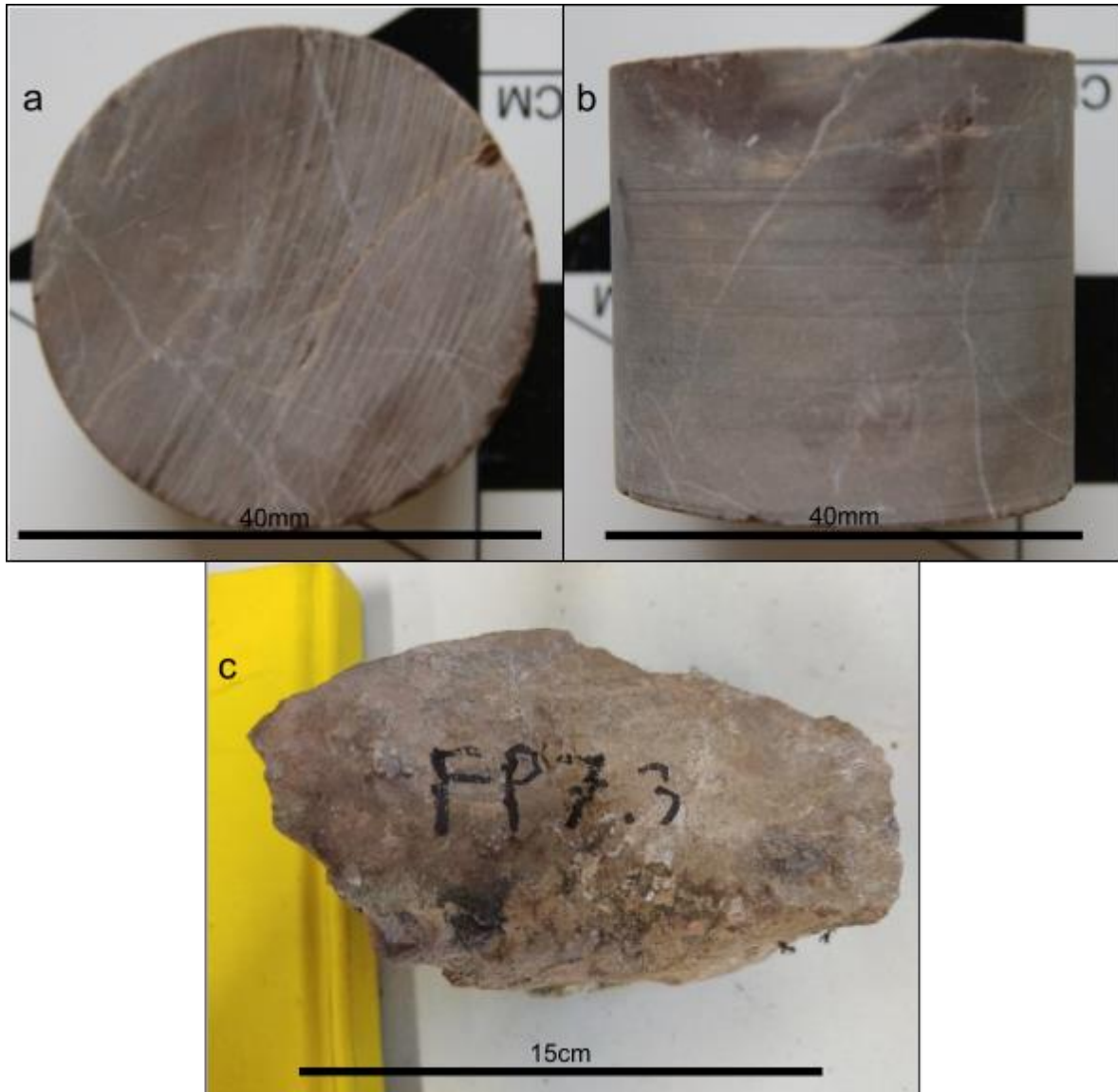
*Figure 67: **a) and b)** 36,48 mm long core plug of the LP7.3 Hornstein Formation in top view (a) and lateral view (b) **c)** Handpiece of the LP7.3 Hornstein Formation), size: 290 cc.*

LP7.3 shows in another rock type of lithologically diverse Hornsteinkalk Formation. This grey-brown (the handpiece and the fresh-cut surface) sample consists of microcrystalline calcite, brown chert lenses, and white calcite veins. The veins are thin and often do not even reach a width of one mm. The chert lenses are oval and have diameters from 1-10 cm in the outcrop. Many of these chert lenses are also part of the 1.6 inches

long plug which was made. There is not much indication of layering in this rock, except for the brown chert lenses: They are elongated in the same direction.

A hydrochloric acid test shows that this sample also has a high content of calcite.

LP7.4

Lithology: Hornstein limestone
Sample Size: 318 cc.
Plugs: 0
Location: 710180 E, 295422 N (MGI_Austria_GK_M34)
FDC: 1

Mostly reminiscent of LP7.1, including the white calcite veins in this brown chert-rich limestone. Overall, the sample looks to be a bit more finely grained, as the calcite crystals are not easy to distinguish.

There is no orientation in this sample and no lenses of chert. The rock is reacting strongly to HCl, which indicates another sample with a high content of calcite. Like the other samples from LP7, it is again massive and does not show any signs of porosities recognizable you could recognize with the naked eye.

Figure 68: Handpiece of the LP7.4 Hornstein Formation, size: 318 cc.

LP7.5

Lithology: Hornstein limestone

Sample Size: 368 cc.

Plugs: 0

Location: 710180 E, 295422 N (MGI_Austria_GK_M34)

FDC: 1

Representing a more greyish variation of the "Hornsteinkalk", the weathered outer layers seem more reddish. This sample is also fine-grained and shows many small not-oriented veins cutting through it. The rock is bulky and free of fractures and pore spaces evident for the naked eye. Like all the LP7 samples, it reacts strongly to hydrochloric acid, which indicates that the Hornstein limestone is a "limestone" first, and chert is only a small fraction in every variation, except for the chert lenses.

There are lens-like forms on this rock´s weathered face, but they are not observable in the freshly cut rock, like in sample LP7.3. The chert lenses are exclusive to that handpiece.

*Figure 69: **a)** Handpiece of the LP7.5 Hornstein Formation, size:368 cc.*

LP11

Lithology: Karstified Wetterstein limestone

Sample Size: 737 cc.

Plugs: 1

Location: 709236 E,293395 N (MGI Austria GK M34)

FDC: 1
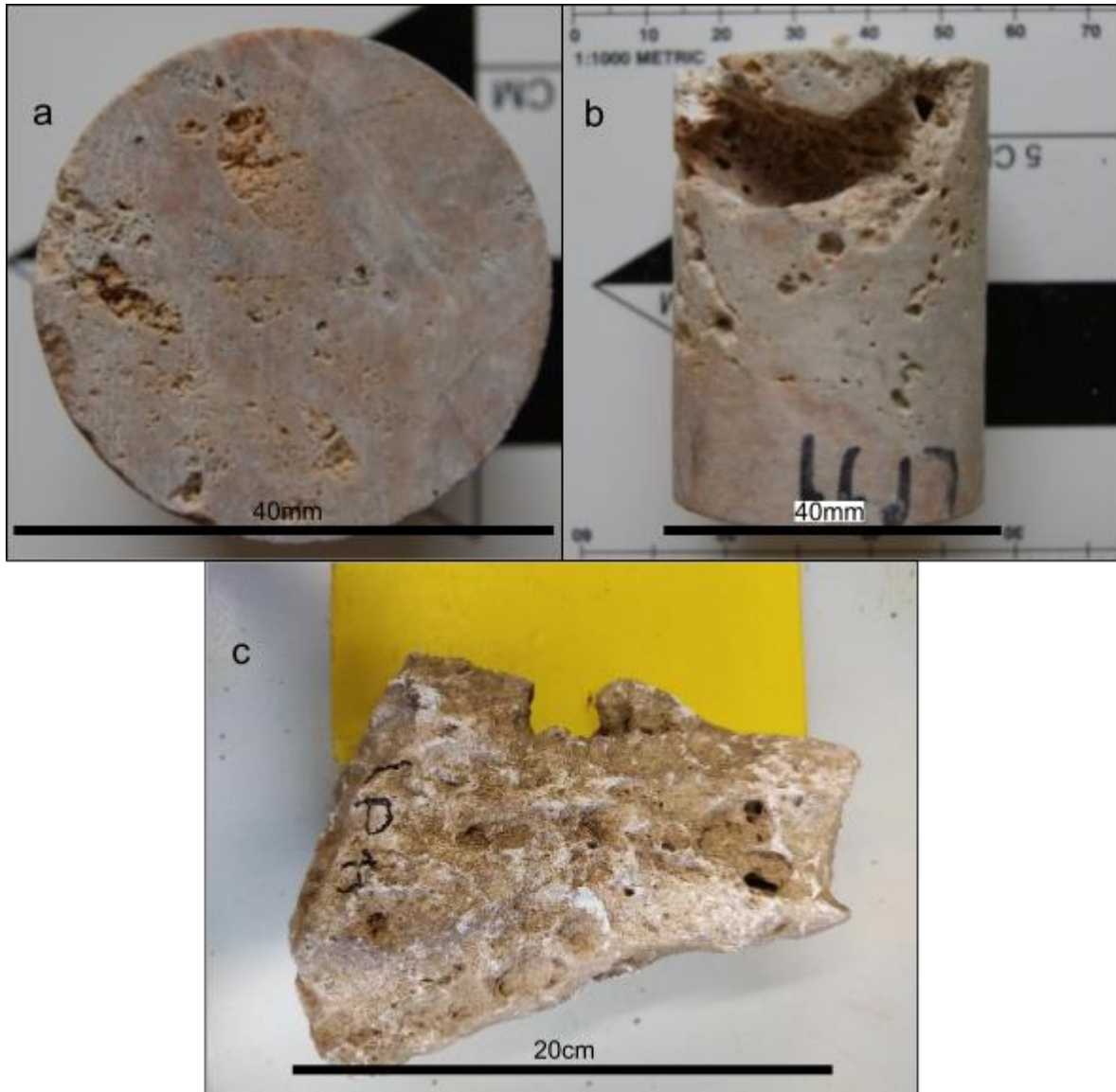
Figure 70: ***a) and b)*** *52,95 mm long core plug of LP11 in top view (a) and lateral view (b), a cavity of a few cc was cut into,* ***c)*** *Handpiece of the LP11 Wetterstein Formation (Karstified), large cavities are found all over the sample, size: 737 cc.*

The visible porosity in this sample provides a good indication of how much karst can influence an environment´s geology. This rock shows reef structures and correlates to the Wetterstein reef facies samples. Important to note is that this sample is the only one, which was not sampled in-situ; it was collected on the central plateau of the Kuh-

schneeberg. Through its good representation of possible karst forms in the area, especially near karst features at the plateau, it is interesting for understanding the entirety of the Kuhschneeberg´s rocks.

The finely grained calcites in the 2-inch plug vary from white to bright pink; they still show some structural reef forms and are intersected by calcite veins. The sample reacts strongly to hydrochloric acid.

Pore sizes vary greatly and can be around a cubic cm in a few cases. A big pore cavity was cut in the plug sample.
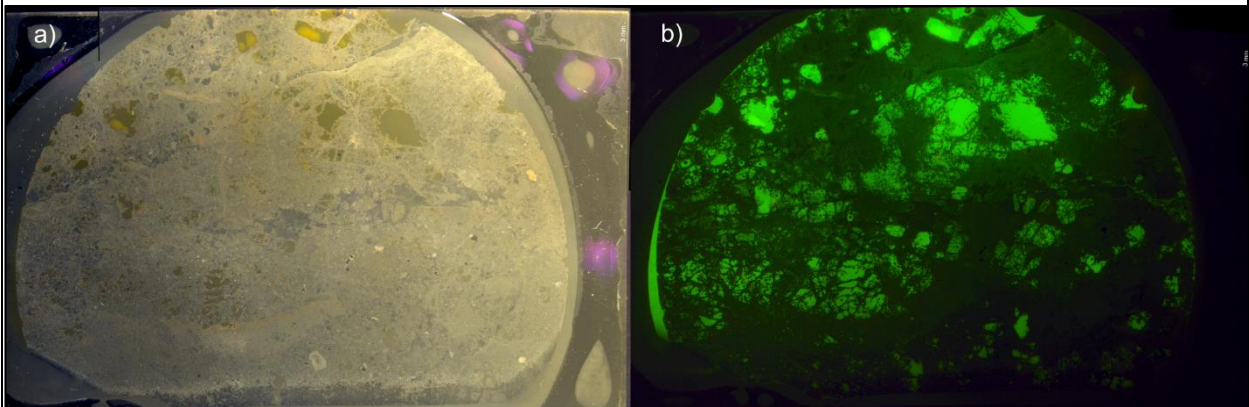
Figure 71: Cut-out from sample LP11 with Fluorol in pores and cleavages. **a)** shows the sample under reflected light. **b)** shows the sample under UV-light. The sample is 1.5 inch wide. The results indicate that the porosity is a relatively prone factor for permeability since the porosity does not interconnect as easily over distance like fractures do. The local high porosity of LP11 does play only a minor role because the porosity a few centimetres down is already much lower. Fractures on the other hand have a far higher reach through their planar development.

Depending on the sample (hand sample, core plug or thin-section) and method, the porosity varies between 4,24 and 20%. This does have to do with the extremely inhomogeneous distribution of pore space in the sample, where parts are extremely weathered and porous but the mostly undisturbed rock a few cm beside is much more solid. The sample shows almost no fractures and the permeability is therefore almost purely pore-dependent. Despite the high porosity, the sample is very impermeable, showing that even much pore space does not guarantee connections for flow-transport, which even more counts over bigger rock volumes. However, this sample keeps a lot of it´s porosity, even under higher confining stresses.

LP19.1

Lithology: Wetterstein reef limestone

Sample Size: 1068 cc.

Plugs: 2

Location: 705278 E, 292366 N (MGI Austria GK M34)

FDC: 2
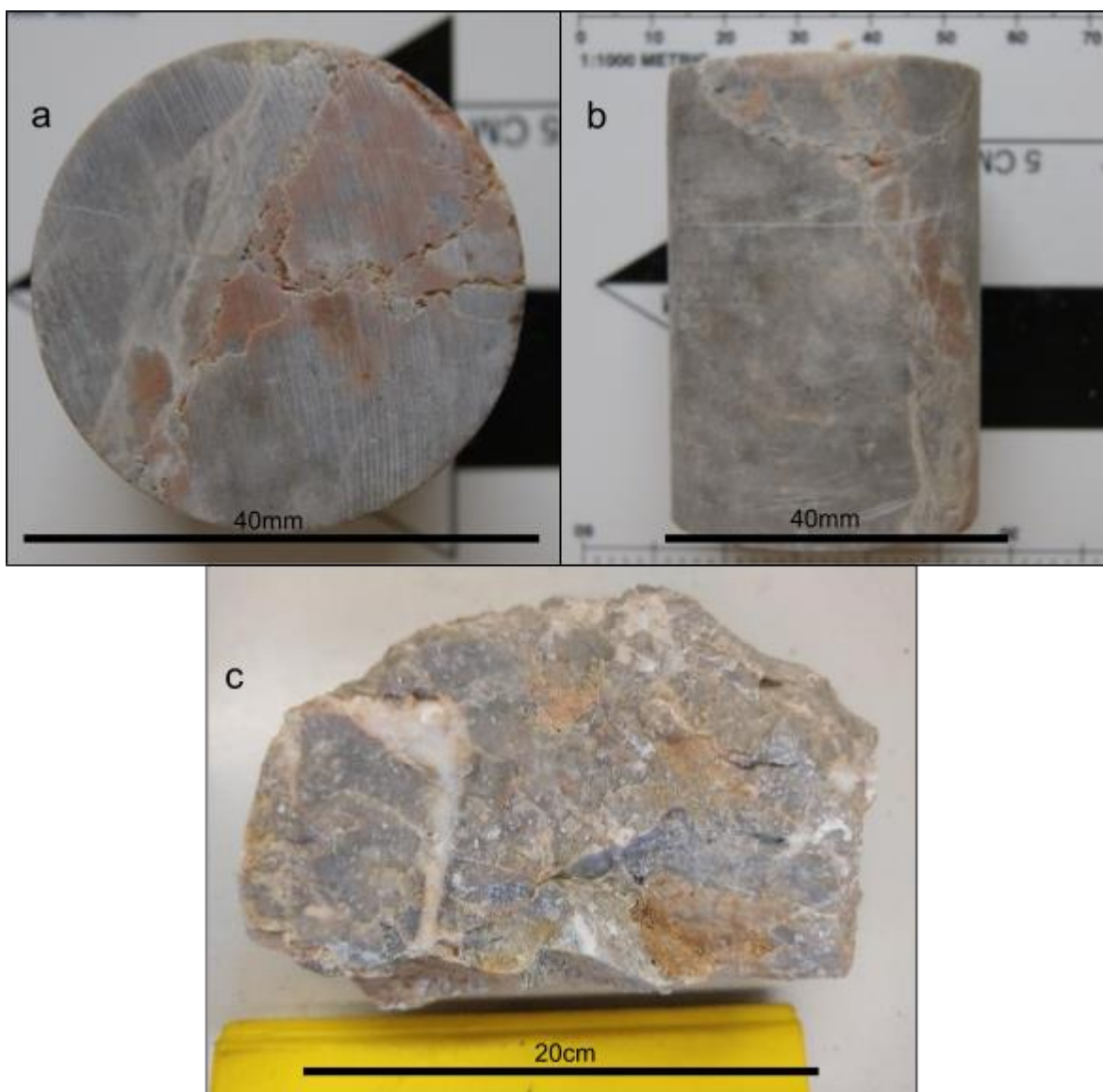
Figure 72: **a) and b)** 55,2 mm long core plug of LP19.1 Wetterstein Formation (Reef Facies Limestone) in top view (a) und lateral view (b), the pink calcite forms are more recognizable in this core plug. **c)** Handpiece of the LP19.1 Wetterstein Formation (Reef Facies Limestone), size: 1068 cc.

LP19.1 represents the reef facies of the Wetterstein limestone. This sample´s colour varies between mostly bright-gray with some pink and red grains; it is fine-grained and rich in fossils, which often are fractured. The sample reacts modestly to hydrochloric acid, so there is some dolomite involved. The limestone is strongly veined with white calcite in both plugs. The veins themselves show no preferred orientation and intersect the whole sample.

LP11 and LP19.2 are similar in the less weathered and sintered areas of the samples to LP19.1, which shows how the rock differs optically and physically with an alteration.
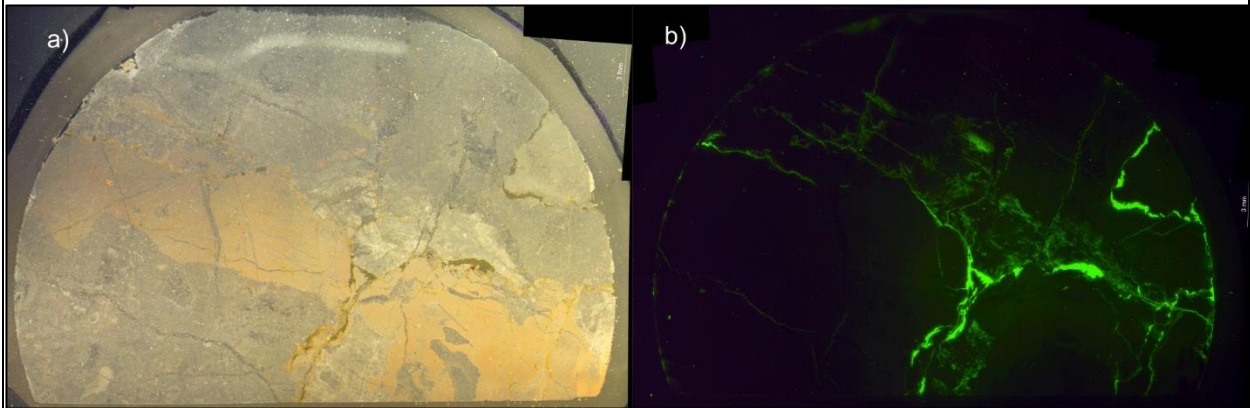
Figure 73: Cut-out from sample LP19.1 with Fluorol in pores and cleavages. **a)** shows the sample under reflected light. **b)** shows the sample under UV-light. The sample is 1.5 inch wide.

LP19.2

Lithology: Karstified Wetterstein limestone

Sample Size: 3154 cc

Plugs: 5

Location: Location: 705278 E, 292366 N (MGI Austria GK M34)

FDC: 1
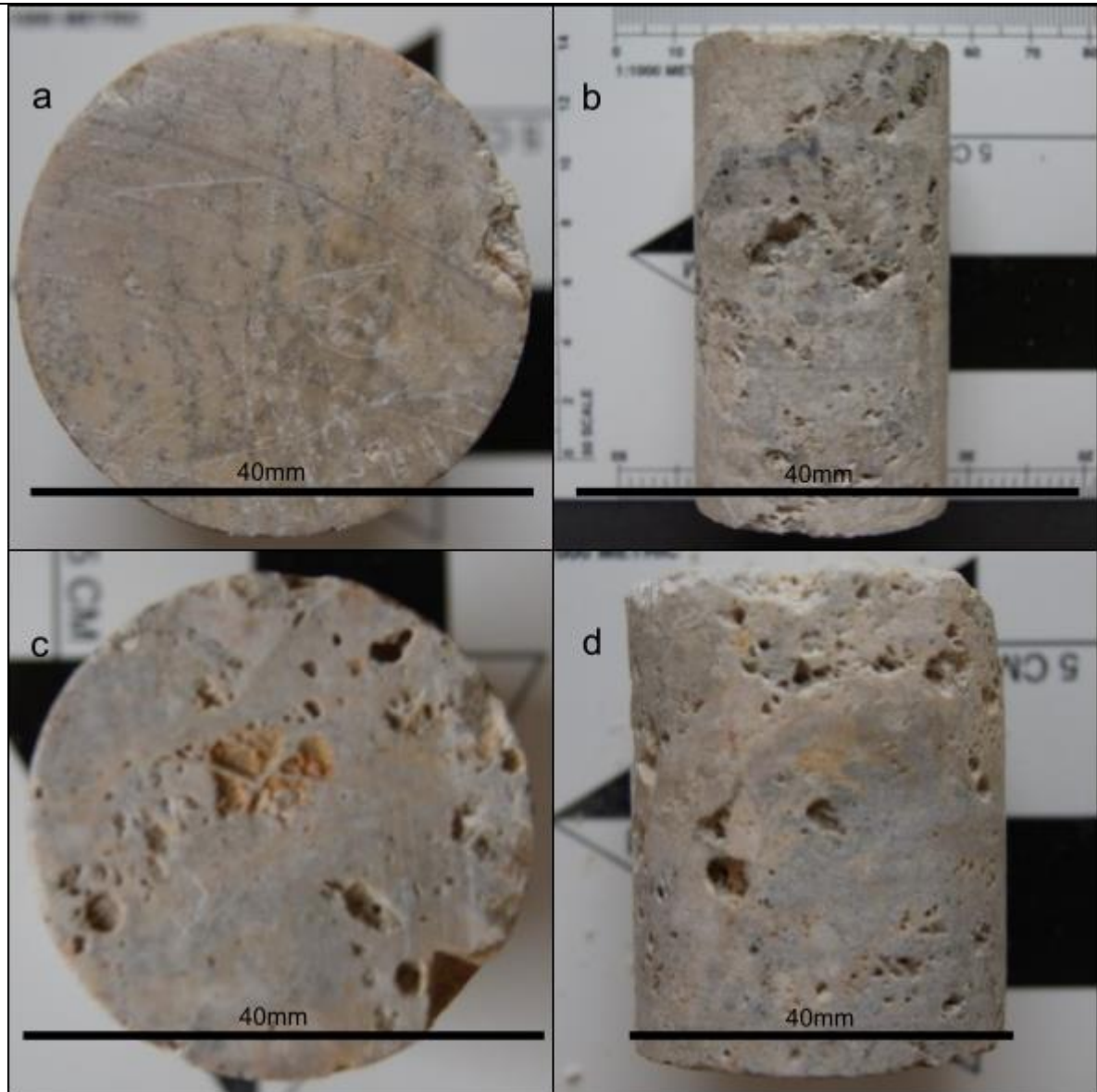
Figure 74: **a) and b)** 68,84 mm long core plug of LP19.2 in top view (a) and lateral view (b), visible porosity is seen over the whole sample material. **c) and d)** 48,2 mm long core plug of LP19.2 in top view (c) and lateral view (d), the reef texture is still visible in this core plug.

This rock originates from the same outcrop as LP19.1 and shows significant alteration through weathering and karstification. Pore spaces are distributed inhomogeneous among the sample and show a "web"-like structure. It seems that the calcite veins, which are found in this sample, are more stable and build up much of the pore walls.

Grain sizes and structures are very similar to LP19.1 and LP11. The rock was stable enough to drill five plugs out of it to compare its porosity and permeability with LP19.1. A larger part of LP19.2 fell off during weight measurements, which meant the weighting had to be repeated and LP19.3 was taken as a new separate sample for the immersion method.
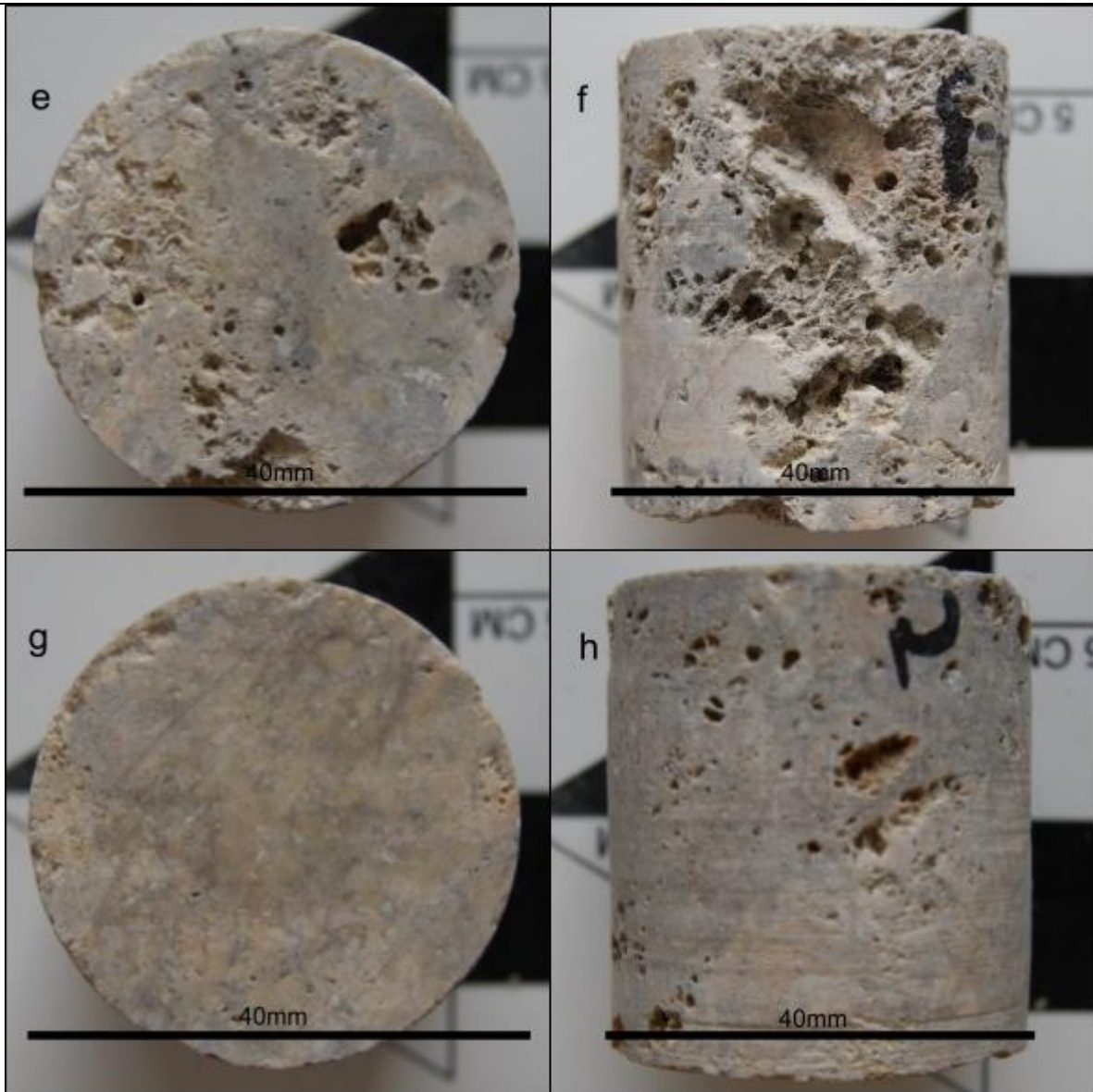
Figure 75: **e) and f)** 44,61 mm long core plug of LP19.2 in top view € and lateral view (f), the pores are often divided by straight walls of calcite, giving them a grid-like appearance. **g) and h)** 42 mm long core plug of LP19.2 in top view (g) and lateral view (h), the plug shows relatively minor karstification, which also shows in density and weight: it is heavier than some of the larger samples.

Figure 76: **i)** and **j)** 30,03 mm long core plug of LP19.2 in top view (i) and lateral view (j) with visible porosity. **k)** Handpiece of LP19.2 Wetterstein Formation (Karstified), the pores are often confined grid-like, the veins are more resistant to karstification and often build up the walls of the pores. size: 3154 cc.
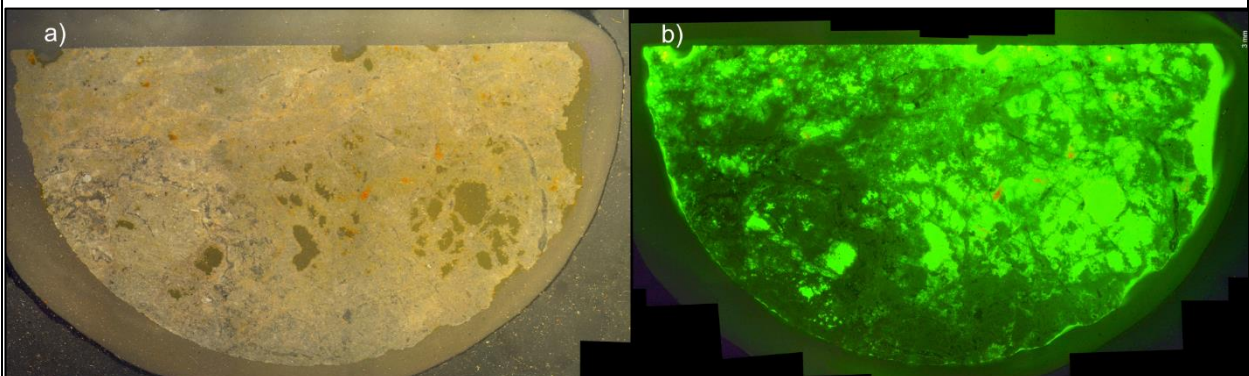
Figure 77: Cut-out from sample LP19.2 with Fluorol in pores and fractures. Almost all Fluorol is found in the pores, only a few small fractures are visible. The grid-like appearance is also visible here, like in Sample Picture 10. **a)** shows the sample under reflected light. **b)** shows the sample under UV-light. The sample is 1.5 inch wide.

Like LP11, this sample shows high porosity-values with relatively little permeability, indicating that pores are not well connected, even when values are exceptionally high.

LP36

Lithology: Wetterstein reef limestone

Sample Size: 520 cc

Plugs: 1

Location: 706254 E, 295167 N (MGI Austria GK M34)

FDC: 1

LP36 was collected from a rock exposed at the mouth of a cave-like karstic opening. The rock is strongly weathered and finely grained with the inner coloration variating between different light greys in this reef facies sample. Calcite veins flow through the rock in different orientations. This sample shows a high reaction to HCl, which does not leave room for a high proportion of dolomite.
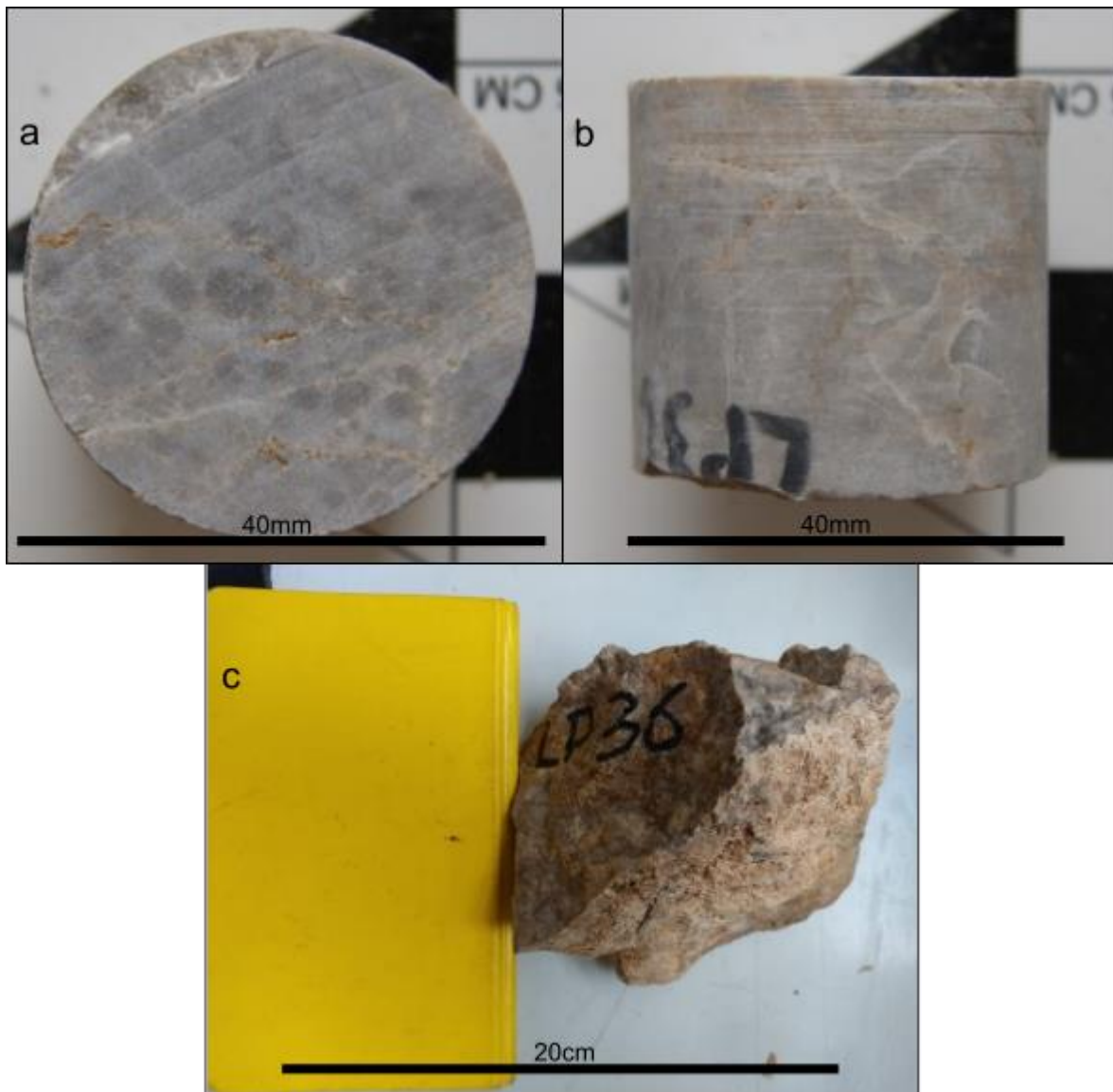
Figure 78: **a) and b)** 36,32 mm long core plug of LP36 in top view (a) and lateral view (b). **c)** Hand-piece of LP36 Wetterstein Formation (Reef Facies), the former adjacency to a cavity only shows itself as a crust in the bottom right surface layer. Size: 520 cc.

Although the sample is extracted from an open cavity, it shows no signs of weathering under the outer few mm´s of the handpiece. There is a high similarity to the samples of LP41 and LP43.
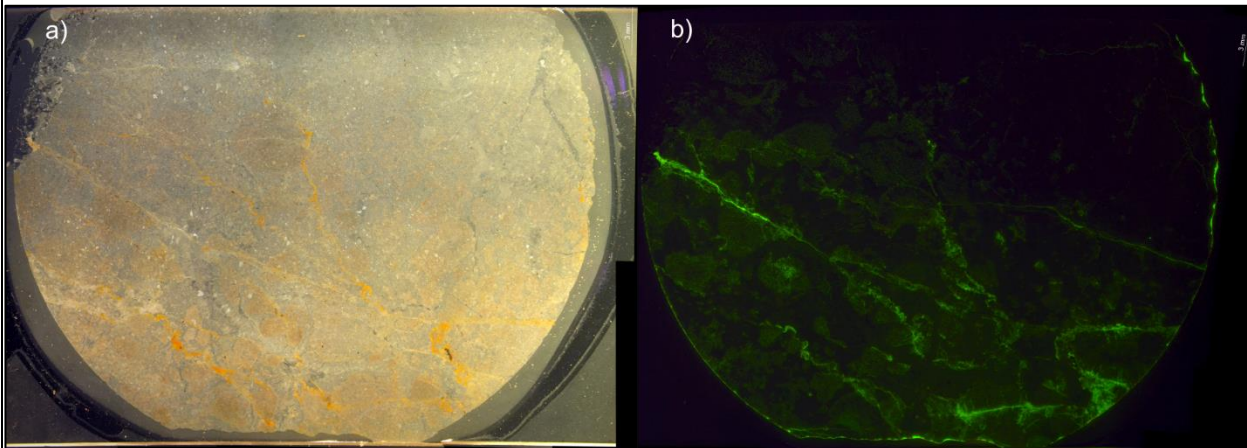
Figure 79: Cut-out from sample LP36 with Fluorol in pores and cleavages. **a)** shows the sample under reflected light. **b)** shows the sample under UV-light. The higher intensity emission of UV-light only happens in the fractures. The sample is 1.5 inch wide.

The core plug of LP36 shows increased permeability through a few open fractures. The main fracture-network in the thin-section contains a few grain fragments and is also very fragmented in the vicinity, which could explain the high resistance of the sample to losses in permeability, since the fracture cannot close as easily with increasing confining pressure.

LP38

Lithology: Stylobreccia from a protolith of Wetterstein reef limestone

Sample Size: 1476 cc

Plugs: 2

Location: 706097 E, 295242 N (MGI Austria GK M34)
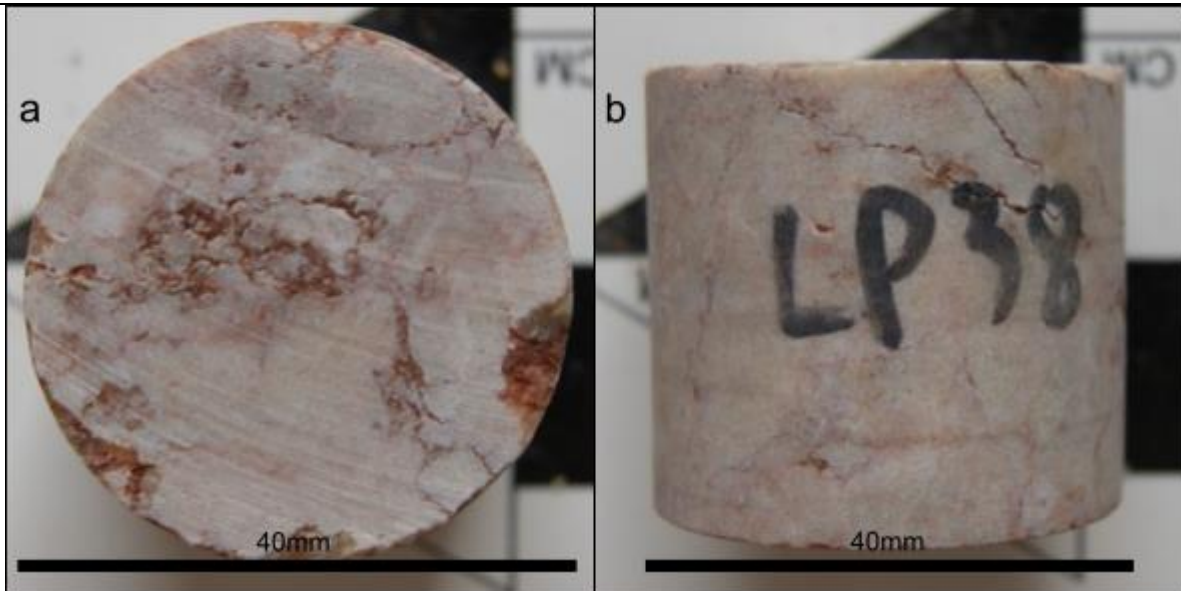
Figure 80: **a) and b)** 36,08 mm long core plug of LP38 in top view (a) and lateral view (b).
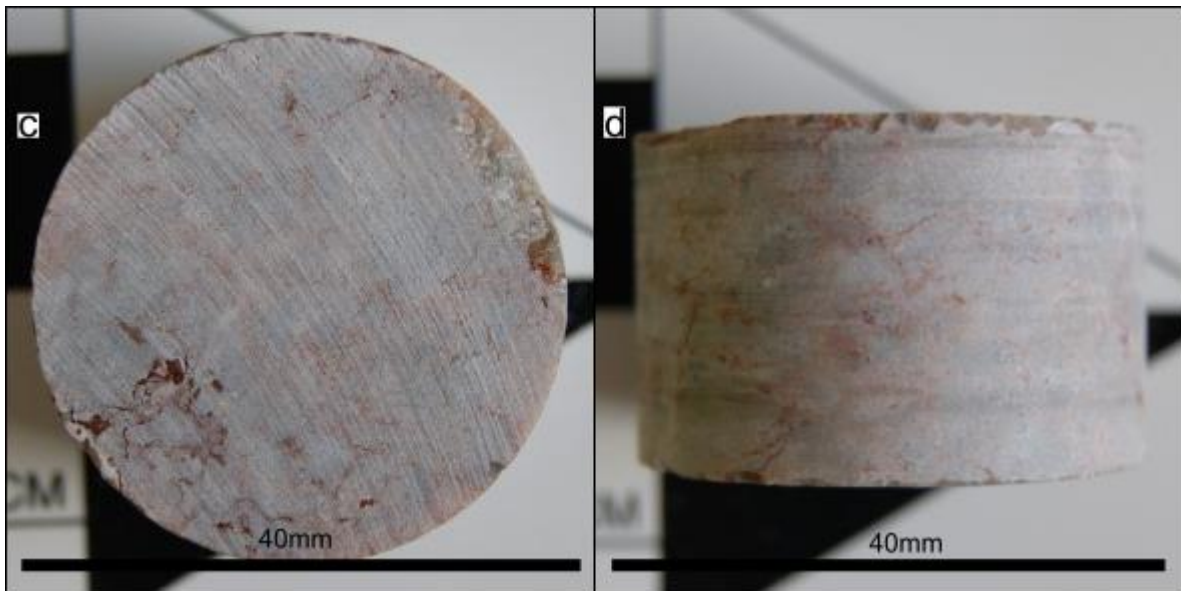
Figure 81: **c) and d)** Core Plug of LP38 in top view (c) and lateral view (d), which was too short for Measurement in the Coreval 700.

This sample was extracted near a cataclastic fault in the Wetterstein limestone. It is classified as a stylobreccia (fault rock) derived from a Wetterstein reef limestone proto-lith and features some angular fragments in the typical reddish matrix in parts of the sample. Naturally, there is a high variation in fragment sizes through the mechanical alteration. There is a reddish clay matrix separating many of the clasts; however, many of them are still in direct grain to grain contact.

Despite the appearance of fractures, the permeability is very low. The pictures of the UV-microscope and the Coreval measurements indicate, that the clay material is an effective aquiclude in this rock. The appearance under the microscope indicates, that the concentration of clay is a result of pressure dissolution, recognizable through the serrated forms of the concentrations.
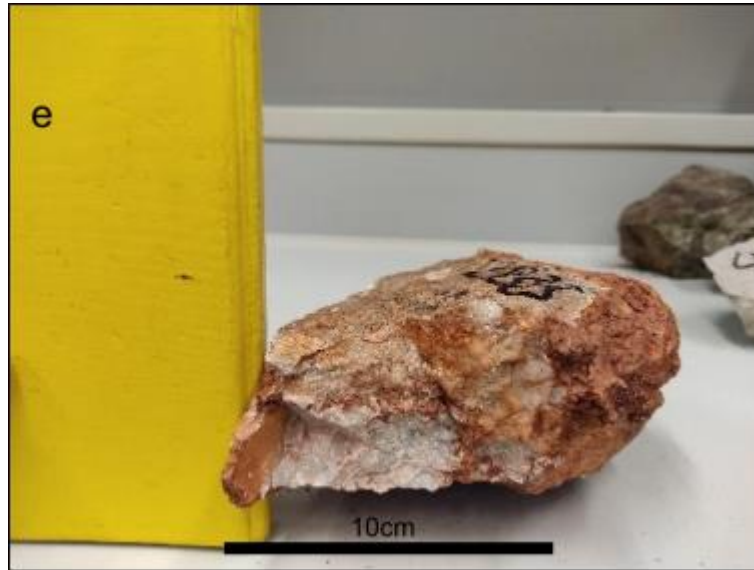
Figure 82: **e)** Handpiece of LP38, the clasts of the rock are heterogeneous in size and often angular.

It was extracted adjacent to the fault near a change in the Wetterstein Formation towards dolomitic facies. However, this sample shows no strong indication of dolomite, as it reacted strongly to HCl.

Figure 83: Cut-out from sample LP38 with Fluorol in pores and cleavages. As there were almost no spaces filled with Fluorol, the pore and cleavage space must be minimal. A stitching of the UV-light picture was not possible due to the low porosity. The sample is 1.5 inch wide.

LP41

Lithology: Wetterstein reef limestone

Sample Size: 725 cc

Plugs: 1

Location: 705751 E, 294907 N (MGI Austria GK M34)

FDC: 1

This Wetterstein limestone, extracted near 30 cm of a cataclastic fault, looks largely unaffected by the fault in macroscopic observation. Under the assumption that there might still be a change in porosity/permeability in the microscopic scale, it was collected.

Features of this sample are its light grey colour with white calcite veins. The veins are thin (< 1 mm) and sparse. They show no preferred orientation. The crystals of this handpiece are sometimes recognizable under macroscopic observation.

Despite its adjacency to a fault, the rock shows no macroscopic signs of increased fracture density and reacts strongly to HCl. Only the thin section reveals regions of intensified fracturing on a microscopic scale.

The partwise cataclastic change in the rock is found in the core plug: fractures are numerous and wall rock fragments are separated without preferred orientation. The porosity is increased through the numerous fractures. The sample shows increased

permeability through the fracture network and is relatively resistant against loss of per-meability and porosity with higher confining pressure.

*Figure 84: **a) and b)** 52,39 mm long core plug of LP41 in top view (a) and lateral view (b), the plug largely reminds of LP43 and LP36, **c)** Handpiece of LP41, there seem to be no fractures induced through the fault, size: 725 cc.*
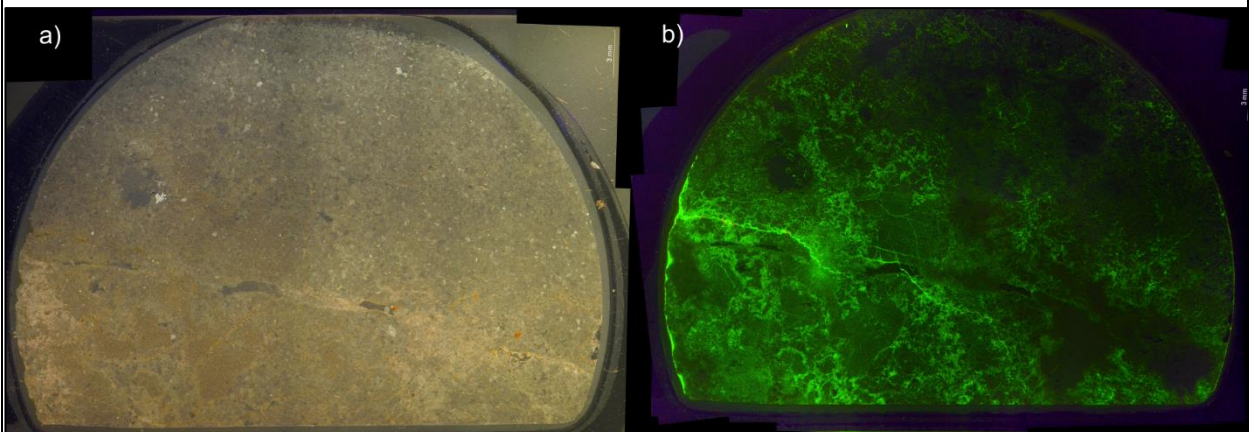
Figure 85: Cut-out from sample LP41 with Fluorol in pores and cleavages. **a)** shows the sample under reflected light. **b)** shows the sample under UV-light. Many small and thin fractures separate clasts into smaller parts and between each other. The sample is 1.5 inch wide.

LP43

Lithology: Wetterstein reef limestone

Sample Size: 865 cc

Plugs: 1

Location: 705875 E, 295115 N (MGI Austria GK M34)

FDC: 2

This rock, in direct proximity to a fault gouge, has fractures visible all over the grey Wetterstein sample surface. Despite the missing integrity at the sample´s fault-facing side (many fractures), the plug, which was made, shows no structural weakness.

The sample looks similar to LP36 and LP41, especially the drilled plug samples. The rock is light grey and shows small fine calcite veins, without preferred orientation. It also shows the same reaction to hydrochloric acid as the other Wetterstein limestone samples.
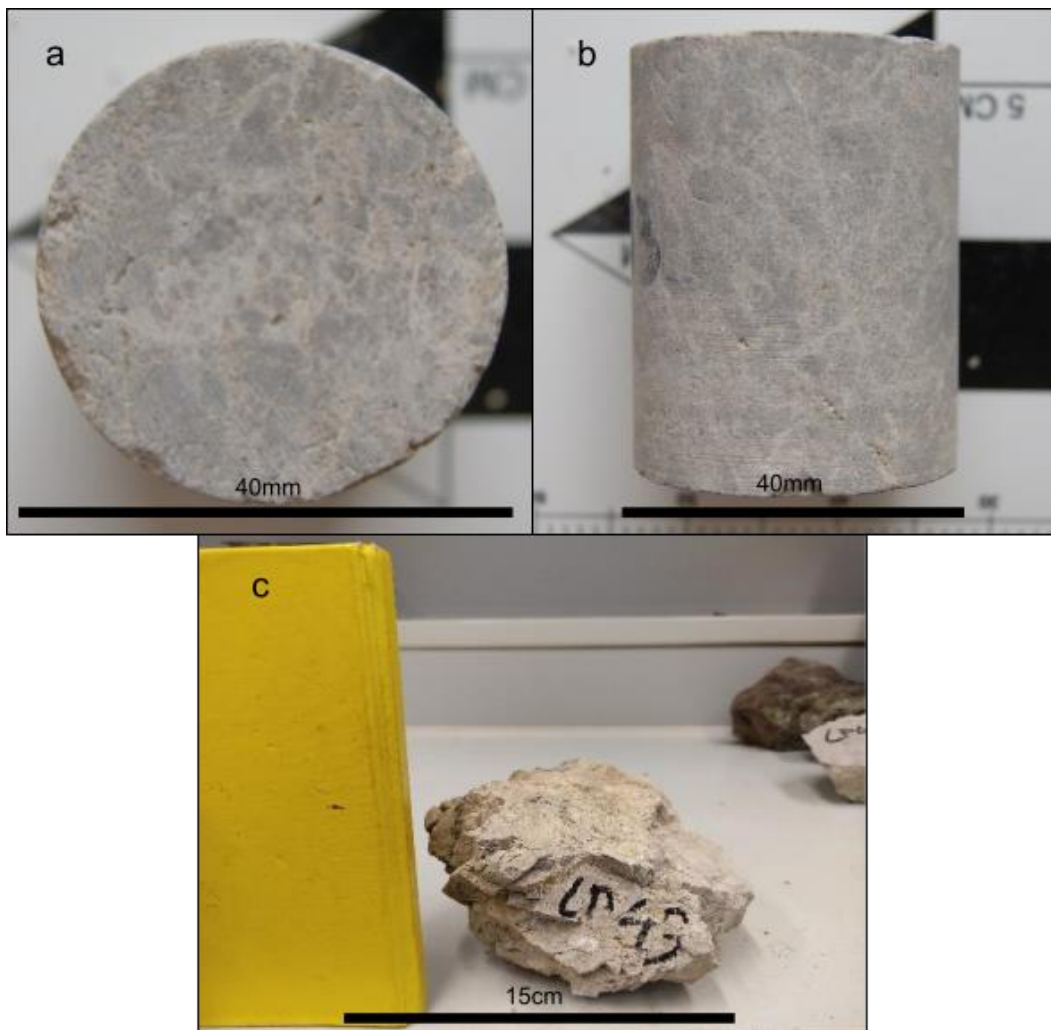
Figure 86: **a) and b)** 49,65 mm long core plug of LP43 in top view (a) and lateral view (b) **c)** Handpiece of LP43, this sample shows fractures, explainable through the fault gouge next to the extraction point. Size: 865 cc.

LP45
Lithology: Hornstein limestone Sample Size: 842 cc Plugs: 3 Location: 706038 E, 295637 N (MGI Austria GK M34) FDC: 1 This sample derives from the strike continuation of the Hornsteinkalk Formation of the Göller Nappe below the Schneeberg Nappe, which also includes the samples of LP7. The characteristic of this sample is its bedding and the red-brownish colour. This sample was found in the North-West of the Kuhschneeberg, facing towards the Baumeckkogel, a nearly thousand-meter-high mountain.   Especially the similarity to LP7.3 is high: The coloration, the strong influence of veins, the chert lenses, and resulting inhomogeneous texture of the sample. The veins are intervening through all other material of the sample. Veins and chert are incorporated in the three plugs, which were drilled. The chert-lacking parts of this sample react strongly to hydrochloric acid.
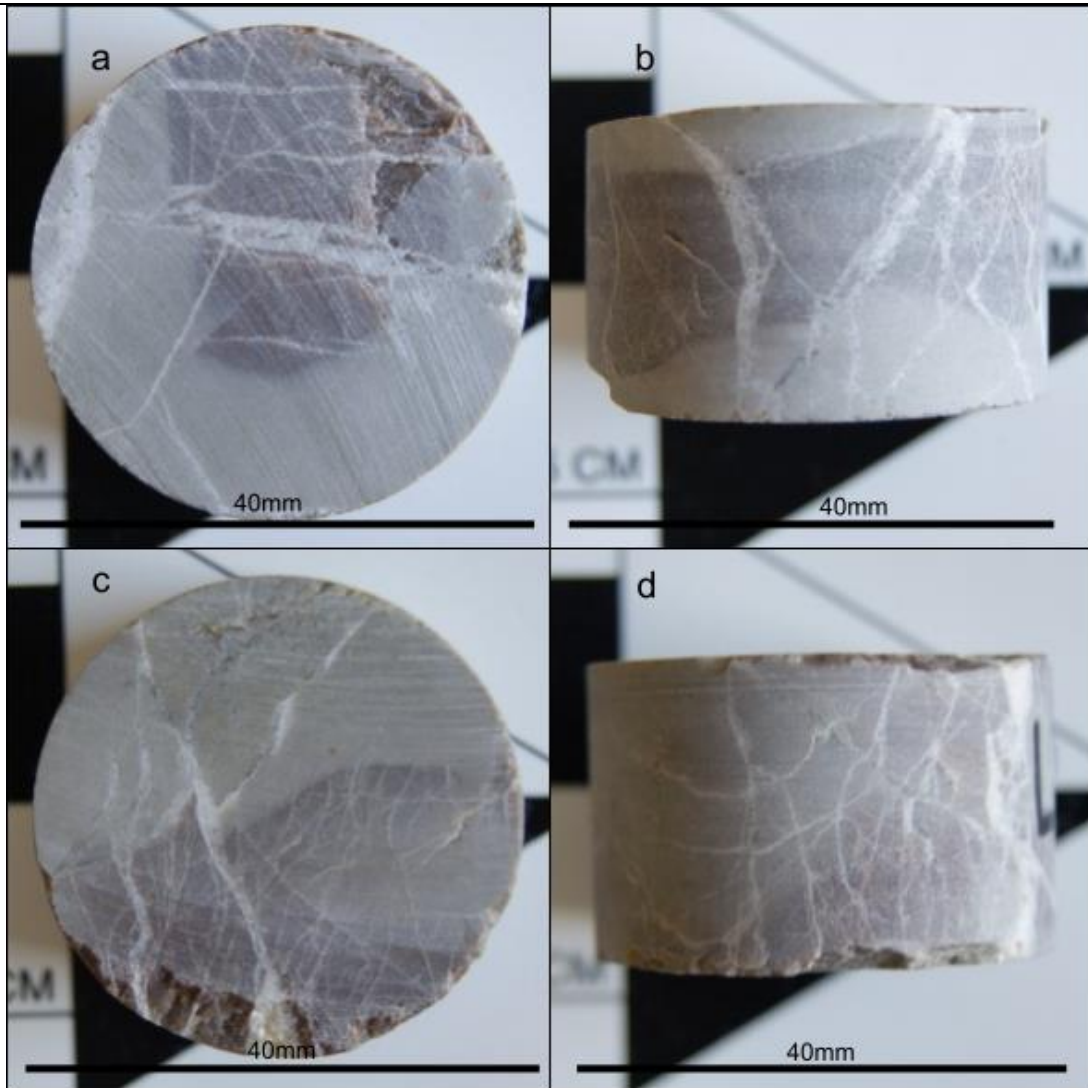
Figure 87: **a) and b)** Core plug of LP45 in top view (a) and lateral view (b), the lithology is relatively stable with exception of the bedding planes. These occur every 2-3 cm, which made it not possible to extract a long enough core plug. **c) and d)** Second LP45 core plug in top view (c) and lateral view (d).
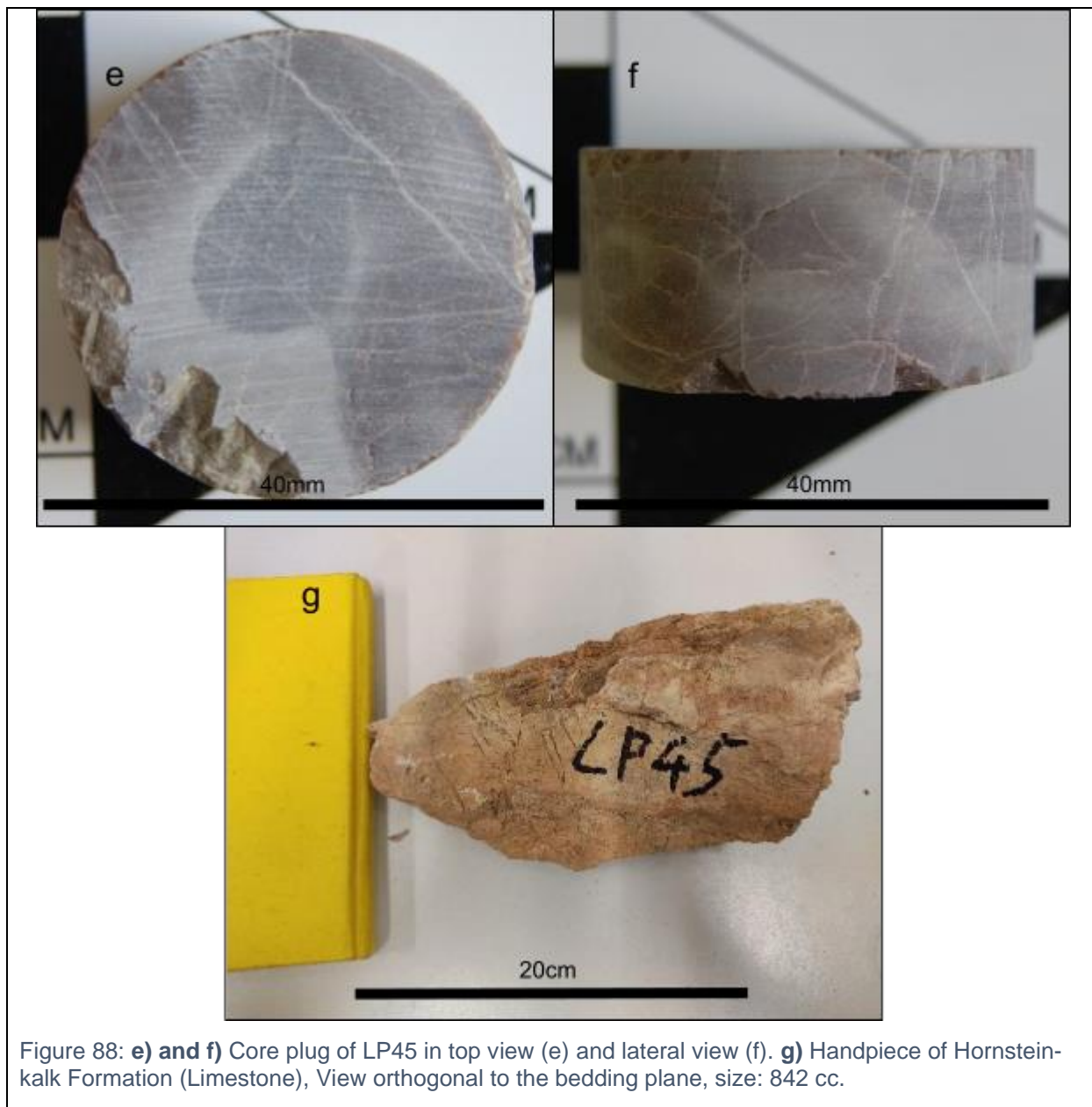
Figure 88: **e) and f)** Core plug of LP45 in top view (e) and lateral view (f). **g)** Handpiece of Hornstein-kalk Formation (Limestone), View orthogonal to the bedding plane, size: 842 cc.

LP46

Lithology: Haupt dolomite

Sample Size: 542 cc

Plugs: 1

Location: 712735 E, 296727 N (MGI Austria GK M34)

FDC: 1

This sample is the only piece of Hauptdolomit Fm. collected during fieldwork and is found as a light-grey rock with small grain-sizes. The Hauptdolomit Fm. plays only a minor role on the surface of the Kuhschneeberg. The sample is not bedded and shows no structurtal weaknesses through fractures.

At first look, it strongly resembles the Wetterstein samples of LP36, LP41, and LP43. In contrast, the drilled plug shows the differences more clearly: Reef-structures are missing, and the sample coloration is very uniform. The grains are very fine, and some small vuggy pores are visible on the drilled sample´s surface.

As expected, the reaction to HCl is weak, which further validates the classification.
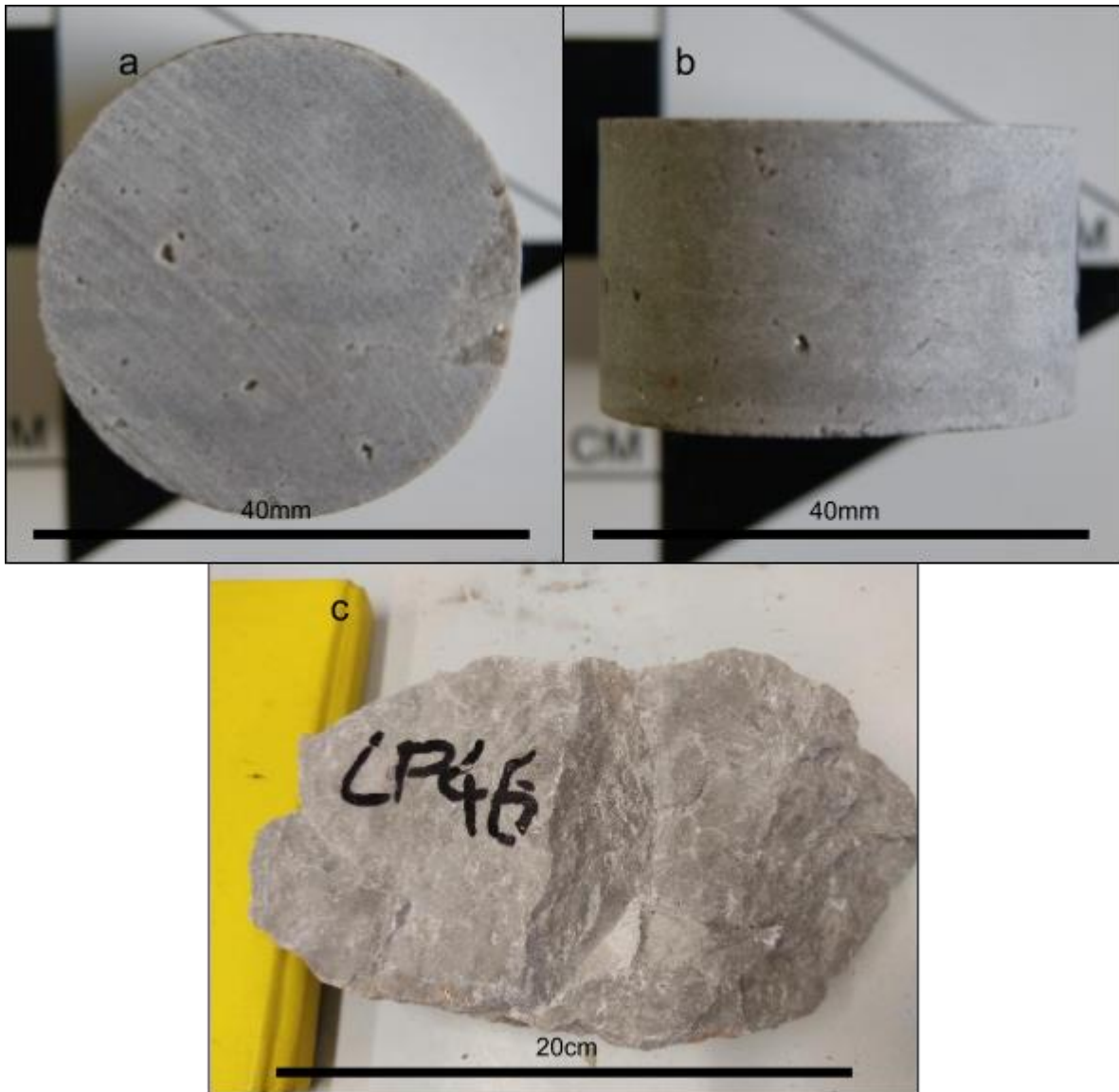
Figure 89: **a) and b)** Core plug of LP46 in top view (a) and lateral view (b), which was too short for measurement in the Coreval, but shows the dissimilarity on freshly cut surfaces to the Wetterstein lime-stone samples, **c)** Handpiece of LP46 Hauptdolomit Formation (Dolomite), The whole rock samples are more similar to some of the Wetterstein samples (like LP41) than the core plugs, size: 542 cc.

LP48

Lithology: Opponitz limestone

Sample Size: 906 cc, 626 cc.

Plugs: 1

Location: 710316 E, 296941 N (MGI Austria GK M34)

FDC: 1

These two grey samples represent two types of the Opponitzer Formation limestones. LP48.1 is the well-bedded bitumen-rich variation of this rock, which is also found in the samples of MT10. The graphite-grey rock is massive with finely grained crystals, the banking repeats in steps of under 10 cm. The plates, as well as the whole rock, fracture very easily and made it impossible to extract a plug of the sample. The same happens to be the case with the samples of MT10.

White veins are oriented at a high angle with respect to bedding and cut through it. The reaction towards HCl is strong.

LP48.2 is a grey-colored example from the Opponitzer Formation. The sample is not as rich in bitumen as LP48.1, and bedding is much less visible. Though it is still there, especially during drilling, the preferred breaking happens in the planar direction.

The veins are still there, but orientation does not seem as clear as it was with sample LP48.1. The rock is massive and reacts strongly to LP48.1.

The Opponitzer Formation is described as a changing sequence of limestones and dolomites with changing contents of bitumen (Mandl, 2006[2]:31f.) with the change being observable in this outcrop.
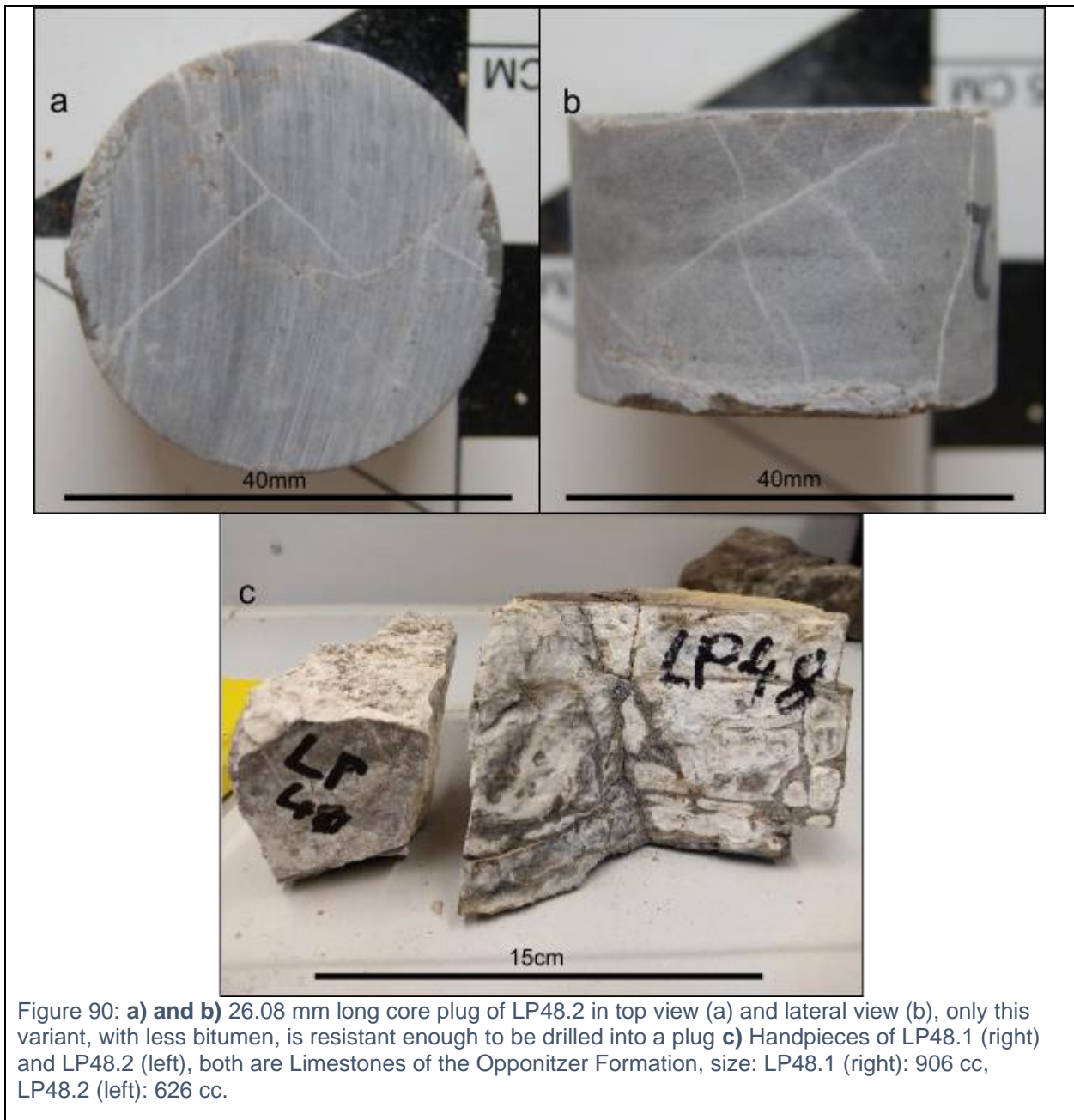
Figure 90: **a) and b)** 26.08 mm long core plug of LP48.2 in top view (a) and lateral view (b), only this variant, with less bitumen, is resistant enough to be drilled into a plug **c)** Handpieces of LP48.1 (right) and LP48.2 (left), both are Limestones of the Opponitzer Formation, size: LP48.1 (right): 906 cc, LP48.2 (left): 626 cc.

MT10

Lithology: Opponitz Limestone

Sample Size: 927 cc, 626 cc.

Plugs: 0

Location: 710743 E, 296985 N (MGI Austria GK M34)

FDC: 1

MT10 and LP48.1 share many characteristics, most prominent being the bituminous smell of their freshly cut surfaces. MT10, too, is graphite-grey and streaked by many white calcite veins. The rock is easily fractured when stress is applied, not only in the planar direction of this sample´s fine lamination. There could be no plug taken by the

bituminous parts of the Opponitzer Formation, because of its fragile behaviour. The finer lamination is a characteristic, which often applies at the lower parts of the Opponitzer Formation, near the Lunzer Formation (Mandl, 2006[2]:31).

As before, the rock has a high concentration of calcite as shown by a test with HCl showed.

Figure 91: Handpiece of MT10 and MT10.2 Opponitzer Formation (Limestone), both samples have a sulphurous odour, size: 626 cc (MT10, left), 927 cc (MT10.2, right).

MT17

Lithology: Stylobreccia from a protolith of Wetterstein reef debris limestone
Sample Size: 1245 cc
Plugs: 3
Location: 706735 E, 294311 N (MGI Austria GK M34)

Like LP2, this rock is s stylobreccia derived from a protolith of the Wetterstein reef debris facies. Some of the different rock fragments are lighter coloured and not as uniform as in LP2, and the clay has a brighter tone. Sutures of pressure dissolution are found on the grain borders of the plugs (3 plugs). The wall rock fragments are around 1 mm to 5 cm in diameter. The angularity is also a little less defined as in LP2. Some white calcite veins are only found in the fragments but not in the clay seams between the fragments. Through the high calcite-content, the rock reacts strongly to HCl.
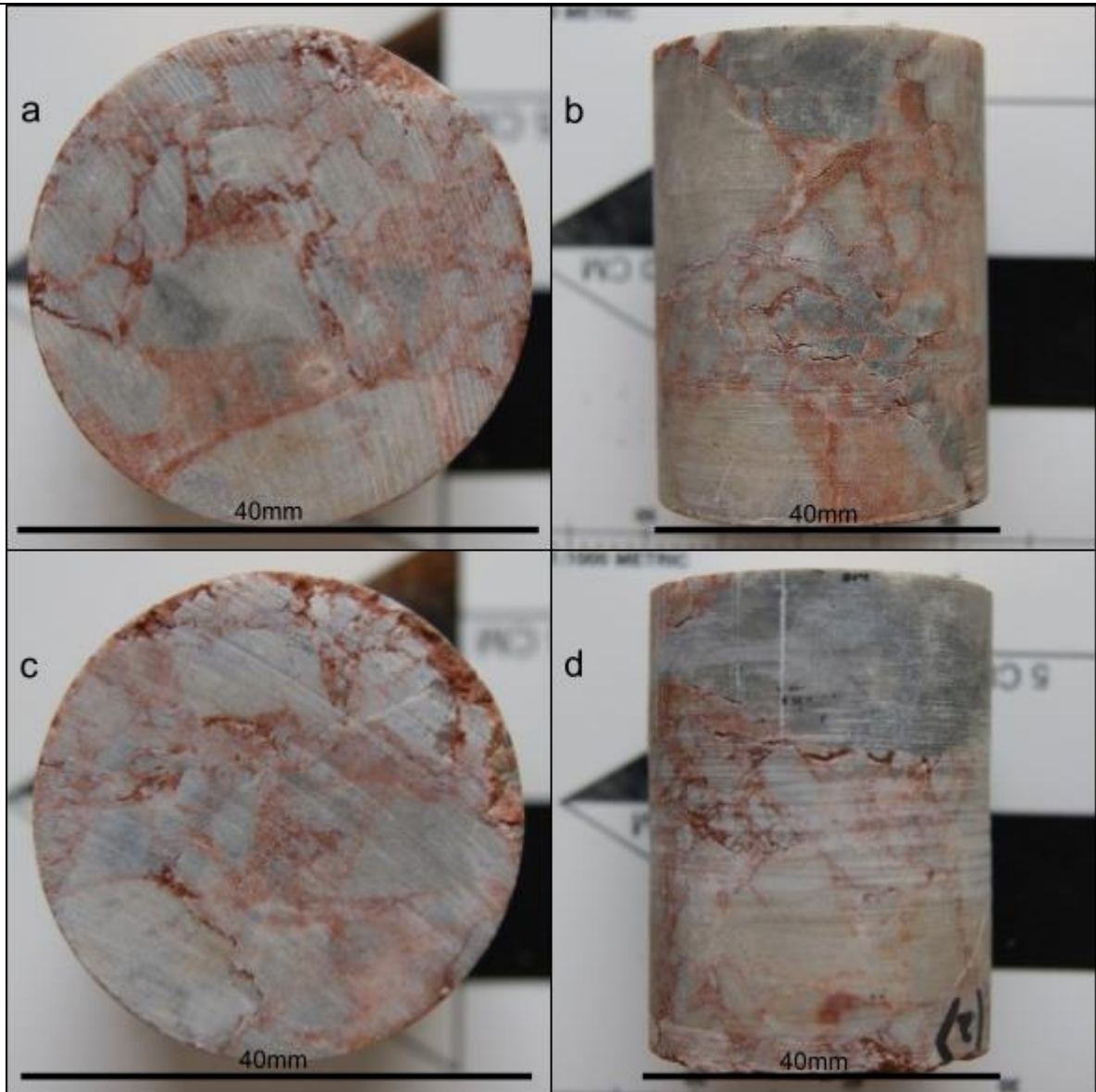
Figure 92: **a) and b)** 51,9 mm long core plug of MT17 in top view (a) and lateral view (b), a clear difference to LP2 is the heterogeneity in clasts, which vary in colour over the whole sample. **c) and d)** 51,27 mm long core plug of MT17 in top view (c) and lateral view (d) with similar features as a) and b), the clasts are strongly angular and often have no clay matrix between clasts.

Despite the clear existence of fractures, the filling of these with clay leads to a de-creased permeability and makes the rock act like an aquiclude.
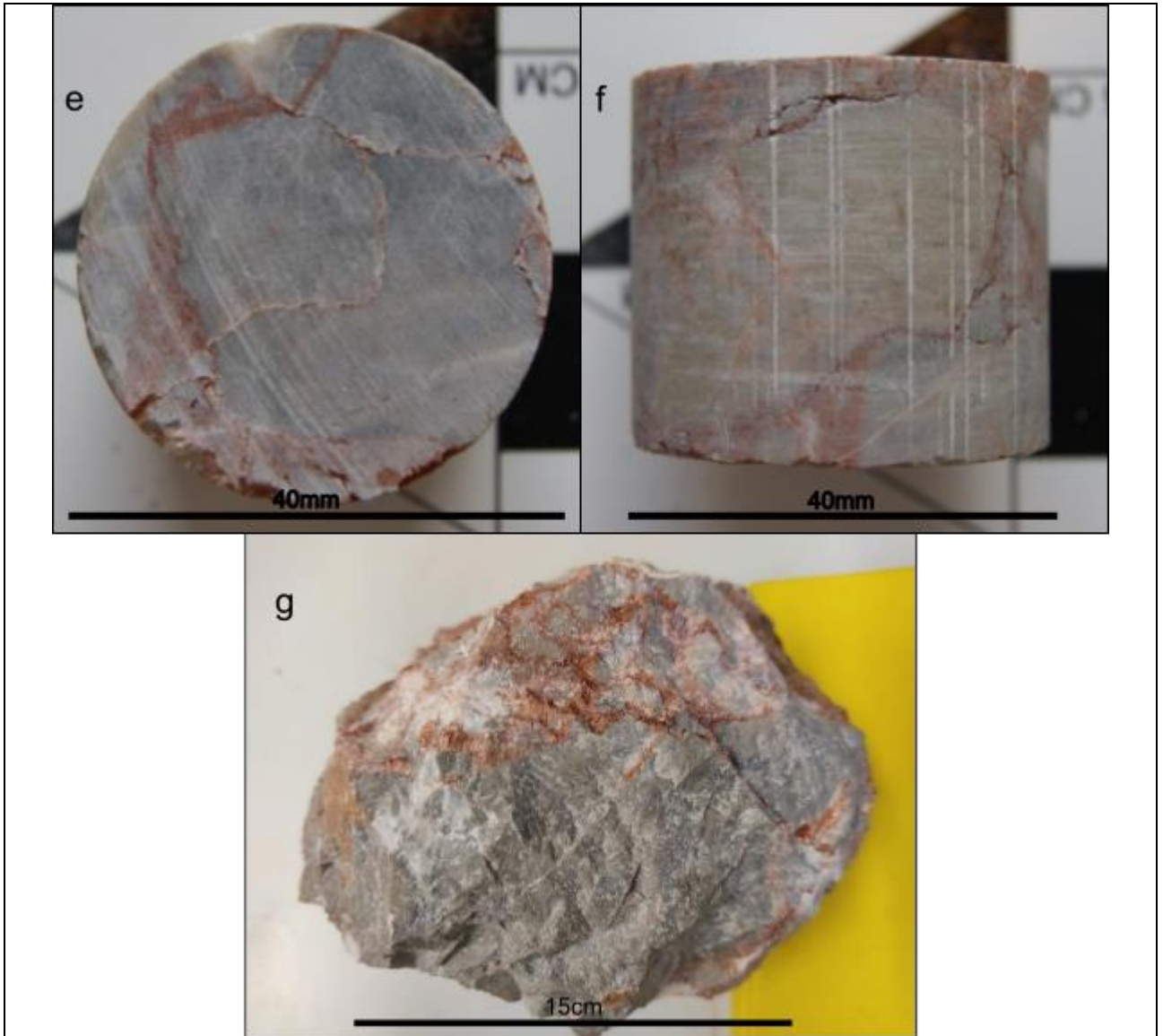
Figure 93: **e) and f)** 34,24 mm long core plug of MT17 in top view (e) and lateral view (f). **g)** Handpiece of MT17, size: 1245 cc.
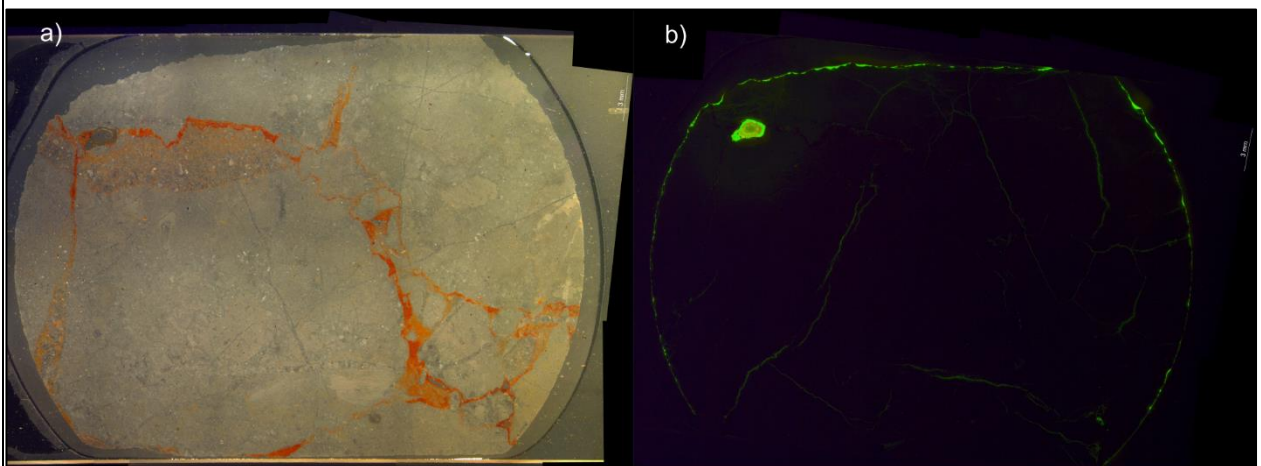
Figure 94: Cut-out from sample MT17 with Fluorol in pores and cleavages. **a)** shows the sample under reflected light. **b)** shows the sample under UV-light. One larger pore makes up most of the pore space, although the largest part of the sample is cleavage-dominated. Despite the relatively high fracturing, not many of these fractures are connected to each other, which has negative effects on the permeability. The sample is 1.5 inch wide.

MT31

Lithology: Cataclasite (Type 1) from a protolith of Wetterstein reef limestone

Sample Size: 1249 cc

Plugs: 0

Location: 705659 E, 293061 N (MGI Austria GK M34)

Type: Cataclasite Type 1

This sample is a cataclasite from a reef limestone of the Wetterstein Formation. It was extracted from a 1.5 m thick cataclastic zone. This plain-gray example shows every typical feature of a cataclasite: From the strong variation in grain size (mm to a few cm) to the poorly rounded fragments and the relatively fragile consistence of the rock itself, which also made it impossible to drill a plug out of it. The clasts are from the Wetterstein reef facies and react strongly to HCl.

Figure 95: Handpiece of MT31, extracted out of a 1.5 m thick band of cataclasite, size: 1249 cc.

PW-Samples

Sample Name: **PW1/6**

Lithology: Wetterstein Dolomite

Length: 35,5 mm

FDC: 4
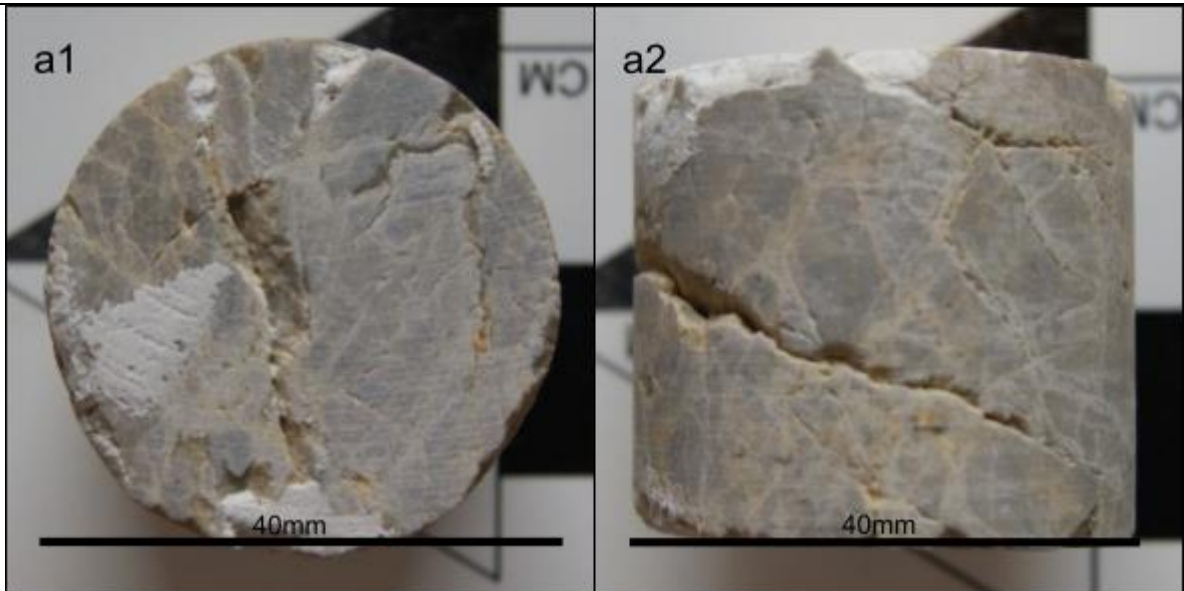
Figure 96: PW1/6 in top view **(a1)** and lateral view **(a2)**. This piece is a perfect example for an FDC 4 rock.
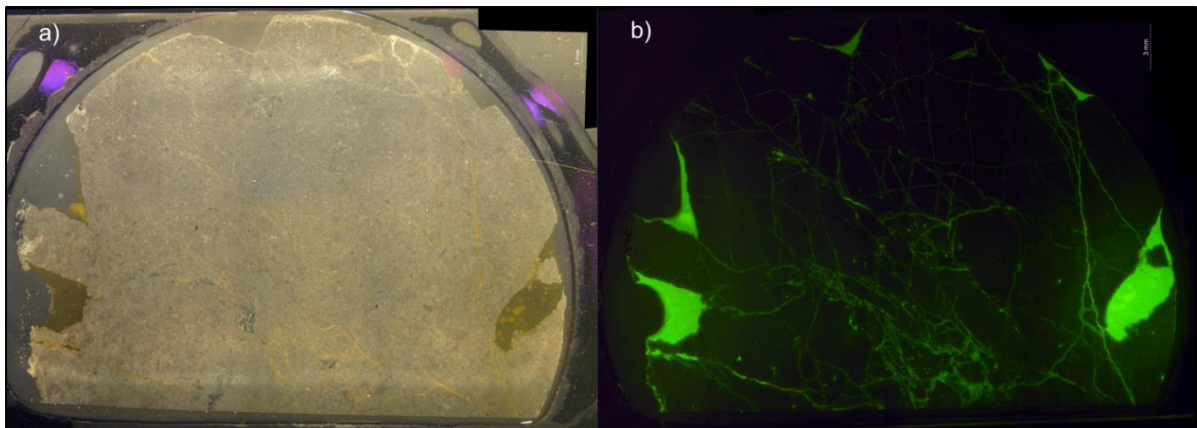
*Figure 97: Cut-out from sample PW1/6 with Fluorol in pores and cleavages. **a)** shows the sample under reflected light. **b)** shows the sample under UV-light. The thin sections of PW1/6 show how strongly evolved the fractures are, with multiple orientations, differences in width, angular cut-outs, and a good interconnectivity between the cleavages. Most of the pore space is caused through fracturing and shows a good example of secondary porosity. The larger green Fluorol-filled areas broke out from the sample and are therefore not counted towards the pore space. The sample is 1.5 inch wide.*

The sample shows an especially high fracture density due to the intensive fracturing of the sample. This rock is very dependent on its fractures in porosity and permeability. Through the undisturbed and connected fractures, the sample is very permeable, far more than the other samples, viewed under UV-light microscopy.

Sample Name: **PW3/1**

Lithology: Wetterstein Reef Limestone

Length: 45,4 mm

FDC: 2
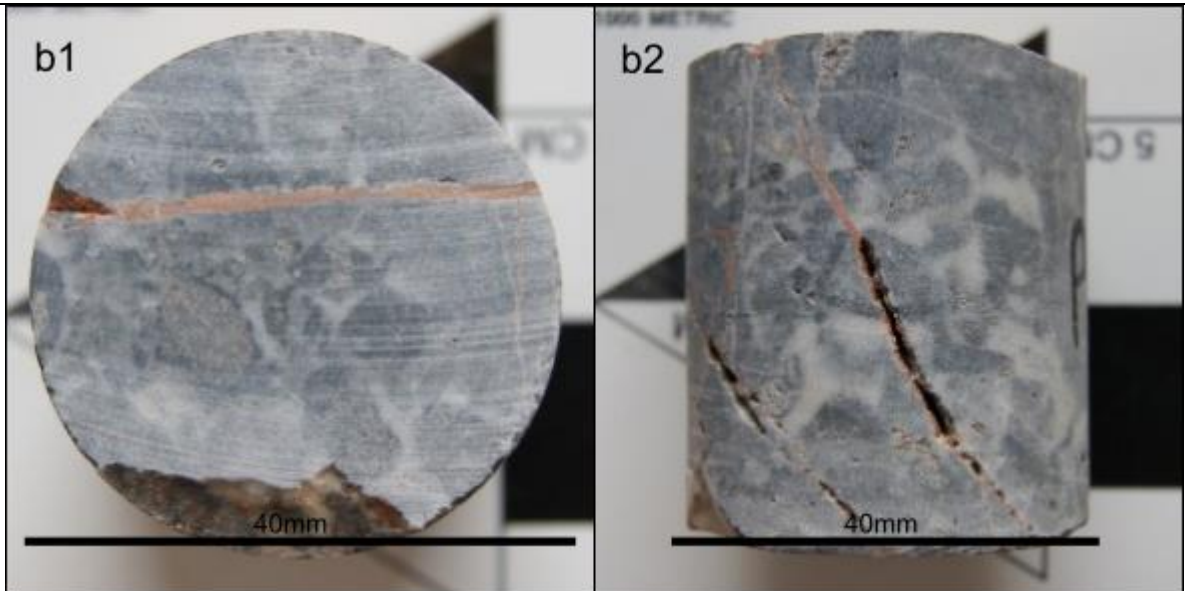
Figure 98: PW3/1 in top view **(b1)** and lateral view **(b2)**.

Sample Name: **PW3/2**

Lithology: Wetterstein Reef Limestone

Length: 53 mm

FDC: 3
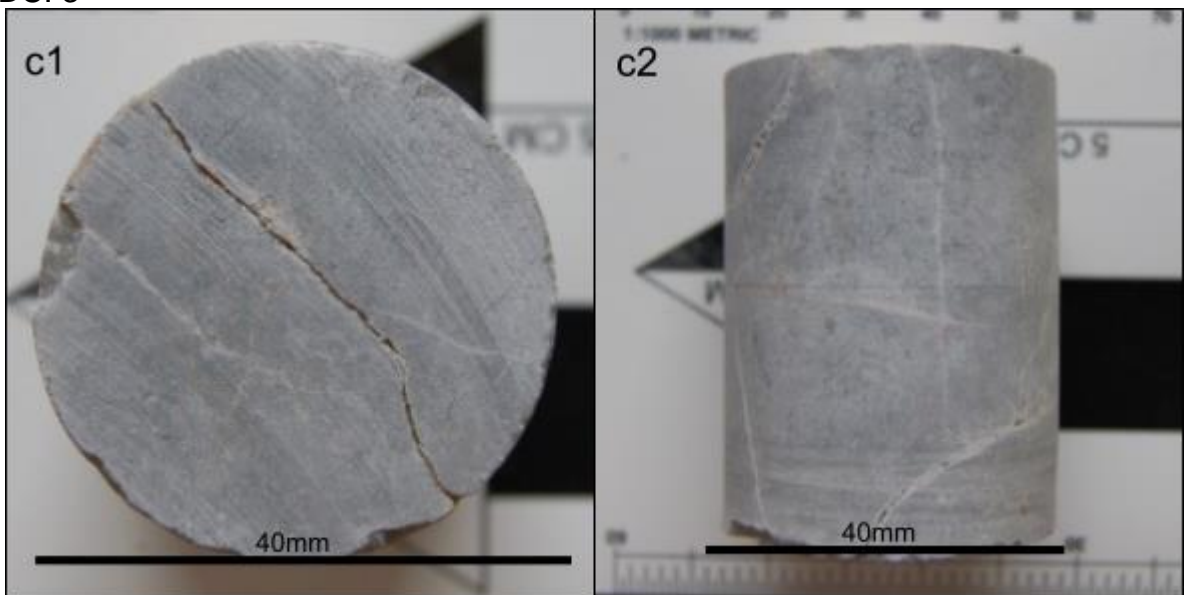
Figure 99: PW3/2 in top view **(c1)** and lateral view **(c2)**

Sample Name: **PW3/3**

Lithology: Wetterstein Reef Limestone

Length: 43,3 mm

FDC: 3
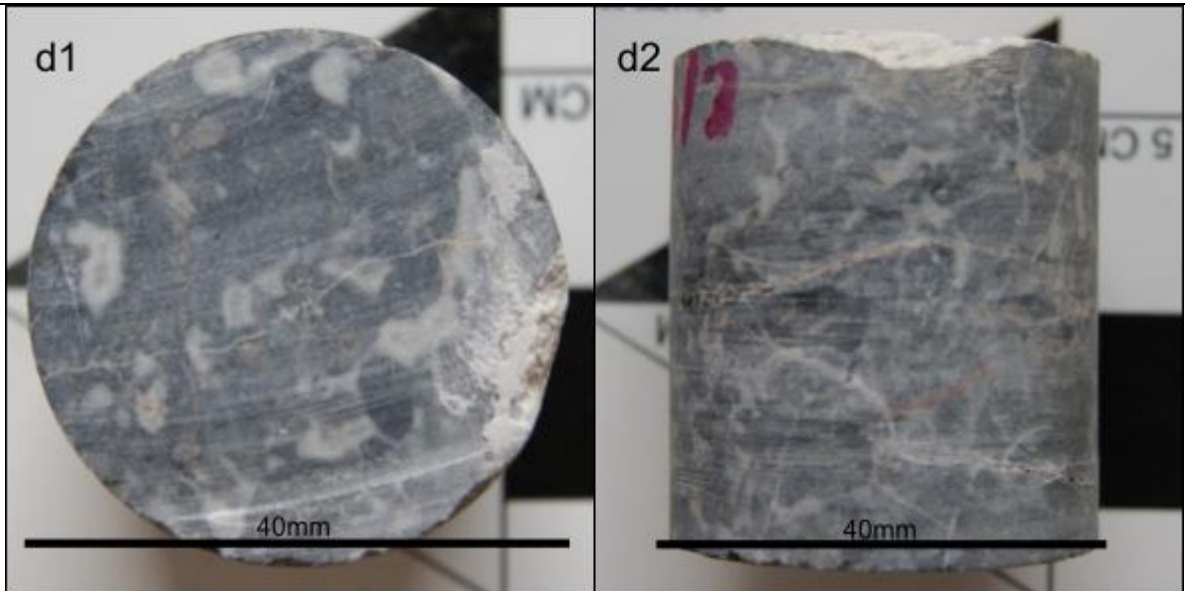
Figure 100: PW3/3 in top view **(d1)** and lateral view **(d2)**.

Sample Name: **PW3/4**

Lithology: Wetterstein Reef Limestone

Length: 35,7 mm

FDC: 2
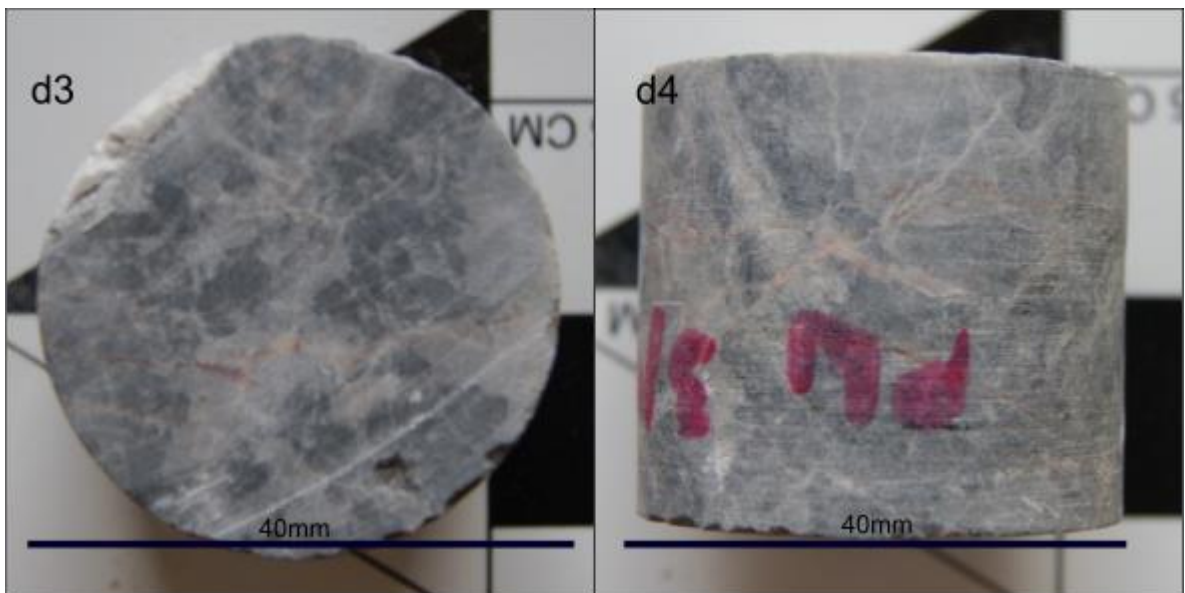
Figure 101: PW3/4 in top view **(d3)** and lateral view **(d4).**

Sample Name: **PW4/4**

Lithology: Wetterstein Reef Limestone

Length: 64,6 mm

FDC: 2
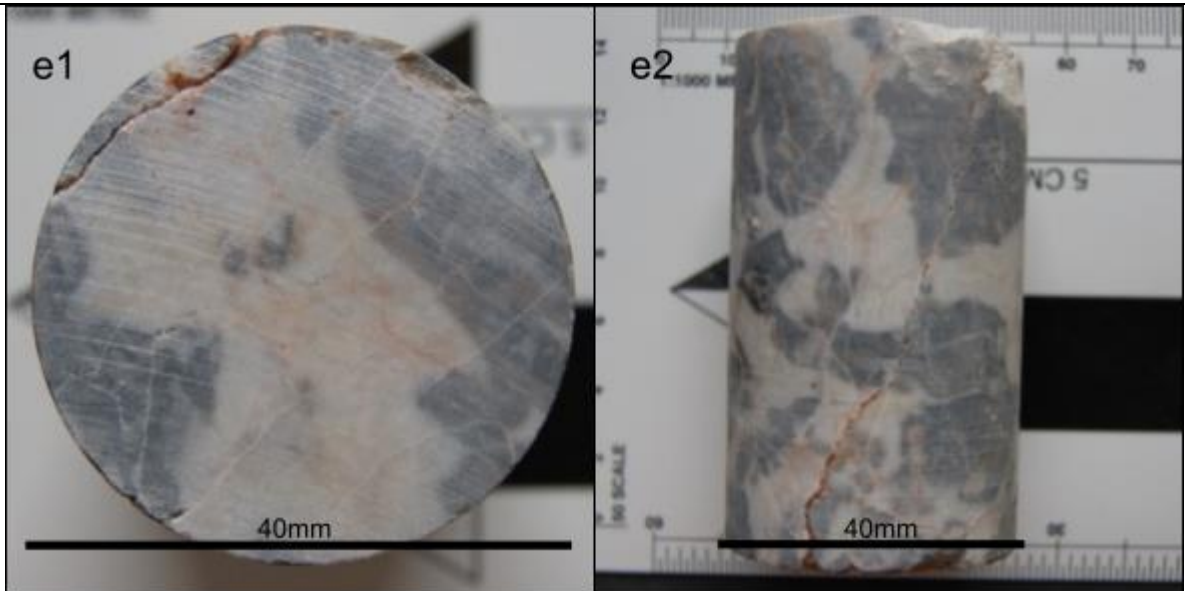
Figure 102: PW4/4 in top view **(e1)** and lateral view **(e2)**.
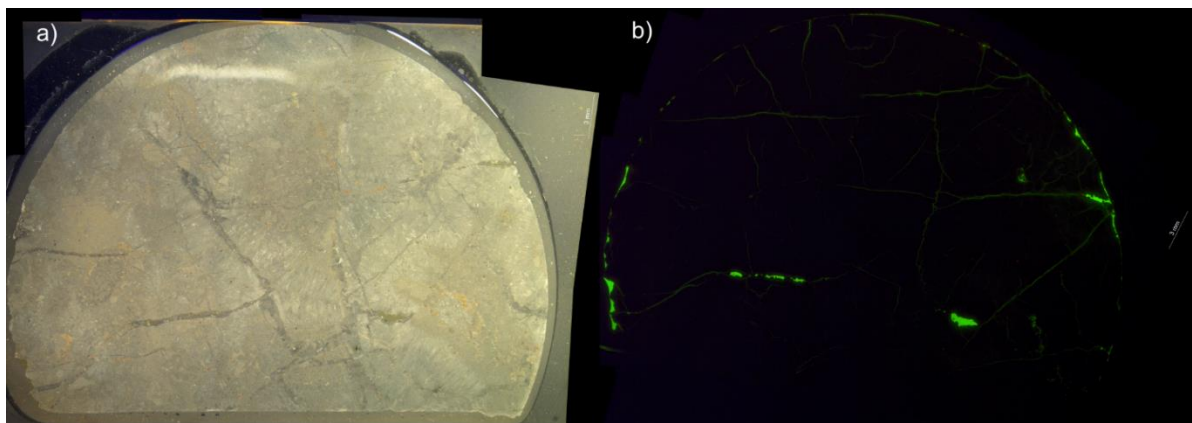
Figure 103: Cut-out from sample PW4/4 with Fluorol in pores and cleavages. **a)** shows the sample under reflected light. **b)** shows the sample under UV-light. Most pores are found adjacent to the fractures. The sample is 1.5 inch wide.

Sample Name: **PW5/1.1**

Lithology: Wetterstein Reef Limestone

Length: 61,5 mm

FDC: 1
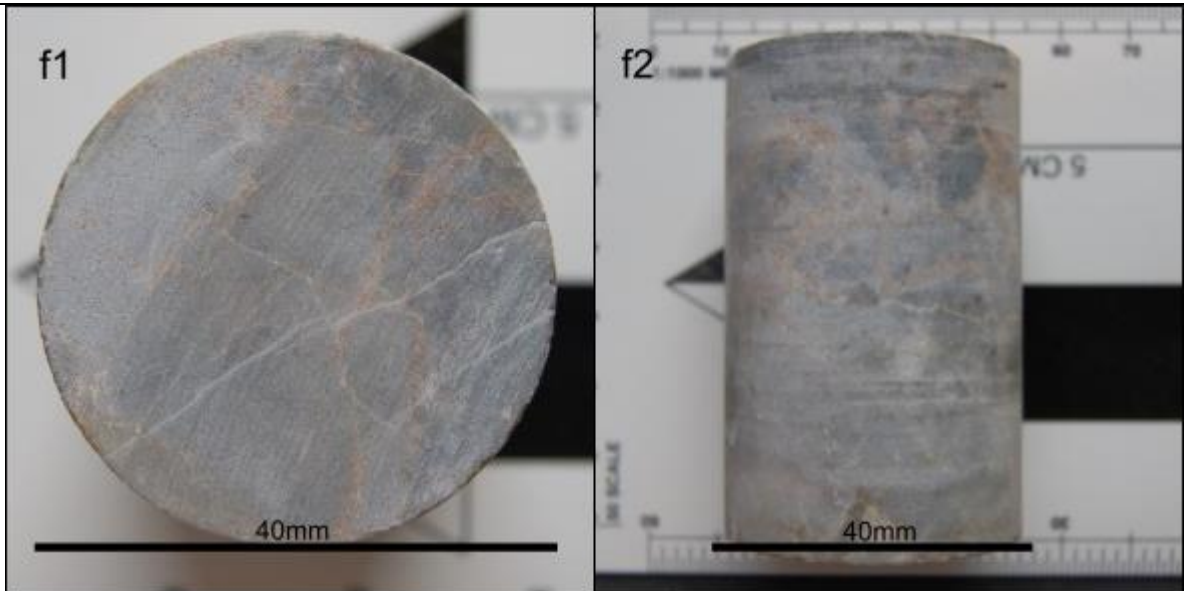
Figure 104: PW5/1.1 in top view **(f1)** and lateral view **(f2)**.
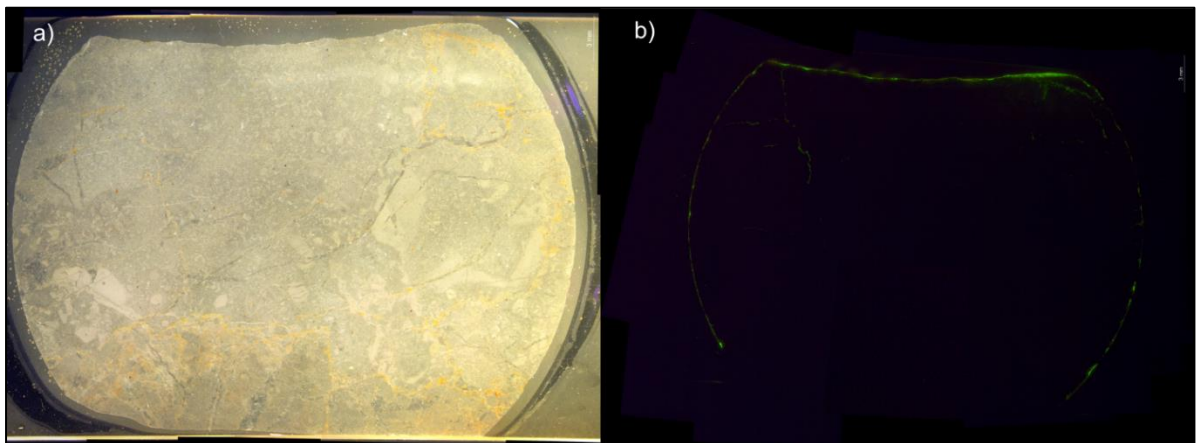
Figure 105: Cut-out from sample PW5/1.1 with Fluorol in pores and cleavages. **a)** shows the sample under reflected light. **b)** shows the sample under UV-light. The outlines of the sample hold most of the Fluorol, only a small part is pore space. The sample is 1.5 inch wide.

PW5/1 and PW5/1.2 show very similar characteristics, with only minor differences in fractures and porosity, with PW5/1 having a little higher fracture length per areas and porosity. This also leads to a little higher permeability value for both samples. Having almost no interconnection between fractures makes the two samples extremely susceptible for losses of permeability and porosity with increased pressure.

Sample Name: **PW5/1.2**

Lithology: Wetterstein Reef Limestone

Length: 38,2 mm

FDC: 1
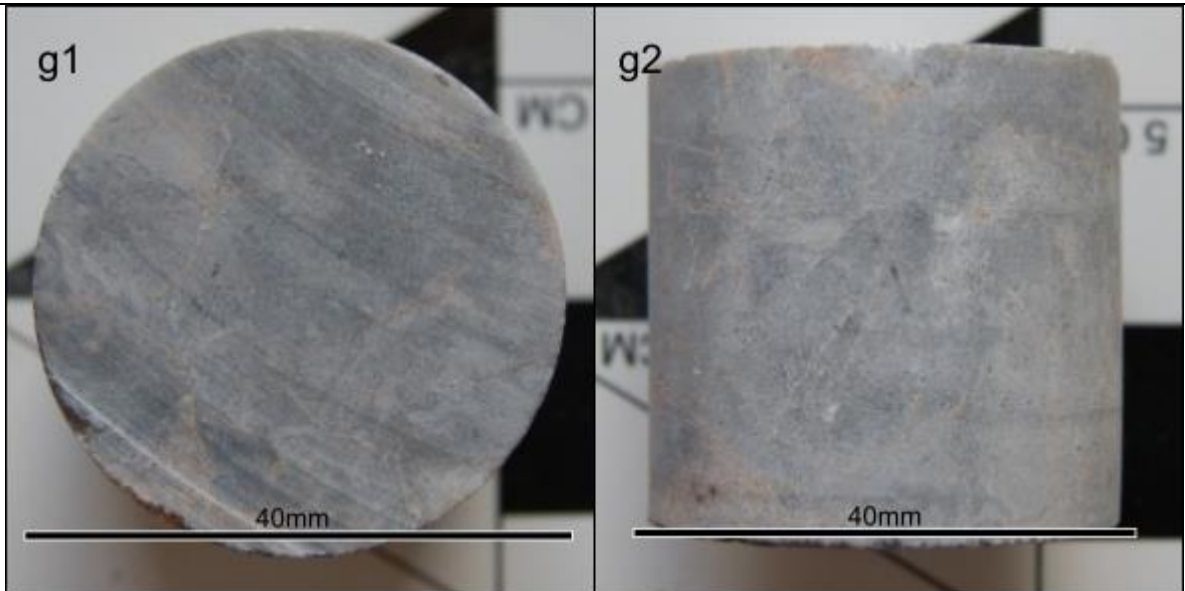
Figure 106: PW5/1.2 in top view **(g1)** and lateral view **(g2)**.
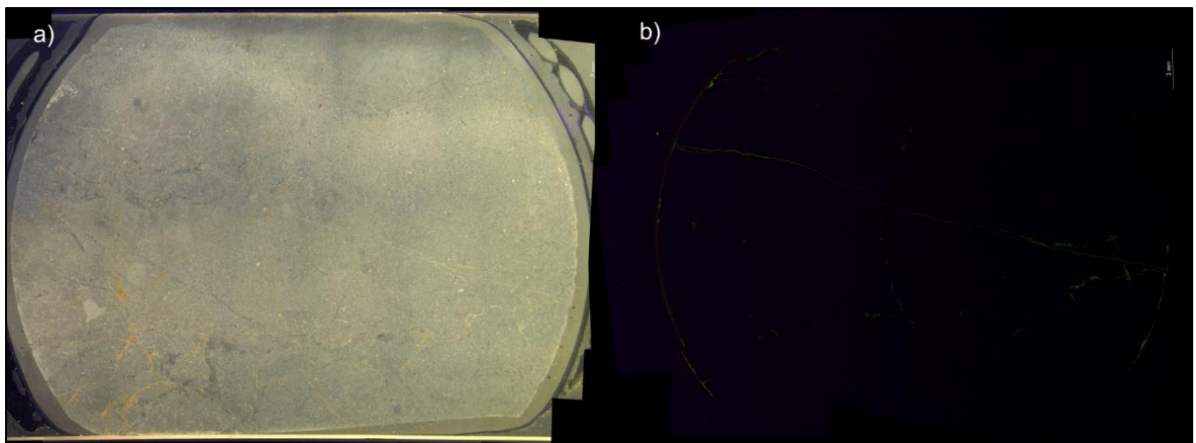
Figure 107: Cut-out from sample PW5/1.2 with Fluorol in pores and cleavages. **a)** shows the sample under reflected light. **b)** shows the sample under UV-light. With almost no pore and cleavage space, the UV light emission is almost non-existent. The sample is 1.5 inch wide.

Sample Name: **PW5/3**

Lithology: Wetterstein Reef Limestone

Length: 64,4 mm

FDC: 2
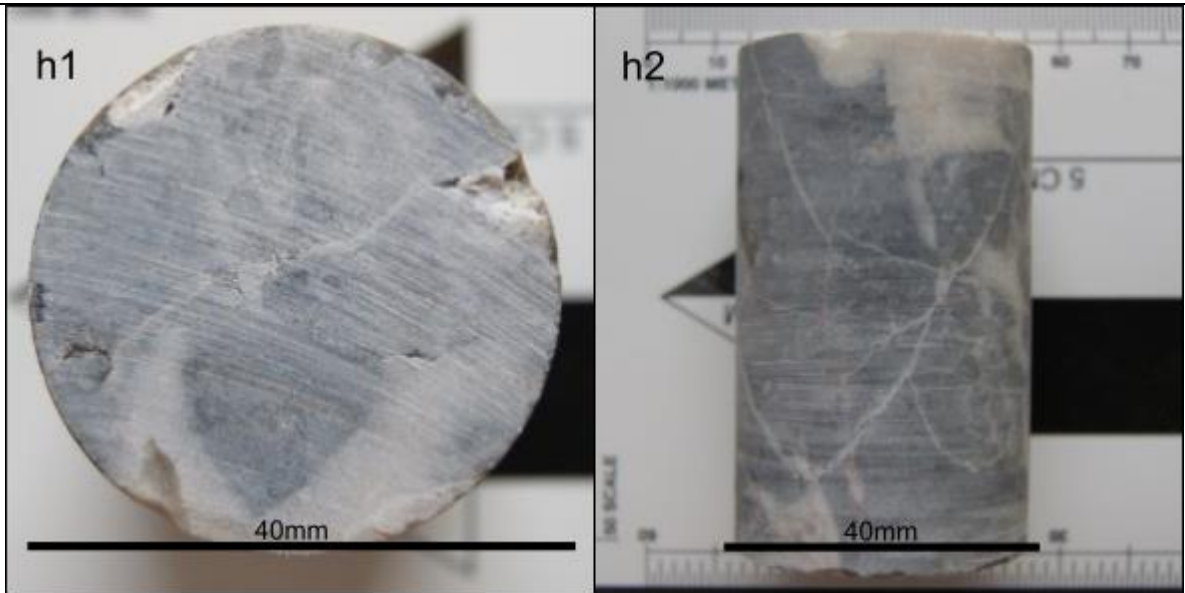
Figure 108: PW5/3 in top view (h1) and lateral view (h2).

Sample Name: **PW5/4**

Lithology: Wetterstein Reef Limestone

Length: 67 mm

FDC: 2
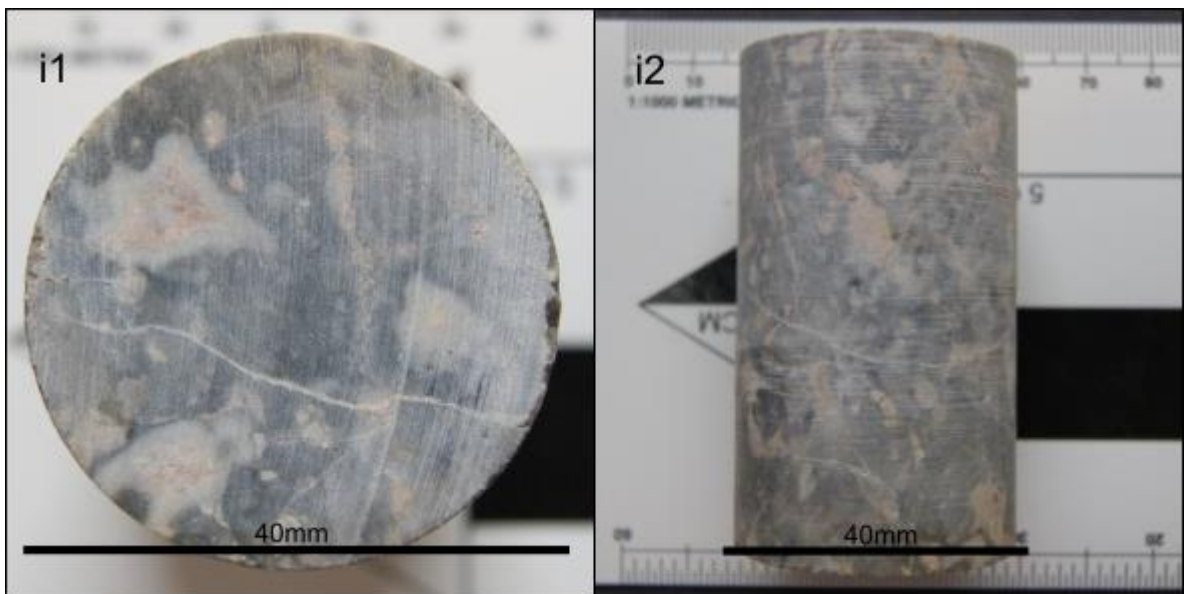
Figure 109: PW5/4 in top view (i1) and lateral view (i2).

Sample Name: **PW5/5**

Lithology: Wetterstein Reef Limestone

Length: 48,8 mm

FDC: 3
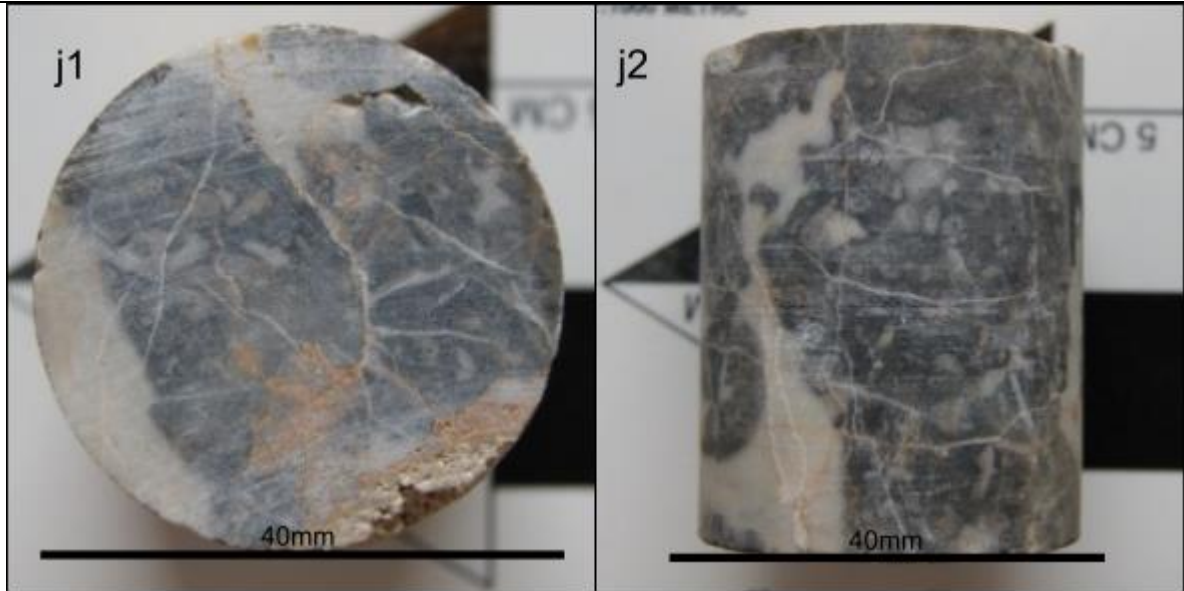
Figure 110: PW 5/5 in top view **(j1)** and lateral view **(j2)**.

Sample Name: **PW5/6**

Lithology: Wetterstein Reef Limestone

Length: 36 mm

FDC: 3
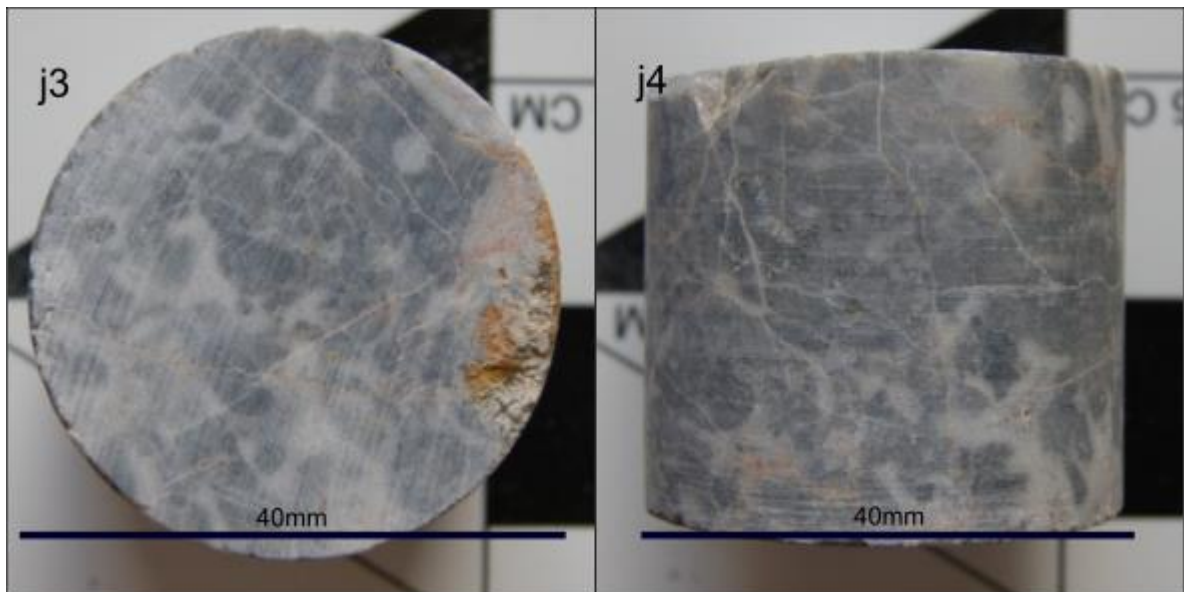
Figure 111: PW5/6 in top view **(j3)** and lateral view **(j4)**.

Sample Name: **PW5/7**

Lithology: Cataclasite (Type 1) from a protolith of the Wetterstein reef limestone

Length: 41,2 mm
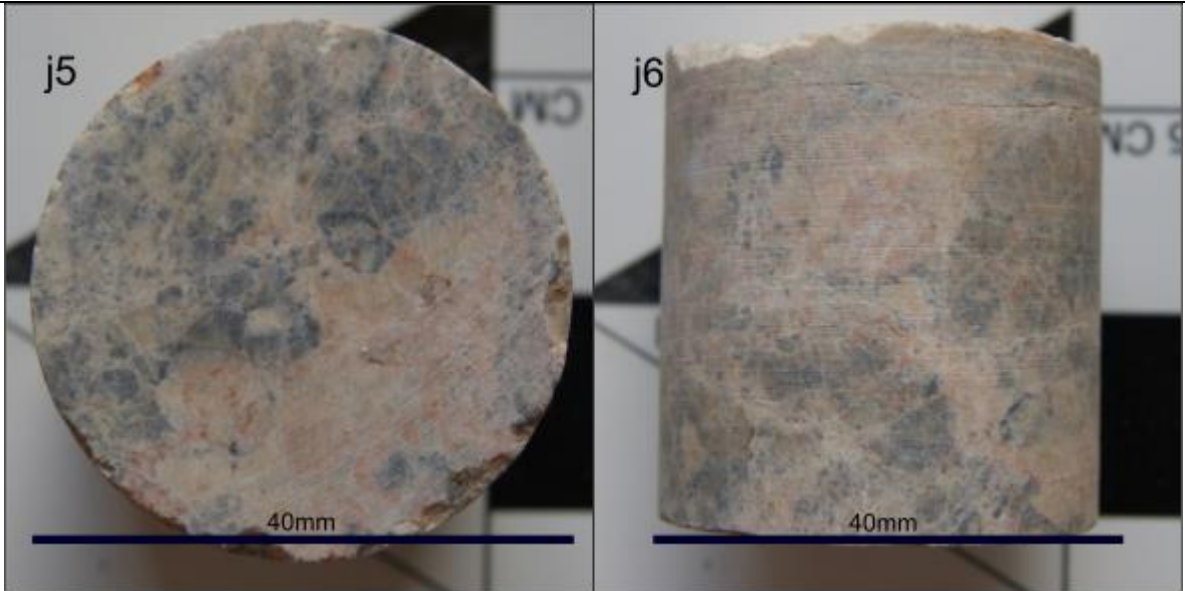
Figure 112: PW5/7 in top view **(j5)** and lateral view **(j6)**.

Sample Name: **PW6/1**

Lithology: Lagoonal Wetterstein Limestone

Length: 51,3 mm

FDC: 3
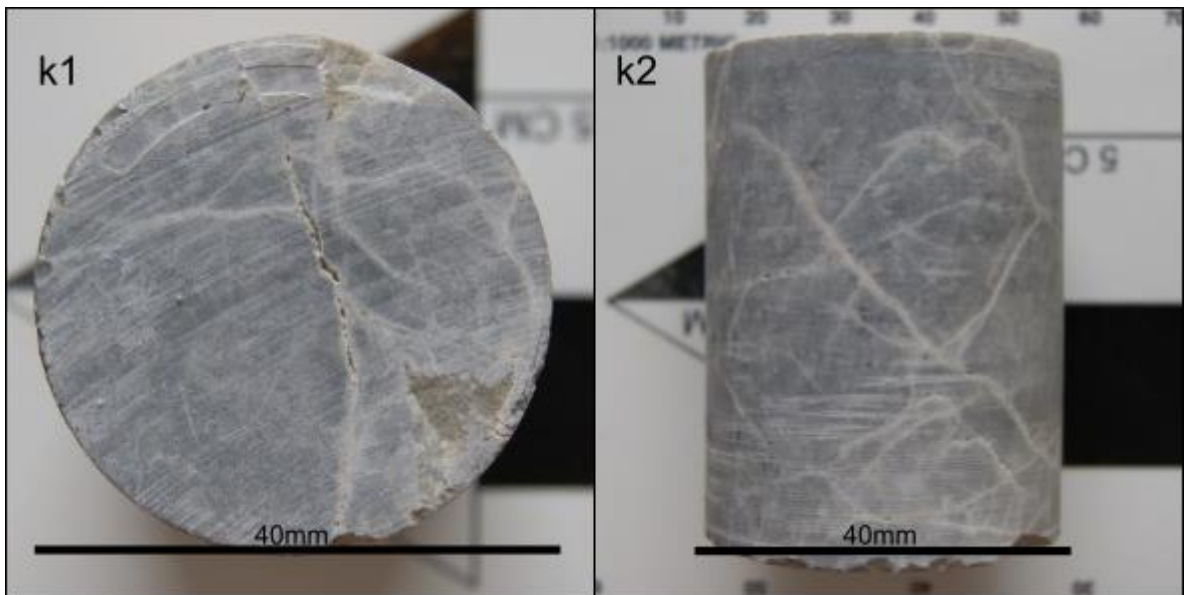
Figure 113: PW6/1 in top view **(k1)** and lateral view **(k2)**.

Sample Name: **PW6/2**

Lithology: Lagoonal Wetterstein Limestone

Length: 58,2 mm

FDC: 2
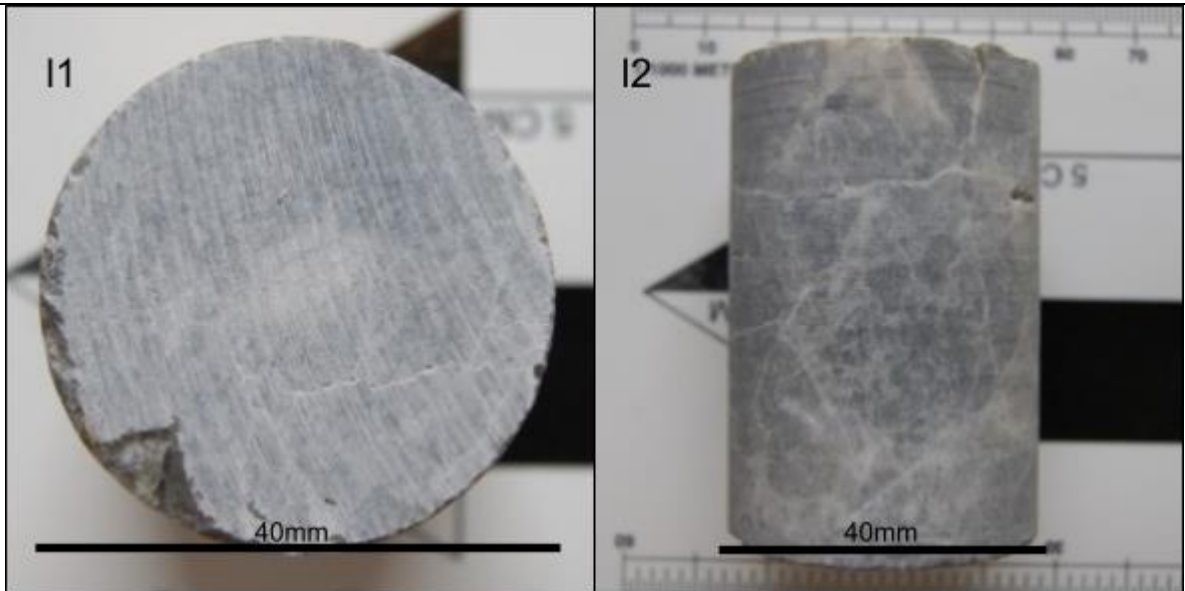
Figure 114: PW6/2 in top view **(I1)** and lateral view **(I2)**.

Figure 115: Cut-out from sample PW6/2 with Fluorol in pores and fractures. **a)** shows the sample under reflected light. There is no picture of the sample under UV-light because no stitch could be made from the almost non-existing UV-emission of this sample.

Sample Name: **PW6/3.1**

Lithology: Lagoonal Wetterstein Limestone

Length: 58 mm

FDC: 2
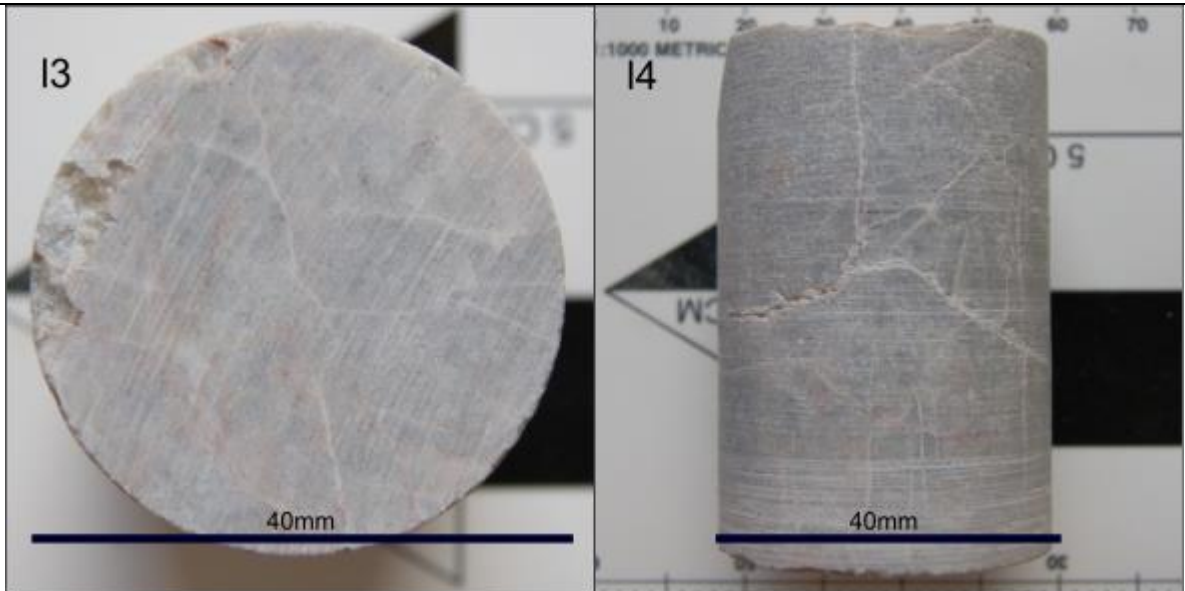
Figure 116: PW6/3.1 in top view **(I3)** and lateral view **(I4)**.

Sample Name: **PW6/3.2**

Lithology: Lagoonal Wetterstein Limestone

Length: 39,8 mm

FDC: 2
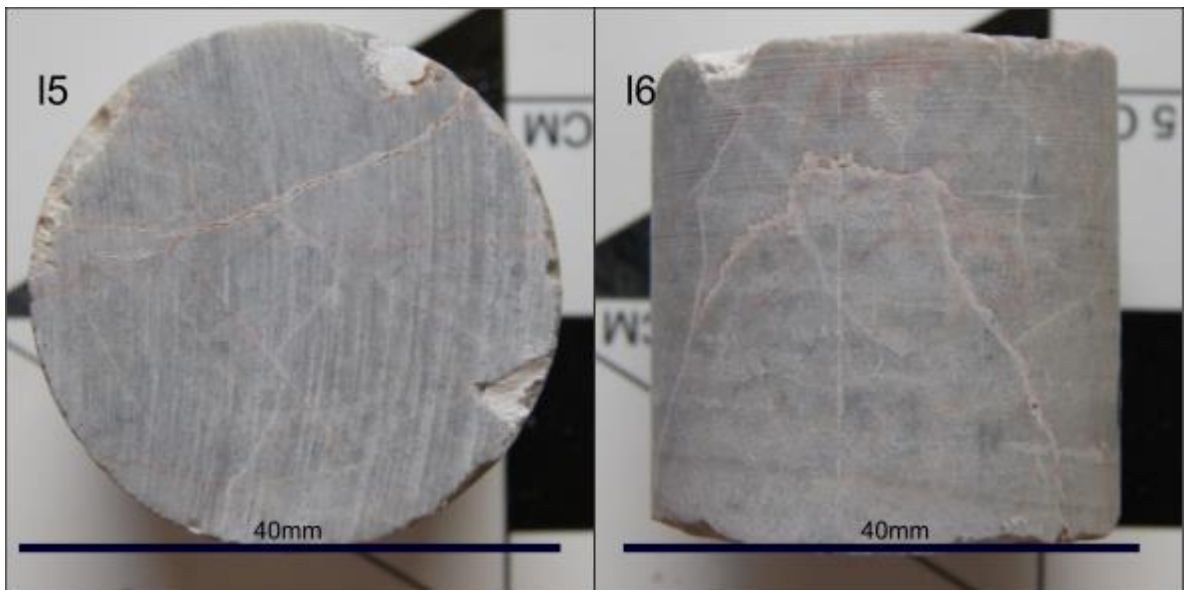
Figure 117: PW6/3.2 in top view **(I5)** and lateral view **(I6)**.

Sample Name: **PW6/4**

Lithology: Lagoonal Wetterstein Limestone

Length: 67,3 mm

FDC: 2
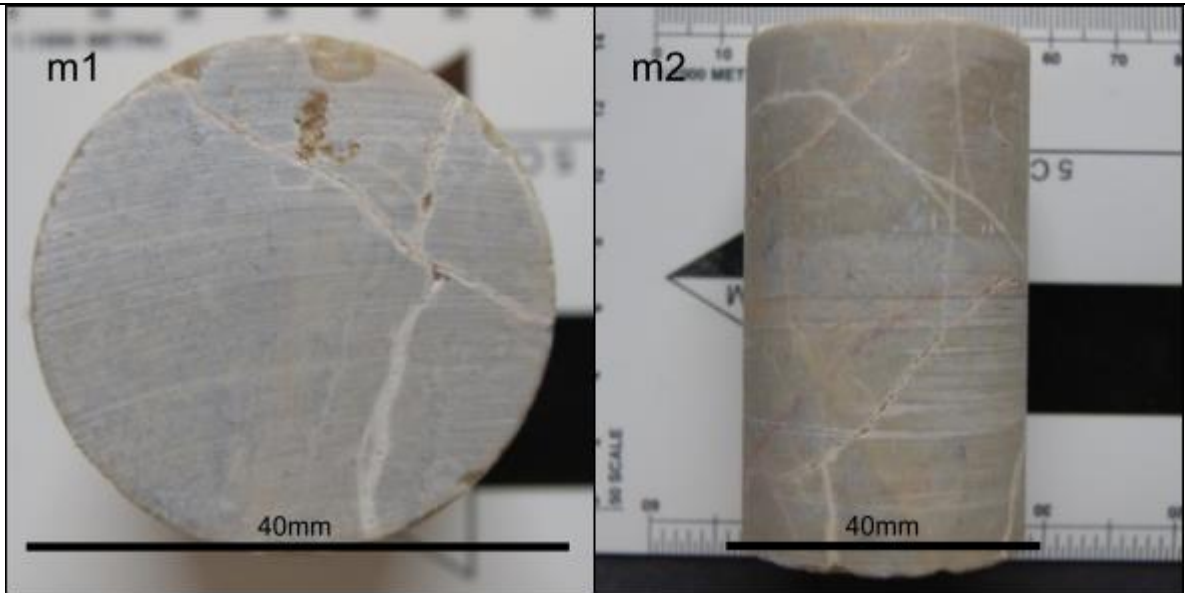
Figure 118: PW6/4 in top view **(m1)** and lateral view **(m2)**.

Sample Name: **PW6/5**

Lithology: Lagoonal Wetterstein Limestone

Length: 32,8 mm

FDC: 3
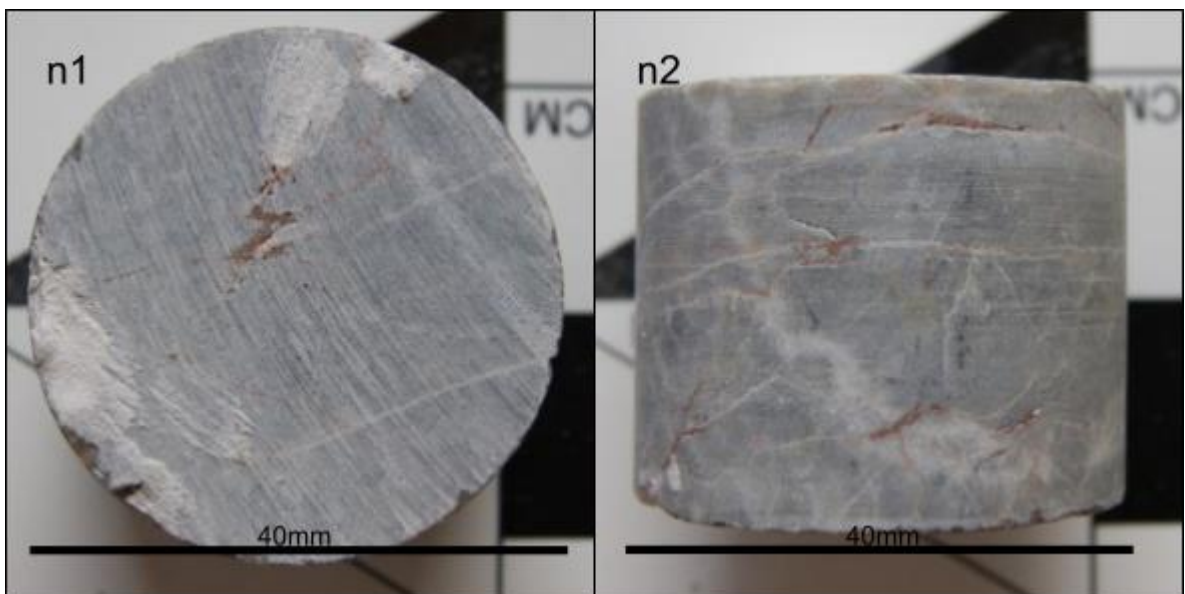
Figure 119: PW6/5 in top view **(n1)** and lateral view **(n2)**.

Sample Name: **PW6/6**

Lithology: Lagoonal Wetterstein Limestone

Length: 45,7 mm

FDC: 3
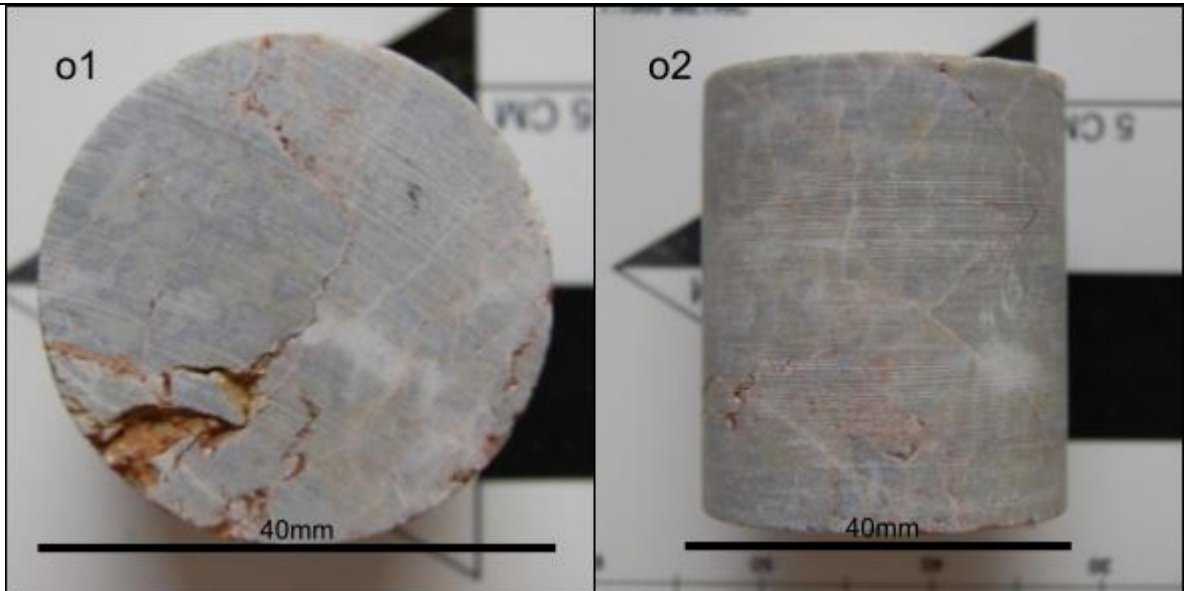
Figure 120: PW6/6 in top view **(o1)** and lateral view **(o2)**.

Sample Name: **PW6/7.1**

Lithology: Stylobreccia from a protolith of lagoonal Wetterstein limestone

Length: 40,9 mm
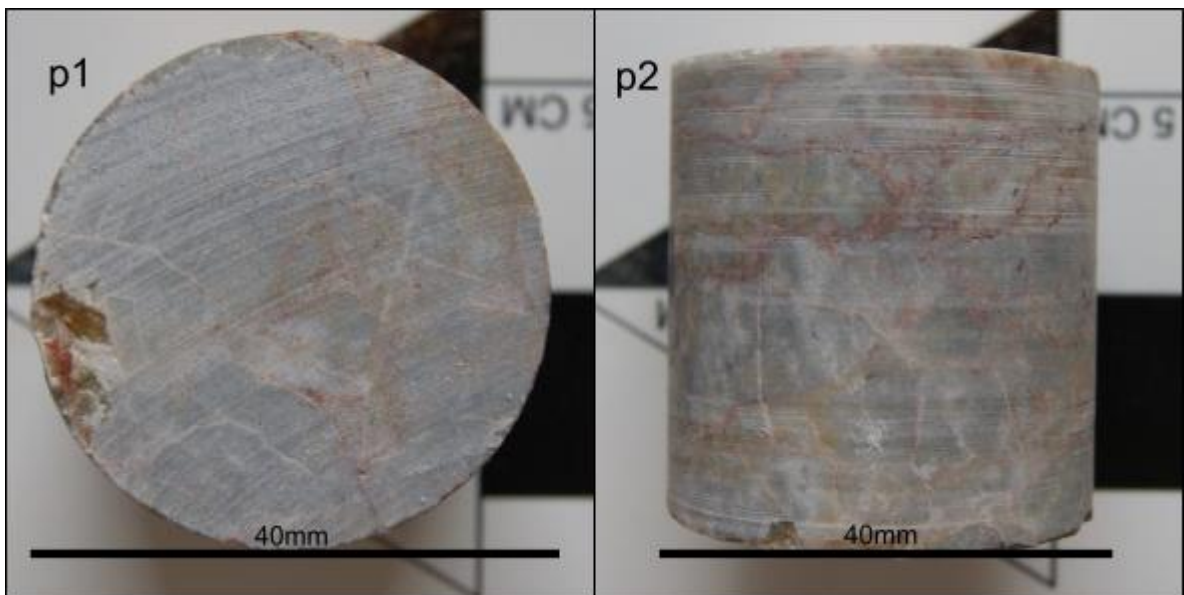
Figure 121: PW6/7.1 in top view **(p1)** and lateral view **(p2)**.

Sample Name: **PW6/7.2**

Lithology: Stylobreccia from a protolith of lagoonal Wetterstein limestone

Length: 50 mm
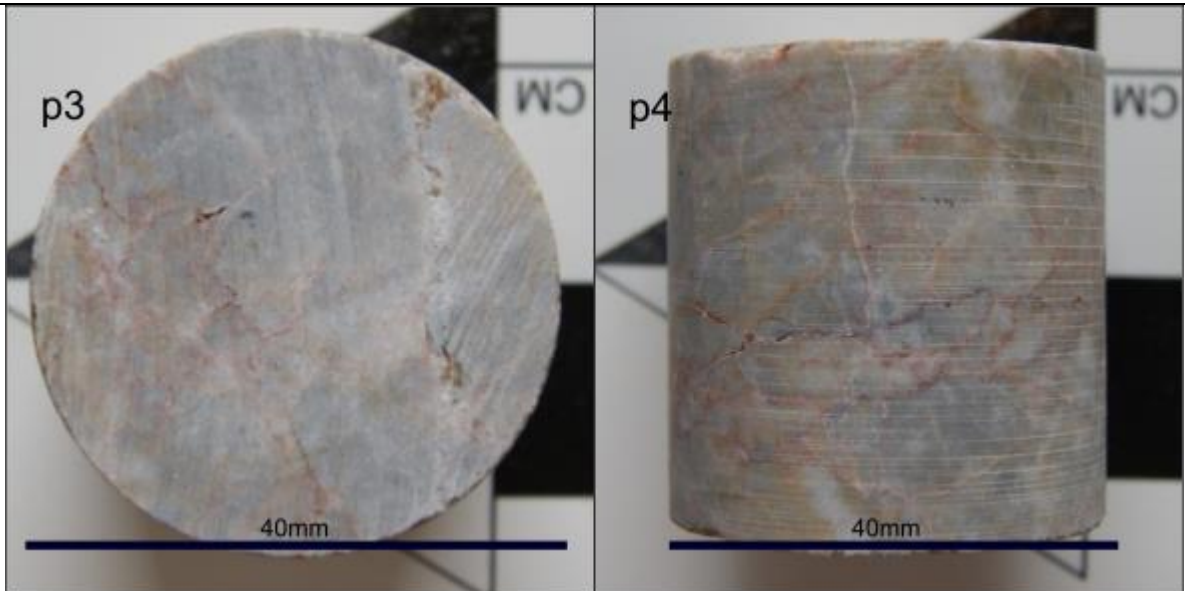
Figure 122: PW6/7.2 in top view **(p3)** and lateral view **(p4)**.

Sample Name: **PW6/8**

Lithology: Lagoonal Wetterstein limestone

Length: 38,3 mm

FDC: 1
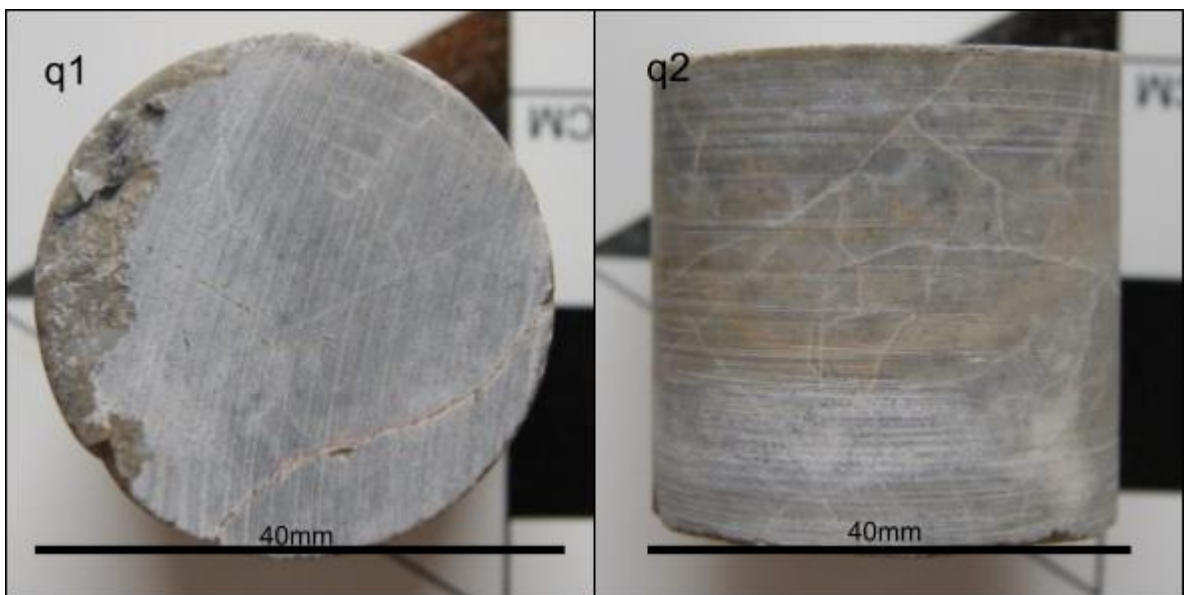
Figure 123: PW6/8 in top view **(q1)** and lateral view **(q2)**.

Sample Name: **PW7/1**

Lithology: Wetterstein Dolomite

Length: 49,8 mm

FDC: 2
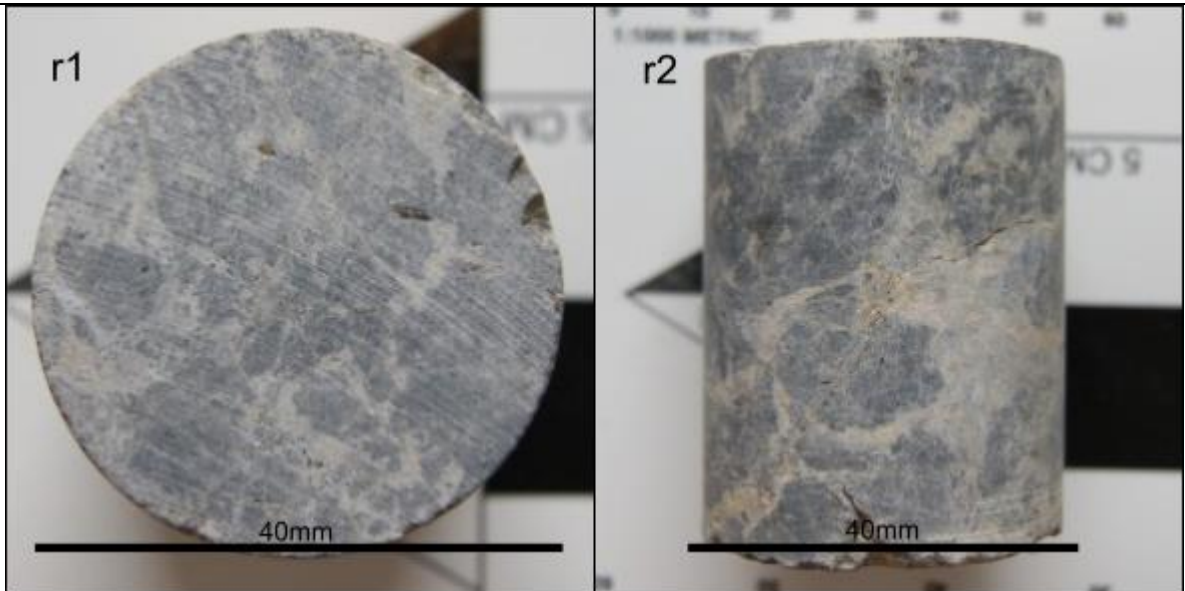
Figure 124: PW7/1 in top view **(r1)** and lateral view **(r2)**.

Sample Name: **PW7/2.1**

Lithology: Wetterstein Dolomite

Length: 37,1 mm

FDC: 2

Figure 125: PW7/2.1 in top view **(s1)** and lateral view **(s2)**.

Sample Name: **PW7/2.2**

Lithology: Wetterstein Dolomite

Length: 37,2 mm

FDC: 2
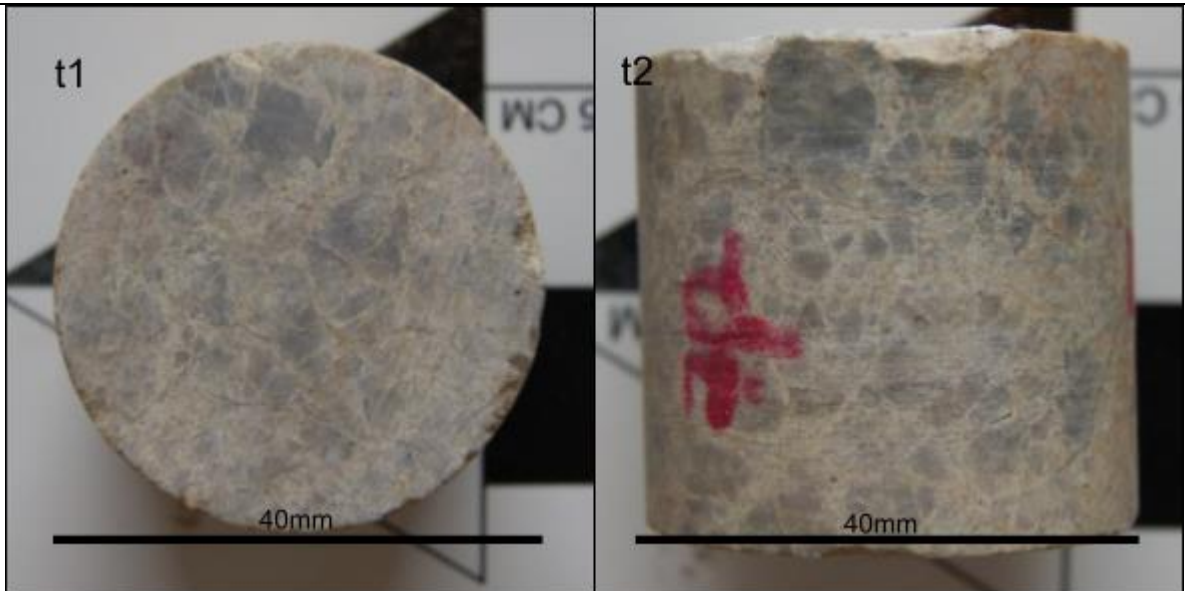
Figure 126: PW7/2.2 in top view **(t1)** and lateral view **(t2)**.

Sample Name: **PW7/3.1**

Lithology: Cataclasite (Type 1) from a dolomitic protolith of the Wetterstein Formation

Length: 61,1 mm

Cataclasite Type 1
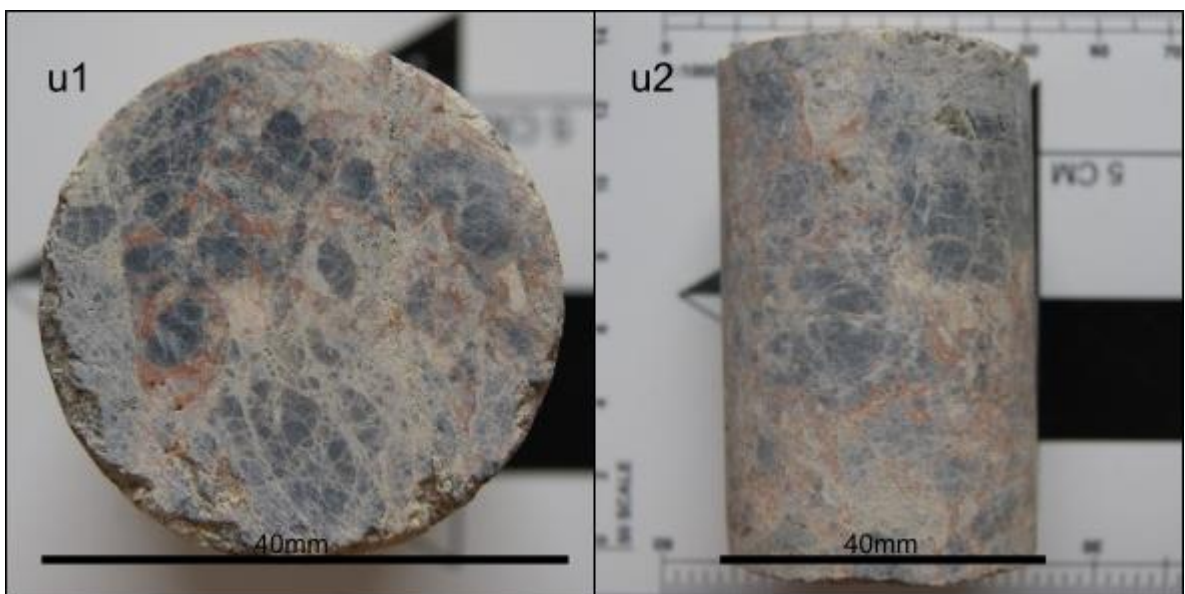
Figure 127: PW7/3.1 in top view **(u1)** and lateral view **(u2)**.
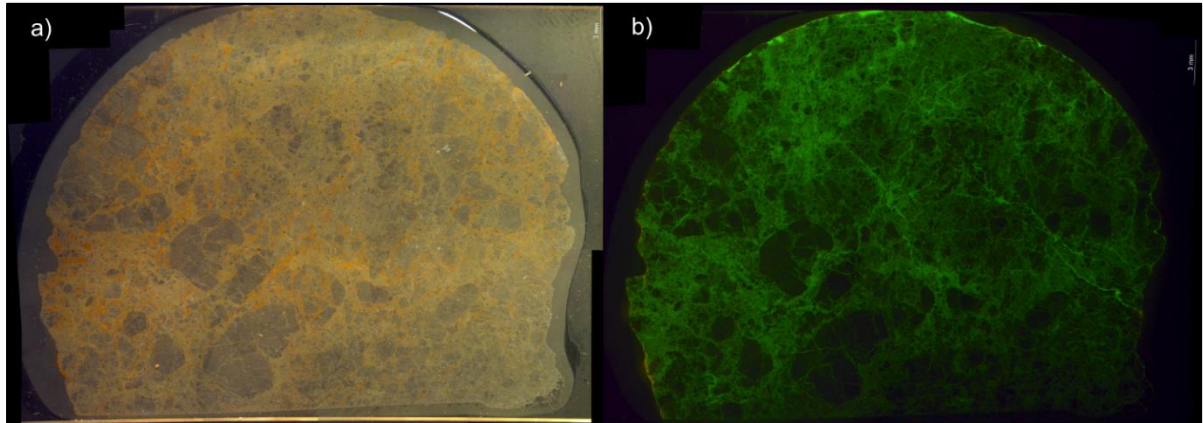
Figure 128: Cut-out from sample PW7/3.1 with Fluorol in pores and cleavages. PW7/3 shows a cataclastic appearance with many fractured grains and a dense network of cleavages without orientation. **a)** shows the sample under reflected light. **b)** shows the sample under UV-light. The sample is 1.5 inch wide.

PW7/3 shows increased porosity through the cataclastic process, which is clearly visible in the UV-photographs. Small but numerous fractures appear over the whole sample and often part even grains. There is no preferred orientation of these fractures. The higher porosity, relative to other Wetterstein Dolomite samples can also be explained through cataclastic flow. The fractures are very interconnected, which enables high permeabilities and makes the sample stable against losses of permeability with pressure, relative to other samples.

Sample Name: **PW7/3.2**

Lithology: Wetterstein Cataclasite (Type 2) from a dolomitic protolith of the Wetterstein Formation

Length: 59,6 mm

Cataclasite Type 2
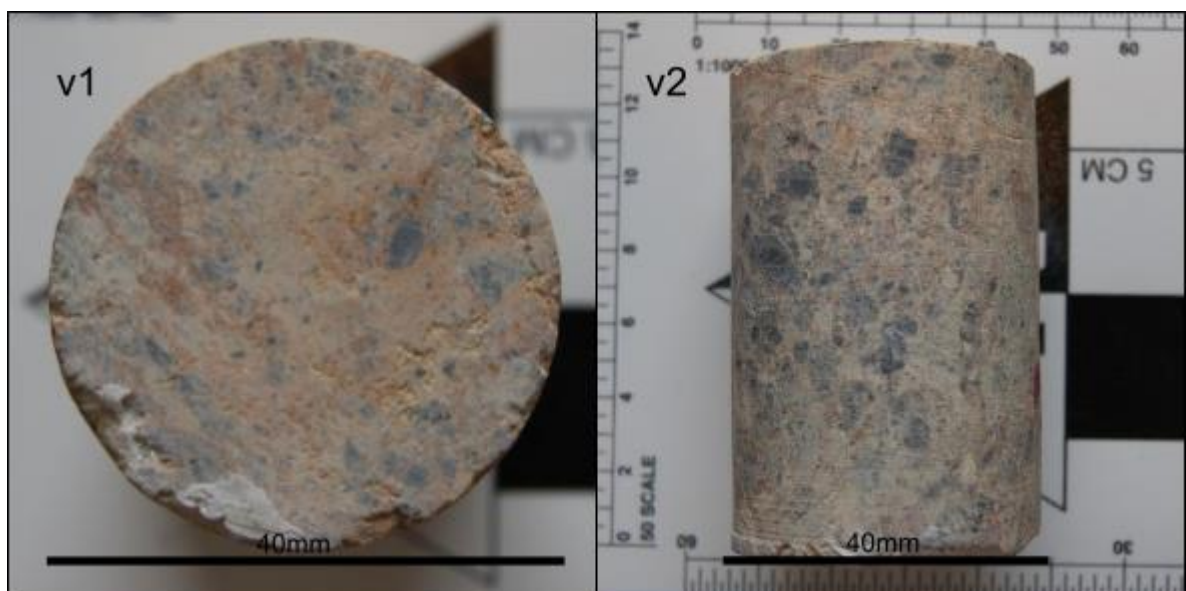
Figure 129: PW7/3.2 in top view **(v1)** and lateral view **(v2)**.

Sample Name: **PW7/4**

Lithology: Cataclasite (Type 1) from a dolomitic protolith of the Wetterstein Formation

Length: 74 mm

Cataclasite Type 1
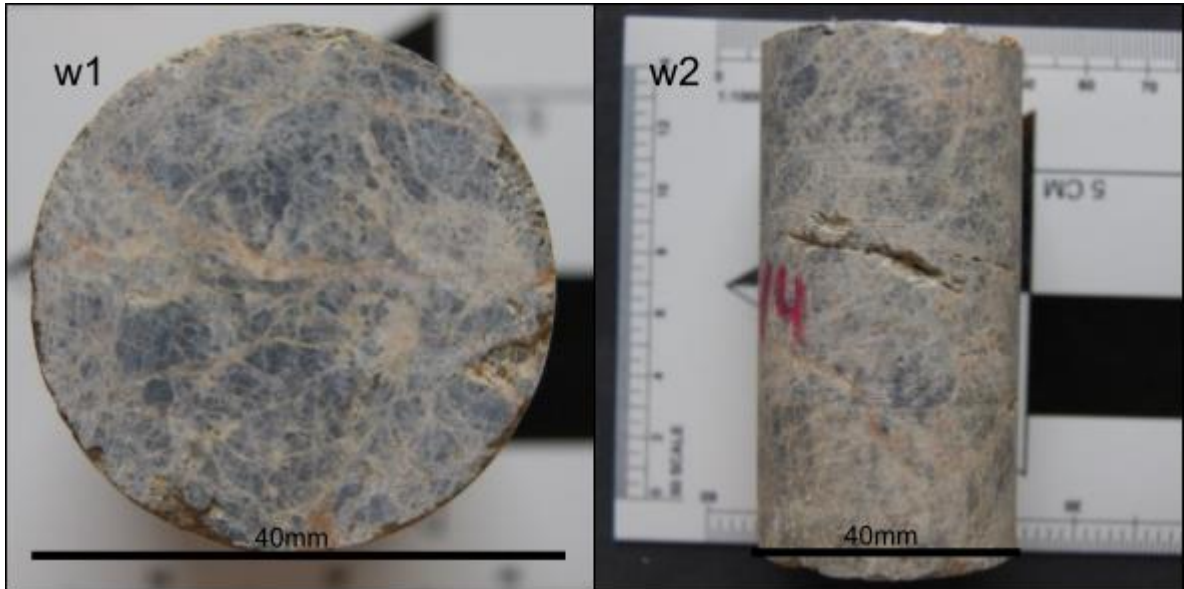
Figure 130: PW7/4 in top view **(w1)** and lateral view **(w2)**.

Sample Name: **PW7/5**

Lithology: Wetterstein dolomite

Length: 59,9 mm

FDC: 1
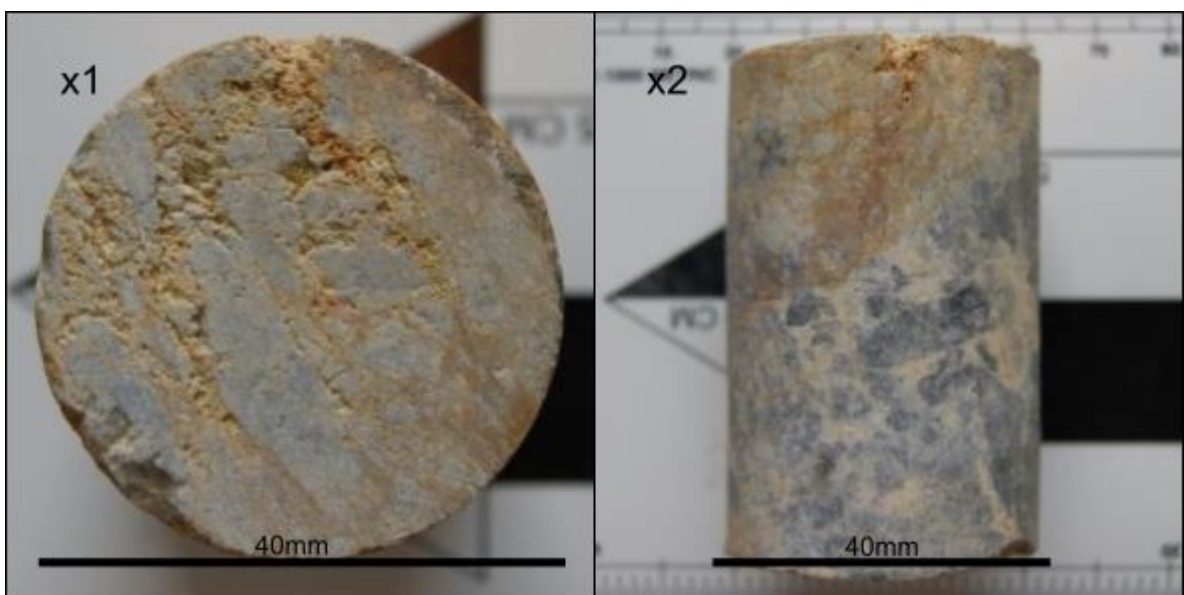
Figure 131: PW7/5 in top view **(x1)** and lateral view **(x2)**.

Sample Name: **PW7/6**

Lithology: Wetterstein dolomite

Length: 36,1 mm

FDC: 1
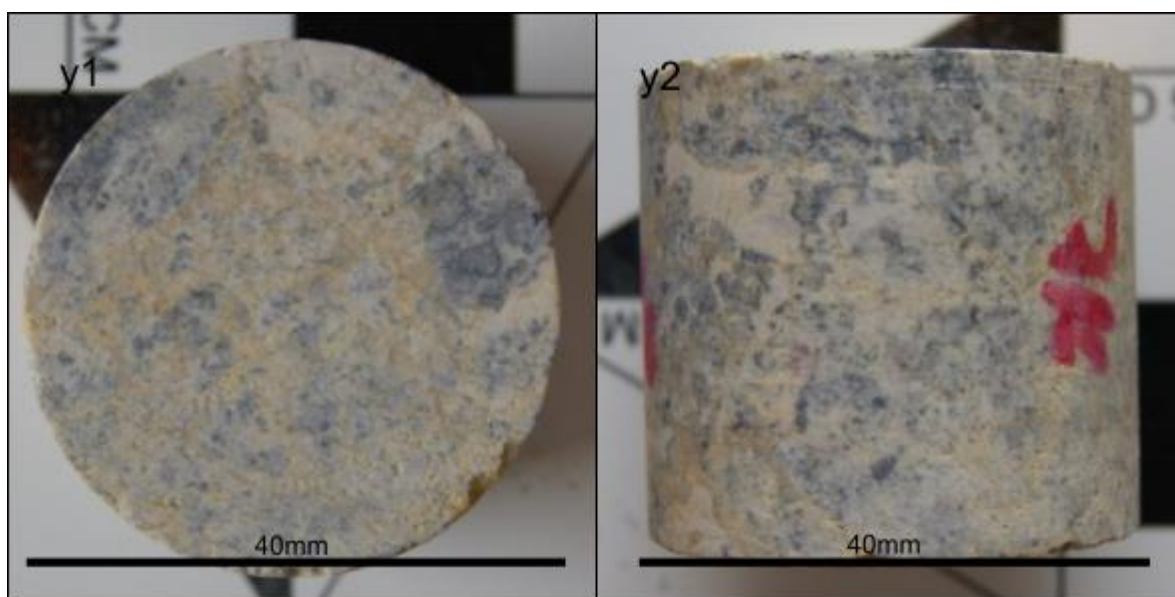
Figure 132: PW7/6 in top view **(y1)** and lateral view **(y2)**.

13 Lists

13.1 List of Figures

13.2 <u>List of Tables</u>

14 References

Adler, P.M., Thovert, J.F., Mourzenko V.V. (2012). Fractured Porous Media. Oxford: Oxford University Press, 173 pp.

API (1998). Recommended Practices for Core Analysis. Recommended Practice 40 Second Edition, February 1998. Washington D. C.: American Petroleum Institute, 236 pp.

Bauer H. (2010). Deformationsprozesse und hydrogeologische Eigenschaften von Störungszonen in Karbonatgesteinen. Magisterarbeit, Department für Geodynamik und Sedimentologie, Universität Wien, 102 pp.

Bauer H., Decker K. (2010). Fault architecture, fault rocks and fault rock properties. In carbonate rocks. Geophysical Research Abstracts, 12:, 1-2.

Bauer H., Schröckenfuchs T. C., Decker K. (2016). Hydrogeological properties of fault zones in a karstified carbonate aquifer (Northern Calcareous Alps, Austria). Hydrogeology Journal, 24:, 1147-1170.

Beidinger, A., Decker, K. (2014), Quantifying Early Miocene in-sequence and out-of-sequence thrusting at the Alpine-Carpathian junction. Tectonics, 3:, 222–252.

Bernoulli D., Jenkyns H. C. (1974). Alpine, Mediterranean and Central Atlantic Mesozoic Facies in Relation to the Early Evolution of the Tethys. In: Society of Sedimentary Geology, Modern and Ancient Geosynclinal Sedimentation, 129–160.

Berre I., Doster F., Keilegavlen E. (2018). Flow in Fractured Porous Media: A Review of Conceptual Models and Discretization Approaches. Transport in Porous Media, 130, 215-236.

Czurda K. (1973). Fazies und Stratigraphie obertriadischer Megalodontenvorkommen der westlichen Nördlichen Kalkalpen. Verh. Geol. B.-A., 1973/3:, 397-409.

Dasgupta T., Mukherjee S. (2020). Porosity in Carbonates. In: Troyee Dasgupta, Soumyajit Mukherjee (eds.), Sediment Compaction and Applications in Petroleum Geoscience. Cham: Springer

Decker, K. (2007): Dolomite fracture and fault analysis, outcrop study Steinbruch Gaaden. Unpublished report to OMV Austria, Vienna

Decker K., Linzer H.-G., Peresson H., Dell´Mour R., Frisch W. (2002). Balancing lateral orogenic float of the Eastern Alps. Tectonophysics, 354, 211-237.

Dirnböck T., Greimler J. (1999). Vegetation mapping in the catchment areas of the City of Vienna (Schneeberg, Rax and Hochschwab) and its application for hydrological and ecological questions. In: AG Ökologie und Diversität der Pflanzen (FB Organismische Biologie), Universität Salzburg (1999): 10 (1999): Biotopkartierung im Alpenraum 1997 (Tagungsbeiträge), Sauteria Bd. 10, s. 201-218.

Egger H. (1990). Zur paläogeographischen Stellung des Rhenodanubischen Flysches (Neokom-Eozän) der Ostalpen. Jb. Geol. B.-A., 133/2:, 147-155.

EN 1936. (2006). Prüfverfahren von Naturstein - Bestimmung der Reindichte, der Rohdichte, der offenen Porosität und der Gesamtporosität (german version). Bruessel, European Committee for Standardization

Frisch W., Gawlick H. J. (2003). The nappe structure of the central Northern Calcareous Alps and its disintegration during Miocene tectonic extrusion — a contribution to understanding the orogenic evolution of the Eastern Alps. Int. J. Earth Sciences, 92:, 712-727.

Frisch W., Kuhlemann J., Dunkl I., Székely B. (2001). The Dachstein paleosurface and the Augenstein Formation in the Northern Calcareous Alps – a mosaic stone in the geomorphological evolution of the Eastern Alps. Int. J. Earth Sciences, 90:, 500–518.

Gangi, A.F. (1978). Variation of whole and fractured porous rock permeability with confining pressure. International Journal of Rock Mechanics and Mining Sciences & Geomechanics, Abstracts, 15/ 5:, 249–257.

Gawlick, H. J., Lein, R., Bucur, I. I. (2021). Precursor extension to final Neo-Tethys break-up: flooding events and their significance for the correlation of shallow-water and deep-marine organisms (Anisian, Eastern Alps, Austria). Int. J. Earth Sciences, 110, 419-446.

Gawlick, H. J., Missoni, S., Schlagintweit F., Lein, R. (2013). Field Trip A3: Triassic to Early Cretaceous shallow-water carbonates in the central Northern Calcareous Alps (Northwestern Tethyan realm). Berichte Geol. B.-A., 99:, 178-190.

Graßler, F. (1984). Alpenvereinseinteilung der Ostalpen (AVE). In: Deutscher Alpenverein (1984): Alpenvereins-Jahrbuch", Berg '84, Bd. 108, s. 215–224.

Grotzinger J., Jordan T.H., Press F., Siever R. (2008). Allgemeine Geologie. 751 pp., Springer (Berlin-Heidelberg).

Grösel K. (2018). Gips im Untergrund: Verbreitung und Entstehung in Niederösterreich sowie behördliche und geotechnische Auswirkungen. Berichte Geol. B.-A., 127:, 29-37.

Hassanzadegan A., Blöcher G., Milsch H., Urpi L., Zimmermann G. (2013). The Effects of Temperature and Pressure on the Porosity Evolution of Flechtinger Sandstone. Rock Mechanics and Rock Engineering, 47/2, 421–434.

Heinemann, Z. E. (2005, Überarbeitung von 2013). PHDG – Textbook Series. Volume 1: Fluid Flow In Porous Media. Leoben: Verein zur Förderung von wissenschaftlichen Arbeiten in Reservoircharakterisierung und -simulation, Leoben, 191 pp.

Heinemann, Z. E. (2014). PHDG – Textbook Series. Volume 5: Natural Fractured Reservoir Engineering. Leoben: Verein zur Förderung von wissenschaftlichen Arbeiten in Reservoircharakterisisierung und -simulation, Leoben, 131 pp.

Heubeck C. (2007). Porosität und Permeabilität in natürlichen Gesteinen. Der belebte Planet, 2:, 36-44, FU Berlin.

Ivy-Ochs, S., Kerschner, H., Reuther, A., Preusser, F., Heine, K., Maisch, M., Kubik, P. W. and Schlüchter, C. (2008). Chronology of the last glacial cycle in the European Alps. J. Quaternary Sci., 23:, 559–573.

Kilian S., Ortner H., Schneider-Muntau B. (2021). Buckle folding in the Northern Calcareous Alps - Field observations and numeric experiments. J. Structural Geology:, 150, 1-19.

Krainer K. (1987). Zusammensetzung und fazielle Entwicklung des Alpinen Buntsandsteins und der Werfener Schichten im westlichen Drauzug (Kärnten/Osttirol). Jb. Geol. B.-A., 130:, 61–91.

Krainer K., Stingl V. (1986). Alluviale Schuttfächersedimente im Ostalpinen Perm am Beispiel der Präbichlschichten an der Typuslokalität bei Eisenerz/Steiermark (Österreich). Austrian Journal of Earth Sciences, 78:, 231-249.

Krystyn L. (1987). Zur Rhät-Stratigraphie in den Zlambach-Schichten (vorläufiger Bericht). In: Sitzungsberichte der Akademie der Wissenschaften mathematisch-naturwissenschaftliche Klasse, 196:, 21-36.

Langguth H. R., Voigt R. (1980). Hydrogeologische Methoden. 1005 pp., Springer (Berlin-Heidelberg-New York).

Linzer H.G., Decker K., Peresson H., Dell´Mour R. Frisch W. (2002). Balancing lateral orofenic float of the Eastern Alps. Tectonophysics 354:, 211-237.

Mandl G. W. (2006a). Explanatory notes to the digital geological map of the Rax-Schneeberg-Region. Unpublished Report, 25 pp., Geologische Bundesanstalt Wien.

Mandl G. W. (2006b). Erläuterungen zur digitalen Geologischen Karte des Rax-Schneeberg-Gebietes. Unveröffentlichter Bericht, 68 pp., Geologische Bundesanstalt Wien.

Matte P. (1986). Tectonics and plate tectonics model for the Variscan belt of Europe. Tectonophysics,126:, 329–374.

Moser M (2014). Die Tremmlgraben-Formation – eine neue Beckenentwicklung in der Mitteltrias der Mürzalpen-Decke. Jb. Geol. B.-A., 154:, 199-207.

Möller G., Brückly E., Weber R. (2011). Active tectonic deformation at the transition from the European and Pannonian domain monitored by a local GNSS network. VGI – Österreichische Zeitschrift für Vermessung & Geoinformation. 2011/2:, 138-148.

NASA Shuttle Radar Topography Mission: https://www2.jpl.nasa.gov/srtm/ - Data is Public Domain and was collected in the year 2000.

Nittel P. (2006). Beiträge zur Stratigraphie und Mikropaläontologie der Mitteltrias der Innsbrucker Nordkette (Nördliche Kalkalpen, Austria. Geo.Alp, 3:, 93-145.

Oates, J. A. H. (1998). Lime and Limestone – Chemistry and Technology, Production and Uses. 472 pp., Wiley-VCH (Weinheim-New York-Chichester-Brisbane-Singapore-Toronto).

Pavuza R., Traindl H. (1983). Über Dolomitkarst in Österreich. Die Höhle Bd. 34:, 15-25.

Piller W. E., Egger H., Erhart C. W., Gross M., Harzhauser M., Hubmann B., van Husen D., Krenmayr H.-G., Krystyn L. Lein R., Lukeneder A., Mandl G., Rögl F., Roetzel R., Rupp C., Schnabel W., Schönlaub H.P., Summesberger H., Wagreich M., Wessely G. (2004). Die stratigraphische Tabelle von Österreich 2004 (sedimentäre Schichtfolgen).

Piros O., Mandl G. W., Lein R., Pavlik W., Bérczi-Makk A. Siblik M. Lobitzer H. (1994). Dasycladaceen-Assoziationen aus triadischen Seichtwasserkarbonaten des Ostabschnittes der Nördlichen Kalkalpen. Jubiläumsschrift 20 Jahre Geologische Zusammenarbeit Österreich-Ungarn, 2:, 343-362, Geol. B.-A. Wien.

Pistotnik U. (1973/1974). Fazies und Tektonik der Hallstädter Zone von Bad Ischl – Bad Aussee (Salzkammergut, Österreich). Mitt. Geol. Ges. Wien. 66-67:, 143-158.

Plan L., Decker K. (2006). Quantitative karst morphology of the Hochschwab plateau, Eastern Alps, Austria. Z. Geomoprh. N. F., Suppl.-Vol. 147:, 29-54.

Prandstätter, L. (2022). Strukturgeologische Kartierung hydrogeologisch bedeutender Störungen am Kuhschneeberg (NOE). MSc Thesis, Department of Geology, Univesity Vienna, 115 pp.

Ratschbacher L., Merle O., Davy P., Cobbold P. (1991). Lateral Extrusion in the Eastern Alps. Tectonics, 10/ 2:, 245-271.

Raumer J. F., Neubauer F. (1993). Pre-Mesozoic Geology in the Alps. 677 pp. Springer (Berlin).

Sayers C. M. (2008). The elastic properties of carbonates. In: Society of Exploration Geophysicists (2008): The Leading Edge. 27/8:, 1020.

Schlager W., Schöllnberger W. (1973/1974). Das Prinzip der Wenden in der Schichtfolge der Nördlichen Kalkalpen. Mitt. Geol. Ges. Wien. 66-67:, 165-193.

Schmid E., Pröll T. (2020). Umwelt- und Bioressourcenmanagement für eine nachhaltige Zukunftsgestaltung. 272 pp. Springer (Berlin).

Schuster R., Daurer A., Krenmayer H. G., Linner M., Mandl G. W., Pestal G., Reitner J. M. (2015). Rocky Austria – Geologie von Österreich – kurz und bunt. 80 pp. Geologische Bundesanstalt, Wien.

Schwarzacher W. (2005). The stratification and cyclicity of the Dachstein Limestone in Lofer, Leogang and Steinernes Meer (Northern Calcareous Alps, Austria). In: Sedimentary Geology, 181:, 93–106.

Spötl C. (1989). The Alpine Haselgebirge Formation, Northern Calcareous Alps (Austria): Permo-Scythian evaporites in an alpine thrust system. Sedimentary Geology. 65:, 113–125.

Tanikawa W., Shimamoto T. (2006). Klinkenberg effect for gas permeability and its comparison to water permeability. In: Hydrology and Earth System Sciences (2006). Hydrol. Earth Syst. Sci. Discuss., 3:, 1315-1326.

Thurner A. (1967). Hydrogeologie. 350 pp. Springer (Wien-New York).

Uehara S., Shimamoto T. (2004). Gas permeability evolution of cataclasite and fault gouge in triaxial compression and implications for changes in fault-zone permeability structure through the earthquake cycle. Tectonophysics, 378:, 183-195.

Vinci Technologies (2013). COREVAL 700 - Unsteady state gas permeameter and porosimeter at overburden pressure: Operating Manual. Rev 01.1. France.

Walsh J. B., Brace W. F. (1984). The effect of pressure on porosity and the transport properties of rock. J. Geophys. Res., 89/ 11:, 9425-9431.

Weigl O. (1937). Stratigraphie und Tektonik des Beckens von Gosau. Jb. Geol. B.-A., 87:,11-40.

Wiener Wasser (2021): https://www.wien.gv.at/wienwasser/versorgung/weg/index.html - Site is part of the official Homepage of the City of Vienna.

Wimmer P. (2020). Struktur- und Hydrogeologische Untersuchung des Grundwasseraquifers der Wettersteinformation am Rax/Schneebergmassiv. Bachelorarberit, 53 pp., Institut für Geologie. Universität Wien

15 Appendix

Lithology	N°	Name	Pc(psi)	K[n2](mD)	K1(mD)	b[n2](psi)	Vp0(cc)	φ0(%)	φ(%)	α(ft^-1)	β(μm)	grain density (g/cc)	raw density (g/cc)	raw density0 (g/cc)	Weight(g)
Wetterstein Dolomite	1	PW1/6	400	8.36	6.79	3.46	1.51	3.91	3.97	8964407908	200.6	2.85	2.74	2.74	105.6
Wetterstein Dolomite	2	PW1/6	500	7.96	6.44	3.53	1.51	3.91	3.91	9315276727	197.8	2.85	2.74	2.74	105.6
Wetterstein Dolomite	3	PW1/6	1000	6.20	4.92	3.89	1.51	3.91	3.70	1.1316E+10	184.1	2.85	2.74	2.74	105.6
Wetterstein Dolomite	4	PW1/6	1500	4.96	3.87	4.24	1.51	3.91	3.41	1.266E+10	162.1	2.85	2.75	2.74	105.6
Wetterstein Dolomite	5	PW1/6	2500	3.40	2.56	4.92	1.51	3.91	3.05	1.6564E+10	141.4	2.85	2.76	2.74	105.6
Wetterstein Dolomite	6	PW1/6	3500	2.48	1.81	5.58	1.51	3.91	2.82	7549109009	45.7	2.85	2.77	2.74	105.6
Wetterstein Dolomite	7	PW1/6	4500	1.90	1.34	6.21	1.51	3.91	2.65	3294458107	15.3	2.85	2.77	2.74	105.6
Wetterstein Dolomite	8	PW1/6	5500	1.50	1.03	6.82	1.51	3.91	2.51	2447527987	9.0	2.85	2.78	2.74	105.6
Wetterstein Dolomite	9	PW1/6	6500	1.22	0.81	7.43	1.51	3.91	2.40	3240996653	9.8	2.85	2.78	2.74	105.6
Wetterstein Reef Limestone	10	PW3/1.1	400	0.22	0.11	15.34	2.52	4.94	2.32	1.3336E+11	67.2	2.73	2.66	2.59	132.2
Wetterstein Reef Limestone	11	PW3/1.1	500	0.18	0.09	16.58	2.52	4.94	2.28	1.771E+11	73.5	2.73	2.66	2.59	132.2
Wetterstein Reef Limestone	12	PW3/1.1	1000	0.11	0.04	21.31	2.52	4.94	2.12	1.0275E+12	219.5	2.73	2.67	2.59	132.2
Wetterstein Reef Limestone	13	PW3/1.1	1500	0.07	0.03	25.68	2.52	4.94	1.99	1.7613E+12	247.6	2.73	2.67	2.59	132.2
Wetterstein Reef Limestone	14	PW3/1.1	2500	0.04	0.01	34.26	2.52	4.94	1.80	1.4263E+13	1088.8	2.73	2.68	2.59	132.2

Wetterstein Reef Limestone	15	PW3/1.1	3500	0.02	0.01	42.53	2.52	4.94	1.65	3.7928E+13	1815.7	2.73	2.68	2.59	132.2
Wetterstein Reef Limestone	16	PW3/1.1	4500	0.02	0.00	50.51	2.52	4.94	1.55	1.3755E+13	441.0	2.73	2.68	2.59	132.2
Wetterstein Reef Limestone	17	PW3/1.1	5500	0.01	0.00	59.08	2.52	4.94	1.45	9.2809E+13	2171.1	2.73	2.69	2.59	132.2
Wetterstein Reef Limestone	18	PW3/1.1	6500	0.01	0.00	60.91	2.52	4.94	1.39	7.3977E+13	1242.8	2.73	2.69	2.59	132.2
Wetterstein Reef Limestone	28	PW3/2	400	0.19	0.09	16.46	0.17	0.29	1.64	1.0885E+12	397.5	3.04	2.99	3.03	175.5
Wetterstein Reef Limestone	29	PW3/2	500	0.18	0.09	16.63	0.17	0.29	1.59	1.1465E+12	388.8	3.04	2.99	3.03	175.5
Wetterstein Reef Limestone	30	PW3/2	1000	0.17	0.08	17.39	0.17	0.29	1.47	5.0296E+12	1438.4	3.04	3.00	3.03	175.5
Wetterstein Reef Limestone	31	PW3/2	1500	0.15	0.07	17.93	0.17	0.29	1.36	7.5744E+12	1999.4	3.04	3.00	3.03	175.5
Wetterstein Reef Limestone	32	PW3/2	2500	0.13	0.05	19.72	0.17	0.29	1.24	5.1008E+12	1047.8	3.04	3.01	3.03	175.5
Wetterstein Reef Limestone	33	PW3/2	3500	0.10	0.04	22.01	0.17	0.29	1.14	3.7087E+12	603.9	3.04	3.01	3.03	175.5
Wetterstein Reef Limestone	34	PW3/2	4500	0.08	0.03	24.59	0.17	0.29	1.06	6.7277E+12	917.4	3.04	3.01	3.03	175.5
Wetterstein Reef Limestone	35	PW3/2	5500	0.06	0.02	27.05	0.17	0.29	0.98	2.6636E+12	300.4	3.04	3.01	3.03	175.5

Wetterstein Reef Limestone	36	PW3/2	6500	0.05	0.02	29.80	0.17	0.29	0.92	1.3661E+13	1334.6	3.04	3.02	3.03	175.5
Wetterstein Reef Limestone	19	PW3/3	400	0.28	0.15	13.74	1.36	2.86	1.20	1.7881E+11	124.8	2.76	2.73	2.68	127.8
Wetterstein Reef Limestone	20	PW3/3	500	0.26	0.13	14.35	1.36	2.86	1.21	2.8538E+10	17.9	2.76	2.73	2.68	127.8
Wetterstein Reef Limestone	21	PW3/3	1000	0.18	0.08	16.83	1.36	2.86	1.17	1.1121E+11	42.3	2.76	2.73	2.68	127.8
Wetterstein Reef Limestone	22	PW3/3	1500	0.12	0.05	19.82	1.36	2.86	1.10	4.5317E+11	123.4	2.76	2.73	2.68	127.8
Wetterstein Reef Limestone	23	PW3/3	2500	0.07	0.03	25.96	1.36	2.86	0.97	1.9685E+12	309.0	2.76	2.73	2.68	127.8
Wetterstein Reef Limestone	24	PW3/3	3500	0.04	0.01	31.79	1.36	2.86	0.89	2.6452E+12	266.6	2.76	2.74	2.68	127.8
Wetterstein Reef Limestone	25	PW3/3	4500	0.03	0.01	37.68	1.36	2.86	0.82	5.5003E+12	387.4	2.76	2.74	2.68	127.8
Wetterstein Reef Limestone	26	PW3/3	5500	0.02	0.01	43.70	1.36	2.86	0.78	1.7377E+13	903.6	2.76	2.74	2.68	127.8
Wetterstein Reef Limestone	27	PW3/3	6500	0.02	0.00	49.58	1.36	2.86	0.74	8.859E+12	346.8	2.76	2.74	2.68	127.8
Wetterstein Reef Limestone	37	PW3/4	400	0.05	0.02	30.60	1.97	5.04	3.32	1.9942E+11	17.7	2.84	2.74	2.69	105.4
Wetterstein Reef Limestone	38	PW3/4	500	0.04	0.01	33.25	1.97	5.04	3.23	5.0157E+12	347.5	2.84	2.74	2.69	105.4

Wetterstein Reef Limestone	39	PW3/4	1000	0.02	0.01	43.54	1.97	5.04	2.93	1.4356E+12	46.0	2.84	2.75	2.69	105.4
Wetterstein Reef Limestone	40	PW3/4	1500	0.02	0.00	49.68	1.97	5.04	2.72	2.9488E+13	642.4	2.84	2.76	2.69	105.4
Wetterstein Reef Limestone	41	PW3/4	2500	0.01	0.00	57.53	1.97	5.04	2.49	2.8598E+14	4359.6	2.84	2.77	2.69	105.4
Wetterstein Reef Limestone	42	PW3/4	3500	0.01	0.00	62.72	1.97	5.04	2.31	4.1871E+14	5172.0	2.84	2.77	2.69	105.4
Wetterstein Reef Limestone	43	PW3/4	4500	0.01	0.00	66.98	1.97	5.04	2.17	3.9251E+14	4129.1	2.84	2.77	2.69	105.4
Wetterstein Reef Limestone	44	PW3/4	5500	0.01	0.00	70.46	1.97	5.04	2.08	3.252E+14	3017.5	2.84	2.78	2.69	105.4
Wetterstein Reef Limestone	45	PW3/4	6500	0.01	0.00	69.14	1.97	5.04	1.99	3.476E+15	31582.5	2.84	2.78	2.69	105.4
Wetterstein Reef Limestone	55	PW4/4	400	2.24	1.61	5.81	2.47	3.43	1.06	1.157E+11	622.8	2.73	2.70	2.64	189.8
Wetterstein Reef Limestone	56	PW4/4	500	1.91	1.36	6.18	2.47	3.43	1.05	1.4832E+11	674.4	2.73	2.70	2.64	189.8
Wetterstein Reef Limestone	57	PW4/4	1000	1.08	0.71	7.81	2.47	3.43	1.02	3.0872E+11	745.1	2.73	2.70	2.64	189.8
Wetterstein Reef Limestone	58	PW4/4	1500	0.74	0.46	9.15	2.47	3.43	0.95	4.4423E+11	698.0	2.73	2.70	2.64	189.8
Wetterstein Reef Limestone	59	PW4/4	2500	0.43	0.24	11.52	2.47	3.43	0.85	6.7698E+11	571.3	2.73	2.71	2.64	189.8

Wetterstein Reef Limestone	60	PW4/4	3500	0.28	0.14	13.86	2.47	3.43	0.78	1.4757E+11	79.7	2.73	2.71	2.64	189.8
Wetterstein Reef Limestone	61	PW4/4	4500	0.20	0.10	16.02	2.47	3.43	0.74	1.8146E+11	70.3	2.73	2.71	2.64	189.8
Wetterstein Reef Limestone	62	PW4/4	5500	0.15	0.07	17.93	2.47	3.43	0.70	6.8934E+11	199.4	2.73	2.71	2.64	189.8
Wetterstein Reef Limestone	63	PW4/4	6500	0.12	0.05	19.74	2.47	3.43	0.67	2.7488E+10	6.2	2.73	2.71	2.64	189.8
Wetterstein Reef Limestone	64	PW5/1.1	400	0.03	0.01	37.56	1.86	2.69	0.64	2.889E+13	1993.2	2.74	2.73	2.67	184.8
Wetterstein Reef Limestone	65	PW5/1.1	500	0.02	0.01	42.69	1.86	2.69	0.63	6.064E+13	3117.1	2.74	2.73	2.67	184.8
Wetterstein Reef Limestone	66	PW5/1.1	1000	0.01	0.00	65.79	1.86	2.69	0.58	1.7003E+14	3556.6	2.74	2.73	2.67	184.8
Wetterstein Reef Limestone	67	PW5/1.1	1500	0.01	0.00	85.40	1.86	2.69	0.55	8.0771E+14	9474.7	2.74	2.73	2.67	184.8
Wetterstein Reef Limestone	68	PW5/1.1	2500	0.00	0.00	123.72	1.86	2.69	0.47	8.2912E+14	4487.3	2.74	2.73	2.67	184.8
Wetterstein Reef Limestone	69	PW5/1.1	3500	0.00	0.00	156.23	1.86	2.69	0.40	3.2894E+15	10480.3	2.74	2.73	2.67	184.8
Wetterstein Reef Limestone	70	PW5/1.1	4500	0.00	0.00	202.72	1.86	2.69	0.33	4.8654E+15	10956.3	2.74	2.74	2.67	184.8
Wetterstein Reef Limestone	71	PW5/1.1	5500	0.00	0.00	218.77	1.86	2.69	0.30	2.228E+15	3453.4	2.74	2.74	2.67	184.8

Wetterstein Reef Limestone	72	PW5/1.1	6500	0.00	0.00	162.36	1.86	2.69	0.27	1.7562E+16	22010.6	2.74	2.74	2.67	184.8
Wetterstein Reef Limestone	73	PW5/1.2	400	0.02	0.00	51.85	0.62	1.49	2.05	8.9322E+13	3294.0	2.73	2.67	2.69	111.3
Wetterstein Reef Limestone	74	PW5/1.2	500	0.01	0.00	64.05	0.62	1.49	2.08	1.1817E+14	2628.6	2.73	2.67	2.69	111.3
Wetterstein Reef Limestone	75	PW5/1.2	1000	0.00	0.00	150.28	0.62	1.49	1.71	5.5111E+14	2995.6	2.73	2.68	2.69	111.3
Wetterstein Reef Limestone	76	PW5/1.2	1500	0.00	0.00	101.96	0.62	1.49	1.57	1.7295E+14	333.2	2.73	2.69	2.69	111.3
Wetterstein Reef Limestone	77	PW5/1.2	2500	0.00	0.00	176.56	0.62	1.49	1.36	1.0737E+15	451.7	2.73	2.69	2.69	111.3
Wetterstein Reef Limestone	78	PW5/1.2	3500	0.00	0.00	281.21	0.62	1.49	1.17	5.0699E+15	585.1	2.73	2.70	2.69	111.3
Wetterstein Reef Limestone	79	PW5/1.2	4500	0.00	0.00	377.76	0.62	1.49	1.06	1.3601E+16	689.7	2.73	2.70	2.69	111.3
Wetterstein Reef Limestone	80	PW5/1.2	5500	0.00	0.00	534.41	0.62	1.49	1.02	4.293E+16	835.3	2.73	2.70	2.69	111.3
Wetterstein Reef Limestone	81	PW5/1.2	6500	0.00	0.00	511.37	0.62	1.49	0.92	3.6817E+16	814.2	2.73	2.70	2.69	111.3
Wetterstein Reef Limestone	82	PW5/3	400	0.07	0.03	25.58	2.25	3.15	1.68	5.1562E+12	792.1	2.74	2.70	2.66	189.8
Wetterstein Reef Limestone	83	PW5/3	500	0.06	0.02	28.40	2.25	3.15	1.63	1.0053E+13	1200.6	2.74	2.70	2.66	189.8

Wetterstein Reef Limestone	84	PW5/3	1000	0.03	0.01	41.38	2.25	3.15	1.46	3.865E+13	1975.7	2.74	2.70	2.66	189.8
Wetterstein Reef Limestone	85	PW5/3	1500	0.02	0.00	53.00	2.25	3.15	1.31	7.0601E+12	203.0	2.74	2.71	2.66	189.8
Wetterstein Reef Limestone	86	PW5/3	2500	0.01	0.00	76.66	2.25	3.15	1.13	2.67E+13	345.6	2.74	2.71	2.66	189.8
Wetterstein Reef Limestone	87	PW5/3	3500	0.00	0.00	101.23	2.25	3.15	0.99	1.3347E+15	10235.4	2.74	2.72	2.66	189.8
Wetterstein Reef Limestone	88	PW5/3	4500	0.00	0.00	128.99	2.25	3.15	0.89	2.0167E+15	9976.7	2.74	2.72	2.66	189.8
Wetterstein Reef Limestone	89	PW5/3	5500	0.00	0.00	152.46	2.25	3.15	0.82	4.6059E+14	1492.1	2.74	2.72	2.66	189.8
Wetterstein Reef Limestone	90	PW5/3	6500	0.00	0.00	122.96	2.25	3.15	0.81	8.4222E+15	24748.2	2.74	2.72	2.66	189.8
Wetterstein Reef Limestone	91	PW5/4	400	0.06	0.02	28.38	2.39	3.19	0.65	4.8307E+12	619.0	2.74	2.73	2.66	198.9
Wetterstein Reef Limestone	92	PW5/4	500	0.05	0.01	31.61	2.39	3.19	0.63	1.5993E+13	1591.3	2.74	2.73	2.66	198.9
Wetterstein Reef Limestone	93	PW5/4	1000	0.02	0.01	46.34	2.39	3.19	0.58	6.3839E+13	2722.8	2.74	2.73	2.66	198.9
Wetterstein Reef Limestone	94	PW5/4	1500	0.01	0.00	59.45	2.39	3.19	0.54	1.8623E+14	4507.5	2.74	2.73	2.66	198.9
Wetterstein Reef Limestone	95	PW5/4	2500	0.01	0.00	83.75	2.39	3.19	0.48	4.3443E+12	48.4	2.74	2.73	2.66	198.9

Wetterstein Reef Limestone	96	PW5/4	3500	0.00	0.00	111.03	2.39	3.19	0.43	1.2579E+15	8656.8	2.74	2.73	2.66	198.9
Wetterstein Reef Limestone	97	PW5/4	4500	0.00	0.00	140.72	2.39	3.19	0.40	1.5417E+15	6919.4	2.74	2.73	2.66	198.9
Wetterstein Reef Limestone	98	PW5/4	5500	0.00	0.00	179.44	2.39	3.19	0.36	1.2323E+15	3887.8	2.74	2.73	2.66	198.9
Wetterstein Reef Limestone	99	PW5/4	6500	0.00	0.00	131.79	2.39	3.19	0.34	1.2287E+17	226472.5	2.74	2.73	2.66	198.9
Wetterstein Reef Limestone	100	PW5/5	400	0.50	0.29	10.80	2.42	4.45	0.83	1.3533E+11	157.4	2.77	2.74	2.64	143.9
Wetterstein Reef Limestone	101	PW5/5	500	0.42	0.23	11.63	2.42	4.45	0.83	6.142E+10	55.1	2.77	2.74	2.64	143.9
Wetterstein Reef Limestone	102	PW5/5	1000	0.23	0.11	15.10	2.42	4.45	0.79	5.1681E+11	213.5	2.77	2.74	2.64	143.9
Wetterstein Reef Limestone	103	PW5/5	1500	0.15	0.07	18.36	2.42	4.45	0.71	1.419E+11	38.9	2.77	2.75	2.64	143.9
Wetterstein Reef Limestone	104	PW5/5	2500	0.08	0.03	24.06	2.42	4.45	0.61	4.3589E+12	662.3	2.77	2.75	2.64	143.9
Wetterstein Reef Limestone	105	PW5/5	3500	0.05	0.02	29.33	2.42	4.45	0.53	1.2215E+13	1193.2	2.77	2.75	2.64	143.9
Wetterstein Reef Limestone	106	PW5/5	4500	0.04	0.01	34.26	2.42	4.45	0.50	1.2715E+12	85.0	2.77	2.75	2.64	143.9
Wetterstein Reef Limestone	107	PW5/5	5500	0.03	0.01	39.37	2.42	4.45	0.47	2.6303E+13	1322.9	2.77	2.75	2.64	143.9

Wetterstein Reef Limestone	108	PW5/5	6500	0.02	0.01	44.12	2.42	4.45	0.45	1.1574E+13	443.2	2.77	2.75	2.64	143.9
Wetterstein Reef Limestone	109	PW5/6	400	0.18	0.08	16.94	1.14	2.91	1.13	3.8491E+11	151.6	2.73	2.70	2.65	103.8
Wetterstein Reef Limestone	110	PW5/6	500	0.16	0.07	17.65	1.14	2.91	1.12	1.101E+11	37.7	2.73	2.70	2.65	103.8
Wetterstein Reef Limestone	111	PW5/6	1000	0.11	0.05	20.76	1.14	2.91	1.02	6.277E+11	143.4	2.73	2.70	2.65	103.8
Wetterstein Reef Limestone	112	PW5/6	1500	0.09	0.03	23.51	1.14	2.91	0.88	4.2448E+11	74.1	2.73	2.71	2.65	103.8
Wetterstein Reef Limestone	113	PW5/6	2500	0.06	0.02	28.53	1.14	2.91	0.73	4.0518E+12	478.9	2.73	2.71	2.65	103.8
Wetterstein Reef Limestone	114	PW5/6	3500	0.04	0.01	32.91	1.14	2.91	0.66	6.9728E+12	609.4	2.73	2.71	2.65	103.8
Wetterstein Reef Limestone	115	PW5/6	4500	0.03	0.01	36.72	1.14	2.91	0.61	1.5088E+11	10.2	2.73	2.72	2.65	103.8
Wetterstein Reef Limestone	116	PW5/6	5500	0.03	0.01	40.51	1.14	2.91	0.56	8.9661E+12	501.5	2.73	2.72	2.65	103.8
Wetterstein Reef Limestone	117	PW5/6	6500	0.02	0.01	44.14	1.14	2.91	0.52	3.3591E+13	1602.6	2.73	2.72	2.65	103.8
Lagoonal Wetterstein Limestone	118	PW6/1	400	0.54	0.32	10.45	2.57	4.54	1.65	1.9316E+10	25.1	2.75	2.70	2.63	148.9
Lagoonal Wetterstein Limestone	119	PW6/1	500	0.50	0.29	10.76	2.57	4.54	1.63	2.0954E+10	24.5	2.75	2.71	2.63	148.9

Lithology	ID	Sample													
Lagoonal Wetterstein Limestone	120	PW6/1	1000	0.40	0.22	11.85	2.57	4.54	1.55	6.8938E+10	53.8	2.75	2.71	2.63	148.9
Lagoonal Wetterstein Limestone	121	PW6/1	1500	0.31	0.17	13.19	2.57	4.54	1.44	2.9017E+10	17.8	2.75	2.71	2.63	148.9
Lagoonal Wetterstein Limestone	122	PW6/1	2500	0.20	0.09	16.12	2.57	4.54	1.28	3.0356E+11	124.9	2.75	2.71	2.63	148.9
Lagoonal Wetterstein Limestone	123	PW6/1	3500	0.13	0.06	19.12	2.57	4.54	1.18	2.0819E+11	62.4	2.75	2.72	2.63	148.9
Lagoonal Wetterstein Limestone	124	PW6/1	4500	0.10	0.04	21.87	2.57	4.54	1.08	3.4564E+11	77.1	2.75	2.72	2.63	148.9
Lagoonal Wetterstein Limestone	125	PW6/1	5500	0.08	0.03	24.37	2.57	4.54	1.02	1.5297E+12	261.9	2.75	2.72	2.63	148.9
Lagoonal Wetterstein Limestone	126	PW6/1	6500	0.06	0.02	27.15	2.57	4.54	0.96	2.9969E+12	410.2	2.75	2.72	2.63	148.9
Lagoonal Wetterstein Limestone	127	PW6/2	400	0.07	0.03	25.17	2.87	4.36	0.87	6.3782E+12	1052.0	2.72	2.70	2.60	171.1
Lagoonal Wetterstein Limestone	128	PW6/2	500	0.06	0.02	27.08	2.87	4.36	0.85	8.9909E+12	1243.6	2.72	2.70	2.60	171.1
Lagoonal Wetterstein Limestone	129	PW6/2	1000	0.04	0.01	33.57	2.87	4.36	0.78	1.5014E+13	1249.0	2.72	2.70	2.60	171.1
Lagoonal Wetterstein Limestone	130	PW6/2	1500	0.03	0.01	38.42	2.87	4.36	0.69	1.5829E+13	959.2	2.72	2.70	2.60	171.1
Lagoonal Wetterstein Limestone	131	PW6/2	2500	0.02	0.00	47.36	2.87	4.36	0.60	7.7145E+13	3000.8	2.72	2.70	2.60	171.1

Lagoonal Wetterstein Limestone	132	PW6/2	3500	0.01	0.00	55.30	2.87	4.36	0.54	1.499E+14	4087.7	2.72	2.71	2.60	171.1
Lagoonal Wetterstein Limestone	133	PW6/2	4500	0.01	0.00	62.97	2.87	4.36	0.50	2.2585E+14	4573.9	2.72	2.71	2.60	171.1
Lagoonal Wetterstein Limestone	134	PW6/2	5500	0.01	0.00	70.50	2.87	4.36	0.46	4.2192E+14	6626.7	2.72	2.71	2.60	171.1
Lagoonal Wetterstein Limestone	135	PW6/2	6500	0.01	0.00	67.71	2.87	4.36	0.44	2.3475E+14	2885.8	2.72	2.71	2.60	171.1
Lagoonal Wetterstein Limestone	136	PW6/4	400	0.33	0.18	12.87	0.60	0.82	1.04	8.1971E+10	70.8	2.71	2.68	2.69	198.3
Lagoonal Wetterstein Limestone	137	PW6/4	500	0.28	0.15	13.72	0.60	0.82	1.07	1.3262E+11	97.8	2.71	2.68	2.69	198.3
Lagoonal Wetterstein Limestone	138	PW6/4	1000	0.17	0.08	17.22	0.60	0.82	0.99	1.8513E+11	78.2	2.71	2.69	2.69	198.3
Lagoonal Wetterstein Limestone	139	PW6/4	1500	0.12	0.05	20.05	0.60	0.82	0.92	8.5006E+11	261.3	2.71	2.69	2.69	198.3
Lagoonal Wetterstein Limestone	140	PW6/4	2500	0.08	0.03	23.85	0.60	0.82	0.83	1.7612E+12	368.2	2.71	2.69	2.69	198.3
Lagoonal Wetterstein Limestone	141	PW6/4	3500	0.07	0.02	26.08	0.60	0.82	0.77	9.5176E+11	157.6	2.71	2.69	2.69	198.3
Lagoonal Wetterstein Limestone	142	PW6/4	4500	0.06	0.02	28.10	0.60	0.82	0.71	3.1037E+12	443.5	2.71	2.69	2.69	198.3
Lagoonal Wetterstein Limestone	143	PW6/4	5500	0.05	0.02	29.98	0.60	0.82	0.67	1.6746E+12	206.2	2.71	2.69	2.69	198.3

Lagoonal Wetterstein Limestone	144	PW6/4	6500	0.04	0.01	32.35	0.60	0.82	0.63	4.2835E+12	455.1	2.71	2.70	2.69	198.3
Lagoonal Wetterstein Limestone	145	PW6/5	400	0.07	0.02	26.63	1.73	4.78	1.37	4.09E+12	612.1	2.74	2.70	2.61	94.6
Lagoonal Wetterstein Limestone	146	PW6/5	500	0.05	0.02	29.18	1.73	4.78	1.37	5.455E+12	636.3	2.74	2.70	2.61	94.6
Lagoonal Wetterstein Limestone	147	PW6/5	1000	0.03	0.01	35.82	1.73	4.78	1.27	8.4303E+12	581.2	2.74	2.70	2.61	94.6
Lagoonal Wetterstein Limestone	148	PW6/5	1500	0.03	0.01	39.29	1.73	4.78	1.10	6.6316E+12	367.4	2.74	2.71	2.61	94.6
Lagoonal Wetterstein Limestone	149	PW6/5	2500	0.02	0.01	43.76	1.73	4.78	0.87	2.2411E+13	1009.0	2.74	2.71	2.61	94.6
Lagoonal Wetterstein Limestone	150	PW6/5	3500	0.02	0.00	46.60	1.73	4.78	0.72	1.5047E+13	585.0	2.74	2.72	2.61	94.6
Lagoonal Wetterstein Limestone	151	PW6/5	4500	0.02	0.00	49.52	1.73	4.78	0.59	8.1501E+12	287.6	2.74	2.72	2.61	94.6
Lagoonal Wetterstein Limestone	152	PW6/5	5500	0.02	0.00	52.38	1.73	4.78	0.51	5.0266E+13	1625.9	2.74	2.72	2.61	94.6
Lagoonal Wetterstein Limestone	153	PW6/5	6500	0.01	0.00	54.89	1.73	4.78	0.41	3.3838E+13	983.3	2.74	2.73	2.61	94.6
Lagoonal Wetterstein Limestone	154	PW6/6	400	0.11	0.05	20.89	1.08	2.16	1.24	2.0154E+12	522.3	2.73	2.70	2.67	133.3
Lagoonal Wetterstein Limestone	155	PW6/6	500	0.09	0.04	22.55	1.08	2.16	1.23	2.7096E+12	582.9	2.73	2.70	2.67	133.3

Lagoonal Wetterstein Limestone	156	PW6/6	1000	0.06	0.02	27.36	1.08	2.16	1.15	4.2899E+12	581.4	2.73	2.70	2.67	133.3
Lagoonal Wetterstein Limestone	157	PW6/6	1500	0.05	0.02	30.48	1.08	2.16	1.04	2.2074E+12	231.5	2.73	2.70	2.67	133.3
Lagoonal Wetterstein Limestone	158	PW6/6	2500	0.04	0.01	35.56	1.08	2.16	0.89	6.1086E+12	463.4	2.73	2.71	2.67	133.3
Lagoonal Wetterstein Limestone	159	PW6/6	3500	0.03	0.01	40.00	1.08	2.16	0.80	1.9217E+13	1151.6	2.73	2.71	2.67	133.3
Lagoonal Wetterstein Limestone	160	PW6/6	4500	0.02	0.01	43.98	1.08	2.16	0.74	1.4694E+13	709.1	2.73	2.71	2.67	133.3
Lagoonal Wetterstein Limestone	161	PW6/6	5500	0.02	0.00	47.64	1.08	2.16	0.69	1.0969E+13	441.0	2.73	2.71	2.67	133.3
Lagoonal Wetterstein Limestone	162	PW6/6	6500	0.02	0.00	51.16	1.08	2.16	0.64	2.1862E+13	748.2	2.73	2.71	2.67	133.3
Lagoonal Wetterstein Limestone	163	PW6/7.1	400	0.03	0.01	37.98	2.44	5.38	1.64	1.388E+13	931.3	2.77	2.72	2.62	118.7
Lagoonal Wetterstein Limestone	164	PW6/7.1	500	0.03	0.01	41.35	2.44	5.38	1.62	3.7672E+13	2079.8	2.77	2.72	2.62	118.7
Lagoonal Wetterstein Limestone	165	PW6/7.1	1000	0.02	0.00	53.88	2.44	5.38	1.52	4.8736E+13	1465.1	2.77	2.72	2.62	118.7
Lagoonal Wetterstein Limestone	166	PW6/7.1	1500	0.01	0.00	62.34	2.44	5.38	1.40	1.1192E+14	2419.3	2.77	2.73	2.62	118.7
Lagoonal Wetterstein Limestone	167	PW6/7.1	2500	0.01	0.00	73.29	2.44	5.38	1.25	2.4658E+13	351.9	2.77	2.73	2.62	118.7

Lagoonal Wetterstein Limestone	168	PW6/7.1	3500	0.01	0.00	82.16	2.44	5.38	1.16	5.5594E+14	6491.9	2.77	2.73	2.62	118.7
Lagoonal Wetterstein Limestone	169	PW6/7.1	4500	0.01	0.00	87.76	2.44	5.38	1.05	2.3086E+14	2200.5	2.77	2.74	2.62	118.7
Lagoonal Wetterstein Limestone	170	PW6/7.1	5500	0.01	0.00	93.55	2.44	5.38	0.99	4.1084E+13	338.0	2.77	2.74	2.62	118.7
Lagoonal Wetterstein Limestone	171	PW6/7.1	6500	0.01	0.00	88.81	2.44	5.38	0.98	8.2755E+14	6861.7	2.77	2.74	2.62	118.7
Lagoonal Wetterstein Limestone	172	PW6/8	400	2.58	1.89	5.49	3.91	8.85	1.95	5.4536E+10	345.8	2.73	2.68	2.49	110.1
Lagoonal Wetterstein Limestone	173	PW6/8	500	2.33	1.69	5.71	3.91	8.85	1.90	6.6782E+10	378.7	2.73	2.68	2.49	110.1
Lagoonal Wetterstein Limestone	174	PW6/8	1000	1.62	1.13	6.61	3.91	8.85	1.76	1.0698E+11	408.3	2.73	2.68	2.49	110.1
Lagoonal Wetterstein Limestone	175	PW6/8	1500	1.28	0.86	7.27	3.91	8.85	1.59	1.2329E+11	363.1	2.73	2.69	2.49	110.1
Lagoonal Wetterstein Limestone	176	PW6/8	2500	0.90	0.58	8.39	3.91	8.85	1.36	1.0845E+11	215.4	2.73	2.69	2.49	110.1
Lagoonal Wetterstein Limestone	177	PW6/8	3500	0.70	0.43	9.31	3.91	8.85	1.21	5.4028E+10	81.1	2.73	2.70	2.49	110.1
Lagoonal Wetterstein Limestone	178	PW6/8	4500	0.57	0.34	10.21	3.91	8.85	1.12	3.9001E+10	49.1	2.73	2.70	2.49	110.1
Lagoonal Wetterstein Limestone	179	PW6/8	5500	0.48	0.28	10.95	3.91	8.85	1.03	1.1437E+10	12.4	2.73	2.70	2.49	110.1

Lagoonal Wetterstein Limestone	180	PW6/8	6500	0.43	0.24	11.51	3.91	8.85	0.97	3.8942E+10	37.1	2.73	2.70	2.49	110.1
Wetterstein Dolomite	181	PW7/1	400	0.14	0.06	18.72	2.26	4.11	3.78	3.3582E+12	882.3	2.86	2.75	2.74	150.6
Wetterstein Dolomite	182	PW7/1	500	0.12	0.05	19.75	2.26	4.11	3.79	3.0477E+12	665.8	2.86	2.75	2.74	150.6
Wetterstein Dolomite	183	PW7/1	1000	0.09	0.04	22.95	2.26	4.11	3.75	5.758E+12	812.6	2.86	2.75	2.74	150.6
Wetterstein Dolomite	184	PW7/1	1500	0.08	0.03	24.87	2.26	4.11	3.72	1.2944E+13	1487.8	2.86	2.75	2.74	150.6
Wetterstein Dolomite	185	PW7/1	2500	0.06	0.02	27.16	2.26	4.11	3.57	9.9089E+12	849.3	2.86	2.75	2.74	150.6
Wetterstein Dolomite	186	PW7/1	3500	0.05	0.02	28.89	2.26	4.11	3.50	1.3704E+13	997.2	2.86	2.76	2.74	150.6
Wetterstein Dolomite	187	PW7/1	4500	0.05	0.02	30.50	2.26	4.11	3.49	4.7176E+13	3200.5	2.86	2.76	2.74	150.6
Wetterstein Dolomite	188	PW7/1	5500	0.05	0.01	31.61	2.26	4.11	3.46	5.7229E+13	3547.1	2.86	2.76	2.74	150.6
Wetterstein Dolomite	189	PW7/1	6500	0.04	0.01	32.55	2.26	4.11	3.44	6.8306E+13	3935.6	2.86	2.76	2.74	150.6
Wetterstein Dolomite	190	PW7/2.1	400	0.05	0.02	30.69	2.01	4.93	3.09	2.0683E+13	1903.9	2.88	2.79	2.74	111.7
Wetterstein Dolomite	191	PW7/2.1	500	0.04	0.01	33.78	2.01	4.93	3.10	3.2726E+13	2284.1	2.88	2.79	2.74	111.7
Wetterstein Dolomite	192	PW7/2.1	1000	0.02	0.01	43.39	2.01	4.93	3.08	4.5512E+13	1555.6	2.88	2.79	2.74	111.7
Wetterstein Dolomite	193	PW7/2.1	1500	0.02	0.00	49.12	2.01	4.93	2.99	5.6712E+13	1347.8	2.88	2.79	2.74	111.7
Wetterstein Dolomite	194	PW7/2.1	2500	0.01	0.00	56.76	2.01	4.93	2.80	3.5151E+14	5880.4	2.88	2.80	2.74	111.7
Wetterstein Dolomite	195	PW7/2.1	3500	0.01	0.00	61.17	2.01	4.93	2.68	3.6999E+13	479.8	2.88	2.80	2.74	111.7
Wetterstein Dolomite	196	PW7/2.1	4500	0.01	0.00	65.20	2.01	4.93	2.59	6.006E+14	7127.8	2.88	2.80	2.74	111.7
Wetterstein Dolomite	197	PW7/2.1	5500	0.01	0.00	67.25	2.01	4.93	2.61	3.0911E+14	3248.7	2.88	2.80	2.74	111.7

Wetterstein Dolomite	198	PW7/2.1	6500	0.01	0.00	64.83	2.01	4.93	2.52	7.6196E+13	803.1	2.88	2.81	2.74	111.7
Wetterstein Dolomite	46	PW7/2.2	400	0.04	0.01	34.68	1.66	4.07	3.23	2.1272E+13	1454.7	2.85	2.76	2.73	111.6
Wetterstein Dolomite	47	PW7/2.2	500	0.03	0.01	38.21	1.66	4.07	3.25	1.3602E+12	66.5	2.85	2.76	2.73	111.6
Wetterstein Dolomite	48	PW7/2.2	1000	0.02	0.00	50.38	1.66	4.07	3.14	1.2913E+14	3056.9	2.85	2.76	2.73	111.6
Wetterstein Dolomite	49	PW7/2.2	1500	0.01	0.00	56.69	1.66	4.07	2.99	2.9022E+14	4850.5	2.85	2.76	2.73	111.6
Wetterstein Dolomite	50	PW7/2.2	2500	0.01	0.00	63.66	1.66	4.07	2.78	1.6914E+14	1990.2	2.85	2.77	2.73	111.6
Wetterstein Dolomite	51	PW7/2.2	3500	0.01	0.00	67.90	1.66	4.07	2.65	3.3642E+14	3380.7	2.85	2.77	2.73	111.6
Wetterstein Dolomite	52	PW7/2.2	4500	0.01	0.00	70.58	1.66	4.07	2.56	4.56E+14	4167.9	2.85	2.78	2.73	111.6
Wetterstein Dolomite	53	PW7/2.2	5500	0.01	0.00	72.51	1.66	4.07	2.49	4.0002E+14	3419.7	2.85	2.78	2.73	111.6
Wetterstein Dolomite	54	PW7/2.2	6500	0.01	0.00	71.31	1.66	4.07	2.42	1.8125E+15	15034.2	2.85	2.78	2.73	111.6
Wetterstein Dolomite	199	PW7/3.1	400	0.34	0.18	12.69	5.36	7.75	5.04	3.9554E+11	224.9	2.87	2.73	2.65	183.2
Wetterstein Dolomite	200	PW7/3.1	500	0.31	0.16	13.22	5.36	7.75	5.02	8.7741E+11	449.0	2.87	2.73	2.65	183.2
Wetterstein Dolomite	201	PW7/3.1	1000	0.24	0.12	14.78	5.36	7.75	4.93	9.4416E+11	338.6	2.87	2.73	2.65	183.2
Wetterstein Dolomite	202	PW7/3.1	1500	0.20	0.10	15.84	5.36	7.75	4.85	1.412E+12	419.4	2.87	2.73	2.65	183.2
Wetterstein Dolomite	203	PW7/3.1	2500	0.16	0.08	17.43	5.36	7.75	4.69	2.0726E+12	474.0	2.87	2.74	2.65	183.2
Wetterstein Dolomite	204	PW7/3.1	3500	0.14	0.06	18.71	5.36	7.75	4.59	3.1087E+12	592.2	2.87	2.74	2.65	183.2
Wetterstein Dolomite	205	PW7/3.1	4500	0.12	0.05	19.84	5.36	7.75	4.50	3.8751E+12	638.3	2.87	2.74	2.65	183.2
Wetterstein Dolomite	206	PW7/3.1	5500	0.11	0.05	20.80	5.36	7.75	4.44	3.0386E+12	437.5	2.87	2.74	2.65	183.2
Wetterstein Dolomite	207	PW7/3.1	6500	0.10	0.04	21.72	5.36	7.75	4.40	5.1947E+12	677.3	2.87	2.74	2.65	183.2

Wetterstein Dolomite	208	PW7/3.2	400	0.58	0.34	10.14	5.41	8.08	6.07	2.9151E+11	339.5	2.87	2.70	2.64	176.8
Wetterstein Dolomite	209	PW7/3.2	500	0.54	0.32	10.42	5.41	8.08	6.07	3.0106E+11	325.6	2.87	2.70	2.64	176.8
Wetterstein Dolomite	210	PW7/3.2	1000	0.42	0.24	11.55	5.41	8.08	6.02	3.45E+11	275.0	2.87	2.70	2.64	176.8
Wetterstein Dolomite	211	PW7/3.2	1500	0.35	0.19	12.46	5.41	8.08	5.94	4.0836E+11	260.6	2.87	2.70	2.64	176.8
Wetterstein Dolomite	212	PW7/3.2	2500	0.27	0.14	13.93	5.41	8.08	5.78	5.2919E+11	245.8	2.87	2.71	2.64	176.8
Wetterstein Dolomite	213	PW7/3.2	3500	0.23	0.11	15.10	5.41	8.08	5.68	7.7806E+11	287.4	2.87	2.71	2.64	176.8
Wetterstein Dolomite	214	PW7/3.2	4500	0.20	0.10	16.09	5.41	8.08	5.60	1.1056E+12	343.0	2.87	2.71	2.64	176.8
Wetterstein Dolomite	215	PW7/3.2	5500	0.18	0.08	16.90	5.41	8.08	5.52	1.1807E+12	315.2	2.87	2.72	2.64	176.8
Wetterstein Dolomite	216	PW7/3.2	6500	0.16	0.07	17.65	5.41	8.08	5.48	1.5701E+12	371.8	2.87	2.72	2.64	176.8
Wetterstein Dolomite	217	PW7/4	400	0.60	0.36	9.97	3.56	4.29	3.47	3.2458E+11	418.0	2.86	2.76	2.74	226.9
Wetterstein Dolomite	218	PW7/4	500	0.56	0.34	10.22	3.56	4.29	3.47	3.6681E+11	440.2	2.86	2.76	2.74	226.9
Wetterstein Dolomite	219	PW7/4	1000	0.43	0.25	11.42	3.56	4.29	3.37	4.8665E+11	426.4	2.86	2.77	2.74	226.9
Wetterstein Dolomite	220	PW7/4	1500	0.35	0.19	12.51	3.56	4.29	3.30	6.6297E+11	459.0	2.86	2.77	2.74	226.9
Wetterstein Dolomite	221	PW7/4	2500	0.26	0.13	14.36	3.56	4.29	3.18	9.1216E+11	432.6	2.86	2.77	2.74	226.9
Wetterstein Dolomite	222	PW7/4	3500	0.20	0.10	16.05	3.56	4.29	3.09	1.4404E+12	513.1	2.86	2.77	2.74	226.9
Wetterstein Dolomite	223	PW7/4	4500	0.16	0.07	17.59	3.56	4.29	3.03	2.3563E+12	663.5	2.86	2.78	2.74	226.9
Wetterstein Dolomite	224	PW7/4	5500	0.14	0.06	19.01	3.56	4.29	2.97	3.2113E+12	739.4	2.86	2.78	2.74	226.9
Wetterstein Dolomite	225	PW7/4	6500	0.12	0.05	20.33	3.56	4.29	2.93	4.5829E+12	885.3	2.86	2.78	2.74	226.9
Wetterstein Dolomite	226	PW7/5	400	0.11	0.05	20.70	4.58	6.84	4.08	2.5222E+12	559.3	2.88	2.76	2.68	179.4

Wetterstein Dolomite	227	PW7/5	500	0.10	0.04	21.63	4.58	6.84	4.03	3.4706E+12	688.5	2.88	2.76	2.68	179.4
Wetterstein Dolomite	228	PW7/5	1000	0.08	0.03	24.38	4.58	6.84	3.90	3.1758E+12	447.2	2.88	2.77	2.68	179.4
Wetterstein Dolomite	229	PW7/5	1500	0.07	0.03	26.00	4.58	6.84	3.82	4.3634E+12	522.2	2.88	2.77	2.68	179.4
Wetterstein Dolomite	230	PW7/5	2500	0.06	0.02	28.04	4.58	6.84	3.71	6.2599E+12	621.1	2.88	2.77	2.68	179.4
Wetterstein Dolomite	231	PW7/5	3500	0.05	0.02	29.44	4.58	6.84	3.62	5.9973E+12	527.0	2.88	2.77	2.68	179.4
Wetterstein Dolomite	232	PW7/5	4500	0.05	0.02	30.54	4.58	6.84	3.56	7.1603E+12	574.2	2.88	2.78	2.68	179.4
Wetterstein Dolomite	233	PW7/5	5500	0.05	0.01	31.49	4.58	6.84	3.51	6.0965E+12	453.3	2.88	2.78	2.68	179.4
Wetterstein Dolomite	234	PW7/5	6500	0.04	0.01	32.36	4.58	6.84	3.47	3.2833E+12	228.2	2.88	2.78	2.68	179.4
Wetterstein Dolomite	235	PW7/6	400	0.16	0.07	17.76	4.10	10.04	4.87	1.7556E+12	528.2	2.89	2.75	2.60	106.2
Wetterstein Dolomite	236	PW7/6	500	0.15	0.07	18.25	4.10	10.04	4.86	4.9691E+11	133.1	2.89	2.75	2.60	106.2
Wetterstein Dolomite	237	PW7/6	1000	0.13	0.06	19.46	4.10	10.04	4.77	1.9595E+11	42.3	2.89	2.75	2.60	106.2
Wetterstein Dolomite	238	PW7/6	1500	0.12	0.05	20.06	4.10	10.04	4.67	5.0692E+11	101.2	2.89	2.76	2.60	106.2
Wetterstein Dolomite	239	PW7/6	2500	0.11	0.05	20.78	4.10	10.04	4.43	4.7013E+11	85.6	2.89	2.76	2.60	106.2
Wetterstein Dolomite	240	PW7/6	3500	0.11	0.04	21.27	4.10	10.04	4.31	1.8525E+11	31.7	2.89	2.77	2.60	106.2
Wetterstein Dolomite	241	PW7/6	4500	0.10	0.04	21.85	4.10	10.04	4.23	3.2013E+12	540.6	2.89	2.77	2.60	106.2
Wetterstein Dolomite	242	PW7/6	5500	0.10	0.04	22.21	4.10	10.04	4.17	3.2E+12	518.2	2.89	2.77	2.60	106.2
Wetterstein Dolomite	243	PW7/6	6500	0.09	0.04	22.54	4.10	10.04	4.13	2.978E+12	463.9	2.89	2.77	2.60	106.2
Wetterstein Reef Debris	244	LP2	400	0.02	0.01	44.54	1.03	2.21	0.88	1.38E+13	733.7	2.72	2.70	2.66	123.8
Hornstein Limestone	245	LP7.1	400	0.01	0.00	62.79	0.79	1.03	0.86	4.93E+14	11829.0	2.71	2.69	2.68	206.7

Hornstein Limestone	246	LP7.2	400	0.02	0.00	50.51	1.01	2.53	2.38	2.1E+13	868.0	2.79	2.73	2.72	108.1
Hornstein Limestone	247	LP7.3	400	0.05	0.02	31.23	2.35	5.75	3.53	1.37E+12	139.7	2.67	2.58	2.52	102.7
Karstified Wetterstein Limestone	248	LP11	400	0.14	0.06	18.47	11.73	19.54	13.86	3.0028E+11	101.5	2.74	2.36	2.20	132.3
Karstified Wetterstein Limestone	249	LP11	500	0.12	0.05	19.86	11.73	19.54	13.60	2.152E+11	59.0	2.74	2.37	2.20	132.3
Karstified Wetterstein Limestone	250	LP11	1000	0.07	0.03	25.60	11.73	19.54	12.64	1.8526E+12	273.7	2.74	2.39	2.20	132.3
Karstified Wetterstein Limestone	251	LP11	1500	0.05	0.02	29.66	11.73	19.54	12.30	3.6126E+12	373.8	2.74	2.40	2.20	132.3
Karstified Wetterstein Limestone	252	LP11	2500	0.03	0.01	36.33	11.73	19.54	11.90	1.7592E+13	1170.1	2.74	2.41	2.20	132.3
Karstified Wetterstein Limestone	253	LP11	3500	0.03	0.01	41.65	11.73	19.54	11.41	1.059E+13	510.3	2.74	2.43	2.20	132.3
Karstified Wetterstein Limestone	254	LP11	4500	0.02	0.00	46.89	11.73	19.54	11.03	7.8504E+13	2994.8	2.74	2.44	2.20	132.3
Karstified Wetterstein Limestone	255	LP11	5500	0.02	0.00	51.46	11.73	19.54	10.70	8.8489E+13	2721.0	2.74	2.45	2.20	132.3
Karstified Wetterstein Limestone	256	LP11	6500	0.02	0.00	50.40	11.73	19.54	10.59	1.5466E+14	4534.4	2.74	2.45	2.20	132.3
Wetterstein Reef Limestone	257	LP19.1_1	400	0.21	0.10	15.73	2.30	3.22	1.02	4.0619E+11	164.4	2.71	2.68	2.62	187.3
Wetterstein Reef Limestone	258	LP19.1_1	500	0.20	0.10	15.99	2.30	3.22	1.02	2.4874E+12	877.7	2.71	2.68	2.62	187.3

Wetterstein Reef Limestone	259	LP19.1_1	1000	0.14	0.06	18.93	2.30	3.22	0.95	1.5445E+12	348.7	2.71	2.69	2.62	187.3
Wetterstein Reef Limestone	260	LP19.1_1	1500	0.10	0.04	21.65	2.30	3.22	0.90	9.8149E+11	164.6	2.71	2.69	2.62	187.3
Wetterstein Reef Limestone	261	LP19.1_1	2500	0.06	0.02	27.43	2.30	3.22	0.84	5.1678E+12	580.2	2.71	2.69	2.62	187.3
Wetterstein Reef Limestone	262	LP19.1_1	3500	0.04	0.01	32.76	2.30	3.22	0.80	3.0874E+12	236.8	2.71	2.69	2.62	187.3
Wetterstein Reef Limestone	263	LP19.1_1	4500	0.03	0.01	38.52	2.30	3.22	0.75	2.0776E+13	1187.8	2.71	2.69	2.62	187.3
Wetterstein Reef Limestone	264	LP19.1_1	5500	0.02	0.01	44.60	2.30	3.22	0.73	2.8564E+13	1266.0	2.71	2.69	2.62	187.3
Wetterstein Reef Limestone	265	LP19.1_1	6500	0.02	0.00	48.58	2.30	3.22	0.70	6.884E+13	2303.4	2.71	2.69	2.62	187.3
Wetterstein Reef Limestone	266	LP19.1_2	400	0.04	0.01	33.59	0.66	1.07	0.80	3.3658E+12	309.3	2.71	2.69	2.68	164.4
Wetterstein Reef Limestone	267	LP19.1_2	500	0.03	0.01	38.56	0.66	1.07	0.79	1.0357E+13	669.7	2.71	2.69	2.68	164.4
Wetterstein Reef Limestone	268	LP19.1_2	1000	0.01	0.00	63.01	0.66	1.07	0.74	3.3137E+13	758.1	2.71	2.69	2.68	164.4
Wetterstein Reef Limestone	269	LP19.1_2	1500	0.01	0.00	88.29	0.66	1.07	0.68	6.3349E+12	71.7	2.71	2.69	2.68	164.4
Wetterstein Reef Limestone	270	LP19.1_2	2500	0.00	0.00	153.41	0.66	1.07	0.62	6.9243E+14	3022.5	2.71	2.70	2.68	164.4

Wetterstein Reef Limestone	271	LP19.1_2	3500	0.00	0.00	258.87	0.66	1.07	0.56	3.2599E+14	728.5	2.71	2.70	2.68	164.4
Wetterstein Reef Limestone	272	LP19.1_2	4500	0.00	0.00	118.97	0.66	1.07	0.52	3.0211E+14	365.7	2.71	2.70	2.68	164.4
Wetterstein Reef Limestone	273	LP19.1_2	5500	0.00	0.00	141.50	0.66	1.07	0.48	5.3855E+14	402.7	2.71	2.70	2.68	164.4
Wetterstein Reef Limestone	274	LP19.1_2	6500	0.00	0.00	243.74	0.66	1.07	0.45	1.4501E+17	56747.3	2.71	2.70	2.68	164.4
Karstified Wetterstein Limestone	275	LP19.2	400	0.22	0.11	15.19	4.79	6.13	12.48	9669811078	4.5	2.44	2.14	2.29	179.4
Karstified Wetterstein Limestone	276	LP19.2	500	0.18	0.09	16.63	4.79	6.13	12.43	6.6288E+11	244.6	2.44	2.14	2.29	179.4
Karstified Wetterstein Limestone	277	LP19.2	1000	0.10	0.04	22.15	4.79	6.13	12.12	4.5496E+12	774.7	2.44	2.15	2.29	179.4
Karstified Wetterstein Limestone	278	LP19.2	1500	0.07	0.02	26.54	4.79	6.13	11.74	1.0172E+13	1039.9	2.44	2.16	2.29	179.4
Karstified Wetterstein Limestone	279	LP19.2	2500	0.04	0.01	34.49	4.79	6.13	10.71	2.3778E+13	1181.3	2.44	2.18	2.29	179.4
Karstified Wetterstein Limestone	280	LP19.2	3500	0.02	0.01	42.36	4.79	6.13	9.56	1.6718E+14	4945.5	2.44	2.21	2.29	179.4
Karstified Wetterstein Limestone	281	LP19.2	4500	0.02	0.00	50.19	4.79	6.13	8.48	3.7153E+14	7226.1	2.44	2.24	2.29	179.4
Karstified Wetterstein Limestone	282	LP19.2	5500	0.01	0.00	58.07	4.79	6.13	7.54	6.2325E+14	8441.3	2.44	2.26	2.29	179.4

Karstified Wetterstein Limestone	283	LP19.2	6500	0.01	0.00	55.41	4.79	6.13	7.44	3.9562E+15	60430.1	2.44	2.26	2.29	179.4
Karstified Wetterstein Limestone	284	LP19.2_2	400	0.84	0.53	8.64	15.04	27.63	24.26	6.9535E+11	1297.1	2.73	2.07	1.97	107.4
Karstified Wetterstein Limestone	285	LP19.2_2	500	0.78	0.49	8.93	15.04	27.63	24.24	8.8775E+11	1515.8	2.73	2.07	1.97	107.4
Karstified Wetterstein Limestone	286	LP19.2_2	1000	0.56	0.33	10.24	15.04	27.63	23.74	2.1041E+12	2500.4	2.73	2.08	1.97	107.4
Karstified Wetterstein Limestone	287	LP19.2_2	1500	0.46	0.27	11.10	15.04	27.63	23.15	3.5331E+12	2984.5	2.73	2.10	1.97	107.4
Karstified Wetterstein Limestone	288	LP19.2_2	2500	0.40	0.22	11.87	15.04	27.63	22.27	5.5822E+12	3993.8	2.73	2.12	1.97	107.4
Karstified Wetterstein Limestone	289	LP19.2_2	3500	0.30	0.16	13.38	15.04	27.63	21.49	8.6964E+12	4188.0	2.73	2.14	1.97	107.4
Karstified Wetterstein Limestone	290	LP19.2_3	400	13.18	11.04	2.91	10.44	20.91	17.76	7720000000	279.8	2.75	2.26	2.18	108.7
Karstified Wetterstein Limestone	291	LP19.2_4	400	0.24	0.12	14.76	6.59	14.00	11.70	8.23E+10	37.8	2.74	2.42	2.35	110.8
Karstified Wetterstein Limestone	292	LP19.2_5	400	36.81	32.54	1.97	8.17	24.85	22.69	2.64E+10	2816.9	2.73	2.11	2.05	67.4
Wetterstein Reef Limestone	293	LP36	400	0.25	0.12	14.62	2.59	6.29	2.72	3.3062E+11	182.2	2.78	2.70	2.60	107.2
Wetterstein Reef Limestone	294	LP36	500	0.22	0.11	15.31	2.59	6.29	2.70	3.9654E+11	194.5	2.78	2.70	2.60	107.2

Wetterstein Reef Limestone	295	LP36	1000	0.19	0.09	16.39	2.59	6.29	2.60	1.1022E+11	42.1	2.78	2.70	2.60	107.2
Wetterstein Reef Limestone	296	LP36	1500	0.17	0.08	17.39	2.59	6.29	2.47	5.8969E+11	201.9	2.78	2.71	2.60	107.2
Wetterstein Reef Limestone	297	LP36	2500	0.13	0.06	19.10	2.59	6.29	2.32	5.4619E+11	147.6	2.78	2.71	2.60	107.2
Wetterstein Reef Limestone	298	LP36	3500	0.11	0.05	20.69	2.59	6.29	2.22	4.9828E+11	110.2	2.78	2.72	2.60	107.2
Wetterstein Reef Limestone	299	LP36	4500	0.10	0.04	22.17	2.59	6.29	2.12	7.8791E+10	14.7	2.78	2.72	2.60	107.2
Wetterstein Reef Limestone	300	LP36	5500	0.09	0.03	23.48	2.59	6.29	2.06	8.9047E+11	143.6	2.78	2.72	2.60	107.2
Wetterstein Reef Limestone	301	LP36	6500	0.08	0.03	24.76	2.59	6.29	2.01	6.6593E+11	94.0	2.78	2.72	2.60	107.2
Wetterstein Cataclasite	302	LP38	400	0.16	0.07	17.57	1.83	4.48	1.24	2.6689E+11	104.7	2.72	2.68	2.60	106.3
Wetterstein Cataclasite	303	LP38	500	0.14	0.06	18.76	1.83	4.48	1.26	9.2176E+11	308.1	2.72	2.68	2.60	106.3
Wetterstein Cataclasite	304	LP38	1000	0.09	0.03	23.48	1.83	4.48	1.13	9.2586E+11	173.8	2.72	2.69	2.60	106.3
Wetterstein Cataclasite	305	LP38	1500	0.06	0.02	27.73	1.83	4.48	1.05	1.7932E+12	234.1	2.72	2.69	2.60	106.3
Wetterstein Cataclasite	306	LP38	2500	0.03	0.01	35.98	1.83	4.48	0.91	2.3898E+12	175.2	2.72	2.69	2.60	106.3
Wetterstein Cataclasite	307	LP38	3500	0.02	0.01	44.85	1.83	4.48	0.83	1.3292E+13	608.6	2.72	2.70	2.60	106.3
Wetterstein Cataclasite	308	LP38	4500	0.01	0.00	54.70	1.83	4.48	0.75	6.2632E+13	1900.4	2.72	2.70	2.60	106.3
Wetterstein Cataclasite	309	LP38	5500	0.01	0.00	65.04	1.83	4.48	0.71	6.0739E+13	1246.8	2.72	2.70	2.60	106.3

Wetterstein Cataclasite	310	LP38	6500	0.01	0.00	63.43	1.83	4.48	0.70	1.1334E+14	2044.8	2.72	2.70	2.60	106.3
Wetterstein Reef Limestone	311	LP41	400	0.31	0.16	13.22	3.95	6.64	4.05	4.4582E+11	287.6	2.83	2.72	2.65	157.2
Wetterstein Reef Limestone	312	LP41	500	0.28	0.14	13.90	3.95	6.64	4.06	1.9169E+11	104.3	2.83	2.72	2.65	157.2
Wetterstein Reef Limestone	313	LP41	1000	0.19	0.09	16.49	3.95	6.64	4.04	3.2295E+11	107.3	2.83	2.72	2.65	157.2
Wetterstein Reef Limestone	314	LP41	1500	0.15	0.07	18.39	3.95	6.64	3.97	5.9282E+11	148.4	2.83	2.72	2.65	157.2
Wetterstein Reef Limestone	315	LP41	2500	0.11	0.04	21.15	3.95	6.64	3.89	1.2267E+12	213.5	2.83	2.72	2.65	157.2
Wetterstein Reef Limestone	316	LP41	3500	0.09	0.03	23.26	3.95	6.64	3.83	3.026E+12	412.8	2.83	2.73	2.65	157.2
Wetterstein Reef Limestone	317	LP41	4500	0.07	0.03	25.08	3.95	6.64	3.78	4.6391E+12	521.9	2.83	2.73	2.65	157.2
Wetterstein Reef Limestone	318	LP41	5500	0.06	0.02	26.70	3.95	6.64	3.74	6.7196E+12	644.8	2.83	2.73	2.65	157.2
Wetterstein Reef Limestone	319	LP41	6500	0.06	0.02	28.19	3.95	6.64	3.72	5.0568E+12	421.5	2.83	2.73	2.65	157.2
Wetterstein Reef Limestone	320	LP43	400	0.41	0.23	11.76	4.20	7.46	4.46	4.573E+11	373.3	2.84	2.71	2.63	147.9
Wetterstein Reef Limestone	321	LP43	500	0.38	0.21	12.15	4.20	7.46	4.48	4.5179E+11	324.7	2.84	2.71	2.63	147.9
Wetterstein Reef Limestone	322	LP43	1000	0.32	0.17	13.01	4.20	7.46	4.47	3.2905E+11	185.1	2.84	2.71	2.63	147.9

Lithology	ID	Sample													
Wetterstein Reef Limestone	323	LP43	1500	0.30	0.16	13.43	4.20	7.46	4.42	4.9458E+11	257.4	2.84	2.71	2.63	147.9
Wetterstein Reef Limestone	324	LP43	2500	0.28	0.14	13.86	4.20	7.46	4.32	4.9397E+11	234.1	2.84	2.72	2.63	147.9
Wetterstein Reef Limestone	325	LP43	3500	0.26	0.14	14.17	4.20	7.46	4.24	6.8799E+11	311.9	2.84	2.72	2.63	147.9
Wetterstein Reef Limestone	326	LP43	4500	0.25	0.13	14.41	4.20	7.46	4.19	7.8877E+11	346.3	2.84	2.72	2.63	147.9
Wetterstein Reef Limestone	327	LP43	5500	0.25	0.13	14.57	4.20	7.46	4.13	7.386E+11	312.8	2.84	2.72	2.63	147.9
Wetterstein Reef Limestone	328	LP43	6500	0.24	0.12	14.75	4.20	7.46	4.09	8.8834E+11	368.4	2.84	2.72	2.63	147.9
Opponitz Limestone	329	LP48.2	400	1.55	1.07	6.73	1.95	6.59	1.55	2.5212E+11	918.5	2.73	2.68	2.55	75.3
Opponitz Limestone	330	LP48.2	500	1.46	1.00	6.89	1.95	6.59	1.52	2.6315E+11	842.4	2.73	2.68	2.55	75.3
Opponitz Limestone	331	LP48.2	1000	1.00	0.65	8.05	1.95	6.59	1.45	4.0448E+11	910.6	2.73	2.69	2.55	75.3
Opponitz Limestone	332	LP48.2	1500	0.80	0.50	8.84	1.95	6.59	1.34	5.4531E+11	946.6	2.73	2.69	2.55	75.3
Opponitz Limestone	333	LP48.2	2500	0.54	0.32	10.42	1.95	6.59	1.17	7.9493E+11	878.2	2.73	2.69	2.55	75.3
Opponitz Limestone	334	LP48.2	3500	0.39	0.22	11.95	1.95	6.59	1.06	1.0267E+12	782.2	2.73	2.70	2.55	75.3
Opponitz Limestone	335	LP48.2	4500	0.30	0.16	13.43	1.95	6.59	0.98	1.4889E+12	830.7	2.73	2.70	2.55	75.3
Opponitz Limestone	336	LP48.2	5500	0.23	0.12	14.93	1.95	6.59	0.92	1.6358E+12	685.0	2.73	2.70	2.55	75.3
Opponitz Limestone	337	LP48.2	6500	0.19	0.09	16.46	1.95	6.59	0.87	1.5376E+12	496.8	2.73	2.70	2.55	75.3
Wetterstein Reef Debris	338	MT17	400	0.02	0.00	52.63	0.91	1.57	0.86	8.94E+12	327.5	2.71	2.68	2.66	154.1

Wetterstein Reef Debris	339	MT17.2	400	0.03	0.01	36.34	2.07	3.56	0.61	3.058E+12	223.9	2.71	2.69	2.61	151.9
Wetterstein Reef Debris	340	MT17.2	500	0.02	0.01	44.91	2.07	3.56	0.62	1.3963E+13	708.1	2.71	2.69	2.61	151.9
Wetterstein Reef Debris	341	MT17.2	1000	0.01	0.00	73.50	2.07	3.56	0.59	5.1192E+13	933.9	2.71	2.69	2.61	151.9
Wetterstein Reef Debris	342	MT17.2	1500	0.00	0.00	105.27	2.07	3.56	0.51	1.6201E+14	1556.2	2.71	2.70	2.61	151.9
Wetterstein Reef Debris	343	MT17.2	2500	0.01	0.00	84.07	2.07	3.56	0.49	9.4228E+13	301.1	2.71	2.70	2.61	151.9
Wetterstein Reef Debris	344	MT17.3	400	0.03	0.01	36.45	2.12	5.46	1.09	4.0635E+12	299.0	2.72	2.69	2.57	99.9
Wetterstein Reef Debris	345	MT17.3	500	0.03	0.01	41.39	2.12	5.46	1.07	3.1397E+13	1724.0	2.72	2.69	2.57	99.9
Wetterstein Reef Debris	346	MT17.3	1000	0.01	0.00	60.54	2.12	5.46	0.90	4.5943E+13	1097.3	2.72	2.70	2.57	99.9
Wetterstein Reef Debris	347	MT17.3	1500	0.01	0.00	76.24	2.12	5.46	0.99	1.2417E+14	1781.7	2.72	2.69	2.57	99.9
Wetterstein Reef Debris	348	MT17.3	2500	0.00	0.00	100.99	2.12	5.46	0.84	1.7726E+13	128.8	2.72	2.70	2.57	99.9
Wetterstein Reef Debris	349	MT17.3	3500	0.00	0.00	121.70	2.12	5.46	0.72	8.2396E+14	3948.4	2.72	2.70	2.57	99.9
Wetterstein Reef Debris	350	MT17.3	4500	0.00	0.00	142.85	2.12	5.46	0.65	3.1724E+15	11292.5	2.72	2.70	2.57	99.9
Wetterstein Reef Debris	351	MT17.3	5500	0.00	0.00	159.73	2.12	5.46	0.59	1.8849E+15	4916.0	2.72	2.71	2.57	99.9
Wetterstein Reef Debris	352	MT17.3	6500	0.00	0.00	140.53	2.12	5.46	0.57	6.1731E+15	15419.5	2.72	2.71	2.57	99.9

Appendix 1: Comprehensive table of the measurements done with the Coreval 700 device.

Sample	md				mh				ms			
	24h	48h	MW	%	24h	48h	MW	%	24h	48h	MW	%
LP2	1530.8	1530.9	1530.85	0.01	962.5	962.6	962.55	0.01	1537.5	1536.2	1536.85	0.08

LP7.1	1400.9	1400.9	1400.9	0.00	882.5	881.9	882.2	0.07	1405	1404.4	1404.7	0.04
LP7.2	823.9	823.6	823.75	0.04	524.8	525	524.9	0.04	829.6	829.9	829.75	0.04
LP7.3	752	752	752	0.00	468.2	468.6	468.4	0.09	758	757.5	757.75	0.07
LP7.4	856.4	856.4	856.4	0.00	539.8	540.3	540.05	0.09	858.3	858.1	858.2	0.02
LP7.5	959.7	959.6	959.65	0.01	600.7	601.1	600.9	0.07	968.6	968.2	968.4	0.04
LP11	1727.5	1727.4	1727.45	0.01	1043.7	1044.6	1044.15	0.09	1779.8	1780.8	1780.3	0.06
LP19.1	2862.8	2862.4	2862.6	0.01	1803.7	1805.2	1804.45	0.08	2870.8	2870.7	2870.75	0.00
LP19.2	7011.6	7010.5	7011.05	0.02	4122.9	4124.6	4123.75	0.04	7269.1	7274.8	7271.95	0.08
LP19.3	255.6	255.4	255.5	0.08	156	155.9	155.95	0.06	270.3	270.1	270.2	0.07
LP36	1363.9	1363.3	1363.6	0.04	864.5	864.5	864.5	0.00	1378.4	1378.3	1378.35	0.01
LP38	3927.1	3926.1	3926.6	0.03	2463.7	2461.7	2462.7	0.08	3938.5	3934.6	3936.55	0.10
LP41	1938.8	1938.8	1938.8	0.00	1244.4	1245.5	1244.95	0.09	1968	1969.5	1968.75	0.08
LP43	2245.5	2244.5	2245	0.04	1432.8	1432.9	1432.85	0.01	2297.1	2296.9	2297	0.01
LP45	2159.1	2157.8	2158.45	0.06	1340.5	1339.6	1340.05	0.07	2180.3	2180.5	2180.4	0.01
LP46	1506.2	1506.1	1506.15	0.01	971.5	970.8	971.15	0.07	1512.9	1512.6	1512.75	0.02
LP48.1	2401.2	2401.1	2401.15	0.00	1503.9	1505.3	1504.6	0.09	2409	2410.4	2409.7	0.06
LP48.2	1161.7	1161.6	1161.65	0.01	727.3	727.1	727.2	0.03	1171.9	1171.6	1171.75	0.03
MT10	2431.6	2431.4	2431.5	0.01	1517.9	1519.4	1518.65	0.10	2444.6	2444.2	2444.4	0.02
MT10.2	1632.4	1632.2	1632.3	0.01	1022	1022.6	1022.3	0.06	1646.5	1648.1	1647.3	0.10
MT17	3333.5	3333.3	3333.4	0.01	2097.4	2099.6	2098.5	0.10	3343	3339.6	3341.3	0.10
MT31	3251.9	3251.3	3251.6	0.02	2038.8	2040.7	2039.75	0.09	3287.2	3286.5	3286.85	0.02
PW1/1	1411.2	1411.3	1411.25	0.01	912.4	913.2	912.8	0.09	1419.3	1420.7	1420	0.10
PW1/2	2599.1	2598.9	2599	0.01	1678.1	1678.3	1678.2	0.01	2614.9	2617	2615.95	0.08
PW1/3	2867	2866.6	2866.8	0.01	1851.4	1853.2	1852.3	0.10	2887.1	2889.5	2888.3	0.08
PW1/4	3407.1	3406.7	3406.9	0.01	2912.7	2914.1	2913.4	0.05	3430.9	3433.1	3432	0.06
PW1/5	2940.9	2940.7	2940.8	0.01	1893.5	1894.3	1893.9	0.04	2967.8	2970.2	2969	0.08
PW1/6	1956.4	1956.4	1956.4	0.00	1263.4	1263.9	1263.65	0.04	1973.3	1974.1	1973.7	0.04

PW3/1	3109.5	3109.5	3109.5	0.00	1953.2	1954.4	1953.8	0.06	3120.7	3121.9	3121.3	0.04
PW3/2	2657.5	2657.6	2657.55	0.00	1676.8	1678.4	1677.6	0.10	2666.3	2666.5	2666.4	0.01
PW3/3	2249.7	2249.5	2249.6	0.01	1416.7	1416.9	1416.8	0.01	2256.4	2257.4	2256.9	0.04
PW3/4	2842.7	2842.5	2842.6	0.01	1819.7	1820.2	1819.95	0.03	2865.6	2867.3	2866.45	0.06
PW4/1	2343.6	2343.8	2343.7	0.01	1474.5	1474.3	1474.4	0.01	2352.8	2353	2352.9	0.01
PW4/2	1769.3	1769.4	1769.35	0.01	1111.6	1111.2	1111.4	0.04	1777.3	1777.6	1777.45	0.02
PW4/3	2110.4	2110.1	2110.25	0.01	1321.5	1322.4	1321.95	0.07	2132.2	2134.3	2133.25	0.10
PW4/4	2598.8	2598.6	2598.7	0.01	1630.5	1632.1	1631.3	0.10	2629.1	2630.2	2629.65	0.04
PW5/1	2304.1	2304	2304.05	0.00	1454.1	1452.9	1453.5	0.08	2308.9	2310.2	2309.55	0.06
PW5/2	1777	1776.7	1776.85	0.02	1116.7	1116.2	1116.45	0.04	1780.1	1781.3	1780.7	0.07
PW5/3	2741.9	2741.6	2741.75	0.01	1733.5	1732.9	1733.2	0.03	2749	2750	2749.5	0.04
PW5/4	3125.2	3125	3125.1	0.01	1969	1967.2	1968.1	0.09	3128	3128.6	3128.3	0.02
PW5/5	1913.2	1913	1913.1	0.01	1204.5	1203.9	1204.2	0.05	1924.6	1925.4	1925	0.04
PW5/6	1872.7	1872.5	1872.6	0.01	1177	1177.6	1177.3	0.05	1889.8	1891.2	1890.5	0.07
PW5/7	2720.7	2720.6	2720.65	0.00	1753.5	1756.1	1754.8	0.15	2750.2	2751.3	2750.75	0.04
PW6/1	3068.6	3068.5	3068.55	0.00	1929.8	1931.5	1930.65	0.09	3082.3	3083.3	3082.8	0.03
PW6/2	2487.3	2487	2487.15	0.01	1564.7	1563.6	1564.15	0.07	2493.1	2494.2	2493.65	0.04
PW6/3	2429.2	2429.2	2429.2	0.00	1529.6	1530	1529.8	0.03	2435.2	2435.6	2435.4	0.02
PW6/4	2551.8	2551.6	2551.7	0.01	1605.8	1606.7	1606.25	0.06	2560.4	2560.3	2560.35	0.00
PW6/5	2670.5	2670.3	2670.4	0.01	1679.9	1680.5	1680.2	0.04	2677.7	2678.7	2678.2	0.04
PW6/6	1722.9	1722.7	1722.8	0.01	1083.8	1083.5	1083.65	0.03	1727.4	1728	1727.7	0.03
PW6/7	2707.6	2707.2	2707.4	0.01	1703.4	1705.1	1704.25	0.10	2714.1	2715.8	2714.95	0.06
PW6/8	2454.1	2453.9	2454	0.01	1542.9	1543.3	1543.1	0.03	2469.6	2470.6	2470.1	0.04
PW7/1	1510.6	1510.6	1510.6	0.00	964	964.8	964.4	0.08	1532.5	1532.5	1532.5	0.00
PW7/2	1811	1810.8	1810.9	0.01	1170.3	1169.7	1170	0.05	1830.7	1832.4	1831.55	0.09
PW7/3	2166.9	2166.8	2166.85	0.00	1399.1	1399.7	1399.4	0.04	2216.6	2218.8	2217.7	0.10
PW7/4	2444.8	2444.7	2444.75	0.00	1581.7	1582.9	1582.3	0.08	2481.6	2482.3	2481.95	0.03

	md				mh				ms			
PW7/5	1825.1	1824.9	1825	0.01	1178.2	1178.9	1178.55	0.06	1850.2	1852.1	1851.15	0.10
PW7/6	1308.1	1308	1308.05	0.01	841.4	840.7	841.05	0.08	1329.5	1330	1329.75	0.04

Appendix 2: Handpieces: Weights of dry samples (md), submerged samples (mh) and wet samples (ms) after 24 hours, 48 hours, the arithmetic median of both measurements (MW) and the percentual deviation of the second from the first measurement.

Sample	md				mh				ms			
	24h	48h	MW	%	24h	48h	MW	%	24h	48h	MW	%
LP2	123.9	123.8	123.85	0.08	77.6	77.6	77.6	0.00	124.2	124.2	124.2	0.00
LP7.1	206.8	206.8	206.8	0.00	129.4	129.4	129.4	0.00	207.1	207.2	207.15	0.05
LP7.2	108.1	108	108.05	0.09	68.8	68.8	68.8	0.00	108.6	108.7	108.65	0.09
LP7.3	102.8	102.8	102.8	0.00	64	64	64	0.00	103.3	103.4	103.35	0.10
LP11	127.2	127.2	127.2	0.00	76.4	76.4	76.4	0.00	129.4	129.5	129.45	0.08
LP19.1_2	164.5	164.4	164.45	0.06	102.9	102.8	102.85	0.10	164.9	164.8	164.85	0.06
LP19.2_1	178.2	178.2	178.2	0.00	107.1	107.2	107.15	0.09	182.1	182.2	182.15	0.05
LP19.2_2	104.3	104.3	104.3	0.00	60.1	60.1	60.1	0.00	108.6	108.7	108.65	0.09
LP19.2_3	107.9	107.9	107.9	0.00	64.6	64.6	64.6	0.00	111.9	112	111.95	0.09
LP19.2_4	110.9	110.9	110.9	0.00	67	67	67	0.00	113.2	113.3	113.25	0.09
LP19.2_5	67.2	67.2	67.2	0.00	39.1	39.1	39.1	0.00	70	70	70	0.00
LP36	107.2	107.2	107.2	0.00	68	68	68	0.00	107.9	107.8	107.85	0.09
LP38	106.3	106.3	106.3	0.00	66.6	66.6	66.6	0.00	106.7	106.6	106.65	0.09
LP41	157.3	157.3	157.3	0.00	100.3	100.4	100.35	0.10	158.8	158.8	158.8	0.00
LP43	148	148	148	0.00	94.2	94.2	94.2	0.00	149.7	149.8	149.75	0.07
LP46	71.2	71.2	71.2	0.00	45	45	45	0.00	71.4	71.4	71.4	0.00
LP48.2	75.4	75.4	75.4	0.00	47.3	47.3	47.3	0.00	75.6	75.6	75.6	0.00
MT17.1	154.1	154.1	154.1	0.00	96.6	96.6	96.6	0.00	154.4	154.4	154.4	0.00
MT17.2	152	152	152	0.00	95.2	95.2	95.2	0.00	152.2	152.3	152.25	0.07
MT17.3	100	100	100	0.00	62.4	62.4	62.4	0.00	100.2	100.2	100.2	0.00

PW1/6	105.4	105.5	105.45	0.09	66.8	66.8	66.8	0.00	106.4	106.4	106.4	0.00
PW3/1_1	132.2	132.2	132.2	0.00	82.5	82.5	82.5	0.00	132.7	132.6	132.65	0.08
PW3/1_2	103.9	103.9	103.9	0.00	64.9	64.9	64.9	0.00	104.2	104.1	104.15	0.10
PW3/2	157.5	157.5	157.5	0.00	98.7	98.7	98.7	0.00	157.9	158	157.95	0.06
PW3/3	127.8	127.8	127.8	0.00	80.4	80.4	80.4	0.00	128.2	128.1	128.15	0.08
PW3/4	105.5	105.5	105.5	0.00	67.2	67.2	67.2	0.00	106	106	106	0.00
PW4/4	189.9	190	189.95	0.05	118.5	118.6	118.55	0.08	190.5	190.4	190.45	0.05
PW5/1_1	184.9	184.9	184.9	0.00	116	115.9	115.95	0.09	185.2	185.2	185.2	0.00
PW5/1_2	111.4	111.3	111.35	0.09	69.9	69.9	69.9	0.00	111.5	111.5	111.5	0.00
PW5/3	190	190	190	0.00	119.3	119.4	119.35	0.08	190.3	190.4	190.35	0.05
PW5/4	199	199	199	0.00	124.7	124.8	124.75	0.08	199.3	199.4	199.35	0.05
PW5/5	144	144	144	0.00	90.4	90.4	90.4	0.00	144.2	144.2	144.2	0.00
PW5/6	103.9	103.9	103.9	0.00	65.2	65.2	65.2	0.00	104.1	104.1	104.1	0.00
PW5/7	123.6	123.6	123.6	0.00	79.3	79.3	79.3	0.00	124.4	124.5	124.45	0.08
PW6/1	148.9	148.9	148.9	0.00	93.4	93.4	93.4	0.00	149.4	149.4	149.4	0.00
PW6/2	171.3	171.2	171.25	0.06	107.2	107.2	107.2	0.00	171.7	171.6	171.65	0.06
PW6/3_1	170	170	170	0.00	106.3	106.4	106.35	0.09	170.4	170.3	170.35	0.06
PW6/3_2	110.3	110.3	110.3	0.00	69	69	69	0.00	110.6	110.6	110.6	0.00
PW6/4	198.5	198.4	198.45	0.05	124.3	124.4	124.35	0.08	198.8	198.9	198.85	0.05
PW6/5	94.6	94.6	94.6	0.00	59.5	59.5	59.5	0.00	94.9	94.9	94.9	0.00
PW6/6	133.4	133.4	133.4	0.00	83.4	83.4	83.4	0.00	133.7	133.7	133.7	0.00
PW6/7_1	118.8	118.7	118.75	0.08	74.4	74.4	74.4	0.00	119	119	119	0.00
PW6/7_2	118.9	119	118.95	0.08	74.5	74.5	74.5	0.00	119.2	119.3	119.25	0.08
PW6/8	110	110.1	110.05	0.09	68.8	68.8	68.8	0.00	110.5	110.5	110.5	0.00
PW7/1	153.4	153.4	153.4	0.00	98.3	98.3	98.3	0.00	154.7	154.8	154.75	0.06
PW7/2	150.7	150.7	150.7	0.00	96.8	96.8	96.8	0.00	152.3	152.4	152.35	0.07
PW4/2	111.8	111.7	111.75	0.09	71.5	71.5	71.5	0.00	112.4	112.5	112.45	0.09

PW7/3_1	183.3	183.2	183.25	0.05	117.8	117.8	117.8	0.00	186.3	186.4	186.35	0.05
PW7/3_2	176.8	176.8	176.8	0.00	113.8	113.9	113.85	0.09	180.4	180.5	180.45	0.06
PW7/4	227	227	227	0.00	145.7	145.8	145.75	0.07	229.5	229.5	229.5	0.00
PW7/5	179.3	179.3	179.3	0.00	114.7	114.8	114.75	0.09	181.1	181.1	181.1	0.00
PW7/6	106.2	106.3	106.25	0.09	67.8	67.8	67.8	0.00	107.5	107.5	107.5	0.00

Appendix 3: Core plugs: Weights of dry core samples (md), submerged core samples (mh) and wet core samples (ms)) after 24 hours, 48 hours, the arithmetic median of both measurements (MW) and the percentual deviation of the second from the first measurement.

Lithology	Sample	Sample type	Porosity (immersion) [%]	Porosity (Coreval 700) [%]	Porosity (thin section) [%]	Klinkenberg permeability (Coreval 700) [mD]	Density (immersion) [g/cc]	Density (Coreval 700) [g/cc]	P21-value [cm/cm²]	FDC
Karstified Wetterstein limestone	LP11	Core plug	4.24	19.54	-	0.065	2.39	2.20	-	1
Karstified Wetterstein limestone	LP11	Hand piece	7.18	-	-	-	2.34	-	-	1
Karstified Wetterstein limestone	LP11	Thin section	-	-	20.87	-	-	-	0.00208	-
Wetterstein reef limestone	LP19.1	Hand piece	0.76	-	-	-	2.68	-	-	2
Wetterstein reef limestone	LP19.1_1	Core plug		3.22	-	0.101	-	2.62	-	2
Wetterstein reef limestone	LP19.1_1	Thin section	-	-	6.59	-	-	-	0.4	-
Wetterstein reef limestone	LP19.1_2	Core plug	0.65	1.07	-	0.012	2.65	2.68	-	2

Karstified Wetterstein limestone	LP19.2	Core plug	5.27	6.13	-	0.112	2.37	2.29	-	1
Karstified Wetterstein limestone	LP19.2	Hand piece	8.29	-	-	-	2.22	-	-	1
Karstified Wetterstein limestone	LP19.2	Thin section	-	-	27.16	-	-	-	0.0172	-
Karstified Wetterstein limestone	LP19.2_2	Core plug	8.96	27.63	-	0.535	2.14	1.97	-	1
Karstified Wetterstein limestone	LP19.2_3	Core plug	8.55	20.91	-	11.038	2.27	2.18	-	1
Karstified Wetterstein limestone	LP19.2_4	Core plug	5.08	14.00	-	0.121	2.39	2.35	-	1
Karstified Wetterstein limestone	LP19.2_5	Core plug	9.06	24.85	-	32.541	2.17	2.05	-	1
Karstified Wetterstein limestone	LP19.3	Hand piece	12.87	-	-	-	2.23	-	-	1
Wetterstein reef debris limestone	LP2	Core plug	0.75	2.21	-	0.006	2.65	2.66	-	1
Wetterstein reef debris limestone	LP2	Hand piece	1.04	-	-	-	2.66	-	-	1
Wetterstein reef limestone	LP36	Core plug	1.63	6.29	-	0.124	2.68	2.60	-	1
Wetterstein Reef Limestone	LP36	Hand piece	2.87	-	-	-	2.65	-	-	1
Wetterstein Reef Limestone	LP36	Thin section	-	-	3.46	-	-	-	0.15	-
Stylobreccia from a protolith of Wetterstein reef limestone	LP38	Core plug	0.87	4.48	-	0.075	2.65	2.60	-	-
Stylobreccia from a protolith of Wetterstein reef limestone	LP38	Hand piece	0.68	-	-	-	2.66	-	-	-

Stylobreccia from a protolith of Wetterstein reef limestone	LP38	Thin section	-	-	very low	-	-	-	very low	-
Wetterstein reef limestone	LP41	Core plug	2.57	6.64	-	0.164	2.69	2.65	-	1
Wetterstein Reef Limestone	LP41	Hand piece	4.14	-	-	-	2.67	-	-	1
Wetterstein Reef Limestone	LP41	Thin section	-	-	5.33	-	-	-	4.42	-
Wetterstein reef limestone	LP43	Core plug	3.15	7.46	-	0.227	2.66	2.63	-	2
Wetterstein Reef Limestone	LP43	Hand piece	6.02	-	-	-	2.59	-	-	2
Hornstein Limestone	LP45	Hand piece	2.61	-	-	-	2.56	-	-	1
Haupt dolomite	LP46	Core plug	0.76	-	-	-	2.69	-	-	1
Haupt dolomite	LP46	Hand piece	1.22	-	-	-	2.78	-	-	1
Opponitz limestone	LP48.1	Hand piece	0.94	-	-	-	2.65	-	-	1
Opponitz limestone	LP48.2	Core plug	0.71	6.59	-	1.071	2.66	2.55	-	1
Opponitz limestone	LP48.2	Hand piece	2.27	-	-	-	2.61	-	-	1
Hornstein limestone	LP7.1	Core plug	0.45	1.03	-	0.002	2.65	2.68	-	1
Hornstein limestone	LP7.1	Hand piece	0.73	-	-	-	2.68	-	-	1
Hornstein limestone	LP7.2	Core plug	1.51	2.53	-	0.004	2.71	2.72	-	1
Hornstein limestone	LP7.2	Hand piece	1.97	-	-	-	2.70	-	-	1
Hornstein limestone	LP7.3	Core plug	1.40	5.75	-	0.015	2.61	2.52	-	1
Hornstein limestone	LP7.3	Hand piece	1.99	-	-	-	2.59	-	-	1
Hornstein Limestone	LP7.4	Hand piece	0.57	-	-	-	2.69	-	-	1
Hornstein Limestone	LP7.5	Hand piece	2.38	-	-	-	2.61	-	-	1
Opponitz Limestone	MT10	Hand piece	1.39	-	-	-	2.62	-	-	1
Opponitz Limestone	MT10.2	Hand piece	2.40	-	-	-	2.61	-	-	1

Description	Sample	Type								
Stylobreccia from a protolith of Wetterstein reef debris limestone	MT17	Core plug	0.52	1.57	-	0.004	2.66	2.66	-	-
Stylobreccia from a protolith of Wetterstein reef debris limestone	MT17	Hand piece	0.64	-	-	-	2.68	-	-	-
Stylobreccia from a protolith of Wetterstein reef debris limestone	MT17	Thin section	-	-	1.22	-	-	-	0.37	-
Stylobreccia from a protolith of Wetterstein reef debris limestone	MT17.2	Core plug	0.44	3.56	-	0.010	2.66	2.61	-	-
Stylobreccia from a protolith of Wetterstein reef debris limestone	MT17.3	Core plug	0.53	5.46	-	0.010	2.64	2.57	-	-
Cataclasite (Type 1) from a protolith of Wetterstein reef limestone	MT31	Hand piece	2.83	-	-	-	2.60	-	-	-
Wetterstein dolomite	PW1/1	Hand piece	1.73	-	-	-	2.78	-	-	3
Wetterstein dolomite	PW1/2	Hand piece	1.81	-	-	-	2.77	-	-	3
Wetterstein dolomite	PW1/3	Hand piece	2.08	-	-	-	2.76	-	-	4
Wetterstein dolomite	PW1/4	Hand piece	2.03	-	-	-	2.75	-	-	4
Wetterstein dolomite	PW1/5	Hand piece	2.62	-	-	-	2.73	-	-	4
Wetterstein dolomite	PW1/6	Core plug	2.40	3.91	-	6.791	2.66	2.74	-	4
Wetterstein dolomite	PW1/6	Hand piece	2.44	-	-	-	2.75	-	-	4

Lithology	Sample	Type								
Wetterstein dolomite	PW1/6	Thin section	-	-	5.4	-	-	-	0.96	-
Wetterstein reef limestone	PW3/1	Hand piece	1.01	-	-	-	2.66	-	-	2
Wetterstein reef limestone	PW3/1.1	Core plug	0.90	4.94	-	0.109	2.63	2.59	-	2
Wetterstein reef limestone	PW3/1.2	Core plug	0.64	-	-	-	2.64	-	-	2
Wetterstein reef limestone	PW3/2	Core plug	0.76	0.29	-	0.089	2.65	3.03	-	3
Wetterstein reef limestone	PW3/2	Hand piece	0.90	-	-	-	2.68	-	-	3
Wetterstein reef limestone	PW3/3	Core plug	0.73	2.86	-	0.147	2.67	2.68	-	3
Wetterstein reef limestone	PW3/3	Hand piece	0.87	-	-	-	2.67	-	-	3
Wetterstein reef limestone	PW3/4	Core plug	1.29	5.04	-	0.016	2.71	2.69	-	2
Wetterstein reef limestone	PW3/4	Hand piece	2.28	-	-	-	2.71	-	-	2
Wetterstein reef limestone	PW4/1	Hand piece	1.05	-	-	-	2.66	-	-	2
Wetterstein reef limestone	PW4/2	Hand piece	1.22	-	-	-	2.65	-	-	3
Wetterstein reef limestone	PW4/3	Hand piece	2.83	-	-	-	2.60	-	-	3
Wetterstein reef limestone	PW4/4	Core plug	0.70	3.43	-	1.611	2.64	2.64	-	2
Wetterstein reef limestone	PW4/4	Hand piece	3.10	-	-	-	2.60	-	-	2
Wetterstein reef limestone	PW4/4	Thin section	-	-	4.14	-	-	-	0.43	-

Lithology	Sample	Type								
Wetterstein reef limestone	PW5/1	Hand piece	0.64	-	-	-	2.69	-	-	1
Wetterstein reef limestone	PW5/1.1	Core plug	0.43	2.69	-	0.009	2.66	2.67	-	1
Wetterstein reef limestone	PW5/1.1	Thin section	-	-	0.83	-	-	-	0.11	-
Wetterstein reef limestone	PW5/1.2	Core plug	0.36	1.49	-	0.004	2.67	2.69	-	1
Wetterstein reef limestone	PW5/1.2	Thin section	-	-	0.74	-	-	-	0.0000329	-
Wetterstein reef limestone	PW5/2	Hand piece	0.58	-	-	-	2.67	-	-	1
Wetterstein reef limestone	PW5/3	Core plug	0.49	3.15	-	0.026	2.67	2.66	-	2
Wetterstein reef limestone	PW5/3	Hand piece	0.76	-	-	-	2.69	-	-	2
Wetterstein reef limestone	PW5/4	Core plug	0.47	3.19	-	0.020	2.66	2.66	-	2
Wetterstein reef limestone	PW5/4	Hand piece	0.28	-	-	-	2.69	-	-	2
Wetterstein reef limestone	PW5/5	Core plug	0.37	4.45	-	0.288	2.67	2.64	-	3
Wetterstein reef limestone	PW5/5	Hand piece	1.65	-	-	-	2.65	-	-	3
Wetterstein reef limestone	PW5/6	Core plug	0.51	2.91	-	0.083	2.67	2.65	-	3
Wetterstein reef limestone	PW5/6	Hand piece	2.51	-	-	-	2.62	-	-	3
Cataclasite (Type 1) from a protolith of Wetterstein reef limestone	PW5/7	Core plug	1.88	-	-	-	2.73	-	-	-

Cataclasite (Type 1) from a protolith of Wetterstein reef limestone	PW5/7	Hand piece	3.02	-	-	-	2.73	-	-	-
Lagoonal Wetter-stein limestone	PW6/1	Core plug	0.89	4.54	-	0.316	2.65	2.63	-	3
Lagoonal Wetter-stein limestone	PW6/1	Hand piece	1.24	-	-	-	2.66	-	-	3
Lagoonal Wetter-stein limestone	PW6/2	Core plug	0.62	4.36	-	0.027	2.65	2.60	-	2
Lagoonal Wetter-stein limestone	PW6/2	Hand piece	0.70	-	-	-	2.67	-	-	2
Lagoonal Wetter-stein limestone	PW6/2	Thin sec-tion	-	-	very low	-	-	-	very low	-
Lagoonal Wetter-stein limestone	PW6/3	Hand piece	0.68	-	-	-	2.68	-	-	2
Lagoonal Wetter-stein limestone	PW6/3_1	Core plug	0.55	-	-	-	2.65	-	-	2
Lagoonal Wetter-stein limestone	PW6/3_2	Core plug	0.72	-	-	-	2.65	-	-	2
Lagoonal Wetter-stein limestone	PW6/4	Core plug	0.54	0.82	-	0.177	2.66	2.69	-	2
Lagoonal Wetter-stein limestone	PW6/4	Hand piece	0.91	-	-	-	2.67	-	-	2
Lagoonal Wetter-stein limestone	PW6/5	Core plug	0.71	4.78	-	0.023	2.67	2.61	-	3
Lagoonal Wetter-stein limestone	PW6/5	Hand piece	0.78	-	-	-	2.67	-	-	3
Lagoonal Wetter-stein limestone	PW6/6	Core plug	0.60	2.16	-	0.046	2.65	2.67	-	3
Lagoonal Wetter-stein limestone	PW6/6	Hand piece	0.76	-	-	-	2.67	-	-	3

Description	Sample	Type								
Stylobreccia from a protolith of lagoonal Wetterstein limestone	PW6/7	Hand piece	0.75	-	-	-	2.67	-	-	-
Stylobreccia from a protolith of lagoonal Wetterstein limestone	PW6/7.1	Core plug	0.56	5.38	-	0.009	2.66	2.62	-	-
Stylobreccia from a protolith of lagoonal Wetterstein limestone	PW6/7.2	Core plug	0.67	-	-	-	2.65	-	-	-
Lagoonal Wetterstein limestone	PW6/8	Core plug	1.08	8.85	-	1.891	2.63	2.49	-	1
Lagoonal Wetterstein limestone	PW6/8	Hand piece	1.74	-	-	-	2.64	-	-	1
Wetterstein dolomite	PW7/1	Core plug	2.39	4.11	-	0.063	2.71	2.74	-	2
Wetterstein dolomite	PW7/1	Hand piece	3.85	-	-	-	2.65	-	-	2
Wetterstein dolomite	PW7/2	Hand piece	3.12	-	-	-	2.73	-	-	2
Wetterstein dolomite	PW7/2.1	Core plug	2.97	4.93	-	0.016	2.71	2.74	-	2
Wetterstein dolomite	PW7/2.2	Core plug	1.71	4.07	-	0.011	2.72	2.73	-	3
Cataclasite (Type 1) from a protolith of Wetterstein dolomite	PW7/3	Hand piece	6.21	-	-	-	2.64	-	-	-
Cataclasite (Type 1) from a protolith of Wetterstein dolomite	PW7/3.1	Core plug	4.52	7.75	-	0.184	2.67	2.65	-	-
Cataclasite (Type 1) from a protolith of Wetterstein dolomite	PW7/3.1	Thin section	-	-	6.79	-	-	-	2.86	-

Lithology	Sample	Type								
Cataclasite (Type 2) from a protolith of Wetterstein dolomite	PW7/3.2	Core plug	5.48	8.08	-	0.343	2.65	2.64	-	-
Cataclasite (Type 1) from a protolith of Wetterstein dolomite	PW7/4	Core plug	2.99	4.29	-	0.359	2.71	2.74	-	-
Cataclasite (Type 1) from a protolith of Wetterstein dolomite	PW7/4	Hand piece	4.13	-	-	-	2.71	-	-	-
Wetterstein dolomite	PW7/5	Core plug	2.71	6.84	-	0.047	2.70	2.68	-	1
Wetterstein dolomite	PW7/5	Hand piece	3.89	-	-	-	2.71	-	-	1
Wetterstein dolomite	PW7/6	Core plug	3.15	10.04	-	0.072	2.67	2.60	-	1
Wetterstein dolomite	PW7/6	Hand piece	4.44	-	-	-	2.67	-	-	1

Appendix 4: Porosities, permeabilities, density, fracture length per area and FDC values of handpieces, core plugs and thin sections.